2007

The Quantitative Genetics of Neurodevelopment: A Magnetic Resonance Imaging Study of Childhood and Adolescence

James Eric Schmitt
Virginia Commonwealth University

The Quantitative Genetics of Neurodevelopment

A Magnetic Resonance Imaging Study of Childhood and Adolescence

A Dissertation submitted in partial fulfillment of the requirements for the degree of Doctor of Philosophy at Virginia Commonwealth University.

by
JAMES E. SCHMITT
B.S., Stanford University, 1998
A.B., Stanford University, 1998

Directors:

KENNETH S. KENDLER, M.D.
DISTINGUISHED PROFESSOR, DEPARTMENTS OF PSYCHIATRY AND HUMAN GENETICS

AND

MICHAEL C. NEALE, PH.D.
PROFESSOR, DEPARTMENTS OF PSYCHIATRY AND HUMAN GENETICS

Table of Contents

List of Tables

List of Figures

List of Abbreviations

CFA	Confirmatory Factor Analysis
CPM	Common Pathway Model
CT	Cortical Thickness
DZ	Dizygotic
EEG	Electroencephalogram
EFA	Exploratory Factor Analysis
FDR	False Discovery Rate
fMRI	functional MRI
HIA	High-resolution Image Analysis
ICV	Intracranial Volume
IPM	Independent Pathway Model
IQ	Intelligence Quotient (Full Scale)
ML	Maximum Likelihood
MLE	Maximum Likelihood Estimate
MRI	Magnetic Resonance Imaging
MTMM	Multitrait Multimethod Matrix
MZ	Monozygotic
NHLBI	National Heart, Lung, and Blood Institute
NIMH	National Institute of Mental Health
NTR	Netherlands Twin Registry
PCA	Principal Component Analysis
PET	Positron Emission Tomography
PIQ	Performance IQ
QTL	Quantitative Trait Loci
r_G	Genetic Correlation
ROI	Region of Interest
SEM	Structural Equation Modeling
SPGR	Spoiled Gradient Recalled
TBV	Total Brain Volume
VBM	Voxel-Based Morphometry
VIQ	Verbal IQ
WAIS	Weschler Adult Intelligence Scale
WISC	Weschler Intelligence Scale for Children

Abstract

THE QUANTITATIVE GENETICS OF NEURODEVELOPMENT:
A MAGNETIC RESONANCE IMAGING STUDY OF CHILDHOOD AND ADOLESCENCE

By James E. Schmitt

A Dissertation submitted in partial fulfillment of the requirements for the degree of Doctor of Philosophy at Virginia Commonwealth University.

Virginia Commonwealth University, 2007

Major Directors:

Kenneth S. Kendler, M.D.
Distinguished Professor, Departments of Psychiatry and Human Genetics

and

Michael C. Neale, Ph.D.
Professor, Departments of Psychiatry and Human Genetics

Understanding the causes of individual differences in brain structure may give clues about the etiology of cognition, personality, and psychopathology, and also may identify endophenotypes for molecular genetic studies on brain development. We performed a comprehensive statistical genetic study of anatomic neuroimaging data from a large pediatric sample (N=600+) of twins and family members from the Child Psychiatry Branch at the NIMH. These analyses included variance decomposition of structural volumetric endophenotypes at several levels of resolution, voxel-level analysis of cortical

thickness, assessment of gene by age interaction, several multivariate genetic analyses, and a search for genetically-mediated brain-behavioral relationships.

These analyses found strong evidence for a genetic role in the generation of individual differences in brain volumes, with the exception of the cerebellum and the lateral ventricles. Subsequent multivariate analyses demonstrated that most of the genetic variance in large volumes shares a common source. More subtle analyses suggest that although this global genetic factor is the principal determinant of neuroanatomic variability, genetic factors also mediate regional variability in cortical thickness and are different for gray and white matter volumes. Models using graph theory show that brain structure follows small-world architectural rules, and that these relationships are genetically-determined. Structural homologues appeared to be strongly related genetically, which was further confirmed using novel methods for semi-multivariate quantitative genetic analysis at the voxel level.

Studies on interactions with age were mixed. We found evidence of gene by age interaction on frontal and temporal lobar volumes, indicating that the role of genetic factors on these structures is dynamic during childhood. Analyses on cortical thickness at a finer scale, however, showed that environmental factors are more important in childhood, and environmental changes were responsible for most of the changes in heritability over this age range. When assessing the relationship between brain and behavior, we found weak negative genetic correlations and positive environmental correlations between IQ and cortical thickness, which appear to partially cancel each other out. More complex models allowing for age interactions suggest that high and low

IQ groups have different patterns of gene by age interactions in concordance with prior literature on cortical phenotypes.

Acknowledgements

Any scientific endeavor represents a symbiosis of many minds, both from present and past. The classical model of a solitary graduate student working on his *magnum opus* no longer adequately represents the reality of scientific research. Given the highly interdisciplinary nature of the analyses to follow, it will soon become apparent that this is certainly the case with my work. Thus, I would like to dedicate this thesis to the spirit of mentorship and collaboration, to honor those who have contributed to its existence. I am particularly grateful to have had advisors such as Ken Kendler and Mike Neale, whom have provided excellent guidance and truly remarkable patience over many years. It is quite a rarity for advisors to allow their students to stray as far as I have from their funded research, and doubly so for advisors to allow themselves to stray a bit as well; I have very much enjoyed our wanderings through the uncharted waters of what may perhaps, in time, become a novel subdiscipline. As this chapter of my life comes to a close, I am certain that I will look upon my days at VIPBG with idyllic fondness, regardless of where Chance carries me in the future.

Thanks to Jay Giedd for the opportunity to work on such a great dataset. In my mind at least, our work together has come close to the ideal collaborative relationship.

To my other committee members Lindon Eaves and Jack Hettema, for agreeing to participate in what has to be the most thankless job in academia. In our discussions over the years, I have gleaned valuable information in the completion of this project, but even more importantly on the nature of an academic career and what it means to be a *good* scientist, in both meanings of the word.

To my collaborators and friends presently or formerly of NIMH: Mike Rosenthal, Sarah Ordaz, Greg Wallace, and Rhoshel Lenroot, who have dedicated mammoth amounts of time to the pediatric twin project. Indeed, it may be somewhat of an insult to acknowledge their "contributions," as the work that follows is as much or more their own: except, of course, for the typos. Though all of these individuals deserve credit for the project, Rhoshel deserves particular accolades for enduring my neuroticism on a near-daily basis. The raw brain maps presented in the chapters on cortical thickness, arguably the most exciting findings of the thesis, were entirely generated by her. Thanks also to the others at NIH and MNI working on this project, only a handful of whom I have met.

My contributions to this project certainly would not have been possible without several years of training in neuroimaging at the Stanford Psychiatry Neuroimaging Laboratory (now the Center for Interdisciplinary Brain Sciences Research at Stanford University), under the expert tutelage of Allan Reiss and Stephan Eliez (now at the University of Geneva). I owe these men an irreparable debt both for their mentorship but also for their assistance in my pregraduate career advancement. In Allan's laboratory, I had the additional honor of learning from many individuals central to the study of genetics and brain development, including Al Galaburda, Ursula Bellugi, Vinod Menon, Ilana Warsofsky, Julie Korenberg, Chris White, David Lyons, Chris Buckmaster, Joe Pinter, and Dan Levitin: I still have not forgotten their kindness and enthusiasm for science.

I also have benefited greatly from many friendships at VIPBG. In addition to the individuals mentioned above, my early training in behavioral genetics owes much to Hermine Maes, Charles Gardner, Steve Aggen, Kristen Jacobson, and Arpana Agrawal. Thanks also to Helen Wang for maintaining the cluster computer and not killing me for trying to wreck it on occasion. Also, I would like to thank Kelly Tracy and Liz Prom for their commiserations on the laborious exercise of dissertation writing, and to the other students and post docs for enduring our incessant outbursts.

No acknowledgement would be complete without mentioning money. In addition to Ken, Mike and the NIH, several other organizations have supported my work on this project. These include Gordon Archer and MCV's MD/PhD program, Jan Chlebowski and the MCV School of Medicine, the Society for Multivariate Experimental Psychology (SMEP), and the VCU chapter of Phi Kappa Phi.

Finally, I would like to acknowledge my oldest collaborator, my wife Kathryn. Thank you for your patience during these difficult times. And thank you for our children. It is with every day that I wonder whether I learn more about neurodevelopment at work or at home; the process of life is truly amazing.

J. Eric Schmitt, January 29, 2007

1

GENERAL INTRODUCTION

"The brain is the last and grandest biological frontier, the most complex thing we have yet discovered in our universe. It contains hundreds of billions of cells interlinked through trillions of connections. The brain boggles the mind."

--James D. Watson, *Discovering the Brain*, 1992

"It is essential to understand our brains in some detail if we are to assess correctly our place in this vast and complicated universe we see all around us"

--Francis Crick, *What Mad Pursuit*, 1988

One of the great gifts to humanity is the capacity to contemplate the nature of the universe and our place in it. It is likely no exaggeration to say that every person who has seen the sunrise or surveyed the earth from a mountaintop, every child on a beach, in short every one of the billions of humans now on this planet and all who preceded us have considered their origins and what makes them who they are. Such contemplations are among the central questions of philosophy, religion, and science, three disciplines that, until quite recently in human history, were inseparable. Modern science differs somewhat from the other two in its insistence on empirical data and acceptance of the subsequent limitations of that constraint, or as the 19th century biologist Thomas Henry Huxley noted, "science is simply common sense at its best that is, rigidly accurate in observation, and merciless to fallacy and logic" (Huxley, 1880).

Neuroscience, broadly speaking, follows the same general pattern as other scientific disciplines, but it is inevitably more intimate. We can witness firsthand the remarkable neurodevelopmental changes transform ourselves and our children from infants into artisans and mathematicians. Our brains enable us to perceive the universe, and our perceptions are colored by our neural organization. Along with opposable thumbs and a few other structural differences, the brain constitutes that which most identifies the human species as unique on our planet. But presumably, differences between human brains also are largely responsible for our uniqueness as individuals: our personalities, cognitive and perceptual abilities, and susceptibilities to mental disease that distinguish one human from one another. These individual differences in brain structures, their

etiology, their dynamics, and their relationship to behavior are the central focus of this thesis.

This work represents but the first volume in a large and ongoing study of the nature of pediatric development by Jay Giedd and his laboratory at NIMH, in collaboration with the Virginia Institute of Psychiatric and Behavioral Genetics (VIPBG) at the Medical College of Virginia. Within these pages, we begin address some of the most basic questions on what factors contribute to individual differences in brain structure and how these factors interact to generate the complexities of neural architecture. Several of the studies represent the first work of their kind. It is my hope that, like an explorer in the wilderness of a new frontierland, the reader will find excitement and novelty in the pages to follow. But also, just as the ancient maps of Herodotus, Ptolemy, or even Columbus represented crude approximations of geographic reality, caution is warranted in trusting the unverified details too greatly. Future "expeditions" to this world will be required to truly understand the role of genes on brain development.

The overall format of this document is something of a hybrid between a traditional American/British "book" style thesis and the continental European model, which represents a collection of scholarly papers. Though most of the work represents manuscripts, published or otherwise, attempts have been made to minimize repetition in the methods sections and redundancies in the discussion. Many of these manuscripts were primarily written by others; I have rewritten them, largely to give me a somewhat illusory sense of ownership over what is in reality a highly collaborative document. As this work

lies at the intersection of several scientific disciplines, it is likely that even some experts will find at least some material unfamiliar. In certain places, I have attempted to provide some background about the underlying sciences, without dwelling on them. Finally, the interested reader with limited time is directed to a review article by Giedd et al., which covers most of the principle findings reported here, but is rather more succinct (Giedd, Schmitt, & Neale, 2007).

Details on the Dataset

The analyses reported in the following chapters utilize data from the Pediatric Twin Study at the Child Psychiatry Branch of the National Institute of Mental Health (NIMH). This study represents an ambitious attempt to acquire both neuroimaging and cognitive data on at least 100 monozygotic (MZ) and 100 dizygotic (DZ) pediatric twin pairs, repeated for at least three time points throughout childhood. The findings reported here are based on cross sectional data from the first time point of data acquisition.

The subjects in this study were recruited by means of local and national advertisements for participation in an ongoing longitudinal pediatric imaging study. Advertisements specified that the MRI study sought twins between the ages of 5 and 18, with no learning disabilities, neurological problems or behavioral disorders. The screening process involved phone interviews, behavioral questionnaires mailed to parents and teachers, an in-person clinical interview, family history assessment, as well as a physical and neurological exam. Exclusion criteria included having a lifetime history of physical, neurological, or psychiatric abnormalities, learning

disabilities, or psychiatric illness oneself, or in either one first-degree relative or more than 20% of second-degree relatives. Approximately one in four families responding to the ads met inclusion criteria. Twins were included in the analysis only if quantifiable MRI scans free from motion or other artifact were obtained on both twins at the same age. Written assent from the child and written consent from a parent were obtained for each participant. The study protocol was approved by the institutional review board of the National Institute of Mental Health. Zygosity was determined by DNA analysis of buccal cheek swabs using 9-21 unlinked short tandem repeat loci for a minimum certainty of 99%, by BRT Laboratories, Inc. (Baltimore, MD).

For some analyses, data from singletons, siblings of twins, or singleton families were used. Singletons and singleton family data were acquired as part of a pediatric study of normal development conducted by NIMH, using similar recruitment strategies and data acquisition methods.

Image Acquisition:

This project centers on data acquired via magnetic resonance imaging (MRI). MRI is a versatile radiological technology that enables the examination of soft tissues *in vivo* with extremely high contrast relative to other imaging modalities (Bushberg, Seibert, Leidholdt, & Boone, 1994). This feature, in combination with its lack of ionizing radiation and subsequent safety, makes MRI particularly useful for neuroanatomic studies on typical populations, especially children, as no clinical indication is required in order to gather data ethically.

The capabilities of MRI are based on the physics underlying nuclear magnetic resonance (NMR). Briefly, all atoms in the universe that contain an odd number of nucleons e.g. elemental hydrogen (^{1}H), ^{17}O, or ^{23}Na, generate small magnetic fields, which can interact with larger fields and be manipulated with electromagnetic waves. Anatomic imaging typically employs hydrogen due to its large magnetic moment and abundance throughout the body, both in aqueous solutions and in lipid. In the presence of a large external magnetic field, protons align either with or against the field and precess, much like a spinning top in the presence of a gravitational field. The application of electromagnetic radiation (i.e. light) of the appropriate frequency simultaneously excites protons to a higher energy state, as well as synchronizes their precessions. Both the rate that protons relax to a lower energy state (T1) and the rate that they become unsynchronized in their precessions (T2) are measurable physical properties that are dependent on the capacity of protons to interact with other atoms, which in turn is affected by properties of tissue. Thus, measurement of T1 and T2 (as well as a few other parameters) provides a means of distinguishing between tissues with different molecular compositions.

In the present study, all subjects were scanned on the same GE 1.5 Tesla Signa MRI scanner (1.5T = 15,000 gauss: for reference, the Earth's magnetic field is about .6 gauss). A three-dimensional spoiled gradient recalled echo in the steady state (3D SPGR) imaging protocol was used for all subjects (axial slice thickness = 1.5 mm, time to echo = 5 msec, repetition time = 24 msec, flip angle = 45 degrees, acquisition

matrix = 192 x 256, number of excitations = 1, and field of view = 24 cm). By phase shifting radio wave pulses, SPGR "spoils" the signal from proton precession and subsequently weights the signal towards the T1 properties of matter (Bushberg et al., 1994), i.e. emphasizing differences in spin relaxation. T1 weighting is particularly good for creating gray versus white matter contrast, and along with high resolution (~1 mm^3) is the reason why SPGR is often used in neuroanatomic studies.

SPGR produces images that resemble actual brain appearance (Figure 1.1), and prior to image processing, a clinical neuroradiologist evaluated all of these scans for gross abnormalities. In this dataset, no abnormalities were identified.

All MRI images are comprised of discrete units called *voxels* e.g. pixels that represent physical volumes. 3D SPGR is conceptually a 3-dimensional matrix of these discrete units, with the grayscale intensity of each voxel representing a scalar signal intensity at a particular spatial location. Thus, the raw image is a downsampled, digital version of the actual volumetric structure of the brain, and voxels can be clustered and their volumes added in order to estimate the volumes of larger structures. Voxels are generally organized into 2-dimensional slices based on the plane of acquisition, but the native 3D "cube" can be viewed from other perspectives, its surface projected onto a 2D space, or transformed into standardized spaces. Details on specific image processing techniques will be discussed in later chapters.

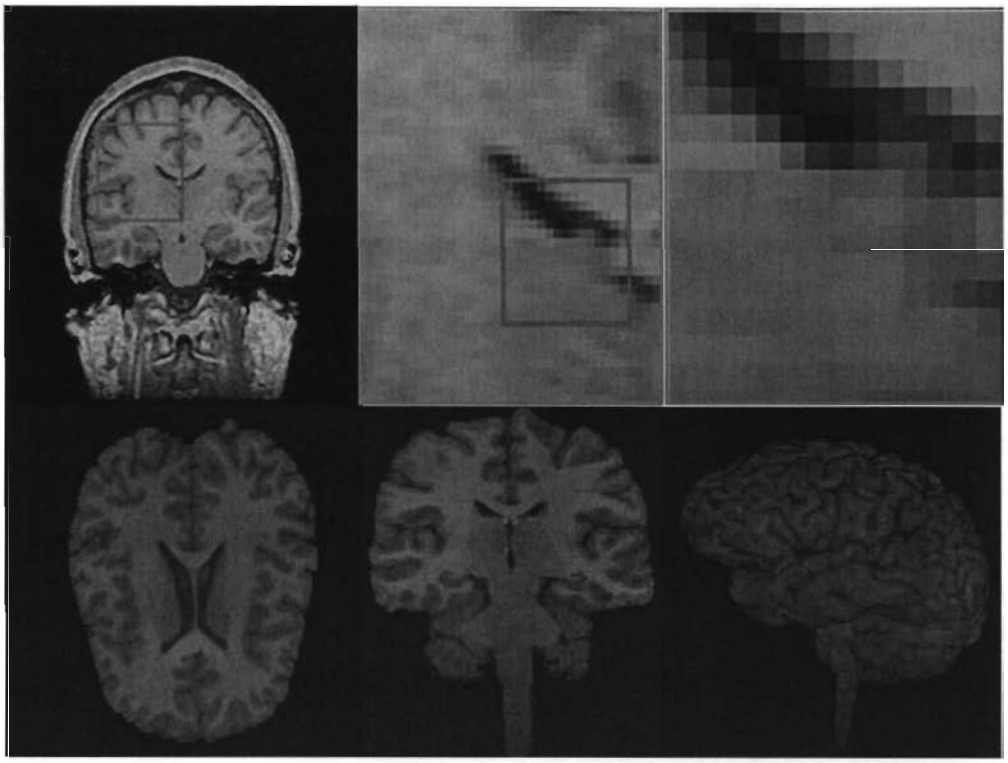

Figure 1.1: Examples of raw data generated with the SPGR pulse sequence. The top row represents the same coronal SPGR at several levels of magnification. At higher levels, the discrete nature of MRI information is apparent. The bottom row represents three representations of the same "skull stripped" image, axial, coronal, and a rendered surface.

Cognitive testing

Several psychometric variables have been assessed in the present dataset, which are summarized in Table 1.1. These tasks range from traditional metrics of general intelligence (IQ cognitive batteries), to tests of spatial working memory (CANTAB), tests of manual dexterity and attention (Trails), and handedness. Considered in total, these tasks represent measures of critical milestones in childhood development, and have direct implications to the pathophysiology of several of the most commonly-acquired psychiatric mental illnesses of childhood, namely autism, attention deficit disorder, and mental retardation.

Table 1.1: Cognitive test batteries employed by the Giedd laboratory. Table courtesy of the Giedd laboratory

Measure	Domains/Purpose	Present Battery	Future Battery	Completed by Parent (P) or Child (C)
WASI/WISC/WPPSI	Intelligence	X		C
CANTAB	Executive Function & Memory	X		C
Trails A & B	Attention, visual search, motor function	X		C
PANESS	Handedness/laterality	X		C
Grooved Pegboard and Hand Dynamometer	Fine motor & laterality	X		C
Verbal Fluency	Verbal organization & output	X		C
Social Responsiveness Scale (SRS)	Autistic Traits	X		P
Social Attribution	Social Cognition		X	C
Morphing Faces Task	Emotion Perception		X	C

The chapters to follow examine the etiology of individual differences in several anatomic measures derived from MRI images, and to a lesser extent, cognitive measures. The focus on the population variance distinguishes this work from more well-established neuroimaging analyses on mean group differences. Or, to borrow from Plomin, DeFries and Fulker, "when we look at children, we see children, not the child" (Plomin, DeFries, & Fulker, 1988). In the next chapter we discuss some of the tools for the analyses of populations, and then follow with a review of extant studies on MRI data that employ them.

2

QUANTITATIVE GENETICS AND STRUCTURAL EQUATION MODELING IN THE AGE OF MODERN NEUROSCIENCE

"The history of science is rich in the example of the usefulness of bringing together two sets of techniques, two sets of ideas, developed in separate contexts for the pursuit of new truth, in touch with each other."

--J. Robert Oppenheimer, *Science and the Common Understanding.*

ADAPTED FROM:

NEALE MC AND SCHMITT JE. QUANTITATIVE GENETICS AND STRUCTURAL EQUATION MODELING IN THE AGE OF MODERN NEUROSCIENCE. IN T. CANNON (ED.). *THE GENETICS OF COGNITIVE NEUROSCIENCE PHENOTYPES.* SOCIETY FOR NEUROSCIENCE CONFERENCE, SHORT COURSE II. (2005).

ABSTRACT

The history of genetics and statistics largely overlap. Before the discovery of molecular genetic tools in the twentieth century, genetics was predominantly an inferential science. The development of appropriate statistical methods was a necessity for identifying heritable traits and to observe the effects of genes within populations. Today, despite technological advances in the basic sciences, the use of inferential statistics remains a powerful tool in elucidating thorny scientific questions, particularly when they involve extremely complex systems with multiple unknown or unmeasurable causal factors. Thus, statistical approaches retain great value when addressing general questions in genetics, psychology, neurobiology, and beyond. This chapter reviews the fundamental principles of behavioral genetics, with particular emphasis on methods central to this thesis.

Partitioning of Variance

The general goal of the classical twin model is to divide the observed variance in a phenotype into genetic and environmental sources (Neale & Cardon, 1992). Since MZ twins are genetically identical, any observed variability between twins of a pair must be due to nongenetic factors (diet, childhood trauma, substance use, measurement error, etc.). Conversely, covariation between MZ twins could be caused by their genetic similarity, or alternatively by characteristics of the environment that both individuals have in common. Using MZ twins alone, it is impossible to disentangle these two possibilities. There are three unknowns (the contributions of genes, shared environment, and unshared environment) and only two statistics (the total phenotypic variance and the MZ correlation):

$$V_P = a^2 + c^2 + e^2$$

$$\text{cov}_{MZ} = a^2 + c^2$$

where a^2, c^2, and e^2 represent the proportion of the total observed phenotypic variance (V_P) due to additive genetic, shared environment, and unshared environmental sources, respectively.

The addition of dizygotic (DZ) twins to the model provides a third statistic that allows one to separate genetic from shared environmental effects. Since DZ twins, as full siblings, share on average half of their genes identical by descent, one would expect that

the genetic correlation driving inter-twin similarity to be half as strong in DZ twins relative to MZ. Therefore:

$$\mathrm{cov}_{DZ} = \frac{1}{2}a^2 + c^2$$

The use of DZ twins, rather than full siblings, provides a better control on potential environmental factors (such as cohort effects) that could be heterogeneous within families. The twin model does assume that the factors influencing the shared environment are, on average, similar for MZ and DZ groups *with respect to the phenotype of interest.* Though often maligned, the Equal Environment Assumption has been shown to hold for most phenotypes examined, with traits such as choice of clothing representing notable exceptions (Evans, Gillespie, & Martin, 2002; Kendler, Heath, Martin, & Eaves, 1986).

In this model, the genetic contribution to phenotype represents cumulative effects of multiple (in theory, infinite) genes, with each gene representing a small effect equal in magnitude to all other effects; thus their effects are additive and normally distributed within the population. Though such an assumption may seem unreasonable, a purely additive model will be well-approximated, even by a handful of genes (Kendler & Kidd, 1986). Additive genetic variance, sometimes called narrow-sense heritability, does not include dominance effects, which also can be estimated with quantitative genetic methodologies (see below). However, an additive model of genetic influence is more likely for complex traits, particularly those with normally distributed phenotypes.

Solving the simultaneous equations 1-3 provides formulae for estimating each variance component. a^2 can be calculated as $2(\text{cov}_{MZ} - \text{cov}_{DZ})$, c^2 as $(2\text{cov}_{DZ}) - \text{cov}_{MZ}$, and e^2 as $V_P - \text{cov}_{MZ}$ or simply $V_P - a^2 - c^2$. These statistics, often called Falconer estimates, can be useful for generating a rough approximation of the sources of phenotypic variance prior to more involved analyses. Falconer estimates can be calculated using Pearson correlations when the phenotypic trait is continuous and normally distributed; in this case the total phenotypic variance is standardized to unity. For dichotomous or ordinal data, tetrachoric or polychoric correlations can be used (PROC FREQ option plcorr in SAS).

As an example, Figure 2.1 represents a scatterplot of caudate nucleus volumes from the Giedd dataset. In general, the scatterplot shows a familial relationship in caudate volume. When the sample is split into MZ (blue) and DZ (red), there is a marked difference in the strength of the relationship based on zygosity, with Pearson correlations of 0.83 for MZ and 0.40 for DZ pairs. Using Falconer estimation, the vast majority of the variability in caudate volume (86%) appears to be generated by additive genetic factors.

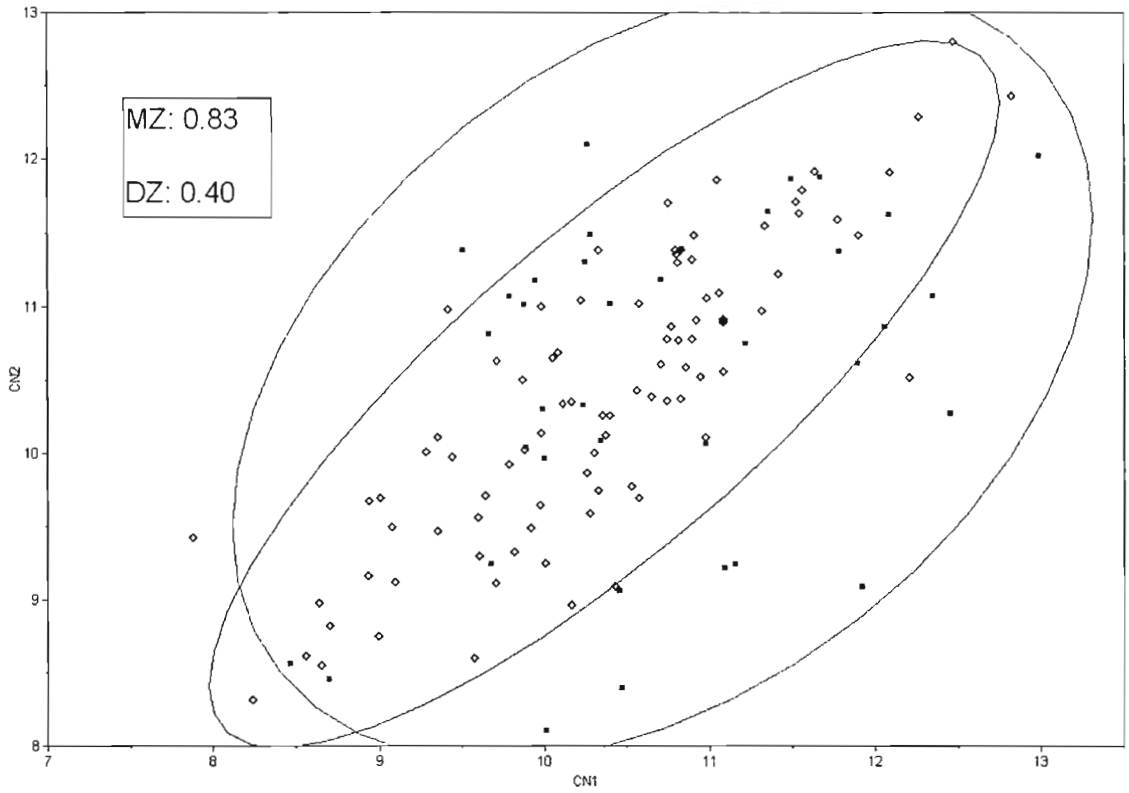

Figure 2.1: Scatterplot of caudate nucleus volumes for MZ (blue) and DZ (red) groups, 95% density ellipses are given for each group separately, and the corresponding Pearson correlation coefficients are given in the inset.

Although useful as a 'rule of thumb', there are at least eight problems with these algorithms for estimating components of variance. One, it is possible to obtain nonsensical estimates of the heritability, both greater than 1.0 and less than zero. Two, it takes no account of the relative precision of the cov_{MZ} and cov_{DZ} statistics, which may be unequal if the sample sizes differ or if the magnitude of the correlation is different, or (as is usually the case) both. Three, there is no assessment of whether the correlations are consistent with the additive genetic model. Four, it does not easily generalize to the multivariate case to permit the examination of why variables correlate with each other. Five, it is not easy to correct estimates for the effects of covariates such as age and sex.

Six, it does not generalize to extended twin studies that involve other relatives. Seven, it is inefficient when there are missing data and eight, it is not suitable for selected samples of twins.

Structural Equation Modeling and Path Analysis

Modern methods overcome these limitations by using more sophisticated computer software algorithms. Structural equation modeling (SEM) and its mathematically-equivalent visual analog, path analysis, represent techniques to model causal and correlational influences on both observed and unobserved (i.e. latent) traits. Most commonly used inferential statistics, such as regression, analysis of variance, correlation, and factor analysis are actually subset families of structural equation models. It can be considered a general framework for statistical analysis that is flexible enough to address specific hypotheses while simultaneously applying principles that are both mathematically elegant and easy to understand. Thus, an initial investment in learning SEM can pay off immensely, as it has broad applicability within many branches of science. SEM is typically used to generate a hypothesis-driven model of a process of interest, but more exploratory analyses also are possible. Though not developed until the mid-twentieth century, SEM has quickly pervaded the social sciences owed to its explicit treatment of measurement error and latent variables.

Path analysis was invented by the great geneticist Sewell Wright and employs symbolic diagrams in order to explicitly describe inter-variable relationships (Loehlin, 1998). By

convention, measured variables are denoted by rectangles while latent variables are shown as circles. Though latent variables are not directly observed, their presence can be detected via their influences on variables that are measured. In addition to observed and latent variables, triangles are often used to denote constants, which can be useful for specifying means, while diamonds represent variables that moderate the strength of the influence of one variable on another.

Two fundamental types of relationships between variables are defined; causal and correlational. While causal relationships are shown by single-headed arrows from causal variables to affected variables, double-headed arrows are used to show correlations. A special type of correlation, that of a variable with itself (i.e. variance) is shown as a double-headed arrow emanating from and returning to the same variable. For example, a simple regression model can be depicted as in Figure 2.2. The path coefficient 'a' quantifies the strength of the causal relationship; for every unit increase in the upstream variable, the downstream variable increases 'a' units. Thus, the path coefficient in this model is simply β, the regression coefficient. If a second causal variable were added, then each path would represent a partial regression coefficient of a multiple regression model; the change in the dependent variable with unit change in one independent variable when the other is held constant.

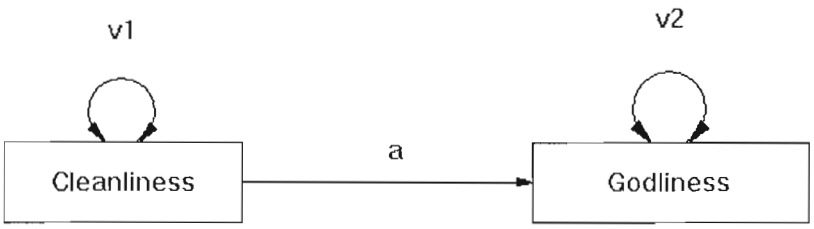

Figure 2.2: Simple linear regression path diagram

Though SEM can solve simple regression models, it is more typically used to investigate the sources of correlations between observed variables due to latent constructs. Consider the model in Figure 2.3, which presents a hypothesized causal structure for observed variables 1-4. The expected covariance between any two observed variables is easily calculated using "Wright's rules" that summarize which paths are allowed:

1) Covariance is calculated as the sum of all possible paths between two variables, where each path represents the product of all path coefficients in the chain.
2) After moving forward along a single-headed arrow, moving backward is illegal
3) A path can contain at most one double-headed arrow
4) Each variable can be crossed only once per path
5) Whenever changing direction (from upstream to downstream) multiply the path by the variance of the upstream variable
6) No loops

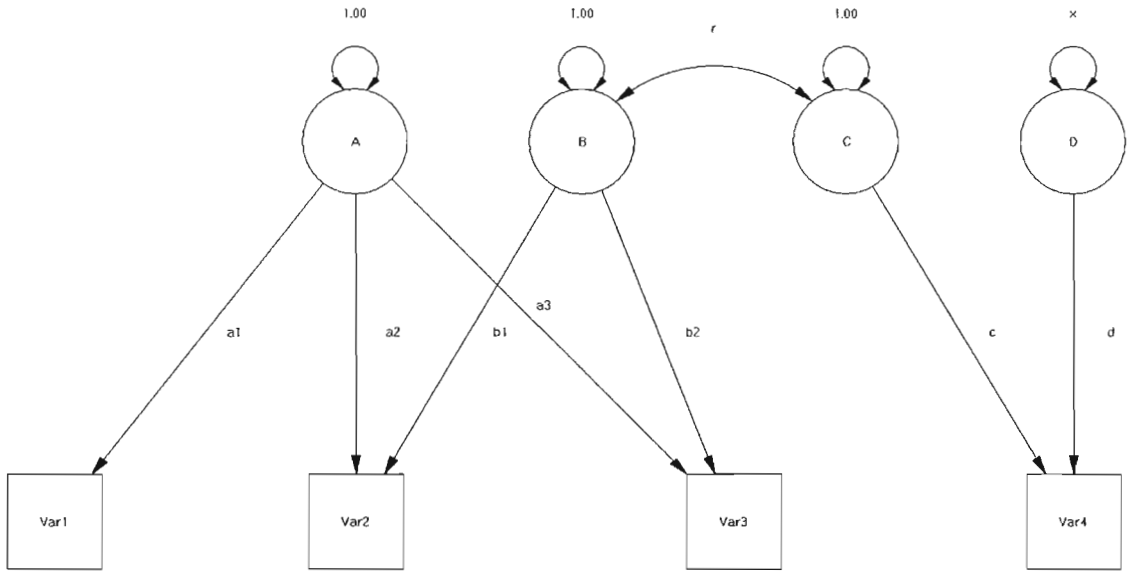

Figure 2.3: Sample path diagram modeling the covariance between observed variables via a hypothesized structure of latent variables

Using these rules, the expected variance-covariance matrix for Figure 2.3 is given in Table 2.1. The path diagram represents a *mathematically complete* representation of the hypothesized inter-variable relationships, and translates directly into matrix algebra. This point is extremely important to keep in mind. For example, variables 1-3 have no explicit variable-specific causal factors; thus the model creates the expectation that *all* of their variance is covariance (i.e. no residual variance). Though some path diagram come with the caveat that "residual paths are not given but assumed," such a practice can be dangerous, as can *implicitly* defining the variance of latent variables equal to unity. This is particularly true when performing computerized analysis, as computers have no capacity for understanding these subtleties.

Table 2.1: Expected variance-covariance matrix for the path diagram in Figure 2.3

	Var1	Var2	Var3	Var4
Var1	a_1^2	$a_1 a_2$	$a_1 a_3$	0
Var2	$a_1 a_2$	$a_2^2 + b_1^2$	$a_2 a_3 + b_1 b_2$	$b_1 rc$
Var3	$a_1 a_3$	$a_2 a_3 + b_1 b_2$	$a_3^2 + b_2^2$	$b_2 rc$
Var4	0	$b_1 rc$	$b_2 rc$	$c^2 + xd^2$

Optimization

Nearly all SEM analyses are solved empirically, using numeric optimization of a likelihood function to produce parameter values that provide the best fit to the data (Neale, Boker, Xie, & Maes, 2002). The general strategy of optimization begins with more or less arbitrary start values for all model parameters, calculation of an initial fit, and then systematic parameter modification and recalculation of model fit in an iterative fashion. There are several flavors of fit metrics (many are variants of least squares algorithms), but maximum likelihood (ML) methods are by far the most frequently used in behavioral genetic studies due to numerous appealing statistical properties. Most pertinent to the present discussion are 1) applicability to a broad range of statistical problems, 2) precise and unbiased parameter estimates with large sample sizes, 3) approximately normal distributions of parameter estimates, 4) robust and maximally informative in situations of missing data or ascertainment biases, and 5) straightforward hypothesis testing in many instances (Edwards, 1972). The primary disadvantage to ML is that it is computationally expensive, though this is becoming less important as processor speeds increase.

There are numerous SEM software packages available, though only a handful (e.g. LISREL, Amos, EQS, Mx) have the capability to perform multiple group analyses, which greatly facilitates twin studies. Of these, only Mx is available for free online (available at http://www.vcu.edu/mx), and two template script libraries have been constructed (http://www.psy.vu.nl/mxbib/ and http://www.vcu.edu/mx/examples.html), which include many of the most commonly used twin designs.

The calculation of likelihood (L) varies based on the type of data available. When model fitting to covariance matrices, the goodness-of-fit function for each group is

$$ML_g = N_g\{(\ln|\Sigma_g| - \ln|S_g| + trS_g\Sigma_g^{-1}) - 2m\}$$

where N_g is the sample size minus one for group g; $\mathbf{S_g}$ is the observed covariance matrix and Σ_g is the covariance matrix predicted by the model for the trial values of the twin covariance matrix. *m* is the number of phenotypes measured on each twin; $|\Sigma|$ and Σ^{-1} denote the determinant and inverse of the matrix Σ, respectively.

Mx also has the capability to fit to raw data, though the calculation of likelihood differs depending on whether the data is continuous or ordinal. Both methods are based in normal theory. For continuous data, if there are *m* observed variables on each twin, the normal probability density function of a column vector of twins observed scores x_i is given by:

$$L = \left|2\pi\Sigma\right|^{-2m/2} \exp\left[-\frac{1}{2}(x_i - u_i)'\Sigma^{-1}(x_i - u_i)\right]$$

where Σ is the predicted covariance matrix and u_i is the (column) vector of predicted means of the variables (Neale, 32767). This represents the likelihood of observing record *i*, given the population mean and variance and assuming normality. The joint likelihood of the N independent pairs in the sample is computed as the product of the likelihoods of all pairs.

In order to calculate likelihood for ordinal data, a liability threshold model is used (Falconer, 1965). This model assumes that ordinal scores are the result of an underlying, normally distributed liability. An individual's ordinal responses are based on whether they are above or below particular thresholds. It follows that the likelihood for an observed vector of ordinal responses will be the integral of a multivariate normal probably density function, with limits corresponding to liability thresholds. For example, a diagnosis of lung cancer would occur in individuals with high liability due to heterogeneous sources (smoking, occupation, heredity, etc.) which places them above threshold for the development of disease. For a vector of observed ordinal responses, the likelihood of observing a twin pair concordant for lung cancer would be:

$$L = \int_{t_1}^{\infty}\int_{t_2}^{\infty}\phi(x), dx$$

where ϕ is the (standardized) multivariate normal probability function (5), and t_1 and t_2 represent liability thresholds for twin 1 and twin 2, respectively. In practice, -2*ln(L) is computed rather than L, both for pragmatic reasons as well as for the favorable statistical behavior described below.

A particularly useful property of using ML is the ability to easily test the importance of subcomponents of a given model using a traditional χ^2 hypothesis test. This is because the difference in -2*ln(ML) between a model and a simplified submodel (by removing one or more parameters, for example) will, in most cases, asymptotically follow a χ^2 distribution with degrees of freedom equal to the difference in the number of parameters between models. If the models are structurally unrelated (one model is not a simplification of the other), however, then an alternative comparison statistic is required. Two of the most popular are Akaike's Information Criterion (AIC) and the Bayesian Information Criteria (BIC) which reward parsimony in models according to Occam's Razor (Akaike, 1987; Spiegelhalter, Best, Carlin, & van der Linde, 2002). Like the χ^2 test, these statistics are based on the ML.

SEM and twins

Path diagrams can be constructed for the classical twin study (Figure 2.4). Three latent variables are defined, A, C, and E, representing additive genetic, shared environmental, and unique environmental dimensions, respectively (Evans et al., 2002; Neale et al.,

1992). It should be apparent that the expected variance and covariance for both MZ and DZ twins is the same in this model as before. However, the SEM framework provides all of the favorable properties described previously, and will provide more accurate parameter estimates. Additionally, parameters a and/or c can be removed from the model to generate submodels that can be tested via χ^2.

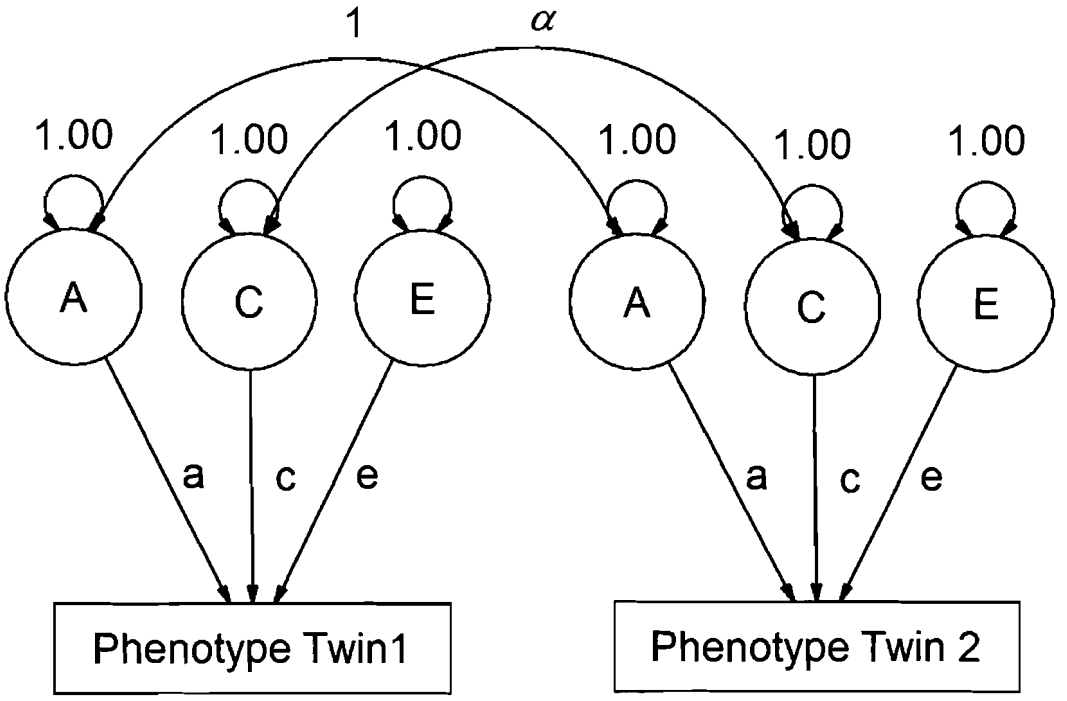

Figure 2.4: The ACE twin model

For example, the data from the caudate nucleus volume example can be reanalyzed in Mx. ML parameter estimation gives estimates of 0.87, 0.00, and 0.42 for path coefficients a, c, and e, respectively. The variance in phenotype due to A, C, and E is simply the square of the path coefficients (since latent variances are standardized to unity), giving values of 0.76, 0.00, and 0.18. To determine the *proportional* variance, each variance

component is divided by the total phenotypic variance (.94) for estimates of a^2 =.81, c^2 =.00, and e^2 =.19. Removing the path 'a' produces a statistically significant worsening in the likelihood (χ_1^2 = 29.53, p <.0001), while removing 'c' has no effect (χ_1^2 = 0, p=.9999). Thus, there are is substantial evidence of genetic effects on the population variability in caudate nucleus volumes, but no evidence for shared environmental effects.

SEM also can theoretically be used to test for dominance or epistatic effects. Like other latent factors, the contributions of dominant genes to phenotypic variance will have predictable effects on MZ and DZ covariance, since the probability of twins inheriting *both* alleles at a loci identical by descent is unity in MZ and only one-quarter in DZ. However, dominance effects are confounded with the shared environment in a classical twin design and cannot be estimated simultaneously. One solution is to compare the ACE and ADE model via goodness of fit statistics. In a twins-only design, however, the power to detect dominance effects can be quite weak (in part because dominance effects are typically small for complex traits). An extended twin design can increase power.

Extensions to Classical Univariate Twin Models

The flexibility of path analysis allows for numerous extensions of twin models. Perhaps the simplest is to regress out potentially confounding factors from an otherwise straightforward analysis. In the caudate example above, sex was unbalanced between MZ and DZ; with a few changes to the Mx script, the effects of sex on mean brain volumes could be taken into consideration. If influences on mean effects are more then a nuisance,

it may be useful to test these factors importance to the model fit via a likelihood ratio χ^2. For example changes in mean brain volumes with age would naturally be of interest in a pediatric or geriatric sample. Though one could achieve similar results by first performing a multiple regression and then using the residuals in a subsequent variance components analysis, adding regression to the SEM model itself has the advantage of estimating all parameters simultaneously, which allows more freedom to determine the best fit to the data.

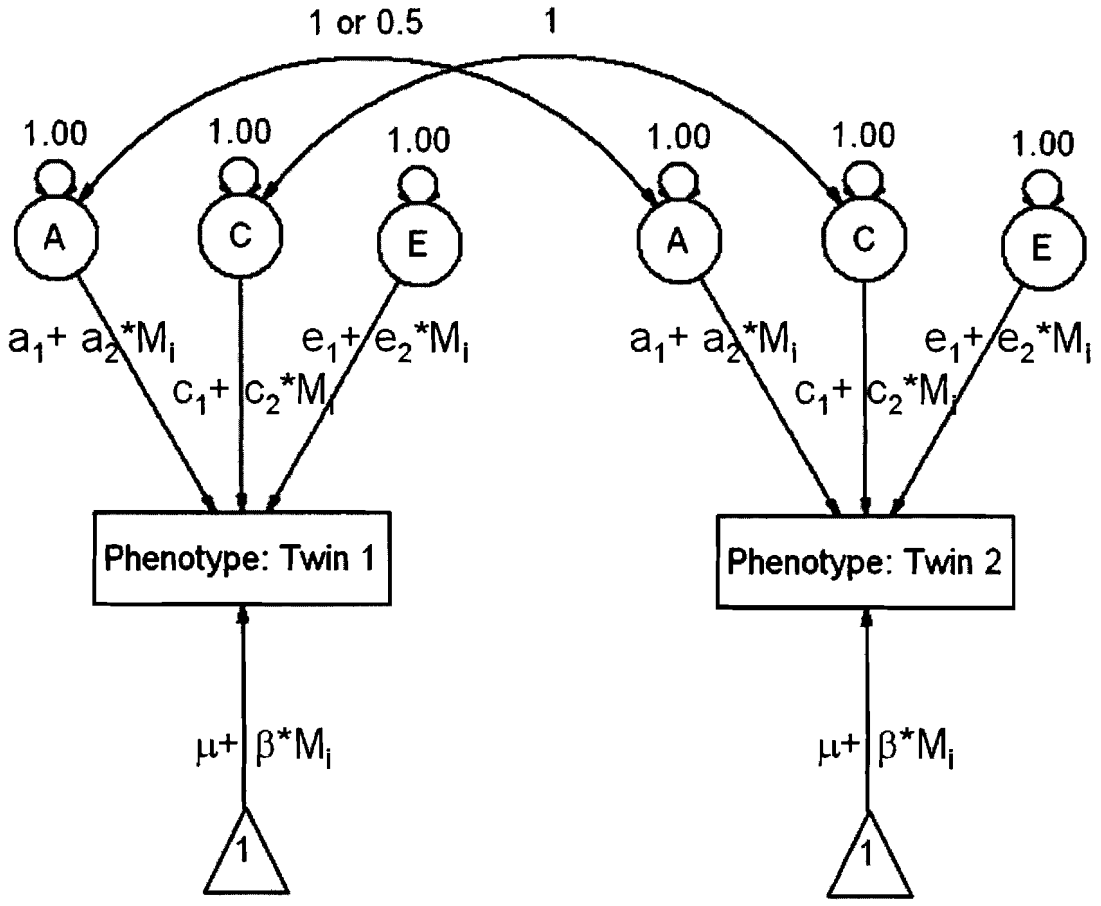

Figure 2.5: The ACE model expanded to allow for interaction effects of moderator *M*. This model also includes a means regression (below phenotype variables) that allows for a linear effect of the moderator on the group mean.

Twin data also can be used to identify gene by environment (g x e) interactions. There are many methods attempting to do so; the most elegant analysis was probably designed by Jinks and Fulker, in which a correlation between MZ twin phenotypic differences and phenotypic sums is indicative of interaction (Jinks & Fulker, 1970). This method is limited because C x E interactions also may produce statistically significant correlations (Evans et al., 2002). A novel approach using extensions of the ACE model is rapidly gaining popularity (Purcell, 2002). The principle is similar to regression, but rather than modulating the mean phenotypic value, the moderator variable adjusts the magnitude of the influence of the latent variables A, C, and E on phenotype (Figure 2.5). Thus, in the interaction model, the influence of the latent variable A on phenotype for individual *i* and moderator variable M is $a_1 + a_2 * M_i$ rather than simply a_1. Since the effects of these latent variables are inferred through phenotypic variance and cross-twin covariance, the result of the expanded g x e model is to allow for changes in variance (i.e. heteroscedasticity) and covariance of phenotype along the dimension of the moderating environmental trait. The twin design allows for the determination of which variance component(s) are responsible for the interaction.

Multivariate Analyses

Though multivariate twin analysis can be substantially more complex than what has been described thus far, the same principles of path modeling are used (Neale et al., 1992). Multivariate models with SEM are often simple extensions of the ACE model. The

classical twin model itself is of course technically multivariate, which is the source of its ability to parse variance. The next conceptual extension would be to run multiple "univariate" twin models for separate variables of interest in parallel; this model would be useful, for instance, if one wanted to test whether additive genetic variance is equal for different phenotypes (Figure 2.6A). A "univariate in parallel" model assumes no covariance between different variables, however. In a true multivariate design, we also obtain information about cross-twin, cross-trait correlations that allows for the determination of which underlying factors cause phenotypes to covary. Multivariate modeling also increases the precision of parameter estimates, since far more statistics are generated. These properties are useful for assessing the underlying causes of cormorbidity, or for modeling changes in phenotypes over time with longitudinal designs.

There are three commonly used multivariate factor models in behavioral genetics analysis, the Cholesky decomposition, the independent pathways (i.e. biometric) model and the common pathways (i.e. psychometric) model; path diagrams for each are given in Figure 2.6. The most parameterized is the Cholesky decomposition (Figure 2.6B), which deconstructs any *n x n* positive definite variance-covariance matrix into an *n x n* triangular matrix, postmultiplied by its transpose, and places few *a priori* constraints on the fitting of the data (Evans et al., 2002; Neale et al., 1992). Cholesky models are typically used for bivariate analyses, as a null model with which to compare more restrictive models, or to calculate unbiased genetic correlations.

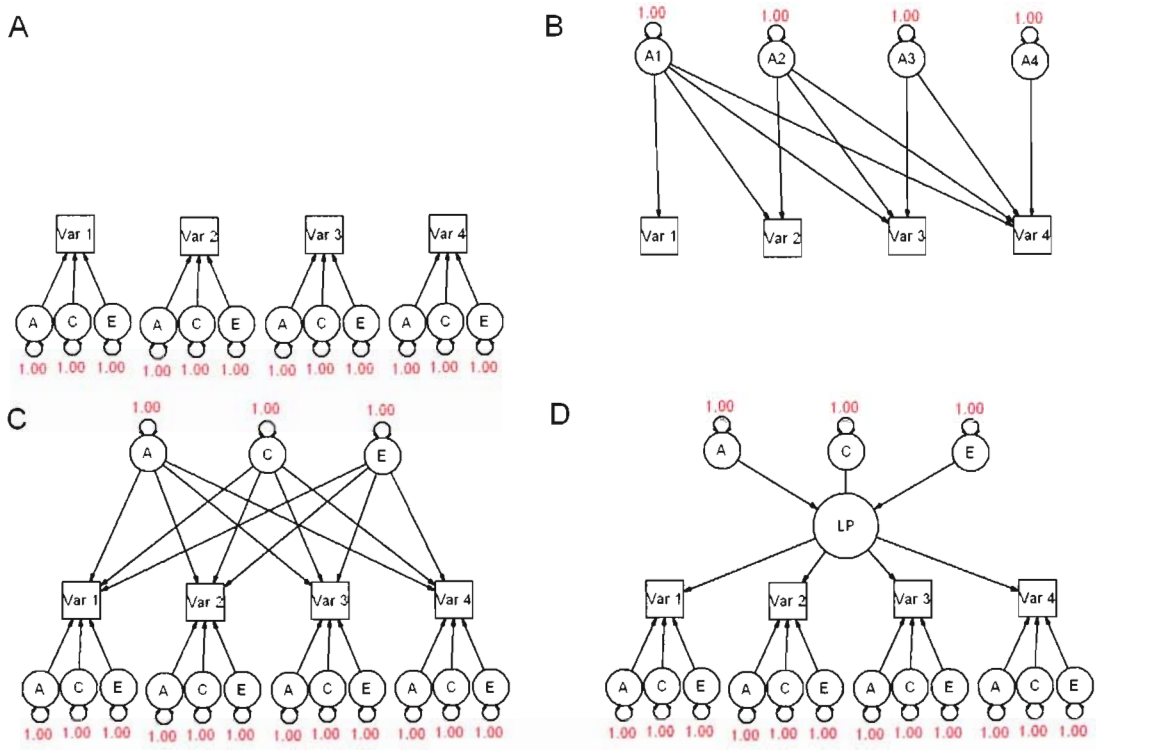

Figure 2.6: Examples of extensions into multivariate analyses. For simplicity, only one member of a twin family is shown in each model. (A) Univariate analyses run in parallel with four observed variables. There is no (modeled) covariance between phenotypes. (B) Cholesky decomposition, with only genetic factors shown. The triple Cholesky would include a series of C and E factors with the same pattern as A. (C) Independent pathways model. (D) Common pathways model; the influences of A, C, and E are mediated through a common, latent phenotype (LP).

Independent pathways models (IPM) allow genetic, shared environmental, and unique environmental common factors to affect observed variables directly, while in common pathways models (CPM) these factors exert their influence through a shared, latent phenotype (Figure 2.6C and D). In both models, each observed variable is permitted a residual variance term, which can also be parsed into A, C, and E. While IPMs are conceptually simpler, CPMs, require fewer parameters and thus are favored by the rules of parsimony. Both CPMs and IPMs are nested submodels of the Cholesky decomposition, and for a given number of common factors, the CPM is nested within IPM. Depending on the number of observed variables, both of these classes of models

can be expanded to allow for multiple genetic, shared environmental, or unique environmental common factors.

Conclusion

Quantitative genetics methodology has broad applicability to many biological questions. Twin and family designs can be useful for understanding complex, polygenic traits and to understand the sources of covariance between phenotypes. This overview gives only a taste of the potential of variance components analyses and SEM; numerous other extensions are possible such as applications in molecular genetics, longitudinal study designs, inclusion of extended families, research into comorbidity, and psychometric modeling, such as latent class and latent trait analysis (Boomsma, Busjahn, & Peltonen, 2002; Takane & de Leeuw, 1987). In the future, research into brain and behavior promises to become increasingly complex and interdisciplinary; the development of powerful mathematical tools will provide the means to cope with the inevitable flood of heterogeneous information that modern instruments will provide.

3

REVIEW OF TWIN AND FAMILY STUDIES ON NEUROANATOMIC PHENOTYPES

"More attention to the History of Science is needed, as much by scientists as by historians, and especially by biologists, and this should mean a deliberate attempt to understand the thoughts of the great masters of the past, to see in what circumstances or intellectual milieu their ideas were formed, where they took the wrong turning or stopped short on the right track."

--Ronald A. Fisher, "Natural selection from the genetical standpoint." *Australian Journal of Science* 22, 16-17, 1959.

ADAPTED FROM:

SCHMITT JE, EYLER LT, GIEDD JN, KREMEN WS, KENDLER KS, AND NEALE MC. REVIEW OF TWIN AND FAMILY STUDIES ON NEUROANATOMIC PHENOTYPES AND TYPICAL NEURODEVELOPMENT. *TWIN RESEARCH AND HUMAN GENETICS*. SUBMITTED.

ABSTRACT

Investigations into the biology of typical neurodevelopment have greatly advanced the understanding of childhood psychiatric diseases. Yet despite extraordinary efforts to identify the molecular genetic factors influencing variability in human neuroanatomic volumes, this approach, thus far, has had limited success. Well-established behavioral genetic methodologies provide a means for investigating relationships between brain and behavior from a global perspective. Behavioral genetics, however, has only just begun to address neuroanatomical questions and to explore the associations between volumetric data and behavioral measures. Knowledge of heritability of brain endophenotypes in children is particularly limited. This chapter reviews the extant studies that report on the relative contributions of genetic and environmental influences on brain volumes via magnetic resonance imaging.

Careful studies of familial relationships have generated a wealth of information on the latent causes of individual differences. This is especially true for complex traits, in which specific underlying causes (such as a single gene or specific environmental factor) play relatively minor roles in creating variability within populations. Behavioral traits, including both psychological and psychiatric variables, are particularly well-informed by such an approach, as their origins promise to be quite complex in most respects. Numerous familial studies, particularly those using twin designs, have provided strong evidence that a multitude of human behavioral traits are strongly influenced by our genetic makeup (Boomsma, Busjahn, & Peltonen, 2002; Strachan & Reed, 2004; Sullivan & Kendler, 1999). Yet despite extensive research on behavioral phenotypes, familial studies into neurobiological characteristics have been substantially more limited.

Direct investigations into *human* neurobiology are particularly valuable, however, due to the lack of an ideal animal model to address questions on brain and behavior. As noted previously, MRI has numerous advantages relative to other imaging modalities, particularly in typical populations (Bushberg et al., 1994). MRI also allows for several options in image processing that enable both volumetric and morphometric analyses at multiple levels of resolution. The use of these novel imaging methodologies within a twin design allows for several important questions to be addressed, including 1) How genes and environment contribute to individual differences in human neuroanatomy, 2) How these effects change with age, and most importantly 3) how biological intermediates link genetic signals with behavior and cognition. In addition to theoretical interest, twin

designs using MRI could help to disentangle the complex interplay of genetic and nongenetic factors in the generation of neurobiological variability; as a novel endophenotype, MRI measures could increase the power to detect quantitative trait loci (QTLs) influencing critical behavioral functions and liability to psychopathology (Gottesman & Gould, 2003).

Heritability of volumetric phenotypes

To date, there have been approximately thirty twin studies on typical neurodevelopment using MRI. These studies employ a diversity of volumetric and morphometric techniques (Table 3.1). The analysis of control families from twin studies on pathological conditions provides some additional information, albeit limited, on MRI-derived phenotypes. Considered together, these studies have demonstrated a strong, statistically significant role of genes in the generation of the high variability in human brain volumes, particularly for larger structures (Baare et al., 2001a; Pennington et al., 2000; Pfefferbaum, Sullivan, Swan, & Carmelli, 2000). For example, Barré et al. reported that the genome was responsible for .90, .82, and .88 of the total variance in total brain, gray, and white matter volumes, respectively, in 112 adult twin pairs (Baare et al., 2001a). Figure 3.1 provides a between-study comparison of heritability estimates for these large structures.

Table 3.1: Comparison of qualitative study design characteristics for all existing twin studies using MRI in typically developing populations. "Substructures measured" is an indication of whether parcellation data for ROIs are reported for structures other than total brain, intracranial volume, or hemispheric volumes. A 'Y' for brain and behavior is indicative that the study not only measured psychometric and imaging variables, but also attempted to describe brain-behavioral relationships. In contrast, the 'Multivariate Analyses' column identifies studies that model relationships between neuroanatomic variables.

Study	Pediatric Population?	Substructures Measured?	Morphological Measures?	Voxel-level Measures?	Brain and Behavior?	Multivariate Analyses?	SEM-based Statistics?	Longitudinal Design?
Reveley, 1984	N	Y[2]	N	N	N	N	Y	N
Oppenheim, 1989	N	Y[2]	Y[2]	N	N	N	N	N
Steinmetz, 1994	N	N	Y	N	N	N	N	N
Steinmetz, 1995	N	Y	N	N	Y[7]	N	N	N
Bartley, 1997	N	Y	Y	N	N	N	Y	N
Biondi, 1998	N	Y	Y	N	N	N	N	N
Bonan, 1998	N	Y	Y	N	N	N	N	N
Carmelli 1998	N	N	N	N	N	N	Y	N
Haidekker, 1998	N	N	Y	N	N	N	N	N
Tramo, 1998	N	Y	N	N	Y	N	N	N
Carmelli, 1999	N	N	N	N	Y	N	N	N
Lohman, 1999	N	N	Y	N	N	N[6]	N	N
Le Goualher, 2000	N	N	Y	N	N	N	N	N
Pennington, 2000	Y[1]	Y	N	N	Y	Y	N	N
Pffefferbaum, 2000	N	Y[2]	N	N	N	Y[3]	Y	N
Posthuma 2000	N	N	N	N	N	Y	Y	N
Barre, 2001	N	N	N	N	N	Y	Y	N
Pfefferbaum, 2001	N	Y[2]	N	N	N	N	Y	N
Sullivan, 2001	N	Y	N	N	N	N	Y	N
Thompson, 2001	N	N	N	Y	Y	N	N	N
Carmelli 2002a	N	Y	N	N	Y	N	Y	N
Carmelli 2002b	N	N[5]	N	N	Y	N	Y	N
Eckert, 2002	Y	Y	N	N	N	N	N	N
Geschwind, 2002	N	Y	N	N	Y[7]	N	Y	N
Hulshoff Pol, 2002	N	Y[2]	N	N	N	N	Y	N
Posthuma 2002	N	N	N	N	Y	Y	Y	N
Reed, 2002	N	Y[2]	N	N	N	N	N	N
White, 2002	N	Y	N	N	N	N	N	N
Wright, 2002	N	Y	N	N	N	Y[3*]	Y[3*]	N
Scamvougeras, 2003	N	Y[2]	N	N	N	N	N	N
Styner, 2003	N	Y	Y	N	N	N	N	N
Mohr, 2004	N	N	Y	N	N	N	N	N
Pfefferbaum, 2004	N	Y[2]	Y[2]	N	N	Y	Y	Y[4]
Hulshoff Pol, 2006	N	N	N	Y	Y	N	Y	N
Giedd Project	Y	Y	?	Y	Y	Y	Y	Y

[1] Greater than 70% of the twin sample had dyslexia
[2] Only midsagittal structures (lateral ventricles and/or corpus callosum) were measured
[3] Bivariate, or bivariate with post-hoc principle component analysis ([3*])
[4] Two timepoints
[5] White matter hyperintensities were the only neuroanatomic variable reported
[6] PCA used, but to assess global, rather than structure-specific, eigenvalues
[7] Handedness only

Figure 3.1: Summary of heritability estimates for large neuroanatomic structures. Studies are listed in parenthesis if heritability is calculated via Falconer estimation. Pediatric studies are denoted with an asterisk. ICV-intracranial volume, Brain-total brain, LH-left hemisphere, RH-right hemisphere, GM-total gray matter, WM-total white matter.

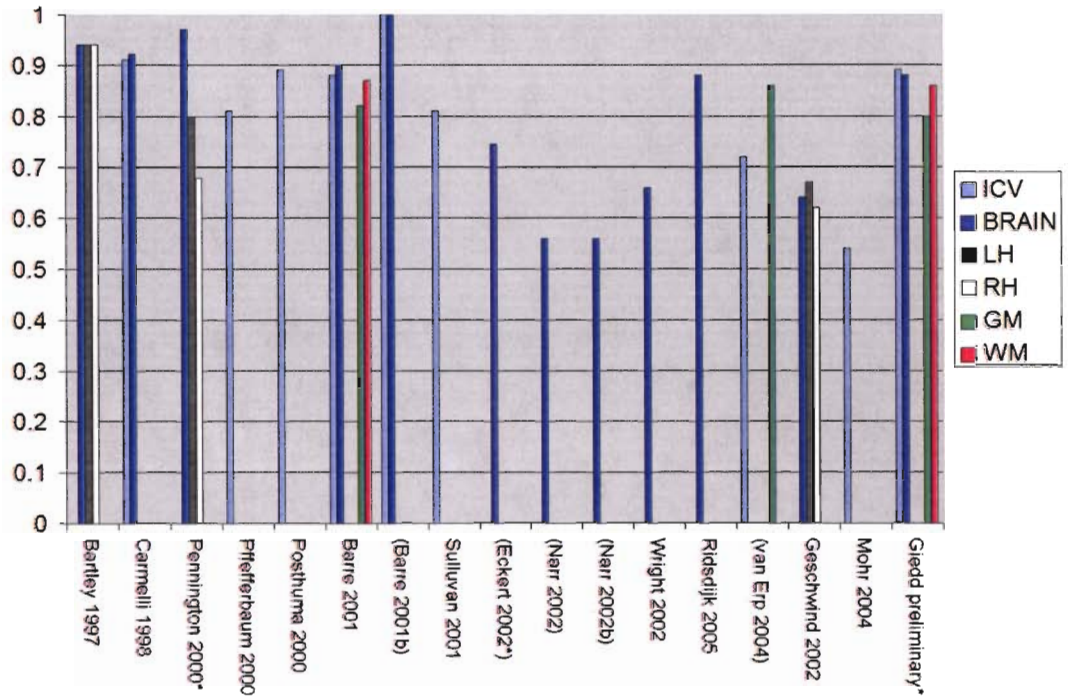

Variance components analyses estimates of neuroanatomic substructures are substantially less frequent than global volumetric measures. It is common that only one or two estimates of heritability have been reported for a given region of interest. For example, there are only two published twin studies that report findings for cerebral lobar tissue (Carmelli, Swan, DeCarli, & Reed, 2002b; Geschwind, Miller, DeCarli, & Carmelli, 2002); both suggest that genes play the predominant role at this level of resolution. Similarly, there are only two extant studies to parse cerebellar variance into genetic and nongenetic components (Posthuma et al., 2000b; Wright, Sham, Murray, Weinberger, & Bullmore, 2002). Though large volumetric measures consistently show high heritabilities, the contribution of the genome to observed individual differences of smaller structures is

more variable. Of these, the lateral ventricles, corpus callosum, and the hippocampus are by far the most well-studied. There is extremely strong evidence that the variance in the area of the corpus callosum is dominated by genetic factors (Oppenheim, Skerry, Tramo, & Gazzaniga, 1989; Pfefferbaum et al., 2000; Scamvougeras, Kigar, Jones, Weinberger, & Witelson, 2003; Sullivan, Pfefferbaum, Swan, & Carmelli, 2001). In contrast, heritability estimates for both the hippocampus (Baare et al., 2001b; Narr et al., 2002; Rijsdijk et al., 2005; Sullivan et al., 2001; van Erp et al., 2004; Van Haren et al., 2004; Wright et al., 2002) and lateral ventricles (Baare et al., 2001a; Baare et al., 2001b; Pfefferbaum et al., 2000; Reveley, Reveley, Chitkara, & Clifford, 1984; Reveley, Reveley, Clifford, & Murray, 1982; Rijsdijk et al., 2005; Wright et al., 2002) are generally lower, but with a great deal of variability from study to study.

Other neuroanatomic structures have been measured extremely rarely in full twin designs, if at all. A few studies on MZ pairs have shown high intertwin correlations for non cerebral structures. For example, White et all reports correlations of .84 for caudate, .75 for putamen, and .75 for thalamic volumes in twelve MZ pairs (White, Andreasen, & Nopoulos, 2002). For most regions of interest, however, the information regarding variance components comes solely from a small study by Wright et al. on 10 MZ and 10 DZ twin pairs, which included measures from individual cerebral gyri (roughly based on Broadmann's areas) as well as subcortical gray, thalamus, cerebellum, and brain stem: 92 parcellated regions (all grey matter) in total (Wright et al., 2002). While numerous regions had statistically significant familial influences, due to low power only the precentral gyrus had statistically significant effects due to genes specifically. Regions

with heritability estimates greater than .50 included the superior parietal lobe, posterior cingulate gyrus, corpus striatum, putamen, and cerebellum. Though this study suffers from low power and multiple testing issues, it is currently the *de facto* source for estimates of the magnitude of genetic influences in typical populations for nearly all substructures in the brain.

With the exception of the lateral ventricles, there is little evidence that the shared environment plays a role in generating neuroanatomic (either morphological or volumetric) variability, although this may be obscured by non-additive effects of genes.

High Resolution Image Analyses

To date, there have been only two published twin studies that examine neuroanatomic structure at high resolution. In a landmark paper, Thompson et al. examined gray matter density in 10 MZ and 10 DZ adult twin pairs and found that genetic factors strongly influenced language and executive processing centers and had weak but significant associations with intelligence (Thompson, Cannon, & Toga, 2002). Probability maps suggested particularly strong genetic effects in middle frontal regions, and an asymmetry in Wernicke's region with the left side highly significant but not the right (Figure 3.2A). More recently, Holshoff Pol et al. examined both gray and white matter density in a substantially larger sample of 258 individuals. Their analysis found several highly significant gray matter foci, including in the superior and middle frontal lobe, Heschl's gyrus, cingulate cortex, and portions of the occipital lobe. Additionally they discovered significant white matter tracts including the superior occipitofrontal fascicle, corpus

callosum, and corticospinal tracts (Figure 3.2B). Some significant genetic correlations between brain and behavior also were observed, including between the right medial frontal gyrus and PIQ and VIQ, and PIQ with the right parahippocampal gyrus.

Figure 3.2: Results from extant studies twin studies on voxel-level data. Panel A is a probability map from Thompson et al. demonstrating regions of significant heritability for gray matter density. Panel B displays findings from an analysis of white matter density by Hulshoff Pol et al. in a glass brain, with significantly heritable regions in orange and reference structures (ventricular system in blue, occipitofrontal fascicle in green).

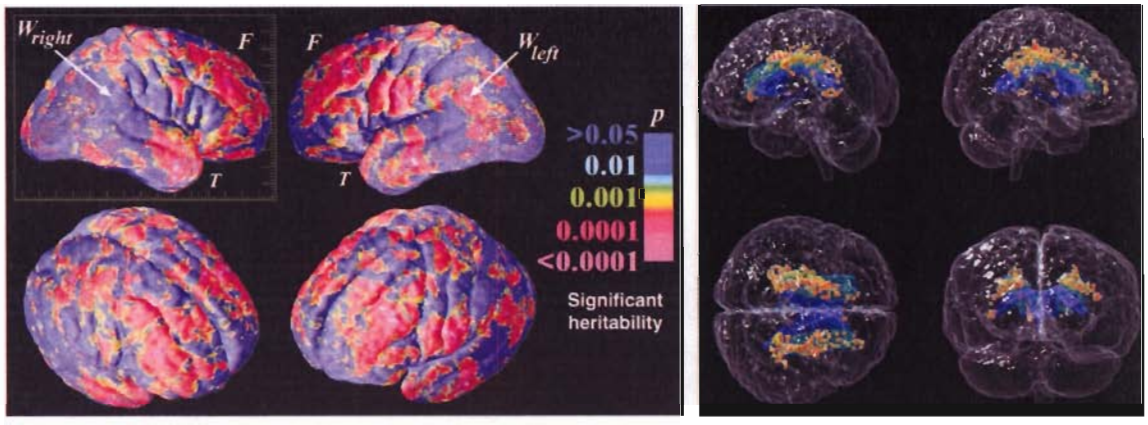

A B

Morphometric measures

The role of the genome on morphological differences appears to be significant, but more modest than its influence on volume. Though less well studied, twin findings on shape differences have been more consistent (Bartley, Jones, & Weinberger, 1997; Biondi et al., 1998; Bonan et al., 1998; Eckert et al., 2002; Haidekker et al., 1998; Lohmann, von Cramon, & Steinmetz, 1999; Mohr, Weisbrod, Schellinger, & Knauth, 2004; Steinmetz, Herzog, Huang, & Hacklander, 1994; White et al., 2002). In general, brain morphology appears to be significantly heritable, but to a lesser extent than volume. For example,

blinded raters are able to successfully match surface renderings of MZ pairs, even though there can be striking qualitative differences (Biondi et al., 1998), which suggests some familial influences but also a role of the unique environment in the development of gyral patterns. More quantitative measures have produced similar findings. A study by Bartley et al. found low heritability for gyral patterning despite high heritability estimates for volumes in 10 MZ and 9 DZ pairs (Bartley et al., 1997). Similarly, a study by White et al. on 24 MZ twin pairs reported that intertwin correlations on volumetric measures were substantially higher than surface measures of cerebral morphology (White et al., 2002). Lohmann also found an effect of genes on sulcal patterns in 19 pairs of MZ twins, with stronger pairwise correlations for deeper (and ontogenetically older) sulci (Lohmann et al., 1999). Other groups have replicated these findings using different metrics of cortical shape and gyral complexity (Haidekker et al., 1998; Mohr et al., 2004). Similar conclusions are found when examining the central sulcus (Bonan et al., 1998; Le Goualher et al., 2000) and the planum temporale (Eckert et al., 2002) specifically rather than global sulcal patterns.

Multivariate and Longitudinal Studies

Despite the importance of understanding the etiology inter-regional neuroanatomic relationships, there are only three studies that investigate questions of this nature. Barré et al. examined relationships between height, intracranial volume (ICV), total gray matter, total white matter, and lateral ventricular volumes in a large sample of 54 MZ and 58 DZ adult twin pairs and 34 sibs of DZ pairs, via variance component analyses (Baare et al., 2001a). Between grey and white matter, they found a genetic correlation of .68, a unique

environmental correlation of .04, and no statistically significant evidence of genetic correlations between the lateral ventricles and other regions of interest. A principle components analyses by Pennington et al. on a sample of 34 MZ and 32 DZ late teen or young adult twin pairs parcellated the brain into 7 cortical gray compartments and 6 noncortical structures (white matter, basal ganglia, brain stem, hippocampus, cerebellum, and the central gray nuclei including the thalamus) found that two factors could account for 64% of the total phenotypic variance. While cerebral structures loaded primarily on the first factor, all other structures loaded on the second (except central gray, which loaded equally on both). Both factors were significantly more correlated in MZ than in DZ pairs, suggesting a strong genetic component to each. The final extant multivariate volumetric study by Wright et al. parcellated the brain into regions with extremely high spatial resolution (Wright et al., 2002). This study identified two putative supra-regional principle components under genetic control. Specifically, a frontoparietal limbic/paralimbic factor and a factor related to audition (lateral temporal cortex, insula, occipitofrontal, and other frontal regions) were found; factor loadings, however, were quite low ($< |0.25|$). These findings would suggest that genes are involved in generating functional relationships between distant brain regions.

There is only one paper that reports longitudinal data on neuroanatomic structures and changes with age. It is based on two volumetric measurements with an interval of 4 years between them, using subjects recruited from the National Heart, Lung and Blood Institute (NHLBI) study on World War II veterans (Pfefferbaum, Sullivan, & Carmelli, 2004). The subsequent analyses on 71 twin pairs suggest genetic stability in both the corpus

callosum and lateral ventricular volumes over this time interval. In contrast, this study found evidence for environmental factors increasing the variability in both measures with time, suggesting ongoing changes in brain structure even in the eighth decade of life. This study, however, does little to explain the sources in neuroanatomic variation over the vast majority of the human lifespan.

Relationships between Brain and Behavior

Though numerous twin studies that have investigated the relationships between atypical behavior and neuroanatomic endophenotypes (Table 3.2), there are relatively few that have attempted to understand how the genetic and environmental effects on typical cognitive and behavioral measures are mediated through brain morphology. Most of the existing work has been on cognition. The detection of brain-cognition correlations has been particularly elusive in typical samples. An initial study on full scale IQ and several brain volumes in a small twin sample failed to find a significant correlation with any structure (range -.04 to .20) (Tramo et al., 1998). There is growing evidence that a small correlation does exist, however. For example, using voxel-based morphometry, Thompson found strong evidence that intelligence (defined as a combination of selected subtests of the WAIS-R) was significantly correlated with frontal gray matter in his sample of 40 twins, but did not attempt to parcellate the correlation into genetic and nongenetic components (Thompson et al., 2001). Spurred by this discovery, Posthuma et al. compared WAIS-IIIR IQ scores to total gray and white matter volumes in an extended twin design with 24 MZ pairs, 31 DZ pairs, and 25 siblings (Posthuma et al., 2002). They

Table 3.2: Comparison of qualitative study design characteristics for the studies on neuropathology. This summary table excludes case reports and studies using twin samples to study non-genetic questions. Studies that provide useful information on typical neurodevelopment, usually because they report statistics on control samples, are shown in boldface.

Study	Condition of Interest	Pediatric Population?	Structure of interest?	Volumetric Analysis?	Morphological Measures?	Voxel-level Measures?	Informs typical development?
Casanova, 1990a	Schizophrenia	N	Corpus Callosum	N	N	N	N
Casanova, 1990b	Schizophrenia	N	Corpus Callosum	N	Y	N	N
Suddath, 1990	Schizophrenia	N	Ventricles, hippocampus	Y	N	N	N
Casanova, 1991	Schizophrenia	N	Corpus Callosum	N	Y	N	N
Weinberger 1991	Schizophrenia	N	Cerebral lateralization	Y	N	N	N
Weinberger, 1992a	Schizophrenia	N	Hippocampus, PFC	Y	N	N	N
Weinberger, 1992b	Schizophrenia	N	Limbic	Y	N	N	N
Bartley, 1993	Schizophrenia	N	Sylvian fissure	Y	N	N	N
Kinnunen, 1993	Lupus	N	Clinical readings	N	N	N	N
Goldberg, 1994	Schizophrenia	N	Prefrontal Cortex, Hippocampus	Y	N	N	N
Thorpe, 1994	Multiple sclerosis	N	Clinical readings	N	N	N	N
Hyde, 1995	Tourette syndrome	Y	Caudate	Y	N	N	N
Noga, 1996	Schizophrenia	N	Global	Y	Y	N	N
Jackson, 1998	Epilepsy	N	Hippocampus	Y	N	N	N
McNeil, 2000	Schizophrenia	N	Hippocampus	Y	N	N	N
Barre, 2001	**Schizophrenia**	**N**	**Multiple substructures**	**Y**	**N**	**N**	**Y**
Briellmann, 2001	Epilepsy	N	Clinical Findings, Hippocampus	Y	N	N	N
Noga, 2001	Bipolar I	N	Mesial Temporal, Basal Ganglia	Y	N	N	N
Bridle, 2002	Schizophrenia	N	Subcortical	Y	N	N	N
Cannon, 2002	Schizophrenia	N	Voxel-level	N	N	Y	N
Kiseppä, 2002	Bipolar I	N	Global	Y	N	N	N
Narr, 2002	**Schizophrenia**	**N**	**Corpus Callosum**	**Y**	**N**	**N**	**Y**
Narr, 2002b	**Schizophrenia**	**N**	**Hippocampus**	**Y**	**N**	**Y**	**Y**
Castellanos, 2003	ADHD	Y	Caudate	Y	N	N	N
Järvenpää, 2004	Cognitive Dysfunction	N	Hippocampus	Y	N	N	N
Kates, 2004	Autism	Y	Global	Y	N	N	N
May, 2004	PTSD	N	Septum Pellucidum	N	N	N	N
Van Erp, 2004	**Schizophrenia**	**N**	**Hippocampus**	**Y**	**N**	**N**	**Y**
Van Haren, 2004	**Schizophrenia**	**N**	**Hippocampus**	**Y**	**N**	**N**	**Y**
Hulshoff Pol, 2004	**Schizophrenia**	**N**	**Global**	**Y**	**N**	**N**	**Y**
Rijsdijk, 2005	**Schizophrenia**	**N**	**Hippocampus**	**Y**	**N**	**N**	**Y**
Spaniel,2005	Schizophrenia	N	Global T1/T2 Relaxation	N	N	N	N
Styner, 2005	**Schizophrenia**	**N**	**Corpus Callosum**	**Y**	**Y**	**N**	**Y**
Hulshoff Pol, 2006	Schizophrenia	N	Voxel-Level	N	N	Y	N

found a small but significant correlation between IQ and neuroanatomic structures, with all of the covariance between IQ and brain anatomy caused by genetic commonalities. A follow up study examining WAIS-III subtests produced similar results, with small brain-behavioral correlations dominated by genetic effects (Posthuma et al., 2003). It is noteworthy that since both IQ and neuroanatomy are strongly genetically mediated, despite the dominance of genes in generating covariance, the relative contributions of shared genes to either IQ or brain volume is rather small. The only brain and behavior study on a typical pediatric twin population was by Pennington (Pennington et al., 2000), which found WISC-R full scale IQ measures to be correlated with total cerebral volume (.42 in their reading disabled sample, .31 in a control group). The genetic correlation between these measures in the combined sample was .48.

The remaining studies on cognition are from the NCLBI, an all male geriatric population (Carmelli et al., 2002b; Carmelli, Reed, & DeCarli, 2002a; Carmelli et al., 1999). Of these, one presents a systematic analysis of two cognitive factors (verbal memory and executive function) (Carmelli et al., 2002b). These factors were based on principle components analyses of data from the Trails A and B, Stroop, California Verbal Learning Test, the Iowa Screening Battery for Mental Decline, and the WAIS Digit symbol substitution subtest, were highly heritable (.62 and .64, respectively). Executive function was found to be positively correlated with frontal and temporal regions and negatively with lateral ventricular volume (magnitude of correlations approximately .20). A similar, slightly weaker pattern was found with brain-verbal memory correlations. However, out of all measures, only lateral ventricular volumes and executive function shared common

genetic origins to a significant level (genetic correlation = -.25). Other studies from the NCLBI focus on the relationships between cognitive and physical performance and white matter hyperintensities in the elderly (Carmelli et al., 2002a; Carmelli et al., 1999).

Limitations of current research

Despite the promise of these methods, numerous limitations of the field are readily apparent. First is a relative dearth of work and lack of replication in this novel field, exacerbated by the limited sample sizes of the great majority of existing studies (Figure 3.3). The information that can be gleaned from control groups from pathological studies suffers this problem to an even greater extent (Figure 3.4). Small samples lead to low confidence in parameter estimates, which is certainly responsible for much of the observed discrepancies between studies. Further, many studies restrict their samples to exclusively MZ twins, which prevents them from distinguishing genetic effects from those of the shared environment (Biondi et al., 1998; Mohr, Knauth, Weisbrod, Stippich, & Sartor, 2001; Mohr et al., 2004; Reed, Pfefferbaum, Sullivan, & Carmelli, 2002; Steinmetz, Herzog, Schlaug, Huang, & Jancke, 1995; Tramo et al., 1998). Of the papers on typical development that apply full twin designs, most are based either on a sample acquired by the Netherlands Twin Registry (NTR) on an adult sample, or on the geriatric sample from NHLBI. To date, there has been only one large twin imaging study on a pediatric sample(Pennington et al., 2000), in which the majority of individuals had been diagnosed with dyslexia.

The variety of image processing methodologies used and target regions of interest also is responsible for the lack of replication. In general, studies that employ state of the art image processing techniques rarely take advantage of advanced statistical genetic methodologies, and vice versa. The few studies that demonstrate well-designed methodological approaches in both domains (e.g. Wright et al.) are ubiquitously limited by extraordinarily small samples. Additionally, the lack of information regarding multivariate, longitudinal, and pediatric neurodevelopmental questions is striking. A better understanding of these processes in a typical population is critical to providing more a more definitive understanding of the genetic substrates of behavioral development.

Figure 3.3: Sample characteristics of the extant MRI twin studies on typical populations. To facilitate comparisons with singleton and sibling subsamples, individual twins are counted rather than twin pairs. Asterisks denote studies on pediatric populations. Several studies share overlapping samples, either derived from the National Heart, Lung, and Blood Institute sample (1), or from the Netherlands Twin Registry (2). For convenience, the sample from the present study, to date, is shown at right.

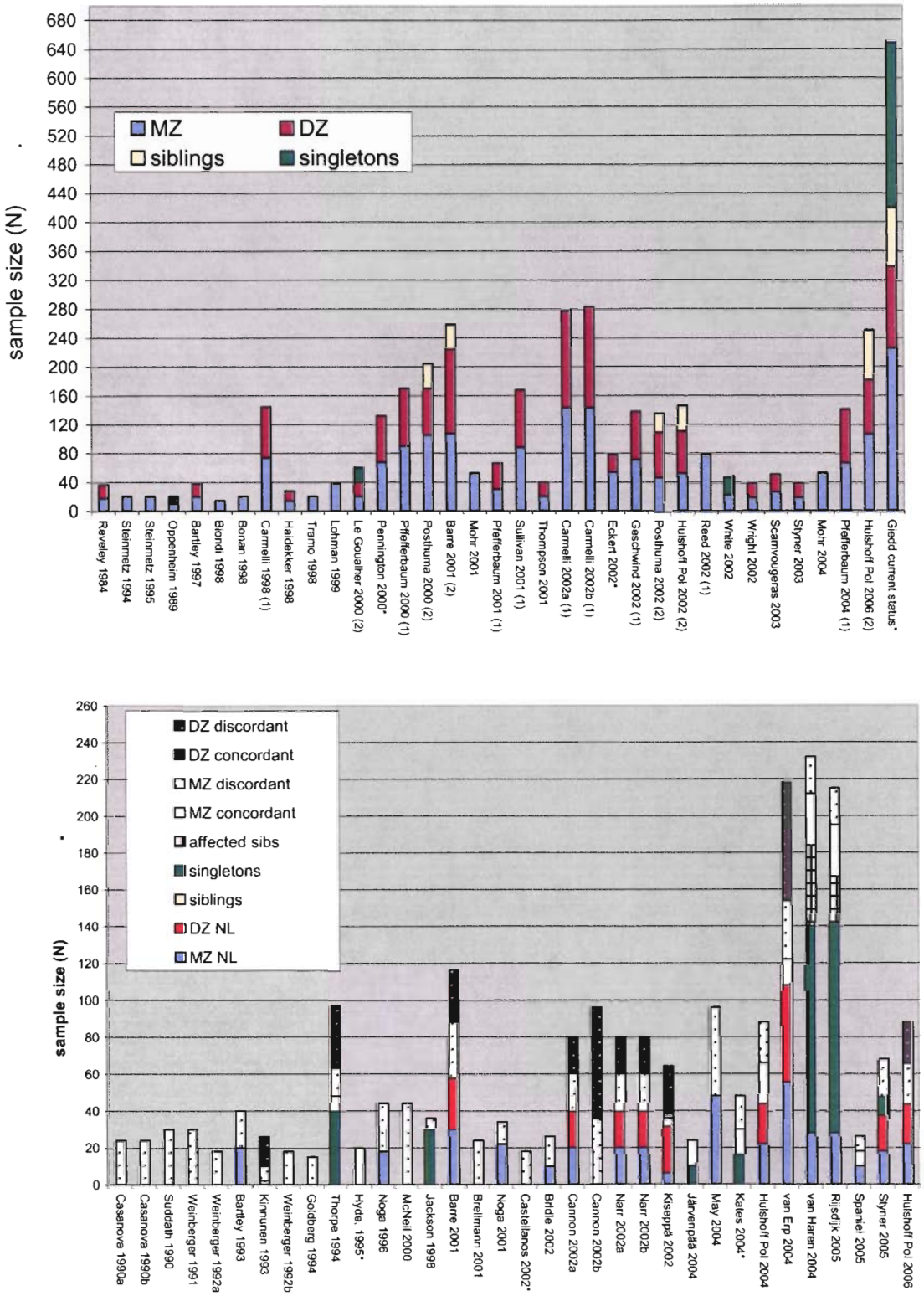

Figure 3.4: Sample characteristics of the extant MRI twin studies on neuropathology. Control subjects are shown in color.

4

THE HERITABILITY OF PEDIATRIC BRAIN VOLUMES

"We thus comprehend, not only that the human mind is united to the body, but also the nature of the union between mind and body. However, no one will be able to grasp this adequately or distinctly, unless he first has adequate knowledge of the nature of our body."

--Baruch Spinoza, *Ethics* (Part II, Prop. XIII), 1677

ADAPTED FROM:

Wallace GW, Schmitt JE, Lenroot R, Viding E, Ordaz S, Rosenthal MA, Molloy EA, Clasen LS, Kendler KS, Neale MC, and Giedd JN. A Pediatric twin study of brain morphometry. *Journal of Child Psychology and Psychiatry*. (2006)

ABSTRACT

The importance of genetic factors in generating variability in neuroanatomic endophenotypes is largely unquantified, particularly for developmental samples. We measured several neuroanatomic volumes via high-resolution MRI in a sample of 90 MZ twin pairs, 37 DZ twin pairs, and 158 unrelated singletons between the ages of 5 and 18. Statistical genetic analyses demonstrated high heritability for nearly all structures measured, with the exception of the lateral ventricles and the cerebellum. Moreover, allowing for changing genetic effects with age, we observed significant gene by age interactions in the frontal and temporal lobes, in both gray and white matter. These results suggest a strong and dynamic role of additive genetic differences on the population variability in pediatric brain structure.

Introduction

Given the limited information on what drives individual differences in neurobiological endophenotypes, particularly in children, a relatively simple but important first step is to quantify how much genetic and nongenetic sources drive the large population variances observed for gross brain volumes. Since many specific brain functions are related to specific brain regions (Kandel & Jessl, 2000), an understanding of what drives differences in volume may help explain differences in brain function, i.e. behavior. The only prior study on a pediatric population (Pennington et al., 2000) reported high heritability for total cerebrum (.97), right neocortex (.68) and left neocortex (.80) in a sample of 34 MZ and 32 DZ twin pairs. Though a factor analysis of smaller substructures was performed in this study, variance components statistics for individual volumes were not reported.

With the exception of prenatal life, childhood is the period with the most dramatic changes in gross neuroanatomic structure and size (Lenroot & Giedd, 2006). It is probably no coincidence that remarkable advances in cognitive function (including concrete reasoning, mathematics, language, metacognition, and greatly reduced processing speeds) also take place during this time, particularly in the school years (Berger & Thompson, 1995; Flavell, Miller, & Miller, 1993). Neuroimaging studies have consistently demonstrated large increases in cerebral white matter volumes, with cerebral gray matter volumes generally decreasing throughout late childhood (Reiss, Abrams, Singer, Ross, & Denckla, 1996). More recent longitudinal studies in large samples have enabled developmental trajectories to be determined with substantially more precision

(Giedd et al., 1999; Gogtay et al., 2004). In these studies, the general trends toward increasing white and decreasing gray matter volume in the second decade are confirmed, but gray appears to peak during this age range and slowly decline in subsequent years. Peak gray matter volume is both sex-dependent and varies based on neuroanatomic region, but the general trend is consistently an "inverted U" shape (Figure 4.1). In contrast, white matter monotonically increases over late childhood and into early adulthood.

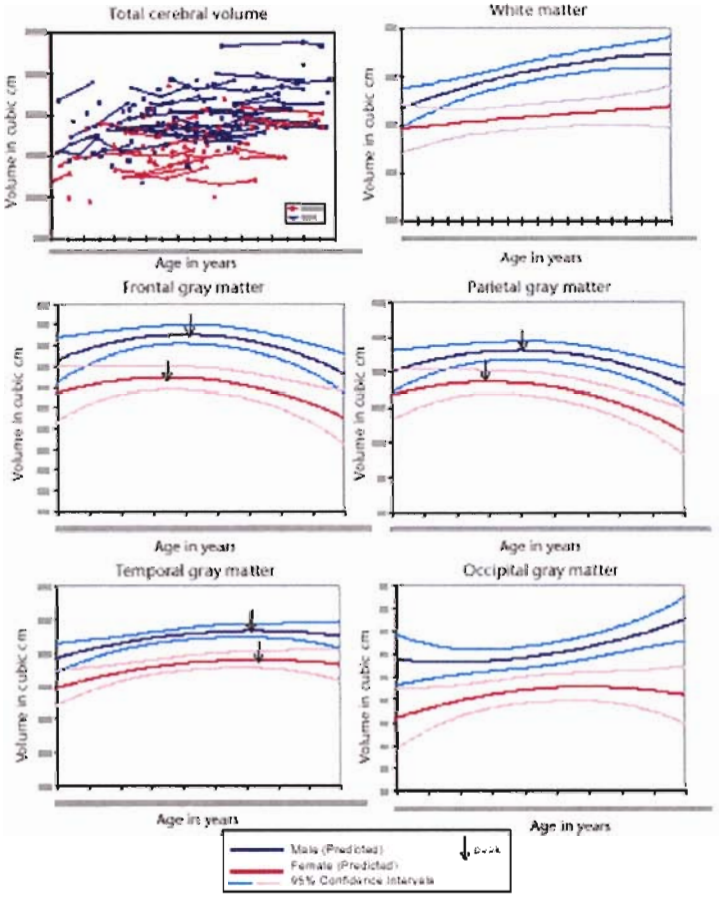

Figure 4.1: Changes in lobar brain volumes with age in a large, longitudinal pediatric sample. Trajectories in blue represent boys, with girls in red. From Giedd et al. *Nature Neuroscience* (2000).

This first volumetric analysis presents the results of classic ACE models for several regions of the pediatric brain, including the four principal cerebral lobes as well as subcortical nuclei. With these models, general information on the strength of genetic and

nongenetic influences on brain variability for this age range are reported. This information represents the first study of its kind in a typically developing pediatric population. As late childhood is a particularly dynamic time with respect to brain volumes, in a second series of analyses we present findings from models in which both genetic and environmental influences on brain volumes are allowed to change linearly with age.

Methods

Subjects

The analyses in this chapter were based on MRI data from one hundred twenty-seven pairs of typically developing same-sex twins (mean age = 11.6, SD = 3.3; age range = 5.6–18.7; 74 male pairs [58%], 53 female pairs) and 158 unrelated typically developing singletons (mean age = 11.3, SD = 3.5; age range = 5.2–18.7; 94 males [59%], 64 females). Of the 127 twin pairs, 90[71%] were MZ(mean age = 11.9,SD = 3.0; age range = 5.8–18.7; 52 male pairs [58%], 38 female pairs), and 37 pairs were DZ (mean age = 10.9, SD = 3.7; age range = 5.6–18.2; 22 male pairs [59%], 15 female pairs). Though singletons provide no information on the relative magnitudes of individual variance components, they could potentially increase precision of total variance estimates, as well as for the role of covariates on mean volumes.

Image Processing

The native MRI scans were first registered into standardized stereotaxic space using a linear transformation (Collins, Neelin, Peters, & Evans, 1994) and corrected for non-

uniformity artifacts (Sled, Zijdenbos, & Evans, 1998). The registered and corrected volumes were segmented into gray matter, white matter, cerebro-spinal fluid, and background using a neural net classifier (Zijdenbos, Forghani, & Evans, 2002). The tissue classification information was combined with a probabilistic atlas to provide region of interest measures (Collins et al., 1994).The output measures of this process that have shown high agreement with conventional hand tracing measures, and were included in this analysis, are the midsagittal area of the corpus callosum, the gray and white matter volumes of the total cerebrum, frontal, temporal, and parietal lobes, the caudate nucleus, the cerebellum, and the lateral ventricles. Figure 4.2 summarizes the image processing pipeline graphically.

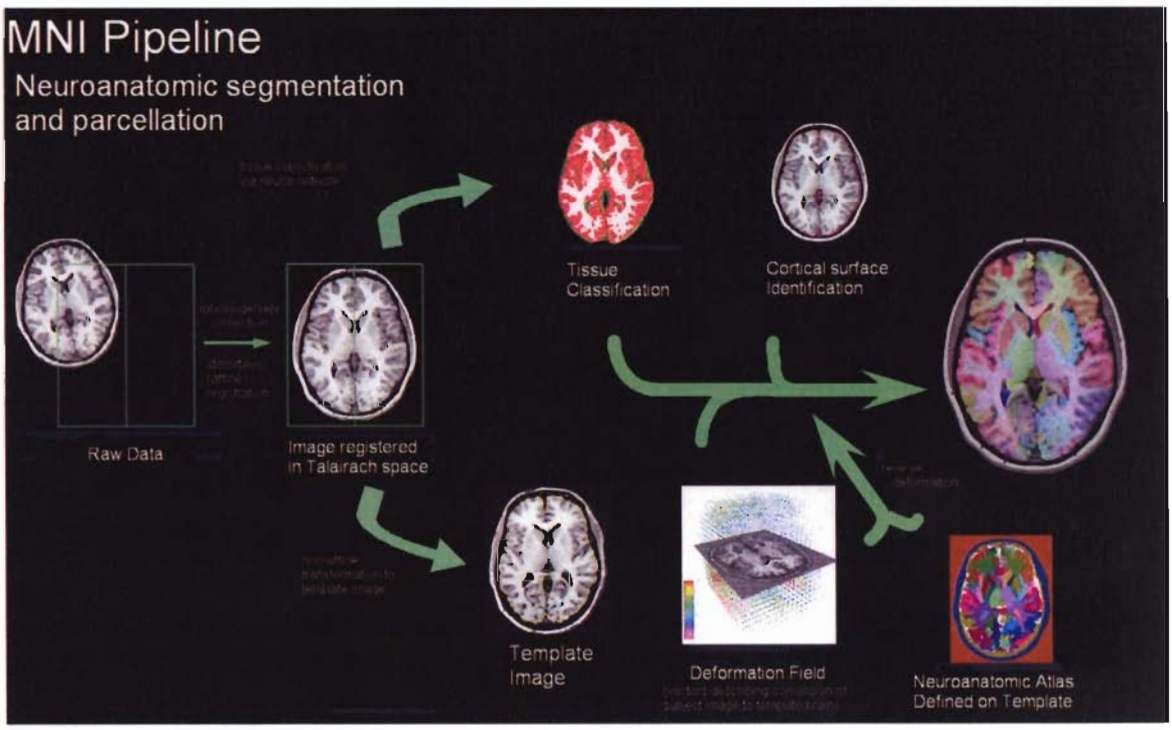

Figure 4.2: Summary of the image processing pipeline for volumetric regions of interest developed by MNI

Statistical Analysis

Neuroanatomic volumes were first assessed for normality, an important assumption of likelihood-based structural modeling. All volumes were highly normal, with the exception of lateral ventricles, which had a slight leftward skew. However, we opted to analyze the raw volumes for all variables including the ventricles, as the raw measurement units (cubic centimeters) are substantially more interpretable than transformed units. Cross twin correlations for each neuroanatomic region were subsequently performed. Additionally, we split both MZ and DZ groups into younger (Y) and older (O) subgroups based on the median age (11.36) in order to get a rough estimate of changes in heritability over time.

Univariate ACE twin models were constructed in Mx (Neale, Boker, Xie, & Maes, 2002). The effect of both age and gender on the mean was simultaneously estimated in addition to variance components. This procedure employed an automated script that included calculations for AE, CE, and 'E only' submodels, providing the optimizer unique starting values for all paths coefficients for each volume analyzed, based on descriptive statistics.

With the addition of individual-specific moderator variables, the standard ACE model can be expanded to account for interactions between A, C, and E with an observed variable (Purcell, 2002). Rather than a simple linear relationship between latent variable and phenotype, an interaction component (in our case, with age) also is included;

$$\hat{y}_i = (a_1 * A + a_2 * A * AGE_i) + (c_1 * C + c_2 * C * AGE_i) + (e_1 * E + e_2 * E * AGE_i)$$

for the i^{th} individual. Therefore, the expected variance and covariances become:

$$\text{Variance} = (a + x * AGE_i)^2 + (c + y * AGE_i)^2 + (e + z * AGE_i)^2$$

$$Cov_{MZ} = (a + x * AGE_i)^2 + (c + y * AGE_i)^2$$

$$Cov_{DZ} = \tfrac{1}{2} (a + x * AGE_i)^2 + (c + y * AGE_i)^2$$

where x, y, and z are additional free parameters.

The best-fit model for each neuroanatomic region was determined using maximum likelihood (ML) (Edwards, 1972). Using the best-fit model for each neuroanatomic region, we calculated broad sense heritability estimates (proportion of the variance due to genetic effects) for each structure and corresponding likelihood-based 95% confidence intervals (Neale & Miller, 1997). Because the difference in ML between any model and a nested submodel follows a χ^2 distribution with degrees of freedom equal to the difference in the number of parameters between models, we were able to directly test several hypotheses, namely the statistical significance of genetic and shared environmental effects, gene x age interactions, and the importance of age and gender on mean volumes. As variance components parameter estimates were virtually identical between ACE and ACE-xyz (age moderated) models, below we report only findings from the latter. Though several tests were performed, given the correlated nature of the data and the modest sample sizes, we used an α of .05 as the threshold for statistical significance.

We also attempted to identify the most informative submodels by systematically removing parameters from the full model. We employed Akaike's information criteria (AIC), mathematically χ^2- 2*df, which rewards model parsimony in addition to goodness of fit (Akaike, 1987). Thus, all things being equal, models with fewer parameters are favored as AIC is a mathematical representation of Occam's razor. This alternative approach also is advantageous since it allows non-nested models to be compared.

Results

Descriptive Statistics

Cross twin correlations are shown in Table 4.1. Monozygotic correlations ranged from .68 to .92 and were, in general, nearly twice that of DZ correlations, which varied from .29 to .73. The difference in magnitude between MZ and DZ correlations suggests that most of the covariance between relatives is caused by genetic factors; the high absolute values for these correlations suggests that genetic factors also account for most of the total variance in these brain volumes. The most striking exceptions to the rule were the lateral ventricles and the cerebellum. The difference in magnitude between MZ and DZ correlations was substantially smaller for these structures.

Table 4.1: Cross-twin volumetric correlations for MZ and DZ groups. Correlations for subgroups (O=Old, Y=Young) also are given.

Structure	MZ	DZ	MZY	DZY	MZO	DZO
Total Cerebrum	0.91	0.44	0.89	0.58	0.91	0.21
Total Gray Matter	0.84	0.41	0.81	0.56	0.86	0.22
Total White Matter	0.91	0.53	0.82	0.43	0.92	0.53
Frontal Gray Matter	0.82	0.46	0.77	0.55	0.84	0.43
Frontal White Matter	0.90	0.47	0.79	0.31	0.91	0.44
Total Frontal Lobe	0.89	0.45	0.84	0.51	0.90	0.37
Parietal Gray Matter	0.80	0.29	0.80	0.45	0.80	0.07
Parietal White Matter	0.90	0.46	0.83	0.39	0.91	0.45
Total Parietal Lobe	0.88	0.30	0.86	0.45	0.87	0.16
Temporal Gray Matter	0.83	0.45	0.74	0.62	0.86	0.23
Temporal White Matter	0.91	0.65	0.80	0.62	0.93	0.60
Total Temporal Lobe	0.92	0.53	0.87	0.65	0.92	0.34
Caudate Nucleus	0.83	0.39	0.72	0.42	0.88	0.38
Corpus Callosum	0.84	0.32	0.90	0.37	0.76	0.20
Lateral Ventricles	0.68	0.40	0.65	0.66	0.69	-0.14
Cerebellum	0.86	0.73	0.86	0.81	0.83	0.41

When splitting the groups by age, MZ correlations tended to be higher in the older age group relative to the younger. In contrast, DZ correlations tended to drop in the older group. These effects were dramatic and are displayed graphically in Figure 4.3. It is important to keep in mind, however, that calculations from the DZ subgroup are based on quite small samples, and that treating age as a continuous variable is a preferable approach, particularly with small N.

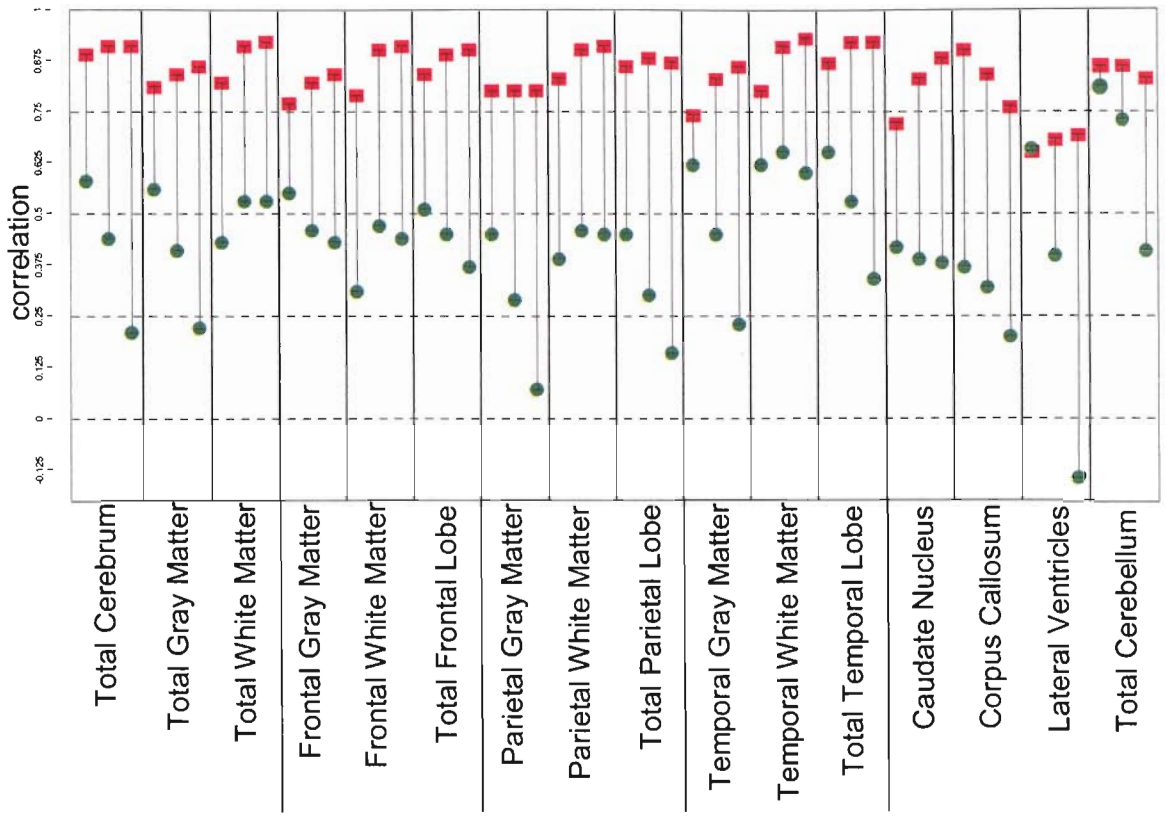

Figure 4.3: Graphical depiction of cross-trait correlations. MZ correlations are shown in red, and DZ correlations in green. For each structure, three pairs of MZ/DZ correlations are shown (young group at left, old group at right, combined at center).

Heritability Estimates

Heritability estimates for neuroanatomic structures were generally high, with additive genetic variance ranging from .49 - .89 (Table 4.2). The principal exception was lateral ventricle volume, where variance was divided about equally between A, C, and E. The cerebral lobar volumes all had heritability estimates of about .80, with virtually none of the variance in volumes attributable to shared environmental effects. Although confidence intervals overlap widely, in general, cerebral white regions appeared to have higher a^2 values when compared to their gray matter counterparts; consistent with this finding, a strong genetic influence on corpus callosum area was also observed. Additive genetic effects also were the predominant source of variance

in subcortical nuclei, with genetic factors accounting for about 70% of the variance in putamen and globus pallidus volumes, and about 80% of thalamus and caudate volumes. The only regions of interest that suggested any substantive role of shared environment on neuroanatomic variance were the putamen (c^2 =.17) and the cerebellum (c^2 =.30) Direct hypothesis testing using submodels found that genetic contributions were statistically significant for all brain regions, including lateral ventricles (χ_2^2 range 7.4 – 51.5, p-value range .0253 - <.0001). The role of shared environment was not found to be significant for any tissue (χ_2^2 range 0.0 – 1.6, p-value range 1.0 - .45).

Table 4.2: Heritability estimates for all neuroanatomic structures, based on maximum likelihood optimization of the full ACE-β_X β_Y β_Z model. $\mathbf{a^2}$, $\mathbf{c^2}$, and $\mathbf{e^2}$, represent the proportion of the variance in volume due to genetic, shared environmental, and unique environmental sources, respectively. Additionally, Chi-squared tests of the significance of genetic (A) and shared environmental (C) variance components were performed by comparing the fit of models with and without their corresponding parameters, and are provided on the right. Since the unique environment includes a contribution from measurement error, it can not be removed from the model. Heritability estimates of these full models (i.e. including interactions) were virtually identical to traditional ACE models (not shown).

							A		C	
STRUCTURE	$\mathbf{a^2}$		$\mathbf{c^2}$		$\mathbf{e^2}$		χ^2_2	p	χ^2_2	p
Total Brain Volume	0.89	[.67 .92]	0.00	[.00 .22]	0.11	[.08 .16]	51.5	**<0.0001**	0.0	1.0000
Total Gray Matter	0.82	[.50 .87]	0.00	[.00 .31]	0.18	[.13 .26]	26.2	**<0.0001**	0.0	1.0000
Total White Matter	0.85	[.56 .90]	0.01	[.00 .28]	0.15	[.10 .22]	35.6	**<0.0001**	0.0	1.0000
Frontal Gray Matter	0.77	[.36 .83]	0.00	[.00 .38]	0.23	[.17 .32]	16.5	**0.0003**	0.0	1.0000
Frontal White Matter	0.84	[.52 .89]	0.00	[.00 .31]	0.16	[.11 .23]	34.3	**<0.0001**	0.0	1.0000
Total Frontal Lobe	0.84	[.56 .89]	0.00	[.00 .27]	0.16	[.11 .23]	34.2	**<0.0001**	0.0	1.0000
Parietal Gray Matter	0.78	[.41 .86]	0.02	[.00 .37]	0.20	[.14 .29]	20.2	**<0.0001**	0.0	0.9915
Parietal White Matter	0.85	[.63 .90]	0.00	[.00 .22]	0.15	[.10 .22]	39.6	**<0.0001**	0.2	0.8900
Total Parietal Lobe	0.86	[.62 .90]	0.00	[.00 .24]	0.14	[.10 .20]	39.9	**<0.0001**	0.0	1.0000
Occipital Gray Matter	0.69	[.16 .77]	0.00	[.00 .48]	0.31	[.23 .44]	7.4	**0.0253**	0.0	1.0000
Occipital White Matter	0.66	[.24 .79]	0.04	[.00 .44]	0.30	[.21 .43]	9.9	**0.0070**	0.7	0.7047
Total Occipital Lobe	0.72	[.26 .81]	0.02	[.00 .45]	0.26	[.19 .37]	11.2	**0.0037**	0.0	0.9965
Temporal Gray Matter	0.80	[.45 .86]	0.00	[.00 .34]	0.20	[.14 .28]	22.1	**<0.0001**	0.0	1.0000
Temporal White Matter	0.82	[.40 .89]	0.02	[.00 .44]	0.16	[.11 .23]	27.9	**<0.0001**	0.0	0.9965
Total Temporal Lobe	0.88	[.60 .91]	0.00	[.00 .27]	0.12	[.09 .17]	44.3	**<0.0001**	0.0	1.0000
Total Cerebrum	0.88	[.65 .91]	0.00	[.00 .23]	0.12	[.09 .17]	48.4	**<0.0001**	0.0	1.0000
Caudate Nucleus	0.80	[.56 .85]	0.00	[.00 .22]	0.20	[.15 .29]	28.7	**<0.0001**	0.0	1.0000
Putamen	0.65	[.30 .87]	0.17	[.00 .52]	0.17	[.13 .24]	17.0	**0.0002**	0.6	0.7312
Globus Pallidus	0.67	[.24 .82]	0.09	[.00 .50]	0.24	[.18 .34]	10.9	**0.0043**	0.1	0.9441
Thalamus	0.82	[.48 .87]	0.00	[.00 .30]	0.18	[.13 .25]	24.3	**<0.0001**	0.0	1.0000
Total Subcortical Nuclei	0.82	[.50 .87]	0.00	[.00 .31]	0.18	[.13 .26]	25.7	**<0.0001**	0.0	1.0000
Corpus Callosum	0.85	[.41 .89]	0.00	[.00 .43]	0.15	[.11 .22]	26.9	**<0.0001**	0.0	1.0000
Lateral Ventricles	0.31	[.00 .67]	0.24	[.00 .58]	0.45	[.33 .60]	9.5	**0.0088**	6.5	**0.0379**
Total Cerebellum	0.49	[.13 .83]	0.30	[.00 .64]	0.21	[.16 .29]	8.9	**0.0118**	1.6	0.4532

Brackets indicate 95% confidence intervals.

Regression Components

Age and gender also had differential effects between neuroanatomic regions (Table 4.3). Male sex predicted substantially larger brain volumes using linear regression. Sex was a significant predictor for all regions with the exception of lateral ventricles ($\chi^2 = 2.19$, df = 1, p = .1392) and corpus callosum area ($\chi^2 = 1.61$, df = 1, p = .2049). Age effects were more variable, but followed the general trend of having a negative relationship with mean gray matter volume, a positive relationship with mean white matter volume, and a positive relationship with gray and white matter volumes combined (i.e., total lobar volumes). The effect of age on neuroanatomic volume was significant for cerebral white matter structures, total temporal lobe volume, and the cerebellum.

Table 4.3: Linear effects of sex and age on mean brain volumes. Columns under the "REGRESSION" heading are parameter estimates from the full model. The column "SEX" indicates changes in predicted brain volumes if the individual is male, while "AGE" is the change in volume per year of age (for the age range of the data, roughly 5-18). The "REGRESSION SUBMODELS" heading provides test statistics comparing the full model to submodels that did not allow for changes in mean volumes with either sex or age. In this figure, an α of .05 was arbitrarily chosen as a threshold for significance.

	REGRESSION			REGRESSION SUBMODELS							
Region	MEAN	SEX	AGE	3) Drop Sex?	X^2	p	AIC	4) Drop Age?	X^2	p	AIC
Total Cranial volume	1027.23	71.63	3.42	NO	14.65	0.0001	12.65	YES	1.68	0.1948	-0.32
CEREBRUM											
Total Cerebral Volume	845.53	845.53	58.46	NO	14.33	0.0002	12.33	YES-trend	3.69	0.0547	1.69
Total Gray Matter	720.27	44.36	-1.44	NO	14.91	0.0001	12.91	YES	0.79	0.3732	-1.21
Total White Matter	306.98	27.37	4.85	NO	11.16	0.0008	9.16	NO	16.37	0.0001	14.37
Total Frontal Lobe	342.77	20.61	1.30	NO	9.79	0.0018	7.79	YES	1.93	0.1649	-0.07
Frontal Gray	222.50	12.07	-0.25	NO	10.47	0.0012	8.47	YES	0.22	0.6429	-1.79
Frontal White	120.34	8.58	1.55	NO	6.79	0.0092	4.79	NO	10.30	0.0013	8.30
Total Parietal Lobe	183.16	10.52	0.67	NO	9.31	0.0023	7.31	YES	1.86	0.1723	-0.14
Parietal Gray	123.54	6.09	-0.46	NO	9.14	0.0025	7.14	YES	2.59	0.1077	0.59
Pariatel White	59.59	4.44	1.14	NO	6.96	0.0083	4.96	NO	20.50	0.0000	18.50
Total Occipital Lobe	88.04	10.06	0.32	NO	17.91	0.0000	15.91	YES	0.94	0.3318	-1.06
Occipital Gray	63.11	6.44	-0.07	NO	16.17	0.0001	14.17	YES	0.10	0.7542	-1.90
Occipital White	24.93	3.63	0.39	NO	14.96	0.0001	12.96	NO	8.49	0.0036	6.49
Total Temporal Lobe	231.52	17.30	1.90	NO	16.64	0.0000	14.64	NO	9.74	0.0018	7.74
Temporal Gray	170.56	10.35	0.68	NO	13.38	0.0003	11.38	YES	2.82	0.0929	0.82
Temporal White	60.99	6.95	1.22	NO	17.05	0.0000	15.05	NO	23.76	0.0000	21.76
Corpus Callosum	476.90	16.52	3.52	YES	1.61	0.2049	-0.39	YES-trend	3.50	0.0614	1.50
SUBCORTICAL											
Total Subcortical Vol.	25.29	1.39	-0.08	NO	12.34	0.0004	10.34	YES	1.97	0.1602	-0.03
Caudate Nucleus	10.48	0.48	-0.02	NO	6.16	0.0131	4.16	YES	0.76	0.3821	-1.24
Globus Pallidus	3.24	0.13	-0.03	NO	4.89	0.0270	2.89	NO	9.12	0.0025	7.12
Putamen	11.57	0.77	-0.03	NO	16.67	0.0000	14.67	YES	1.17	0.2802	-0.83
Thalamus	15.93	0.89	0.07	NO	12.25	0.0005	10.25	YES-trend	3.38	0.0660	1.38
Lateral Ventricles	8.28	1.46	0.19	YES	2.19	0.1392	0.19	YES	1.82	0.1774	-0.18
Cerebellum	114.44	12.35	0.77	NO	38.10	0.0000	36.10	NO	8.27	0.0040	6.27

Table 4.4: Testing age invariance in neurodevelopment. For each structure, maximum likelihood estimates for the variance components of full ACE-β_X β_Y β_Z models are given. Chi-squared tests of age invariance (i.e. heteroscedasticity) were performed by removing all age interaction parameters (i.e. β_X, β_Y, and β_Z) simultaneously from the full model. Tests of gene*age and (unique) environment* age interactions were performed on models in which nonsignificant shared environment interaction parameters were removed. Examining best-fit submodels is an alternative approach to traditional hypothesis testing. Using AIC, the best fit submodels of the full model are shown (where X, Y, and Z denote β_X, β_Y and β_Z, respectively).

	Parameter estimates						Age invariance[1]		Gene * age		Environment * age		Best-Fit Submodels	
Structure	**a**	**c**	**E**	β_X	β_Y	β_Z	χ^2_3	**P**	χ^2_1	**p**	χ^2_1	**p**		**AIC**
Total Brain Volume	58.54	0.01	20.82	2.43	0.00	0.85	6.9	0.0752	4.0	***0.0447***	1.14	0.2857	AE_X/AE_XZ	-4.86/-4.00
Total Gray Matter	41.09	0.01	10.11	1.27	0.01	1.41	11.0	***0.0119***	1.9	0.1648	5.43	***0.0198***	AE_Z/AE_XZ	-4.07/-4.00
Total White Matter	24.44	8.20	18.32	1.10	-0.98	-0.25	4.7	0.1927	4.7	***0.0307***	0.6	0.4386	AE_X	-5.39
Frontal Gray Matter	10.26	0.01	4.19	0.59	0.01	0.44	14.8	***0.0020***	4.2	***0.0398***	4.35	***0.0370***	AE_XZ	-4.00
Frontal White Matter	6.74	1.61	8.75	0.68	-0.23	-0.21	9.6	***0.0223***	9.4	***0.0022***	2.13	0.1444	AE_XZ/AE_X	-4.00/-3.87
Total Frontal Lobe	14.59	0.19	11.29	1.24	-0.20	0.11	10.9	***0.0124***	8.4	***0.0037***	0.11	0.7401	AE_X	-5.89
Parietal Gray Matter	6.46	3.56	2.86	0.28	-0.17	0.18	8.1	***0.0446***	2.2	0.1362	2.56	0.1096	AE_XZ/AE_Z	-3.98/-3.76
Parietal White Matter	4.99	4.97	3.04	0.24	-0.48	0.02	6.2	0.1014	5.0	***0.0248***	0.07	0.7913	AE_X	-5.70
Total Parietal Lobe	10.36	1.62	4.57	0.51	-0.11	0.17	8.5	***0.0362***	4.8	***0.0286***	1.02	0.3125	AE_X/AE_XZ	-4.98/-4.00
Occipital Gray Matter	6.68	0.05	4.26	0.05	-0.00	0.05	0.5	0.9123	0.1	0.7773	0.25	0.6171	AE	-7.47
Occipital White Matter	2.52	4.26	2.19	0.12	-0.29	0.04	2.6	0.4557	0.7	0.3994	0.54	0.4624	AE	-5.39
Total Occipital Lobe	9.29	2.53	5.84	0.11	-0.06	0.04	0.6	0.9078	0.3	0.6171	0.12	0.7290	AE	-7.45
Temporal Gray Matter	7.88	0.01	2.92	0.52	0.00	0.34	14.6	***0.0022***	5.0	***0.0251***	3.91	***0.0480***	AE_XZ	-4.00
Temporal White Matter	4.46	0.17	5.03	0.28	-0.12	-0.15	8.5	***0.0366***	6.5	***0.0110***	4.11	***0.0426***	AE_XZ	-3.99
Total Temporal Lobe	11.35	0.01	4.74	0.74	0.00	0.23	11.0	***0.0117***	6.9	***0.0086***	1.59	0.2073	AE_X/AE_XZ	-4.41/-4.00
Total Cerebrum	45.84	0.01	16.75	2.20	0.00	0.81	8.6	***0.0356***	4.9	***0.0273***	1.41	0.2351	AE_X/AE_XZ	-4.59/-4.00
Caudate Nucleus	0.31	0.00	0.48	0.05	0.00	0.00	10.1	***0.0177***	9.3	***0.0023***	0.17	0.6801	AE_X	-5.83
Putamen	0.43	0.36	0.20	0.03	0.00	0.02	9.1	***0.0280***	3.7	0.0532	2.3	0.1307	AE_XZ/AE_X	-3.37/-3.09
Globus Pallidus	0.18	0.06	0.08	0.01	0.00	0.01	7.5	0.0583	2.1	0.1502	2.89	0.0895	AE_XZ/AE_X	-3.89/-3.00
													AE_XZ/AE_X/	-4.85/-4.30/-4.00
Thalamus	0.92	0.00	0.35	0.02	0.00	0.02	4.2	0.2457	1.2	0.2835	1.7	0.1923	AE_Z	
Total Subcortical Nuclei	0.85	0.00	0.69	0.08	0.00	0.01	10.2	***0.0172***	7.2	***0.0072***	0.29	0.5902	AE_X	-5.71
Corpus Callosum	76.28	0.01	17.49	-1.05	0.01	0.86	3.6	0.3131	1.2	0.2674	2.99	0.0838	AE_Z/AE	-4.77/-4.44
Lateral Ventricles	5.43	3.54	1.28	-0.71	-0.09	0.18	50.7	***<0.0001***	11.4	***0.0007***	6.91	***0.0086***	AE_XZ	-1.94
Total Cerebellum	7.86	6.58	3.20	-0.11	-0.12	0.10	1.5	0.6800	1.1	0.3055	0.95	0.3297	AE/ACE	-4.89/-4.49

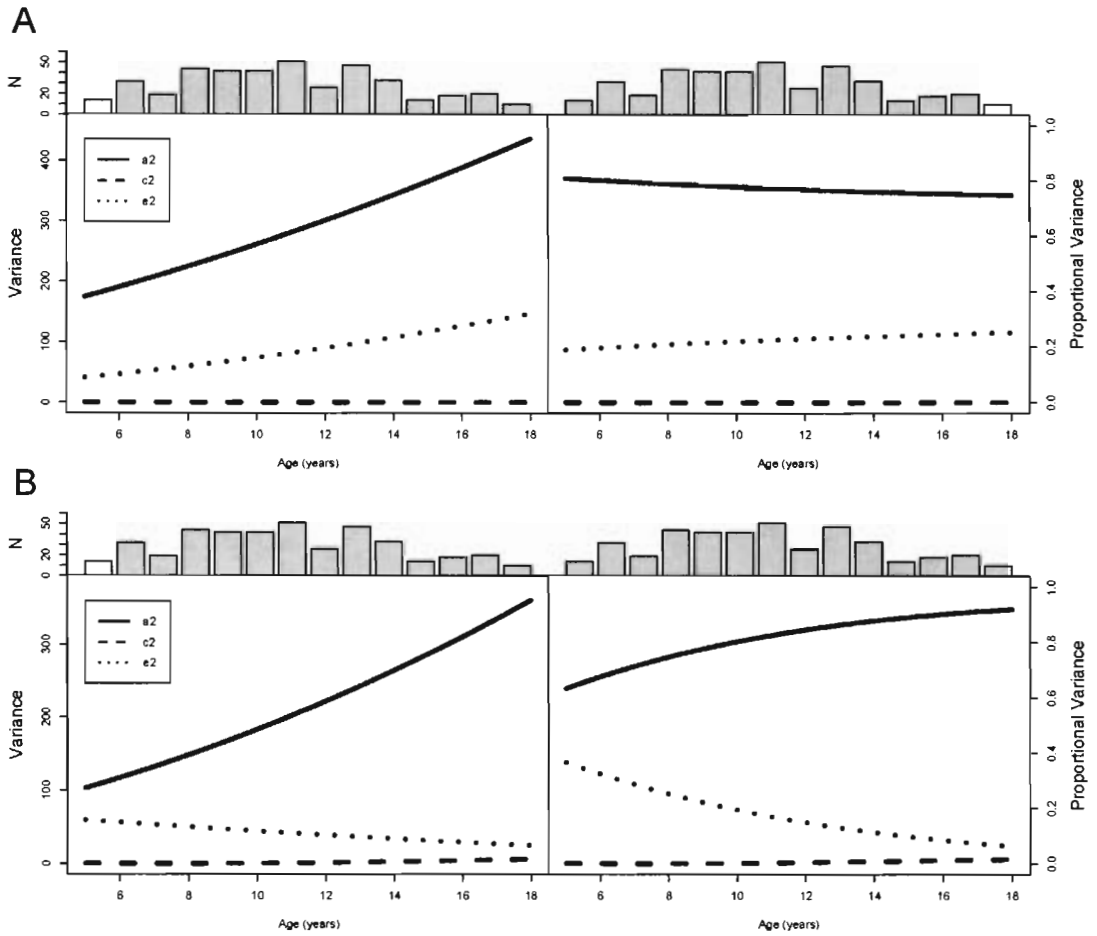

Figure 4.4: Changes in the variance of frontal lobe gray (A) and white (B) matter with age. Plots show absolute and proportional variance attributable to genetic (solid), shared environmental (dashed) and unique environmental (dotted) factors. Histograms above the plots show the distribution of the sample across the age range.

Interactions with Age

Parameter estimates for the full age-moderated models are given in Table 4.4. In general, total variance increased for most structures, particularly those in the cerebrum. Heteroscedasticity was observed most prominently in the frontal and temporal lobes and the caudate nucleus. In contrast, the cerebellum appeared to have no statistically

significant change in variance over the second decade of life ($\chi_3^2 = 1.5$, p-value = .6800); the best fit model via AIC, correspondingly, had no interaction parameter for cerebellar volumes.

Changes in variance in the cerebrum were largely driven by an increase in the magnitude of the genetic path with age, though variance due to the unique environment also tended to increase with age. In contrast, the role of the shared environment was insignificant, both in main effect and interaction with age. Figures 4.4 and 4.5 plot changes in variance components with age for frontal and temporal lobar compartments, the two cerebral regions with the most prominent age interactions. From these figures, it is readily apparent that raw variance attributable to additive genetic factors is increasing dramatically in children, regardless of tissue type. In contrast, it appears that raw unique environmental variance also increases with age for gray matter, but decreases slightly in white matter over this age range. The net effect is that it appears that *proportional* variance owed to genetic factors, i.e. the heritability, changes little in gray matter but increases somewhat in white matter.

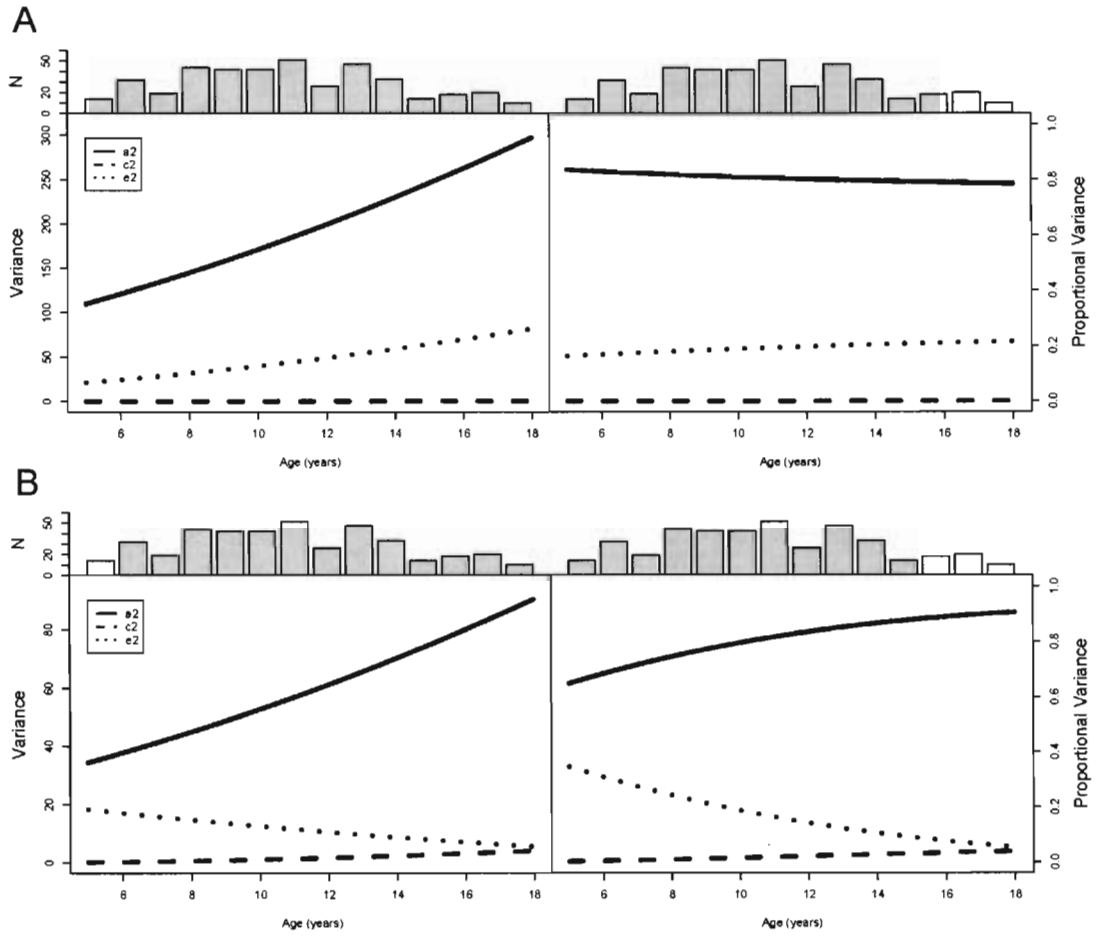

Figure 4.5: Changes in the variance of temporal lobe gray (A) and white (B) matter with age. Plots show absolute and proportional variance attributable to genetic (solid), shared environmental (dashed) and unique environmental (dotted) factors. Histograms above the plots show the distribution of the sample across the age range.

Discussion

These analyses clearly demonstrate the strong role of genetic factors in observed individual differences in pediatric brain volumes. High heritability for global brain volumes (e.g. total cranial volume, total gray matter, and total white matter) is consistent with prior studies in adults, as well as data from a study on pediatric dyslexia from

Pennington et al.. While a genetic role in brain formation will come as no surprise, it is significant that nearly all of the population variance in human brain volume is caused by genetic variance.

Additionally, we observed that maximum likelihood estimates for cerebral white matter were generally larger than that of cerebral gray; the only other twin study to segment the brain into gray and white matter compartments (Baare et al., 2001a) also reported that gray matter heritability (.82) was somewhat lower than white (.88) in a sample of 54 MZ and 58 DZ adult twin pairs.

Twin studies employing lobar parcellation schemes also are uncommon. To date, only two (Carmelli et al., 2002b; Geschwind et al., 2002) have provided parameter estimates for heritability, both in adult samples (Figure 4.6). Both found that genetic factors account for about half of the variance in lobar volumes (with the possible exception of occipital lobe). These estimates were substantially lower than that of the present study, however. There are several possible reasons for the discrepancy. Perhaps the most likely is that our measures combine left and right hemispheres, while the other two studies do not. In general, larger structures tend to have higher heritability values, perhaps due to decreased measurement error. Other possible reasons for differences include differing image processing methods, or true effects of age.

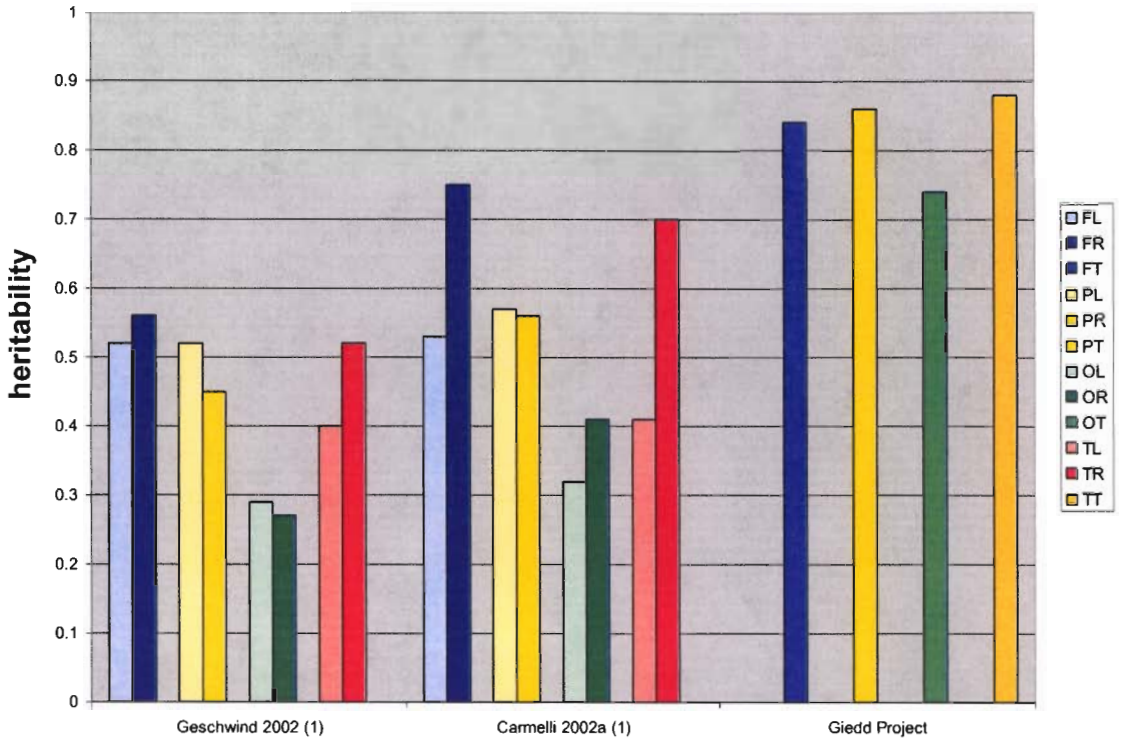

Figure 4.6: Extant heritability estimates for lobar brain volumes. In the legend, the first letter indicates lobe (F=frontal, P=parietal, O=occipital,T=temporal) and the second indicates hemisphere (L=left, R=right, T=total).

Our analyses also found some evidence for interactions between latent factors and age, particularly for frontal and temporal lobar compartments. To our knowledge, the present analyses are the first to address gene by age interaction for brain volumes. We observed increasing variance in these regions with age, driven primarily by genetic factors. Prominent increases in the genetic variance may be related to the late maturation of the frontal and temporal lobes relative to the rest of the cerebral cortex (Gogtay et al., 2004). During childhood, the age of highest synaptic proliferation varies widely throughout the cerebrum. The synaptic density of the occipital cortex reaches peak density before four months of age, but peak synaptic density in the frontal lobe occurs at approximately four years of life and does not decline appreciably until near the end of the second decade

(Huttenlocher, 1979; Huttenlocher & Dabholkar, 1997). This heterogeneity is in contrast to nonhuman primates, in which peak synaptogenesis occurs shortly after birth throughout the cortex (Rakic, Bourgeois, Eckenhoff, Zecevic, & Goldmanrakic, 1986). Other measures of developmental changes in neuropil, such as dendritic arborization, also show postnatal changes and regional heterogeneity (Becker, Armstrong, Chan, & Wood, 1984; Mrzljak, Uylings, Kostovic, & Vaneden, 1992). Genetic variability that produces individual differences in the proteins involved in the synaptic pruning and neural plasticity seen in childhood would be expected to produce increased variability in gray matter volumes, as gray matter is dependent on these factors.

Similar patterns were seen in white matter, though the magnitude of the genetic effect was somewhat larger. Significant gene by age interactions were detected in the frontal, temporal, and parietal lobes. The process of white matter maturation is dominated by axonal myelination and continues through childhood into the third decade of life (Benes, Turtle, Khan, & Farol, 1994). Diffusion tensor imaging (DTI) studies have demonstrated developmental changes in white matter in this age range *in vivo*, with prefrontal cortex, the sensory-motor strip, superior temporal gyrus, precuneus, and several occipital subregions showing increased fractional anisotropy throughout the second decade (Barnea-Goraly et al., 2005). Additionally, measures of white matter density in children have shown age-related increases in fronto-temporal (i.e. language association) and corticospinal (i.e. voluntary motor) tracts (Paus et al., 1999). Thus, it is likely that gene

by age interactions with white matter volumes involve variations in the process of myelination during late childhood and adolescence.

Interaction models such as these are not without limitation, and it is important to carefully evaluate assumptions before placing too much weight on their results. One potential confound is that it is assumed that the moderator variable is not influenced by the phenotype of interest. For some G x E interaction studies, determining the causal relationships between moderator and phenotype is difficult, if not impossible. Fortunately, in the case of age as a moderator, the causal arrow, if it exists, certainly points from age to brain volume and not vice versa.

A more important concern for the present study is the effect of scaling. For example, increases in mean volumes with age would, all things equal, generate increasing variance in volumes in older subjects. A change of scale, to log-transformed volumes, for example, could potentially eliminate the observed statistical interactions. This criticism of interaction is somewhat of a red-herring, however, as all statistical interactions could theoretically be eliminated by rescaling data. The observation that variance is increasing even in structures that have decreasing means with age (such as all cerebral gray matter measures) suggests against scaling as the sole cause of heteroscedasticity in the present study. Unlike many other variables in psychiatric genetics, neuroanatomic variables are not scaled arbitrarily or to generate favorable statistical properties; rather, volumes are the "true" measures of interest. Transformation of the data could serve to complicate interpretation, even assuming that the interaction is subsequently eliminated. Finally, it is

unlikely that scale could generate the observed differential interaction between different variance components. If scaling artifact was the sole source of heteroscedasticity, then variance components would be expected to change in parallel with one another.

In summary, these analyses establish heritability values for brain volumes in typical children. They also provide some evidences of a dynamic, generically mediated process underlying changes in variance over time.

5

HERITABILITY AT HIGH RESOLUTION: STUDIES OF CORTICAL THICKNESS AT THE VOXEL LEVEL

"God, or nature, or whatever else you wish to call the mysterious creative force of this world, which in the course of millions of years on the scale of phylogenetic development has shaped out of the simple cell all the diverse and complex varieties of life, has, of all living beings, endowed only the human species with the capacity to create new things. Creation has impressed a part of its own creative craft upon the brain of humans."

> -- Constantin Baron von Economo, Antwort zur Festrede des Präsidenten des Aeroklubs Alexander Cassinone, 1927

Adapted From:

LENROOT RK, SCHMITT JE, ORDAZ SE, WALLACE G, NEALE MC, LERCH JP, KENDLER KS, EVANS AC, GIEDD JN. QUANTITATIVE GENETIC ANALYSIS OF CORTICAL THICKNESS IN A PEDIATRIC TWIN POPULATION. *HUMAN BRAIN MAPPING.* UNDER REVISION.

ABSTRACT

Using data from a large sample (N=600) of twins and family members, we combined voxel-level neuroimaging and statistical genetic analyses to produce the first high-resolution pediatric heritability maps of the human brain. The role of additive genetic factors on variance in cortical thickness varied substantially over the brain surface. Heritability was strongest in the frontal lobe (particularly on the right side and orbitofrontal regions bilaterally), superior parietal lobule, language centers (Broca's and Wernicke's area), inferior pre- and postcentral gyrus, and superior temporal gyrus bilaterally. In contrast, heritability was quite low in the occipital lobe and the inferior tempro-occipital cortex. The role of shared environmental factors on variance was insubstantial. These findings demonstrate regional effects of genes on cortical development, and could aid the hunt for genetic polymorphisms that affect variability in human brain structure.

Introduction

Nearly all prior research on neuroanatomic endophenotypes is on volumes. These analyses, including those reported in the previous chapter, have consistently demonstrated that brain volumes are highly heritable throughout the brain. But though region of interest (ROI) based parcellation of the brain has numerous advantages, it also carries with it several limitations. In particular, ROIs have low resolution relative to the native resolution of the raw SPGR images (about 1 mm^3). Thus, fine scale effects can be blurred or obscured when considering voxels in aggregate. Additionally, parcellation schemes are necessarily based on *a priori* knowledge of structural and functional neuroanatomy. Although using knowledge gleaned from prior research is desirable in a hypothetico-deductive model, this approach has the capacity to overlook unanticipated gene-brain relationships. Given the lack of information in this area, it seems likely that many localized effects of genes on brain structure go undetected when using ROIs-alone (Ashburner & Friston, 2000).

A complementary approach to ROIs is the use of high-resolution image analysis (HIA). The most commonly-used version of this technique is voxel-based morphometry (VBM), originally developed by Ashburner and Friston (Ashburner et al., 1998; Ashburner et al., 2000). In this approach, raw MRI images are spatially normalized, and then a characteristic of interest (e.g. gray matter density) generated for all voxels in the image. At each voxel, standard statistical tests can be used. HIA has the advantage both of increased resolution and decreased reliance on gross neuroanatomic divisions. But these

new capabilities do not come without a cost; new problems, such as reduced power and multiple testing must be addressed.

In this chapter, we combine HIA and statistical genetics to produce the first heritability maps of the pediatric brain. We employ novel methods developed for the measurement of cortical thickness. The measurement of cortical thickness, which has long been of interest to neuroscientists, has traditionally been difficult to measure using MRI. Advances in image processing, however, have allowed for measurements that are in high agreement with measures from more traditional histological methods (Lerch & Evans, 2005a). Prior studies on cortical thickness using MRI are sparse, but have shown significant changes in neural architecture in diseases such as Alzheimer's disease, autism, attention deficit hyperactivity disorder, and schizophrenia (Greenstein et al., 2006; Hardan, Muddasani, Vemulapalli, Keshavan, & Minshew, 2006; Lerch et al., 2004; Lerch et al., 2005b; Narr et al., 2005b; Narr et al., 2005a; Shaw et al., 2006b; Singh et al., 2006) as well as normal changes with age (Shaw et al., 2006a; Thompson et al., 2005). The cerebral cortex is of particular interest to genetic studies given its novel structure in mammals relative to other vertebrates and its massive and disproportionate increase in humans relative to other primates (e.g. Appendix A).

Methods

Subjects

Six hundred normally developing children (mean age 11.1 years, range 5-18), including 214 same sex monozygotic and 94 dizygotic twins, 64 siblings of twins, and 228 singletons from non-twin families were included in these analyses (Table 5.1). Of the non-twin families, there were 34 sibships with two members, 9 with three members, 4 with four members, and one family with five members.

Table 5.1: Demographic data and global mean cortical thickness for each group.

	MZ	DZ	Sibs of twins	Singletons	Total
N	214 (35.7%)	94 (15.7%)	64 (10.7%)	228 (38.0%)	600
Mean Age	11.03 (3.16)	11.20 (3.80)	11.62 (3.53)	10.92 (3.48)	11.08 (3.43)
(SD)	Ran:5.37-18.72	Ran:5.55-19.34	Ran:4.99-19.11	Ran:5.16-18.88	Ran:4.99-19.34
Sex	117 M (55%)	53 M (56%)	31 M (48%)	132 M (58%)	332 M (55%)
	97 F (45%)	41 F (44%)	33 F (52%)	96 F (42%)	268 F (45%)
Race	202 W (94%)	92 W (98%)	63 W (98%)	172 W (75%)	529 W (88%)
W=Caucasian	6 B (3%)	0 B	0 B	36 B (16%)	42 B (7%)
B=African	2 A (<1%)	0 A	0 A	8 A (4%)	10 A (2%)
A=Asian	4 H (2%)	2 H (2%)	1 H (2%)	11 H (5%)	18 H (3%)
H=Hispanic	0 U	0 U	0 U	1 U (<1%)	1 U (<1%)
U=Other					
Handedness	189 R (88%)	78 R (83%)	56 R (88%)	199 R (87%)	513 R (86%)
R=Right	19 M (9%)	11 M (12%)	7 M (11%)	21 M (9%)	36 M (6%)
M=Mixed	18 L (8%)	9 L (10%)	10 L (16%)	32 L (14%)	37 L (6%)
L=Left	6 NA (3%)	2 NA (2%)	4 NA (6%)	2 NA (<1%)	14 NA (2%)
SES	43.49 (18.40)	42.92 (13.87)	40.11 (16.89)	40.70 (20.57)	41.99 (18.49)
	Ran: 20-89	Ran: 20-70	Ran: 20-77	Ran: 20-95	Ran: 20-95
Mean CT	4.20 (0.34)	4.13 (0.32)	4.12 (0.37)	4.12 (0.38)	
(SD)	4.20 (0.34) M	4.14 (0.32) M	4.11 (0.48) M	4.15 (0.37) M	
	4.19 (0.34) F	4.14 (0.32) F	4.14 (0.23) F	4.08 (0.39) F	

Image Analysis

The native MRI scans were registered into standardized stereotaxic space using a linear transformation (Collins et al., 1994) and corrected for non-uniformity artifacts (Sled et al., 1998). The registered and corrected volumes were segmented into white matter, gray matter, cerebro-spinal fluid and background using a neural net classifier (Zijdenbos et al., 2002). The white and gray matter surfaces are then fitted using deformable models resulting in two surfaces with 81920 polygons each (MacDonald, Kabani, Avis, & Evans, 2000). The white and grey matter surfaces are resampled into native space and cortical thickness was then computed in native space . In order to improve the ability to detect population changes, each subject's cortical thickness map was blurred using a 30mm surface based blurring kernel, which respects anatomical boundaries. A kernel size of 30mm was chosen to maximize statistical power while minimizing false positives (Lerch et al., 2005a). The output is cortical thickness at each of 40,962 cortical points, with information from each individual stored as a single vector (Figure 5.1). Statistical results at each point are projected upon the smoothed brain template using in-house software developed by the Montreal Neurological Institute. A probabilistic atlas was used to assign cortical points to specific neuroanatomic regions (Collins, Zijdenbos, Barre, & Evans, 1999).

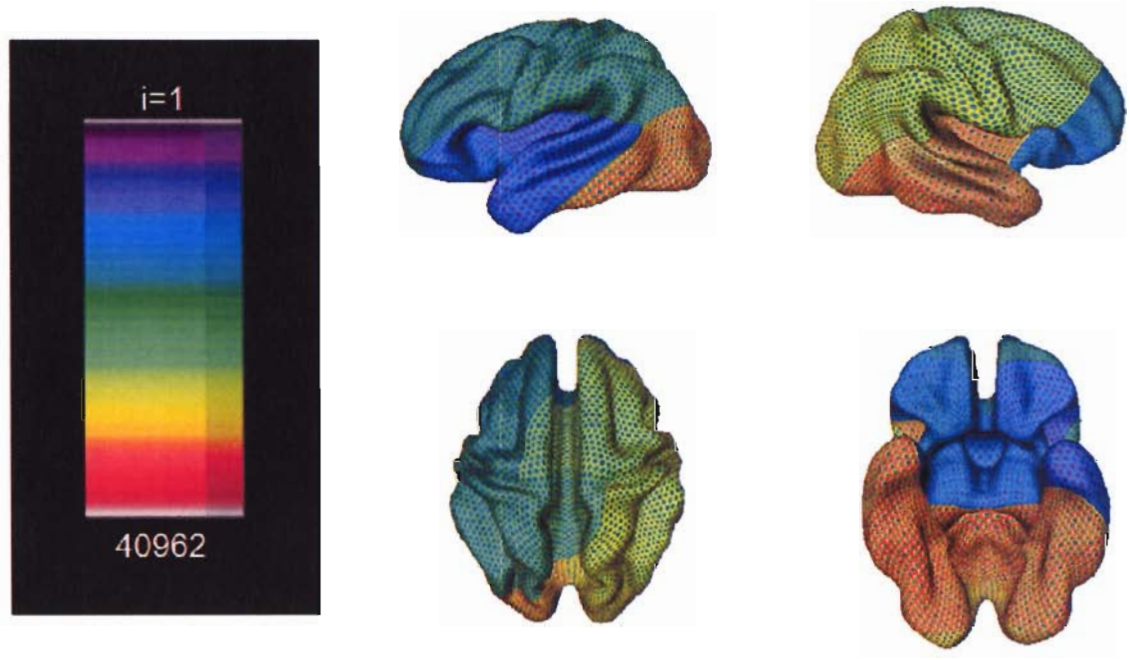

Figure 5.1: Vector to manifold relationship for cortical thickness data. The color look up table on the left represents a 40962 element vector, with colors corresponding to neuroanatomic locations at right.

Statistical Analysis

The resultant neuroanatomic output consisted of two matrices; one an N x I matrix of I cortical points for N subjects, and the second and N x V matrix of demographic information (age, sex, zygosity, etc.). We used the statistical package R to generate separate datasets for each cortical point, which iteratively passed to Mx for analysis. For the i^{th} cortical point, the interfacing algorithm extracted cortical thickness information for all subjects and then linked them to demographic information. This new dataset was then reorganized such that each record represented data from families rather than that of individuals, and the dataset was then written to a text file (Figure 5.2). From within R, Mx was called to perform statistical genetic analysis, and append the results to an output file. This procedure was then repeated for all cortical points in the dataset.

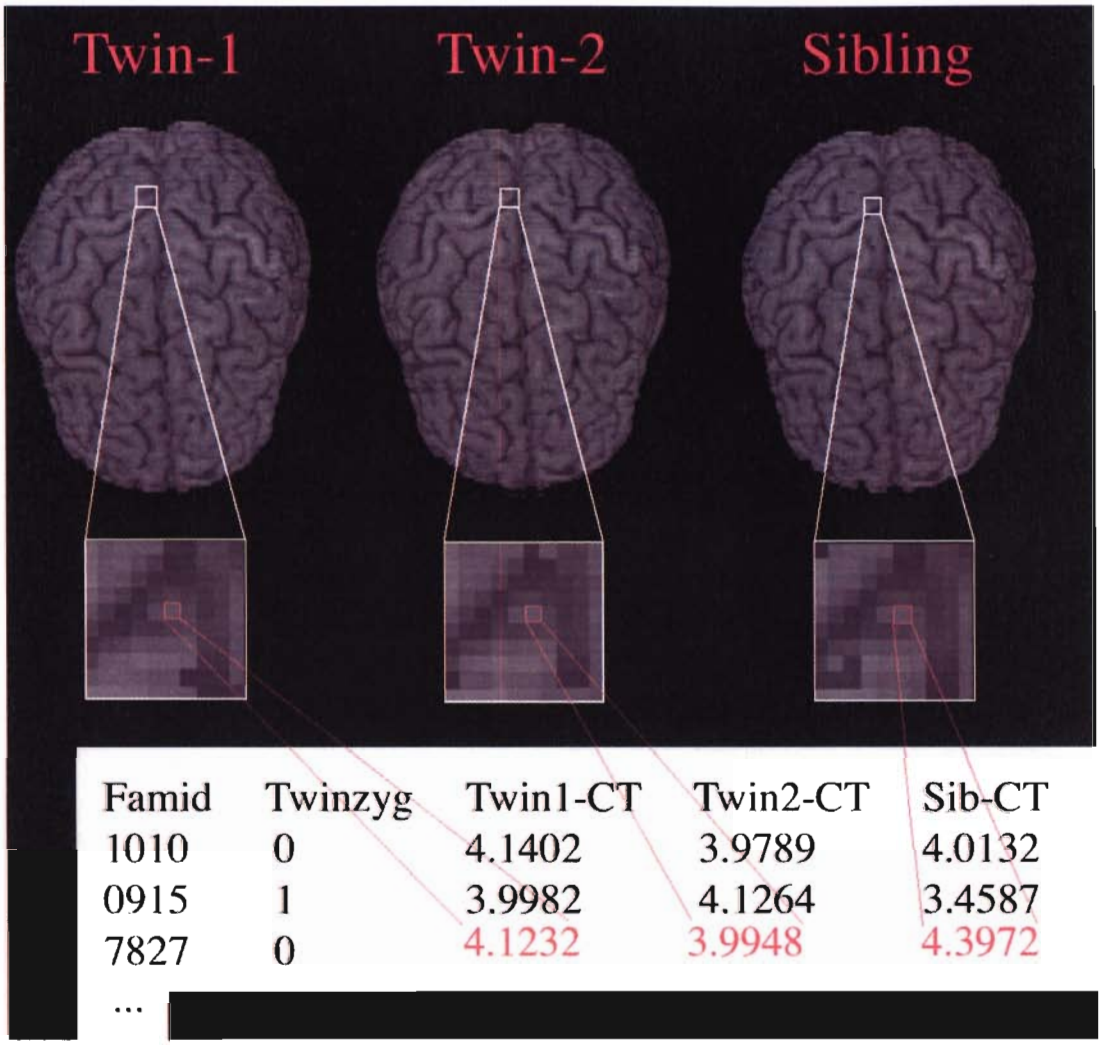

Figure 5.2: Conversion of spatially-referenced voxel information into the familywise data vectors typically used for genetic analyses in Mx. Information at a single spatial point in the image is associated with demographic information from the individual, and then each individual's data is systematically associated with that from family members. Mx models can then be used to analyze the information at this point in space. After sequentially iterating over all vertices, the output vector(s) have parallel structure to the original data

The dualistic nature of the interface has several useful properties. First, it simultaneously takes advantage of the strengths of each program, i.e. the powerful dataset manipulation and graphical tools in R and the statistical modeling utility of Mx. Second, it modularizes the analyses. This allows for relatively easy modification of either the data structure or the statistical models with a minimum impact on the other component. Thus, simple

expansions to univariate analyses can be added to Mx scripts without affecting the R code. Conversely, adjustments to the R code can be used to determine a subrange of voxels to be studied, create novel neuroanatomic CT measures by averaging over regions, or substitute one non-anatomic measure for another (e.g. substituting full scale IQ with performance IQ in a bivariate analysis) without requiring modification of Mx scripts. The value of such straightforward modification will become increasingly apparent below and in subsequent chapters that use data on cortical thickness.

For these analysis, we analyzed the data using classical ACE models, with the exception that an extended twin design was used (Posthuma et al., 2000b; Posthuma & Boomsma, 2000a). The addition of siblings of twins and a large sample of siblings from singleton families (i.e. families with no twins) provided substantially increased power to detect genetic signal due to a greater number of observed covariance statistics (Figure 5.3). This extended design assumes that the shared environment operates similarly in both twins and singleton births, with respect to the phenotype of interest. In our sample, families contained a twin pair and up to three additional siblings, or singleton families with up to five members in total.

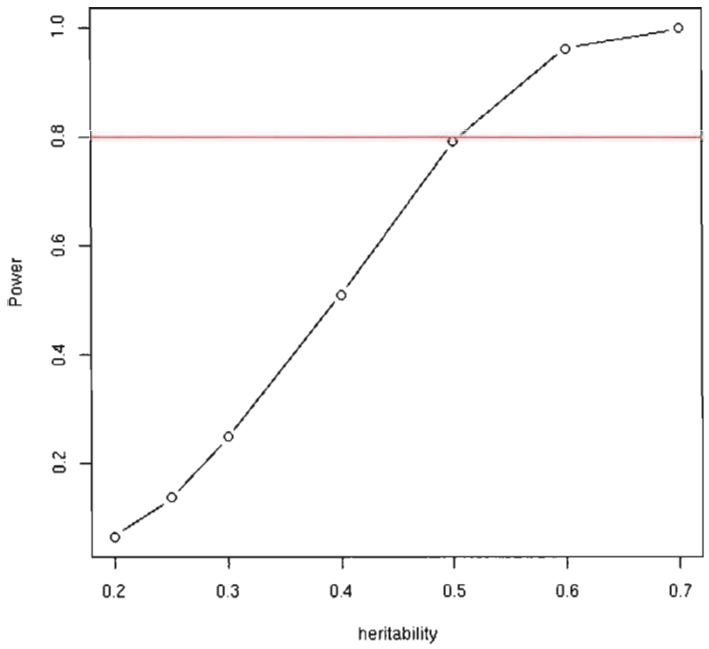

Figure 5.3: Power as a function of heritability in a series of simulations. Simulations used sample size and family structure identical to that of the actual data. Each data point represents the proportion of true positives (i.e. the power) from 1000 simulations of N=600.

These models also contained parameters to account for the effects of age and sex on mean cortical thickness, which were estimated concurrently with the variance components. Sex effects were estimated using a linear model and age was estimated using a cubic model based on prior evidence of age interactions with cortical thickness (Lenroot, 2005). Optimum model fit was determined using maximum likelihood (Edwards, 1972), which produces unbiased parameter estimates and allows for the identification of statistically significant parameters in the model. Likelihood based 95% confidence intervals also were calculated at each point (Neale et al., 1997). Fit statistics for submodels removing the parameters for genetic, shared environmental, or familial

(genetic plus shared environment) also were calculated, and parameter estimates from the full model, as well as X^2 and AIC statistics of submodels, were appended to an output file as a single record.

The resultant output consisted of parameter estimates for all cortical points as well as p-values of the statistical significance of A, and C. Brain maps were reconstructed from these data to visualize the maximum likelihood estimates of proportion of variability owed to additive genetic (a^2), shared environmental (c^2) and unique environmental (e^2) factors. Probability maps also were constructed to assess the significance of genetic factors on individual differences in cortical thickness. An $\alpha < .05$ was set as the threshold for statistical significance.

A false discovery rate (FDR) adjustment was applied to control for type I error (Genovese, Lazar, & Nichols, 2002); unless otherwise specified, FDR was set to allow for a 5% chance of false positives. Power analyses were generated using simulations as no other comparable studies are currently available. First simulated datasets identical in sample size and family structure of the true data were generated under various values of heritability. For each heritability value, one-thousand simulated datasets were created, and the models described above were subsequently fitted in order to generate a distribution of χ^2 test statistics comparing model fit with and without the presence of a genetic factor. From this distribution, power at our α could subsequently be calculated.

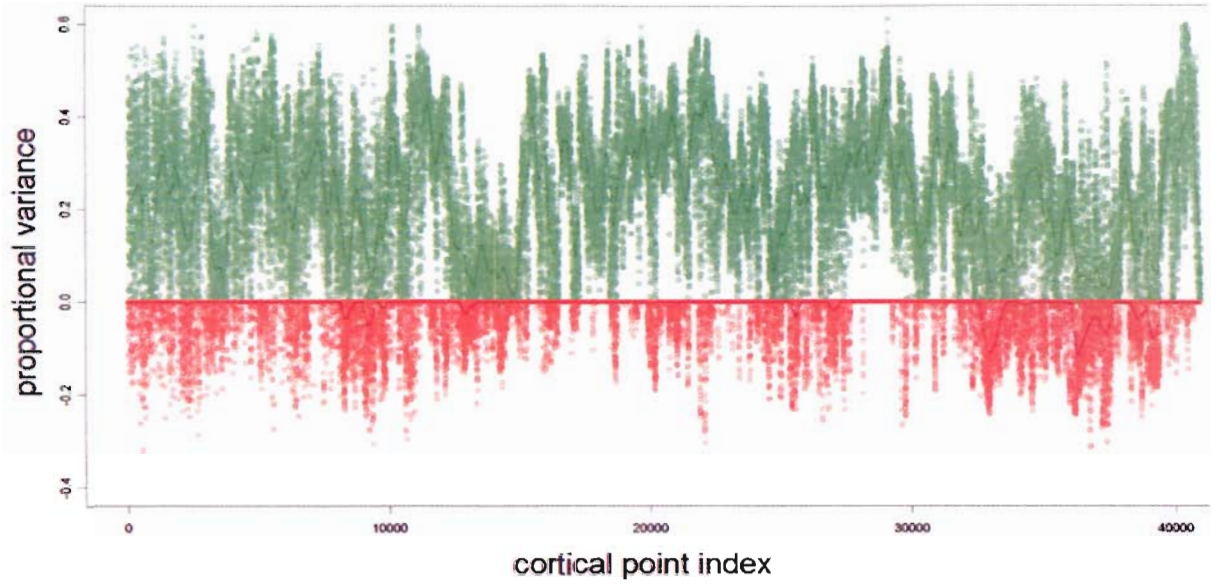

Figure 5.4: Example of raw output from statistical genetic pipeline. Green points display heritability for all 40962 cortical points, while red values represent variance due to the shared environment, reflected into negative space. Cortical points with similar index numbers tend to be spatially proximal.

Results

Preliminary inspection of the raw output showed substantial heterogeneity in the heritability of cortical thickness, with heritability ranging from 0 to about .60 (Figure 5.4). The patterns of heritability are readily apparent when parameter estimates are projected on the brain surface (Figure 5.5). Heritability was highest in inferior pre- and post-central gyrus, orbitofrontal gyri, superior frontal gyrus, lateral frontal gyrus, particularly on the right side, superior parietal lobe, and language centers including

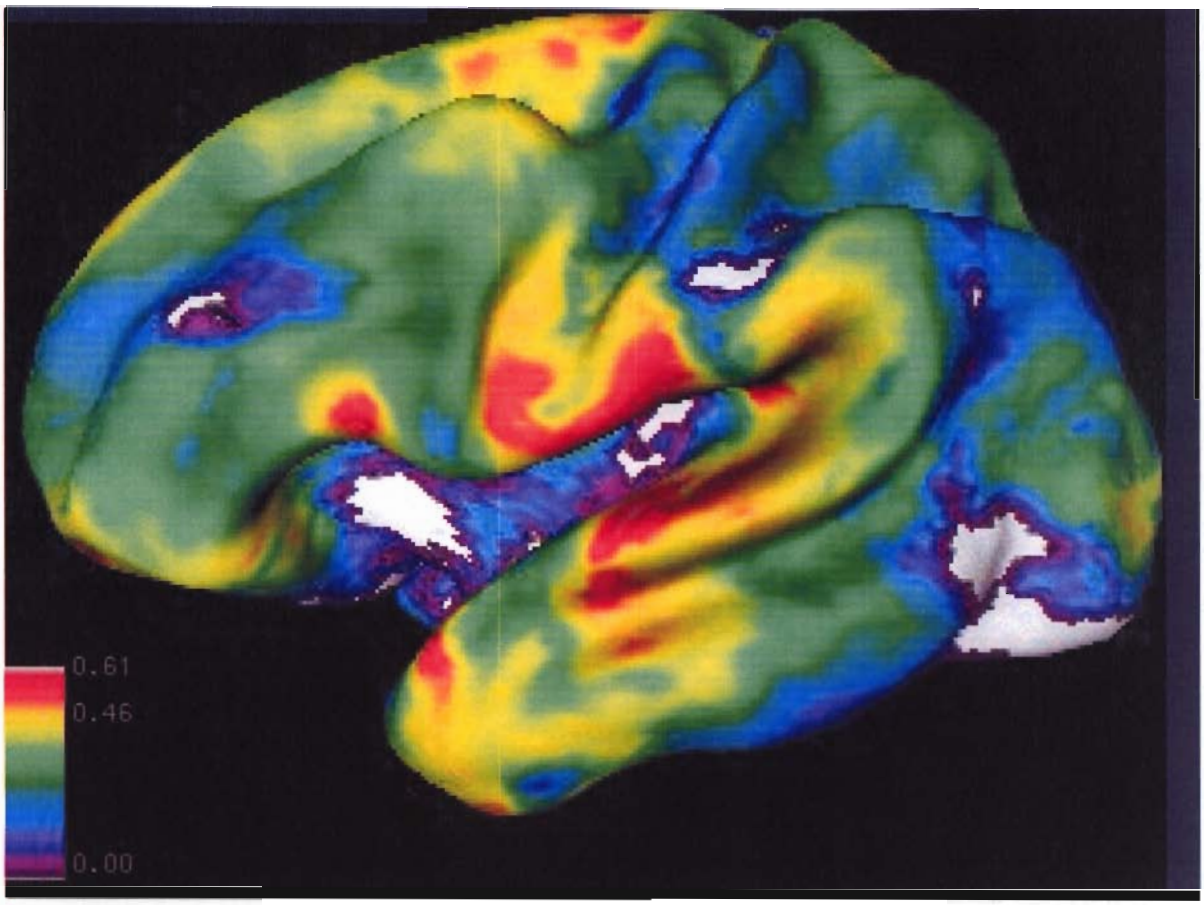

Figure 5.5: Brain heritability map for cortical thickness, as derived from ACE twin models using an extended twin design on MRI data from 600 twins, siblings, and unrelated singletons. Regions in white represent vertices with no heritability.

Broca's area, Wernicke's area, superior temporal gyrus, and the temporal pole. In contrast, shared environmental variance maximum likelihood estimates for nearly all vertices were zero, and approached zero for the remaining vertices (Figure 5.6). Variance caused by the unique environment and measurement error accounted for the greatest variance in most regions.

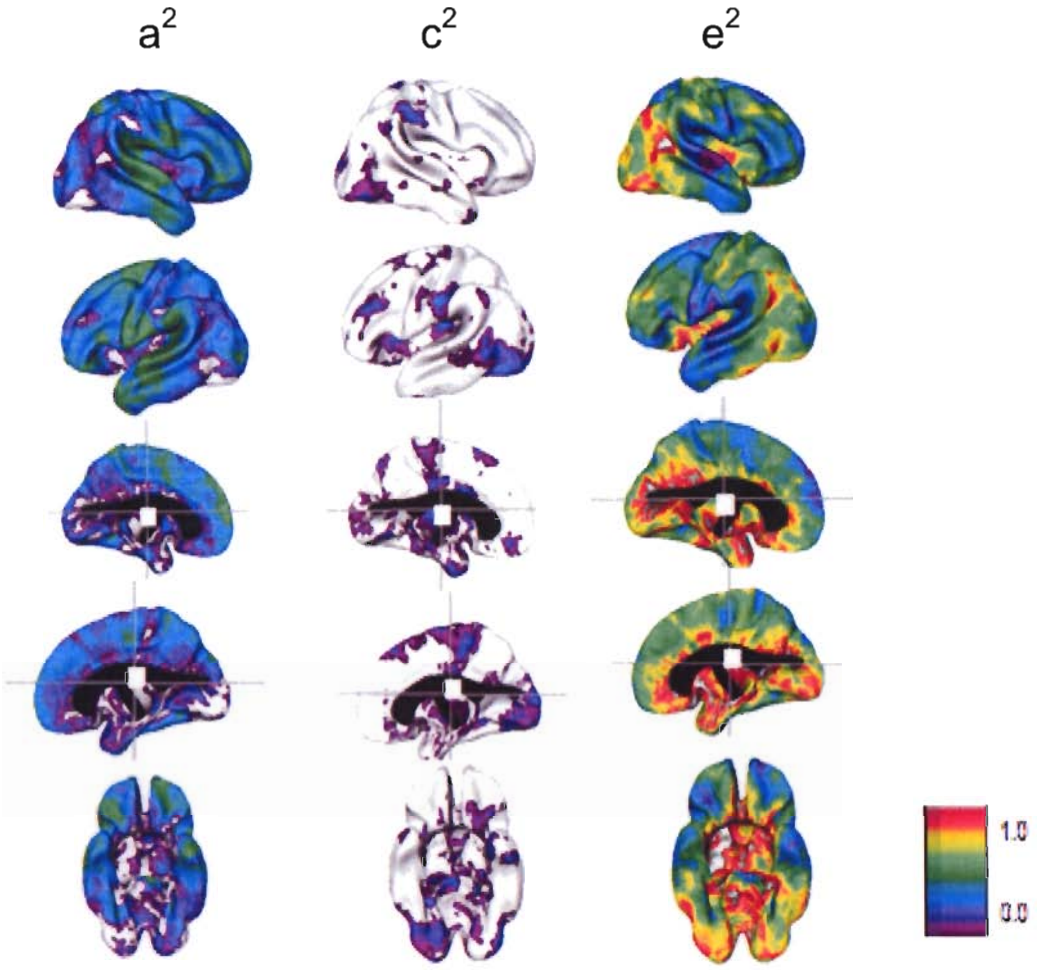

Figure 5.6: Maximum likelihood Parameter estimates for ACE models of cortical thickness

In addition to maximum likelihood estimates, 95 % confidence intervals also were calculated (Figure 5.7). Intervals were broad, as expected given the relatively small sample size and fine scale of this study. With the exception of a few vertices in the inferior occipital lobe, the lower bound for shared environmental variance was zero. In contrast, the lower bound for heritability was above zero in the regions described above.

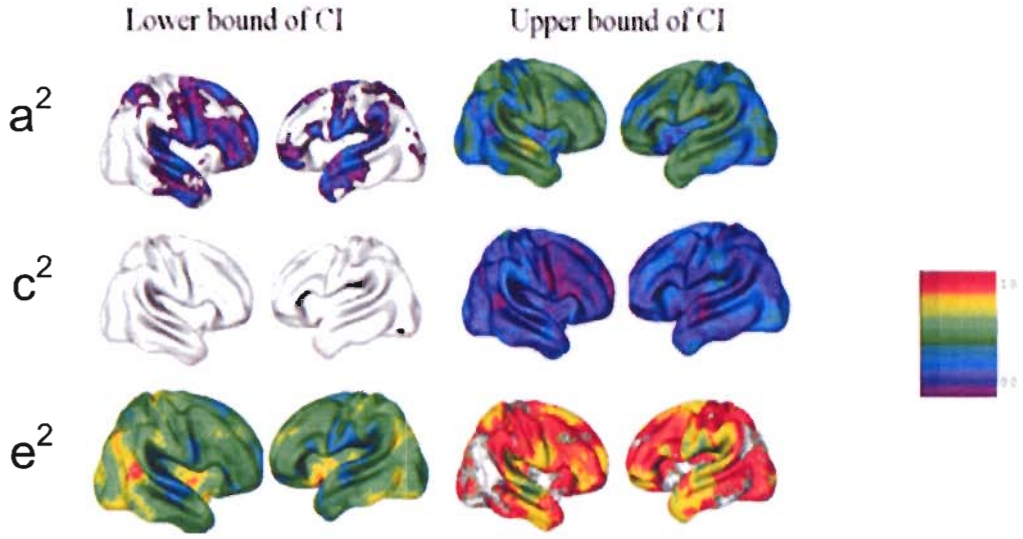

Figure 5.7: Likelihood-Based 95% Confidence Intervals for estimated variance components

Probability maps testing the importance of the genetic factors also generated similar patterns as the point estimates and confidence intervals (Figure 5.8). A very stringent FDR = .05 had relatively few significant vertices, but these were found at the core of regions with previously demonstrated high heritability. As the FDR threshold was increased to .10 or .15, the significant vertices at higher FDRs tended to form core regions which were surrounded by less significant regions. This produced a "bulleseye" pattern rather than random noise throughout the cortex.

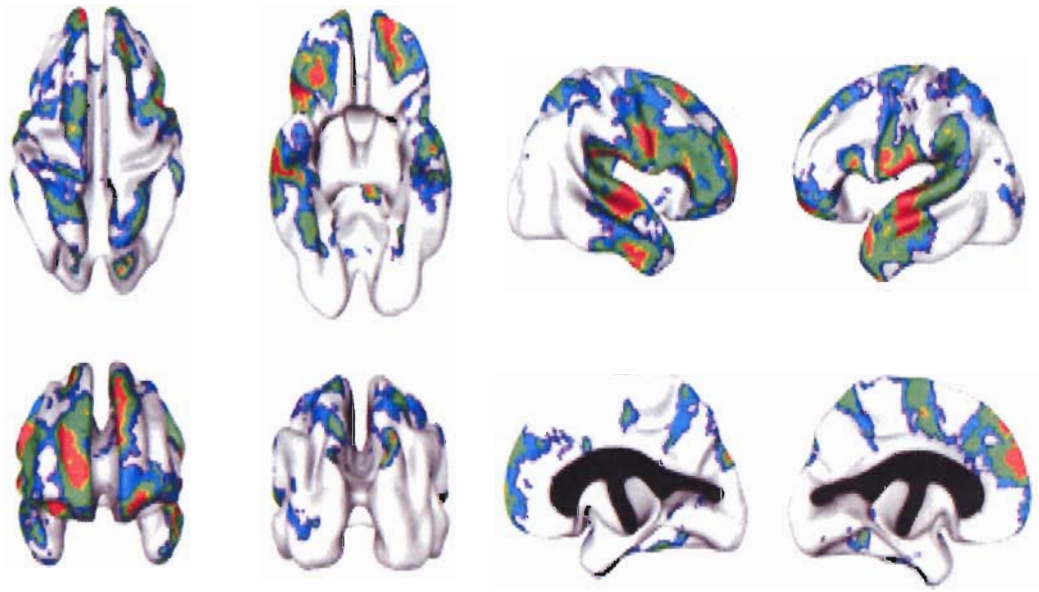

Figure 5.8: Probability map giving regions of statistically significant heritability. Colors represent significance at three false discovery rates (FDRs). Red represents an FDR of .05, green at .10, and blue at .15 (corresponding to uncorrected p-values of .002, .016, and .042, respectively.

Discussion

In his seminal text *The Cytoarchitectonics Of The Human Cortex,* Austrian psychiatrist Constantin Baron von Economo presented his now classic maps on the variability in cortical gray matter thickness throughout the cerebral hemispheres (von Economo & Koskinas, 1925). In this chapter, we continue in this tradition by creating the first maps of the heritability of cortical thickness. Like von Economo's work, these analyses reveal distinct patterns of regional specificity. The most heritable regions include several

portions of the frontal cortex, parietal association areas, language centers, and anterior temporal cortex.

It is noteworthy that many of the regions with the highest heritability estimates have well-documented roles in cognition, speech, sociality, and language; functions thought to have developed or been enhanced in humans relatively recently in evolutionary time (Fisher & Marcus, 2006). Comparative anatomic studies have demonstrated that many of the most prominent anatomic differences between humans and nonhuman primates lie within these regions as well, including the gyri encompassing Brodman's areas 9, 10,11 (prefrontal and orbitofrontal cortices), areas 44,45 (Broca's area), and areas 21, 22, 37, 39, and 40 (superior temporal and supramarginal cortex) (Carroll, 2003). Though studies in animal models demonstrate that genes are critical for patterning of the brain as a whole (Grove & Fukuchi-Shimogori, 2003; Monuki & Walsh, 2001), the present findings show that genetically-mediated variance is topologically variable, at least with respect to cortical thickness.

An ongoing evolutionary process could potentially explain why high genetic variability persists in relatively novel cortical regions, but not in others, as genes influencing evolutionarily "older" regions have had more time to reach allelic fixation. An alternative, albeit related, explanation would be that regions with low genetic variance have greater functional constraints on their determinants of cortical thickness, such that functional mutations in these regions have a higher probability of resulting in purifying selection. Comparative genomic experiments have shown that a subset of neurally-

expressed genes have evolved more rapidly in humans than in other primates (Dorus et al., 2004; Khaitovich et al., 2005; The Chimpanzee Sequencing and Analysis Consortium, 2005); both gene expression changes and protein sequence modification have accelerated in humans relative to nonhuman primates (Caceres et al., 2003; Enard et al., 2002; Gu & Gu, 2003; Hsieh, Chu, Wolfinger, & Gibson, 2003; Uddin et al., 2004). The findings of increased genetic variance in evolutionarily recent structures may represent a remnant of these rapid neurogenetic changes that accompanied our divergence from other primates.

In the last years of his short life, von Economo's interests turned from cataloging the architecture of the cortex towards fundamental questions on human origins (Triarhou, 2006). His final works on comparative neuroanatomy are dedicated to describing the brain regions that are most unique to humans relative to other animals; Broca's area, frontal lobe, and the superior parietal lobe. His hypothesis of 'progressive cerebration' included within it the belief that human brain evolution did not end before dawn of civilization, but was an ongoing process even in the modern era. The presence of specific patterns of genetic variation in the cortex may be evidence that this belief was not too far off the mark.

6

GENE BY AGE INTERACTION IN PEDIATRIC BRAIN DEVELOPMENT

"Children are very active, constructive thinkers and learners. They are clearly not blank slates that passively and unselectively copy whatever the environment presents to them."

--John H. Flavell "Cognitive development: Past, present, and future." *Developmental Psychology* (28:6),1992.

ADAPTED FROM:

LENROOT RK, SCHMITT JE, ORDAZ SE, WALLACE G, NEALE MC, LERCH JP, KENDLER KS, EVANS AC, GIEDD JN. QUANTITATIVE GENETIC ANALYSIS OF CORTICAL THICKNESS IN A PEDIATRIC TWIN POPULATION. *HUMAN BRAIN MAPPING.* UNDER REVISION.

ABSTRACT

In this chapter, we have expanded our analyses of cortical thickness to allow for changes with age. Both genetic and environmental variance decreased in most regions, though genetic variance increased in the superior parietal lobule and environmental variance increased in superior primary motor and somatosensory cortex. As total phenotypic variance decreased, the relative importance of genetic factors increased in most regions, including superior temporal, frontal lobes, and the superior parietal lobule. The increase in heritability in these regions is temporally coincident with the development of many cognitive functions that have been associated with them. Though underpowered, these results are suggestive of a dynamic process underlying both genetic and nongenetic contributions to cortical variability.

Introduction

Although the human brain reaches 80 percent of its adult weight by the fifth year of life (Dekaban & Sadowsky, 1978), mid and late childhood represents a dynamic period in which several critical modifications to brain structure occur. In addition to the gross volumetric changes described in Chapter 4, related qualitative changes are observed. These include increasing myelination of CNS axons and rapid arborization of dendritic trees (Lenroot et al., 2006). During childhood, specific patterns of global gray density reduction are observed, with primary motor and sensory regions first to develop, followed by regions responsible for speech, language and parietal attention centers, and finally predominantly frontal lobe regions involved in motor coordination and executive function (Gogtay et al., 2004).

The introduction of methods for estimating cortical thickness from MRI data have allowed for new assessments of developmental changes of the cerebral surface. For example, Sowell et al. found substantial decreases in mean cortical thickness in right dorsolateral prefrontal cortex, inferior temporal cortex, and occipitoparietal regions in a sample of 45 children ages 5-11, scanned twice at approximately 2 year intervals (Figure 6.1) (Sowell et al., 2004a). Increases in mean cortical thickness were observed in the regions surrounding the Sylvian fissure and left anterior cingulate cortex and anterior-medial superior frontal gyrus.

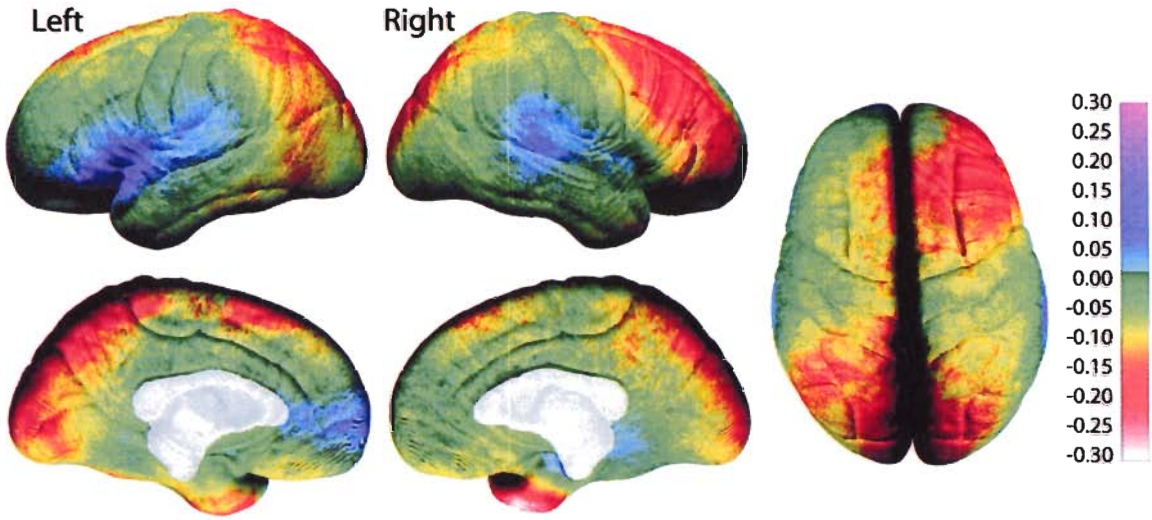

Figure 6.1. Yearly changes in mean cortical thickness in a sample of 45 children ages 5-11. From Sowell et al. (Sowell et al., 2004a).

These studies provide striking depictions of the dynamic changes in brain structure that occur in childhood at high resolution (Gogtay et al., 2004; Sowell et al., 2004a; Sowell et al., 2004b). In this chapter, we attempt to determine how variability in cortical thickness changes with age, and whether the strength of genetic and nongenetic factors on the phenotypes might affect this variability.

Methods

The methods for these analyses are similar to those described in the previous chapter. The subjects (n=600), image processing, and the automated generation of datasets for each vertex are identical. The analyses differ in that an alternative genetic model was used. The model was an extended twin design version of the age-moderator model described in Chapter 4, which allowed for changes in the influence of genetic and nongenetic latent factors on cortical thickness with time (Posthuma et al., 2000b; Posthuma et al., 2000a;

Purcell, 2002). Because univariate ACE models indicated that there was little variance due to the shared environment, we used AE models rather than the full ACE in order to increase statistical power. Thus, four parameters modeling the relationships between latent variables and cortical thickness: the main genetic and unique environmental effects (A and E) as well as parameters allowing age to moderate these variance components (X and Z) analogous to beta weights. As with the models described in the previous chapter, the effect of age and sex on mean cortical thickness was estimated simultaneously.

Figure 6.2: Example of predicted changes in variance components with age (x axis) by vertex (y axis) from the raw output. Color maps depict predicted changes in variance with age for each vertex, with red and white colors indicating high variance, green low variance, and black intermediate variance.

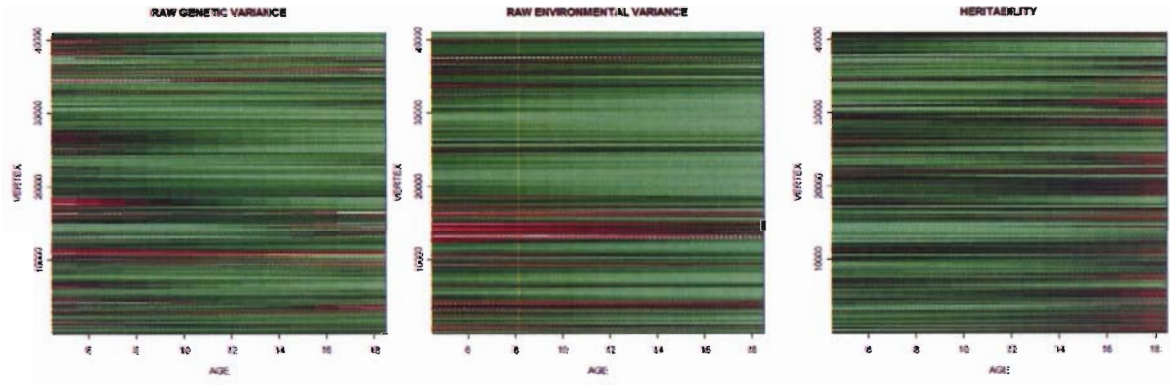

Raw Genetic Variance Raw Environmental Variance Heritability

Results

In general, total variance in cortical thickness decreased with age throughout the cerebrum. Interpretation of the raw predictions of variance changes with age is difficult (Figure 6.2), but does demonstrate heterogeneity in the data. When projected on the brain surface, regionalized differences in both genetic and environmental variance with age are more apparent (Figure 6.3). Though as a rule both genetic and environmental variance decreased globally, there were some interesting exceptions. For example, increases in

genetic variance were observed in the superior parietal lobule, and environmental increases were seen in pre- and postcentral gyri.

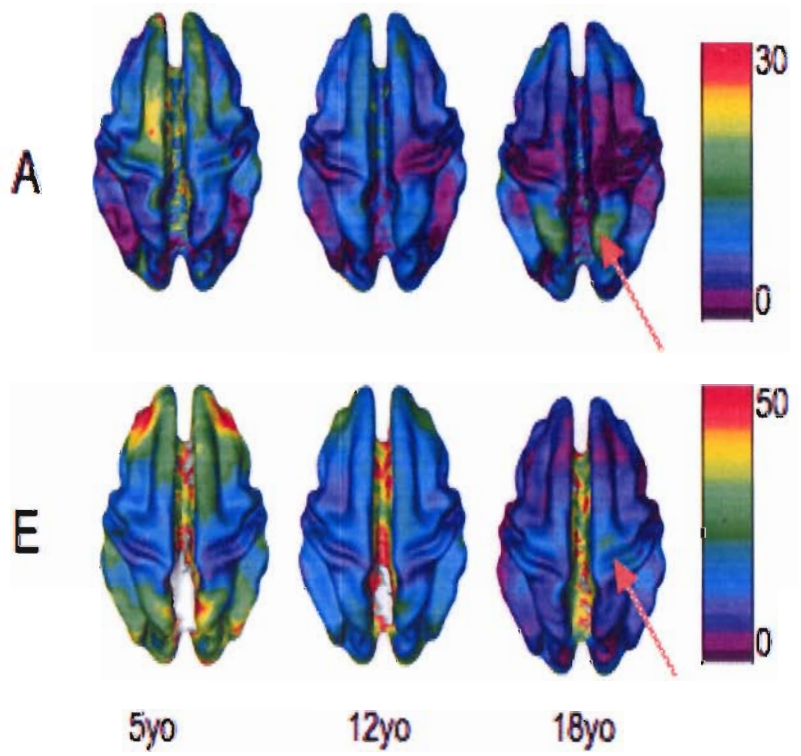

Figure 6.3: Changes in raw genetic (A) and environmental (E) variance predicted by maximum likelihood parameter estimates. Arrows point to example regions where increasing variance is observed.

When considering more traditional metrics of genetic variance, namely heritability, dramatic changes were seen with age (Figure 6.4). The most striking increases were seen in the inferior frontal gyri, particularly on the left side, superior parietal lobule, and left supramarginal gyrus, with decreases in primary somatosensory and motor cortex, parieto-occipital cortex, and the inferior surface of the temporal lobe. As heritability is dependent on total variance, it important to keep in mind that observed increases in heritability are

largely driven by genetic variance decreasing at a slower rate when compared to decreasing environmental variance, rather than outright increases in genetic variance.

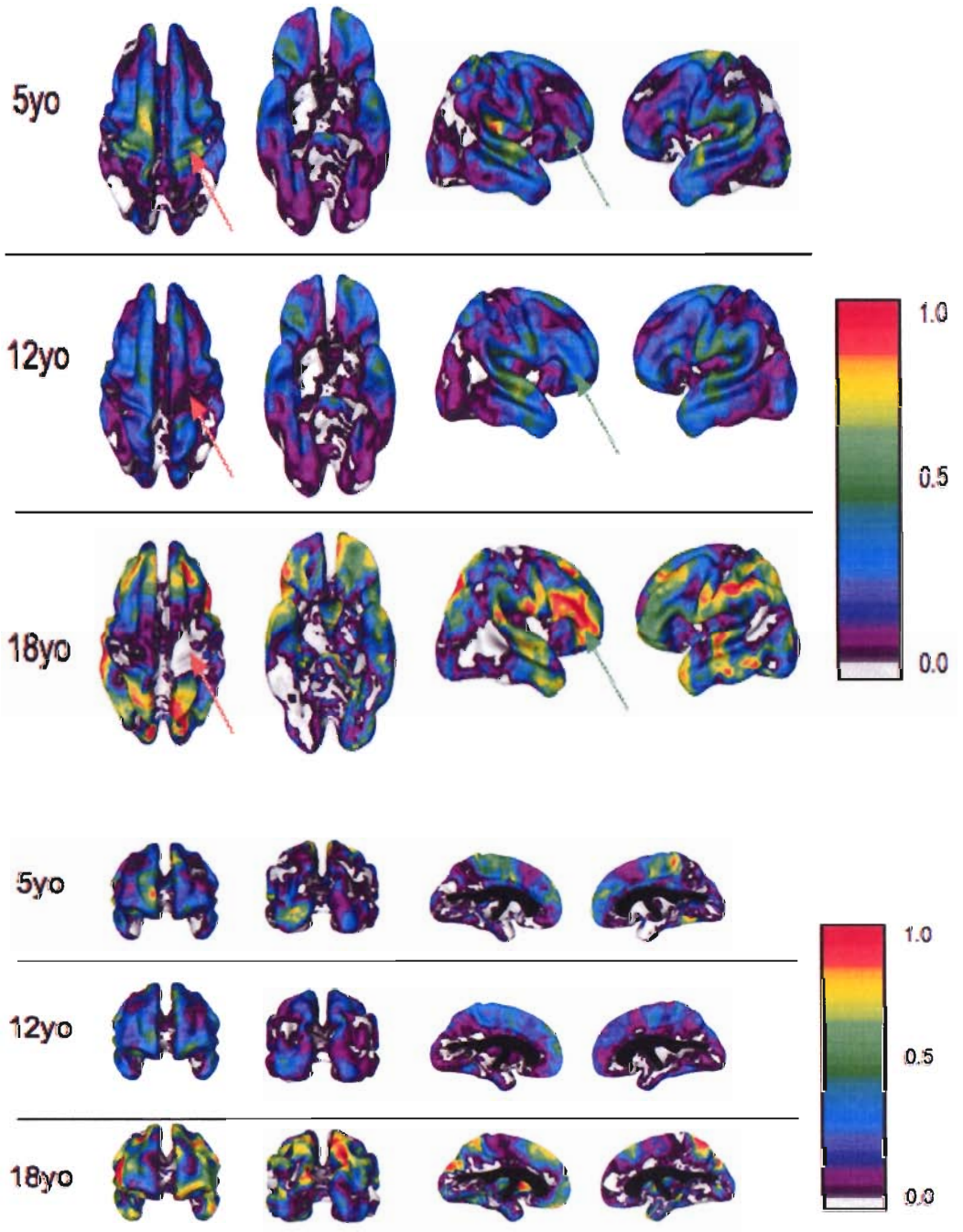

Figure 6.4: Predicted heritability at 5, 12, and 18 years of age based on maximum likelihood estimates from models that allow for age to moderate genetic and environmental influences on cortical thickness. The larger images in the top half of the figure represent superior, inferior, left lateral, and right lateral views, while the smaller images on the bottom show anterior, posterior, and left and right medial views.

Statistical Significance

In order to test the statistical significance of age interactions, we removed the gene x age and environment x age parameters and compared likelihoods to the full model. Figure 6.5 plots p-values by vertex. Even without controlling for multiple testing, very few vertices had statistically significant gene x age interactions. In contrast, strong environmental interactions with age were observed throughout the data.

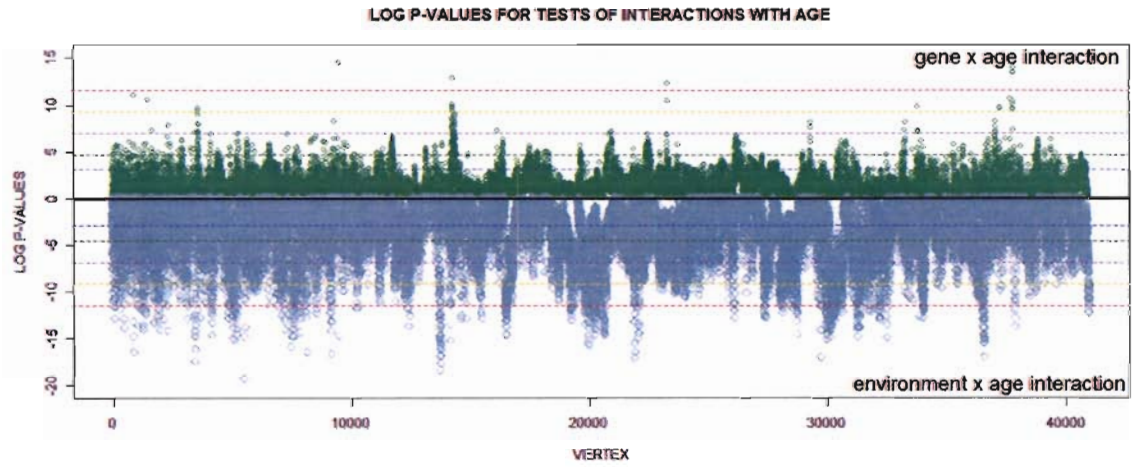

Figure 6.5: Log of p-values by vertex for gene x age interaction (green) and –Log p-values for environment x age interaction (gray). Dotted lines indicate p-values of .05, .01, .001, .0001, and .00001.

When projected on the brain surface (Figure 6.6), the probability map for gene x age effects was quite sparse, with focal clusters of significant vertices in left inferior supramarginal gyrus and the superior frontal gyrus, particularly on the left. Regions of the superior temporal lobe bilaterally also had a few significant voxel clusters. In contrast, a large fraction of the cortex had significantly significant age x environmental interactions. The most significant changes in environmental variance occurred in the frontal lobes bilaterally, the lateral parieto-occipital cortex, and the inferior temporal lobes.

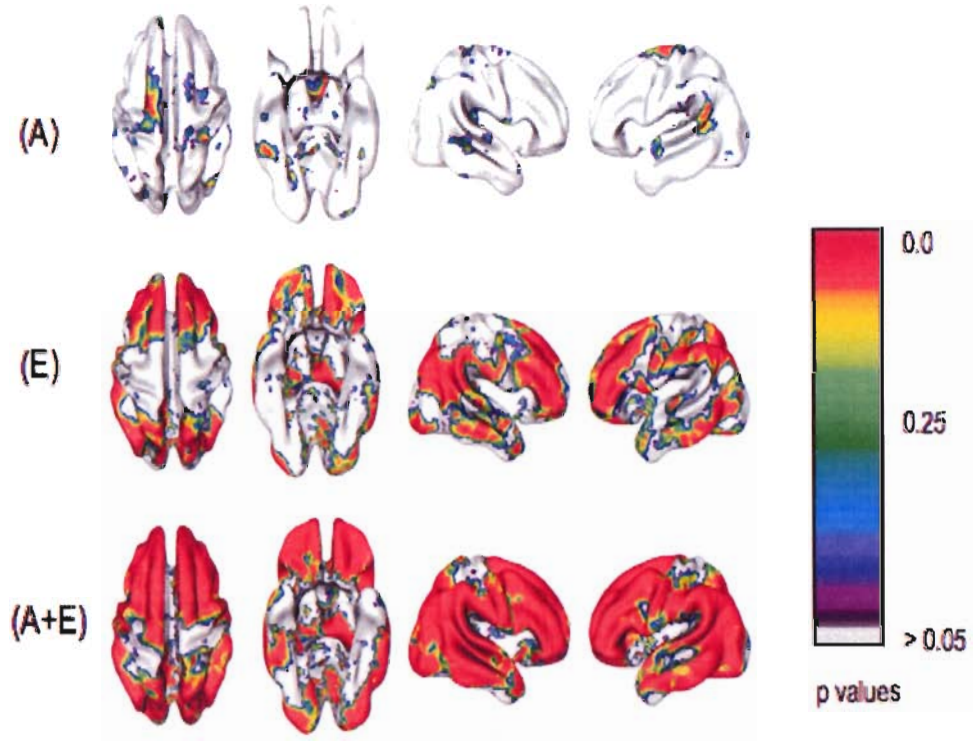

Figure 6.6: Probability maps displaying statistically significant interactions between variance components and age.

Discussion

Prior to MRI, surprisingly little was known about childhood brain development (Casey, Giedd, & Thomas, 2000; Giedd et al., 1996). MRI studies have dramatically increased the knowledge on *how* the brain changes as children grow but have only started to elucidate *why* the changes occur. The present study begins to answer the latter question. Our analyses suggest decreasing global variation in cortical thickness with age. When estimated separately, both genetic and environmental variance tends to decrease, but there are prominent exceptions to the rule. Most notable is an increase in genetically-

mediated variability in the superior parietal lobule, a region previously associated with high heritability.

Yet the power to detect significant gene x age interaction was weak. The most significant interactions were in the superior frontal gyri and supramarginal gyrus, which, like the superior parietal lobule, were *a priori* regions of interest due to their high heritability. As no vertices met threshold for global significance, the utility of probability maps for these analyses is unclear. Maximum likelihood parameter estimates of heritability, however, were quite interesting. Broad sense heritability decreased in primary association cortices and the inferior surface of the brain, with increases in frontal lobe, parietal and temporal association cortices, and language centers. These changes temporally coincide with the development of refined skills in executive function, semantics, and abstraction commonly observed in the second decade of life (Berger et al., 1995; Flavell et al., 1993).

Though these analyses provide a first glimpse of gene by age interactions in cortical development, the results are substantially limited by several difficulties in interpretation. First is the aforementioned lack of power. While it can be argued statistical significance is commonly overemphasized compared to maximum likelihood estimation, given the sheer number of models in these analyses the fact that relatively few vertices were significant at a relatively generous alpha should generate no small degree of skepticism. Concerns may be somewhat ameliorated by the fact that regions with the largest gene x age interactions were already regions of interest, though this observation is made *post hoc* and not mathematically integrated into the model. Changes in heritability with time

were predominantly driven by decreases in environmental variance rather than increases in genetic variance. It is noteworthy, however, that heritability maps in late childhood are very similar to maps previously generated in adults (Thompson et al., 2001). Nevertheless, further longitudinal modeling will be required in order to definitively establish gene x age interactions in children.

7

MULTIVARIATE MODELS OF ONGOGENETICALLY DIVERSE STRUCTURES

"In complex organisms, early stages of ontogeny are remarkably refractory to evolutionary change, presumably because the differentiation of organ systems and their integration into a functioning body is such a delicate process so easily derailed by early errors with accumulating effects. Von Baer's fundamental embryological laws (1828) represent little more than a recognition that early stages are both highly conservative and strongly restrictive of later development."

> --Stephen J. Gould and Richard C. Lewontin, "The spandrels of San Marco and the panglossian paradigm." Proceedings of the Royal Society of London. B 205(1161), 1979.

ADAPTED FROM:

SCHMITT JE, WALLACE GL, ROSENTHAL MA, ORDAZ, S.J., MALLOY EA, CLASEN LS, BLUMENTHAL JD, ROSE AB, KENDLER KS, NEALE MC, GIEDD, JN. MULTIVARIATE ANALYSES OF NEUROANATOMY IN A GENETICALLY INFORMATIVE PEDIATRIC SAMPLE. *NEUROIMAGE*. 2007.

ABSTRACT

An important component of brain mapping is an understanding of the relationships between neuroanatomic structures, as well as the nature of shared causal factors. Prior twin studies have demonstrated that much of individual differences in human anatomy are caused by genetic differences, but information is limited on whether different structures share common genetic factors. We performed a multivariate statistical genetic analysis on volumetric MRI measures (cerebrum, cerebellum, lateral ventricles, corpus callosum, thalamus, and basal ganglia) from a pediatric sample of 326 twins and 158 singletons. Our results suggest that the great majority of variability in cerebrum, cerebellum, thalamus and basal ganglia is determined by a single genetic factor. Though most (75%) of the variability in corpus callosum was explained by additive genetic effects these were largely independent of other structures. We also observed relatively small but significant environmental effects common to multiple neuroanatomic regions, particularly between thalamus, basal ganglia, and lateral ventricles. These findings are concordant with prior volumetric twin studies and support radial models of brain evolution.

Introduction

The inception of neuroembryology might be considered to be when von Baer, over 175 years ago, first observed the neural tube in a vertebrate species and described its primordial subdivisions (von Baer, 1828). In the later half of the nineteenth century, Orr continued this work and detailed the initial segmentation of the nervous system into structural subunits, coined neuromeres, during embryogenesis in reptiles (Orr, 1887). Since these initial discoveries, neuroembryologists have chronicled the remarkable anatomical and cellular changes of the brain in great detail. Somehow, from the relative disorganization of the embryo evolves structure of extraordinary complexity. Despite its well-documented developmental sequence and our ever-expanding understanding of functional neuroanatomy, relatively little is known about the underlying forces responsible for the creation of the human brain. Presumably, our brain development is largely preordained by the genetic program given to us by our parents. Though heroic efforts in molecular genetics have identified thousands of genes with expression within the central nervous system (CNS) (Kandel et al., 2000), attempts to explain normal human variation via genetic polymorphisms responsible for normal human variation in CNS structure have thus far had limited success.

The use of twin designs, wed with magnetic resonance imaging (MRI), provides a powerful non-invasive method to directly estimate the overall effects of genes and environment on human brain structure and function. Several previous studies have presented converging evidence that the predominant sources of variance in brain volumes

are genetic in origin. Most studies performed to date have used small sample sizes (Bartley et al., 1997; Biondi et al., 1998; Steinmetz et al., 1995; Tramo et al., 1998), but a few more recent studies on larger samples have largely confirmed previous results (Baare et al., 2001a; Pennington et al., 2000). More recent twin designs also have included dizygotic twins, which enable the parsing of familial similarities into genetic and shared environmental sources. Though image processing methodologies differ substantially, univariate studies generally estimate that genes account for well over half of the variance in most volumetric regions of interest, particularly of the cerebral cortex. For example, Barré et al. reported that genes accounted for of .90, .82, and .88 of the total variance in total brain, gray, and white matter volumes, respectively, in 112 adult twin pairs (Baare et al., 2001a). Similarly, measures of the corpus callosum areas reveal heritabilities of .80 or larger (Pfefferbaum et al., 2004; Pfefferbaum et al., 2000; Scamvougeras et al., 2003). In contrast, there is virtually no evidence that environmental factors shared between twins influence cortical brain volumes (Pennington et al., 2000; Posthuma et al., 2000b), although this may be obscured by non-additive effects of genes.

The sources of variability of non-cortical structures are less well established, partially due to increased errors in measurement and partly because they are measured less often and usually in studies with quite small sample sizes. For example, the most comprehensive parcellation of the brain published in twins thus far was a study of 10 monozygotic (MZ) and 10 dizygotic (DZ) twin pairs (Wright et al., 2002). This study estimated heritabilities of .60 for corpus striatum, .79 for putamen, and .67 for the cerebellum, and .00 for the thalamus. These estimates, however, were not statistically different from zero owed to

low statistical power. A study by White et al. found high interclass correlations in caudate, putamen, and thalamic volumes in a sample of 12 MZ twins compared to 12 control subjects (White et al., 2002). The role of genes in measures of ventricular volumes also has been uncertain. While the first examination of lateral ventricular volume in twins suggested high heritability (Reveley et al., 1984), subsequent investigations have found a more modest role of genes, if any (Baare et al., 2001a).

Though understanding the genetic epidemiology of individual brain regions is important in elucidating the biological substrates of neuroanatomic structure, determining how structures share common origins is equally vital. As yet, few imaging studies that have examined structural data in from a multivariate perspective, and with the exception of a handful of twin studies (2000; Baare et al., 2001a; Pennington et al., 2000; Posthuma et al., 2000b; Wright et al., 2002), those have focused more on psychopathological disorders with putative disruptions in neural connectivity than on control populations (Faraone et al., 2003; Herbert et al., 2003; Tien et al., 1996; Wright et al., 1999). Such a dearth of information from in vivo structural studies is surprising given the great interest in functional connectivity and multivariate approaches in functional and diffusion tensor imaging (Ramnani, Behrens, Penny, & Matthews, 2004). Determining typical patterns of anatomic relatedness, particularly in comparison to functional models, could be informative in disentangling the relative contributions of ontological origin, subcranial environment, and functional connectivity in the development of neuroanatomic regions.

In this chapter, we attempt to fuse two lines of research, that of twin studies describing the genetic and environmental substrates of neuroanatomic endophenotypes with the rather limited literature examining the multivariate relationships between MRI volumetric measurements. Specifically, we employ factor analysis of several large brain structures (cerebrum, thalamus, lateral ventricles, telencephalic subcortical nuclei, corpus callosum, and cerebellum), of differing ontological origins and diverse functions. Given our genetically informative sample, we also were able to investigate whether global factors exert their influence via genetic or non-genetic mechanisms.

Methods

Sample Selection

127 pairs of monozygotic twins (mean age = 11.6, SD = 3.3; age range = 5.6-18.7; 74 [58%] male, 53 female) and 36 pairs of same-sex dizygotic twins (mean age = 11.0, SD = 3.7; age range = 5.5-18.2; 18 [60%] male, 12 female) were included in this analysis. The sample also included a group of 158 singletons (mean age = 11.3, SD = 3.5; age range = 5.2-18.7; 94 [59%] male, 64 female). Though singletons provide no genetic information, their addition substantially increased the precision of within-individual, cross-region correlations as well as total variance estimates for the phenotypes described below.

Image Processing

Images were analyzed using the same voxel-intensity based classification and probabilistic atlas technique described in chapter 4. The resultant regions of interest obtained from image segmentation were gray and white lobar volumes, cerebellum, thalamus, lateral ventricles, globus pallidus, putamen, caudate nucleus, and corpus callosum. To make the experiment computationally manageable, we chose 6 gross regions of interest that represent different ontological origins and neurological functions. Namely, we measured total cerebral volume (sum of gray plus white lobar volumes), the midsagittal area of the corpus callosum (CC), lateral ventricles (LV), thalamic nuclei, basal ganglia (sum of caudate nucleus, globus pallidus, and putamen; BG), and the total cerebellar volume.

Statistical Analyses

Since our structural models assume normally distributed variables, prior to analyses the distribution of the volumes of each structure was visually inspected for normality. All volumes appeared to be normally distributed, with the exception of lateral ventricles which had a leftward skew, caused by several outliers above the bulk of the distribution. Using SAS, we calculated descriptive statistics for all regions of interest (2000). We also calculated correlations between all volumes for visual inspection prior to modeling. Since preliminary simple linear regressions demonstrated a significant effect of age, race, and sex, we used residuals from multiple regressions including age sex and race as

explanatory variables. Thus, the resultant partial correlation matrix represents inter-anatomic relationships after removing the effects of age, sex, and race.

Raw data were imported into Mx (Neale et al., 2002) for multivariate genetic analyses. Multivariate approaches enable the detection of common factors that influence multiple regions similarly, or alternatively can demonstrate independence of one structure relative to another. The multivariate approach also substantially increases power, as the use of inter-structure correlations provides additional information which improves statistical precision (Schmitz, Cherny, & Fulker, 1998). The presence of genetically informative data additionally allows the parsing of total variance of each structure into contributions from additive genetic (A), shared environmental (C) and unique environmental components (E) based on the differences in genetic correlations between MZ and DZ twins (Neale et al., 1992).

We attempted to model the relationships between structures via two alternative techniques. In addition to traditional factor analytic approaches (described below), we also constructed Cholesky decompositions to calculate descriptive statistics of broad sense heritability and genetic correlations. In all models, we employed maximum likelihood (Edwards, 1972) in order to generate the most probable parameter estimates (i.e. maximum likelihood estimates) for any given model. All models also included a means component that regressed out the contributions of sex, age, and race to the variance in each neuroanatomic region of interest (ROI).

Cholesky Decompositions

We used Cholesky factorization to calculate genetic and environmental correlation matrices, as well as estimates of the proportion of variance due to genetic (a^2), shared environment (c^2), and unique environment (e^2). Since the parameters of a Cholesky decomposition imply directionality of the latent factors, their direct interpretation is probably inappropriate for the present data (Loehlin, 1996). However, the approach permits unbiased estimation of inter-structure correlations, parceled into relationships of either genetic or environmental origin (Crawford & DeFries, 1978). The genetic correlation, which measures the degree of overlap between the genetic forces on two phenotypes, can be written mathematically as:

$$r_{x,y} = \frac{A_{xy}}{\sqrt{(A_x * A_y)}}$$

where A_{xy} is the genetic covariance between structures x and y, and A_x and A_y represent the proportion of the variance due to genetic factors for x and y, respectively (Falconer & Mackay, 1996). Similar calculations can be used to measure the role of shared and unique environment. We also determined the proportion of genetic, shared environmental, and unique environmental covariance relative to the total phenotypic variance. Finally, we calculated eigenvalues from standardized covariance matrices (i.e. correlation matrixes)

for these analyses for A, C, and E separately, to estimate the best number of latent factors to employ in subsequent analyses.

Factor Analyses

A common goal of multivariate analysis is to extract latent constructs that explain the covariance between observed measures. Ideally, the relationship between a large set of variables can be accounted for by a relatively small number of factors. In our analyses, we tested two families of models; that of the independent pathway (i.e. biometric) and the common pathway (i.e. psychometric) models (Kendler, Heath, Martin, & Eaves, 1987; Mcardle & Goldsmith, 1990; Neale et al., 1992). Independent pathways models (IPM) allow genetic, shared environmental, and unique environmental common factors to affect observed variables directly, while in common pathways models (CPM) these factors exert their influence through a shared, latent phenotype (Figure 7.1). In both models, each observed variable is permitted a residual variance term, which can also be parsed into A, C, and E (Evans, Gillespie, & Martin, 2002). Though IPMs are conceptually simpler, CPMs require fewer parameters and are thus favored by the rules of parsimony, all things being equal. However, in the case of neuroanatomic data, a biometric structure would seem the superior hypothesis, as genetic and environmental factors would be expected to impact brain volumes directly via independent channels.

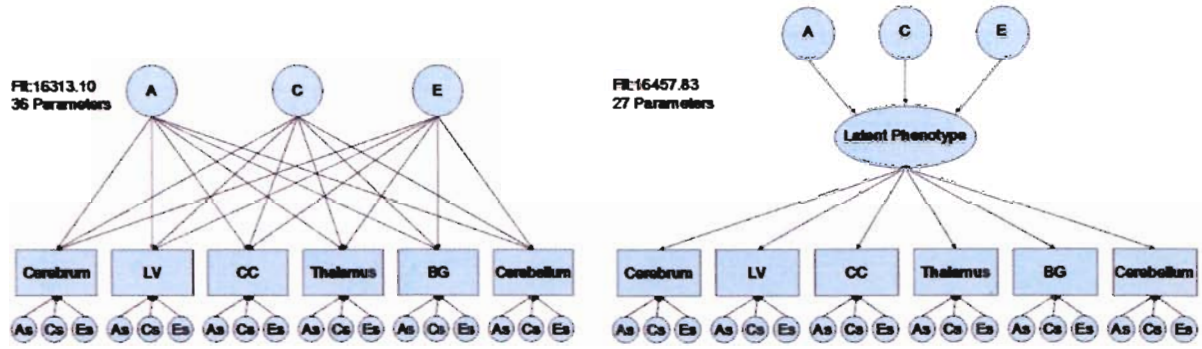

A B

Figure 7.1: Two putative factor models for explaining covariance in neuroanatomic data. While the independent pathways model (a) allow genes A, C, and E to directly influence the observed variables, the common pathways model (b) their effects are mediated via a shared latent variable. A, C, and E are modeled to have means of zero and variances of one. For both models, residual variance can be partitioned as well; thus if common factors are removed, both models collapse to univariate analyses run in parallel.

In addition to models with a single common factor for each of the three etiological sources (A, C, and E), we also constructed more complex models which allowed for 2 common factors for each variance component (Figure 7.2); two-factor solutions were suggested by a scree plot of eigenvalues from the Cholesky decomposition. The models are near the upper limit of mathematical feasibility (i.e. they are close to being underidentified) for a six-variable multivariate analysis. We designated the most complex of these the 2-2-2 IPM and 2-2-2 CPM models since they each contain 2 additive genetic, 2 shared environmental, and 2 unique environmental common factors. For models with 2 common factors of identical etiology (i.e. genetic), we arbitrarily removed one path from the second factor to an observed variable (cerebrum) in order to fix the rotational indeterminacy inherent in models with two or more factors.

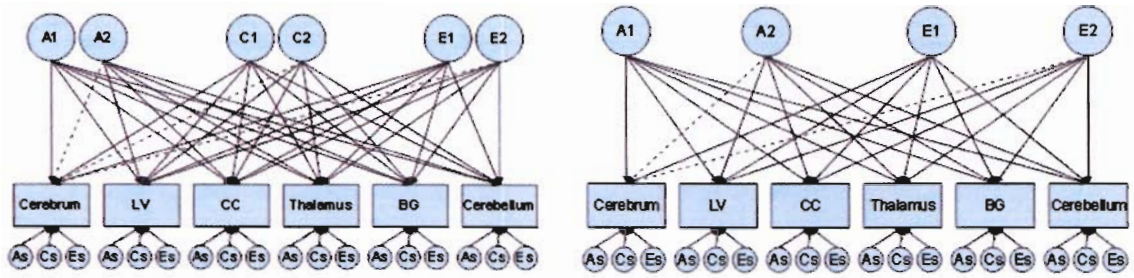

A B

Figure 7.2: Examples of expanded models allowing for multiple factors for each variance component. The 2-2-2 IPM (a) represented the most complex model that was fit to the data; all other models were nested submodels of the 2-2-2 IPM. Dotted lines represent parameters that were fixed to zero in order to make factors orthogonal. The 2-0-2 IPM (b) represents the best-fit model, both by χ^2 tests and AIC.

Under certain regularity conditions, the difference in -2 times the log likelihood (-2LL) of any model and a nested submodel follows a χ^2 distribution with degrees of freedom equal to the difference in the number of parameters. Therefore, we could directly test whether simpler models fit the data significantly worse than more complex versions. In particular, we were interested in determining whether shared environmental factors are important in explaining covariance, since prior univariate analyses would suggest that the shared environment has little to no impact on the variability of most brain regions. For all comparisons, we also calculated Akaike's information criteria (AIC), as $\chi^2 - 2 * df$, which rewards parsimony in addition to goodness of fit (Akaike, 1987); negative values imply that the nested submodel is a more parsimonious fit than the full comparison model.

From the best-fit model (2-0-2 IPM), we standardized parameter estimates to facilitate interpretation and performed orthogonal rotation via the VARIMAX procedure in SAS (2000). In order to generate likelihood-based confidence intervals on the rotated parameter estimates (Neale et al., 1997), we reran the best-fit model in Mx, but freed the

two paths previously fixed to zero and instead fixed the rotated factor loadings of the 2nd A and E common factors that were closest to zero. As an alternative and perhaps more familiar metric of the statistical significance of individual parameters, we also attempted to drop each parameter from the model and test whether the fit to the data deteriorated significantly. This approach is therefore completely analogous to tests of significance of individual beta weights in a multiple regression model.

Gray/White Cerebral Comparisons

Our primary analyses combined cerebral gray and white matter volumes into a single variable, since we had no tissue-specific information for non-cerebral structures. However, since other studies have analyzed gray/white differences (Baare et al., 2001a), we calculated genetic and environmental correlations from a Cholesky decomposition that split total cerebral volume into gray and white matter in order to facilitate comparisons between studies.

Covarying for Total Brain Volume

To investigate *relative* differences in inter-structure covariance rather than *absolute* differences, we repeated the factor analysis procedure described above, but included total brain volume (TBV) as a regressor. With this exception, our mathematical modeling approach was identical to that described previously.

Table 7.1: Descriptive statistics for all anatomic structures analyzed in the present study, split by zygosity status. Mid sagittal corpus callosum is measured in square mm, while volumetric measures are in cubic centimeters.

	MZ (N = 180)		DZ (N = 72)		Singletons (N = 158)	
	Mean	SD	Mean	SD	Mean	SD
Total Cerebrum	1104.59	107.03	1111.63	100.62	1106.06	111.72
Lateral Ventricles	11.71	6.13	10.80	5.21	10.90	6.01
Corpus Callosum	529.99	69.48	527.50	62.32	530.83	81.53
Thalamus	17.22	1.35	17.21	1.38	17.50	1.55
Basal Ganglia	25.04	2.17	25.47	2.17	25.67	2.41
Cerebellum	131.43	11.79	129.84	12.06	129.83	12.26
Cerebral Gray Matter	725.07	68.09	730.88	60.66	726.05	75.14
Cerebral White Matter	379.52	49.79	380.75	48.09	380.01	51.18

Results

Descriptive Statistics

Means and standard deviations for all measures are given in Table 7.1. Singletons, MZs, and DZs had comparable means and variances for all structures measured. A cross-twin correlation matrix for both MZ and DZ groups is provided in Table 7.2. In general, within-structure, cross-twin correlations were substantially higher in the MZ than in the DZ twins, suggesting a strong role of genetic factors on the variance in brain volumes. The role of genetic factors in the cerebellum appeared to be more modest, and even less prominent for the lateral ventricles. When examining within-individual, cross-structure

correlations the cerebrum, thalamus, and basal ganglia were highly intercorrelated. Correlations with the lateral ventricles were low; indeed a small negative correlation was observed between the basal ganglia and lateral ventricular volumes. The corpus callosum also was not correlated with other structures. The cross-twin, cross-structure correlations are much greater in MZ than DZ twins, suggesting that much of the observed correlations between structures are genetically-mediated.

Table 7.2: Cross twin correlation matrix of six neuroanatomic regions. MZ correlations are shown below the diagonal, while DZ twins are above (shaded). Within-structure, cross-twin correlations are shown in bold. Abbreviations are as follows: Cer-cerebrum, LV-lateral ventricles, CC-corpus callosum, Thal-thalamus, BG-basal ganglia, Cb-cerebellum.

	Cer1	LV1	CC1	Thal1	BG1	Cb1	Cer 2	LV2	CC2	Thal2	BG2	Cb2
Cer1	**1.00**	0.22	0.29	0.75	0.77	0.68	**0.34**	0.08	-0.37	0.37	0.42	0.38
LV1	0.34	**1.00**	-0.09	0.06	-0.05	0.27	0.19	**0.39**	-0.08	0.11	0.15	0.10
CC1	0.15	0.02	**1.00**	0.31	0.15	0.22	0.18	-0.08	**0.26**	0.18	0.14	0.22
Thal1	0.80	-0.06	0.15	**1.00**	0.90	0.50	0.20	0.04	-0.41	**0.32**	0.34	0.42
BG1	0.76	-0.11	0.27	0.91	**1.00**	0.53	0.26	0.07	-0.46	0.27	**0.33**	0.41
Cb1	0.58	0.26	0.23	0.48	0.43	**1.00**	0.13	0.09	-0.10	0.13	0.22	**0.54**
Cer2	**0.88**	0.10	0.17	0.66	0.69	0.57	**1.00**	0.12	0.28	0.77	0.85	0.67
LV2	0.14	**0.65**	-0.01	-0.05	-0.15	0.15	0.28	**1.00**	-0.16	-0.03	-0.05	0.15
CC2	0.29	0.09	**0.83**	0.24	0.17	0.23	0.09	0.04	**1.00**	0.30	0.19	0.23
Thal2	0.75	0.03	0.19	**0.80**	0.79	0.51	0.86	-0.09	0.22	**1.00**	0.96	0.56
BG2	0.76	0.00	0.21	0.75	**0.83**	0.52	0.78	-0.16	0.27	0.94	**1.00**	0.56
Cb2	0.59	0.09	0.18	0.52	0.53	**0.79**	0.69	0.30	-0.01	0.63	0.63	**1.00**

Variance components estimates from the Cholesky decomposition are given in Figure 7.3. As expected, neural tissue demonstrated high heritability, with the cerebellum slightly lower than other structures. The variance in lateral ventricular volume was equally divided between genetic, shared environmental and unique environmental

Figure 7.3: Variance components estimates obtained from Cholesky decomposition. a^2, c^2, and e^2 represent the proportion of variance due to additive genetic, the shared environment, and the unique environment, respectively. Bars denote likelihood-based 95% confidence intervals.

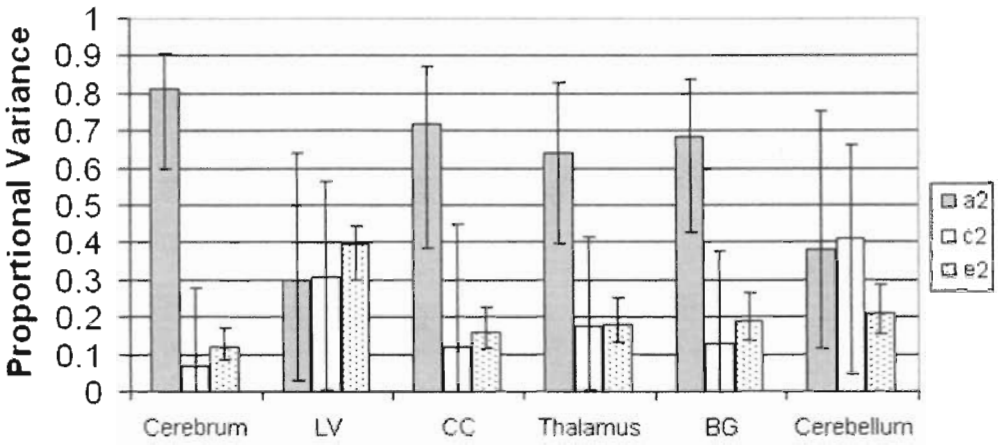

sources. Table 7.3 reports genetic and environmental correlations and reveals the extent to which different structures share genetic and environmental sources of variance. The genetic substrates of cerebrum, thalamus, basal ganglia, and cerebellum are highly intercorrelated. There was a small but statistically significant genetic correlation between corpus callosum and cerebrum, thalamus, and basal ganglia. Cross-structure correlations attributable to the unique (i.e. individual-specific) environment were generally lower, but were still substantial between thalamus and basal ganglia and between cerebrum and cerebellum. Interestingly, there was a small but statistically significant negative environmental correlation between the lateral ventricles and both thalamus and basal ganglia.

Table 7.3: Sources of correlation between neuroanatomic regions. Genetic correlations are given below the diagonal; unique environmental correlations are above it (shaded). 95% confidence intervals are given in parenthesis. Estimates of shared environmental correlations all had extremely wide confidence intervals and were uninformative; therefore they are not reported.

	Cerebrum	LV	CC	Thalamus	BG	Cerebellum
Cerebrum	1	.26 (.06 .43)	.37 (.17 .54)	.35 (.16 .51)	.23 (.03 .42)	.58 (.43 .70)
LV	.18 (-.33 .69)	1	-.05 (-.25 .15)	-.22 (-.40 -.03)	-.23 (-.41 -.03)	.29 (.10 .46)
CC	.30 (.05 .52)	.22 (-.54 .74)	1	.49 (32 .63)	.39 (.19 .55)	.10 (-.11 .30)
Thalamus	.97 (.83 1.0)	.00 (-.49 .65)	.42 (.11 .66)	1	.65 (.52 .75)	.07 (-.13 .27)
BG	.82 (.71 .92)	-.37 (-.80 .24)	.35 (.07 .64)	.91 (.81 .98)	1	.13 (-.07 .33)
Cerebellum	.82 (.59 1.0)	.20 (-.59 .71)	.12 (-.38 .57)	.79 (.44 1.0)	.63 (.29 .93)	1

The role of the environment, however, was quite minor relative to the impact of genetic structures on neuroanatomic covariance. Since the environmental correlation represents the proportion of unique *environmental* variance shared between two structures, it excludes variance attributable to other sources. In other words, these values are standardized relative to the unique environmental variance components, which can be quite small. Table 7.4 reports how genetic and environmental covariance relates to the *total* phenotypic variance in each structure. The highest shared environmental correlation was .17, and the highest unique environmental correlation was .12, with most values near zero. In contrast, the majority of the genetic correlations were greater than .20, with the highest (basal ganglia vs. thalamus) estimated at .70.

Table 7.4: Variance components relative to the total phenotypic variance, with 95% confidence intervals provided. Additive genetic effects are given below the diagonal, and environmental effects (shaded) above the diagonal. The correlations for shared environment are given in italics, below the calculations for the unique environment. The values on the diagonal represent parameter estimates for e^2, c^2, and a^2.

	Cerebrum	LV	CC	Thalamus	BG	Cerebellum
Cerebrum	0.12 (.09 .17) *0.05 (.00 .29)* 0.82 (.59 91)	0.06 (.01 .11) *0.08 (-.12 .27)*	0.05 (.02 .09) *0.01 (-.13 .20)*	0.05 (.02 .09) *0.02 (-.06 .23)*	0.03 (.00 .07) *0.07 (-.03 .28)*	0.09 (.06 .14) *0.13 (-.05 .37)*
LV	0.09 (-.12. 23)	0.40 (.29 .53) *0.30 (.00 .57)* 0.31 (.03 .64)	-0.01(-.07 .04) *-0.08 (-.27 .19)*	-0.06 (-.12 -.01) *0.04 (-.17 .23)*	-0.06 (-.13 -.01) *0.12 (-.11 .27)*	0.08 (.03 .15) *0.07 (-.20 .33)*
CC	0.23 (.03 .39)	0.10 (-.18 .31)	0.16 (.11 .23) *0.13 (.00 .46)* 0.71 (.38 .87)	0.08 (.05 .13) *-0.01 (-.16 .21)*	0.07 (.03 .12) *-0.03 (-.18 .17)*	0.02 (-.02 .06) *0.10 (-.15 .33)*
Thalamus	0.70 (.50 .80)	0.00 (-.20 .22)	0.29 (.06 .45)	0.18 (.13 .25) *0.18 (.00 .38)* 0.64 (.39 .83)	0.12 (.08 .18) *0.11 (-.03 .34)*	0.01 (-.02 .06) *0.15 (-.06 .38)*
BG	0.62 (.40 .74)	-0.17 (-.33 .08)	0.26 (.04 .42)	0.61 (.37 .76)	0.19 (.14 .27) *0.12 (.00 .38)* 0.69 (.42 .84)	0.02 (-.02 .07) *0.17 (-.05 .40)*
Cerebellum	0.46 (.22 .66)	0.07 (-.18 .35)	0.07 (-.17 .32)	0.40 (.17 .62)	0.33 (.10 .56)	0.21 (.15 .29) *0.40 (.04 .67)* 0.39 (.11 .76)

Factor Analyses

Our most parameterized model, the 2-2-2 IPM, did not fit the data significantly worse than the fully saturated Cholesky, despite its comparative simplicity ($\chi^2_{12} = 10.2$, p = .5980, AIC = -13.8). The 2-2-2 CPM also did not differ significantly from the full Cholesky ($\chi^2_{27} = 35.08$, p = .1369, AIC = -18.92) but was more parsimonious. The relative equivalence between the IPM and CPM models was driven by the eleven shared environmental common parameters in the IPM that were largely uninformative.

Removing these parameters (producing the 2-0-2 IPM) did not significantly affect the fit of the model (vs. full Cholesky: $\chi^2_{23} = 17.0$, p = .8093, AIC = -29.0; vs. 2-2-2 IPM: $\chi^2_{11} =$ 6.8, p = .8147, AIC = -15.2) and produced superior explanation of the data compared to the 2-2-2 CPM. Further attempts at reduction of the 2-0-2 IPM were unsuccessful (vs. 1-0-2 IPM: $\chi^2_5 = 20.4$, p = .0011, AIC = 10.4; vs. 2-0-1 IPM: $\chi^2_5 = 61.8$; p < .0001; AIC = 51.8), as were other factorial combinations of IPM and CPM submodels.

The varimax-rotated parameter estimates for the 2-0-2 IPM are given in Table 7.5. Of the two common genetic factors identified, one strongly influenced variance of cerebrum, thalamus, and basal ganglia, with factor loadings (analogous to standardized partial regression coefficients) of about .85. This factor also accounted for a substantial proportion of the genetic variance of the cerebellum, and had a low but statistically significant effect on corpus callosum, but no impact on lateral ventricular volumes. The second genetic factor predominantly comprised the modest genetic effects on ventricular volume, with a statistically significant negative factor loading on the basal ganglia compartment.

Table 7.5: Parameter estimates for the best-fit factor model (2-0-2 IPM). A1 and A2 represent common genetic factors, while E1 and E2 are environmental sources unique to individuals, but shared between brain regions. Shared environmental common factors were not statistically significant. Values represent factor loadings, with 95% confidence intervals given in brackets. Factor loadings for structure-specific factors also are given, as are proportional variance components estimates under this model, for each structure in the analysis.

	Common Factors				Structure-Specific Factors			Heritability Estimates		
	A1	A2	E1	E2	As	Cs	Es	a^2	c^2	e^2
Cerebrum	.85* (.76 .95)	.22‡ (.07 .35)	.13* (.06 .21)	.29* (.21 .37)	.33‡ (.23 .42)	.02 (-.48 .52)	.14 (.01 .30)	.88 (.77 .91)	.00 (.00 .13)	.12 (.09 .17)
LV	.05 (-.09 .19)	.57* (.29 .84)	-.17‡ (-.31 -.03)	.27* (.14 .41)	.00 (-.93 .93)	.53 (.29 .78)	.54 (.46 .62)	.32 (.09 .68)	.28 (.00 .48)	.39 (.29 .53)
CC	.28* (.16 .40)	.06 (-.11 .24)	.24* (.15 .33)	.06 (-.02 .14)	.83* (.57 .95)	.26 (-.61 1)	.33 (.28 .38)	.75 (.40 .88)	.06 (.00 .14)	.17 (.12 .24)
Thalamus	.85* (.76 .95)	.01§	.40* (.32 .49)	.00§	.00 (-91 .92)	.30 (.22 .37)	.17 (.07 .28)	.72 (.64 .85)	.09 (.00 .14)	.19 (.14 .26)
BG	.84* (.74 .94)	-.17‡ (-.36 -.05)	.31* (.22 .40)	-.01 (-.09 .07)	.28 (.13 .43)	.00 (-.37 .36)	.31 (.01 .25)	.81 (.70 .86)	.00 (.00 .08)	.19 (.14 .26)
Cerebellum	.64* (.53 .75)	.14‡ (.004 .34)	.02 (-.08 .12)	.31* (.20 .42)	.33 (-.01 .66)	.49 (.27 .70)	.34 (.01 .26)	.55 (.36 .81)	.24 (.00 .40)	.21 (.16 .29)

* $p < .001$; ‡ $p < .05$; §Fixed to make factors orthogonal

Similarly, two unique environmental common factors were identified, though the pattern of effects was quite different than that of the genetic factors. One environmental factor primarily contributed to variance in all deep structures (thalamus, BG, LV, and corpus callosum), with antagonism between the ventricles and the other variables. The second represented relationships between the cerebrum, lateral ventricles, and cerebellum.

Structure-specific factors contributed far less variance than the common factors with the exception of the corpus callosum where genetic factors specific to that structure accounted for 69% of the variance. Less than 10% of the variance in corpus callosum size could be explained by genetic sources that also affected other structures in the analysis.

Gray/White Correlations

Genetic correlations between cerebral tissue compartments and other structures are given in Table 7.6. The genetic effects influencing gray and white were highly correlated (.84; 95% CI [.65 .99]), while there was virtually no environmental correlation (.-.04; 95% CI [-.24 .17]). In general, correlations did not differ when comparing either cerebral gray or white to other structures. The primary exception was corpus callosum, which had higher genetic (.49 versus .09) and environmental (.43 versus .16) correlations with cerebral white matter volumes relative to gray. Additionally, the environmental correlation between cerebellum and cerebral gray (.57) was significantly higher than cerebellum with cerebral white (.22).

Table 7.6: Genetic and environmental correlations between the cerebrum and other neuroanatomic structures, after segmenting cerebral tissue into gray and white matter. 95% confidence intervals are given in parentheses.

	Additive Genetic		Unique Environment	
	Gray	White	Gray	White
Cerebral Gray	**1.00**	.84 (.65 .99)	**1.00**	-.04 (-.24 .17)
Cerebral White	.84 (.65 .99)	**1.00**	-.04 (-.24 .17)	**1.00**
LV	.11 (-.42 .65)	.18 (-.32 .72)	.19 (-.01 .37)	.14 (-.05 .33)
CC	.09 (-.21 .39)	.49 (.25 .69)	.16 (-.06 .36)	.43 (.25 .59)
Thalamus	.88 (.69 .99)	.96 (.82 1)	.25 (.05 .44)	.38 (.20 .54)
BG	.77 (.60 .91)	.80 (.67 .94)	.24 (.03 .43)	.16 (-.05 .36)
Cerebellum	.73 (.44 .99)	.88 (.56 1)	.57 (.41 .69)	.22 (.03 .41)

Total brain volume as a covariate

As expected from the previous finding that a single genetic factor dominated inter-structure covariance, the genetic correlations between structures dropped substantially when adjusting for total brain volume (Table 7.7). We still detected a high, statistically significant genetic correlation between thalamus and basal ganglia (r_G = .72), and a negative genetic correlation between basal ganglia and the lateral ventricles (r_G = -.88). The non-genetic inter-structure correlations, however, differed substantially when the analyses was adjusted for global effects. Rather than a general pattern of positive correlations between structures detected previously (with the exception of negative correlations involving lateral ventricles), the environmental correlations had a more complex pattern. Both the thalamus and basal ganglia structures were *negatively* correlated with cerebral volumes, but positively correlated with each other. The lateral ventricles retained their mostly negative environmental correlations with other structures.

There was a small but statistically significant negative environmental correlation between the cerebellum and the thalamus, and all telencephalic tissues showed negative correlations with the cerebellum, though none approached statistical significance.

Table 7.7: Genetic and environmental correlations derived after regressing on total brain volume. Genetic correlations are given below the diagonal, and environmental above the diagonal and shaded.

	Cerebrum	LV	CC	Thalamus	BG	Cerebellum
Cerebrum	1	.17 (-.02 .36)	.15 (-.06 .34)	-.41 (-.56 -.22)	-.41 (-.57 -.21)	-.16 (-.35 .05)
LV	.13 (-.87 .59)	1	-.09 (-.28 .12)	-.36 (-.52 -.19)	-.33 (-.49 -.15)	.20 (.00 .38)
CC	.34 (.01 .82)	.12 (-.61 .68)	1	.33 (.14 .50)	.22 (.01 .41)	-.12 (-.32 .09)
Thalamus	.34 (-.16 1)	-.59 (-.99 .32)	.64 (.00 .99)	1	.59 (.44 .71)	-.27 (-.44 -.07)
BG	.02 (-.19 .80)	-.88 (-1 -.34)	.26 (-.10 .64)	.72 (.21 1)	1	-.10 (-.29 .11)
Cerebellum	-.09 (-.96 1)	.12 (-1 .85)	-.23 (-1 .39)	-.25 (-.99 .82)	-.03 (-.90 1)	1

When performing factor analyses, the 2-2-2 IPM (χ^2_{12} = 8.1; p = .7807; AIC = -15.94) did not fit the data significantly worse than a Cholesky decomposition. However, the 2-2-2 CPM was rejected relative to either the full Cholesky (χ^2_{30} = 175.26; p < .0001; AIC = 115.26) or the 2-2-2 IPM (χ^2_{18} = 167.21; p < .0001; AIC = 131.21). A stepwise removal of latent factors indicated that the 2-0-2 IPM was once again the best fit model (vs. Cholesky: χ^2_{24} = 19.3; p = .6814; AIC = -26.66, vs. 2-2-2 IPM: χ^2_{18} = 11.2; p .4199; AIC = -10.72). However, the patterns of genetic and environmental associations differed substantially when examining residual variance after adjusting for TBV (Table 7.8). In general, the structures shared less variance with each other, though one common factor indicated that the thalamus and the basal ganglia shared a substantial proportion of their genetic variance, and a second genetic factor influenced both the cerebral compartment

and the corpus callosum. Two common individual-specific environmental factors also emerged; one influencing thalamus and the subcortical compartment in an opposite direction to cerebrum and lateral ventricles, and one whose effects influenced cerebrum and cerebellum in opposite directions.

Table 7.8: Parameter estimates for the best fit model (2-0-2 IPM) after covarying for total brain volume.

	Common Factors				Structure-Specific Factors			Heritability Estimates		
	A1	A2	E1	E2	As	Cs	Es	a2	c2	e2
Cerebrum	.00	.48	-.39*	.40*	.68‡	.00	.01	.68 (.35 .77)	.00 (.00 .30)	.32 (.22 .44)
LV	.37	.10	-.23*	-.14‡	.13	.66	.57	.17 (.06 .66)	.43 (.00 .55)	.40 (.30 .52)
CC	.17	.50	.08	.18*	.60	.44	.35	.65 (.34 .88)	.19 (.00 .49)	.16 (.11 .22)
Thalamus	.52	.28	.50*	.16‡	.27	.47	.30	.42 (.23 .71)	.22 (.00 .38)	.36 (.27 .48)
BG	.79	-.03	.41*	.06§	.00	.00	.44	.64 (.49 .74)	.00 (.00 .09)	.36 (.26 .50)
Cerebellum	.05	.04§	-.06	-.23*	.50	.69‡	.46	.24 (.00 .70)	.49 (.05 .74)	.27 (.20 .37)

* $p < .001$; ‡ $p < .05$; §Fixed to make factors orthogonal

Discussion

One of the fundamental questions in neurogenetics is how our relatively simple genetic programming combines with environmental exposure to produce variation in human brain volumes. Our data suggest that not only do genes play the predominant role in generating the observed volumetric diversity, but that most of the genetic variance is determined by genes that are shared between the major gross neural subdivisions. Concordant with previous univariate studies, the contribution of the shared environment to variance was negligible, while the individual-specific environment had smaller but statistically significant factors common to multiple regions; an environmental factor influencing ROIs beneath the cortical surface (corpus callosum, thalamus, and basal ganglia), and a non-subcortical factor (cerebrum, lateral ventricles, and cerebellum) were identified. Though both genetic and non-genetic effects are critical for explaining neuroanatomic covariance, these data additionally suggest that, at this level of spatial resolution, genes and environment exert their influences on brain variation largely independently of one another.

Such a strong role of genes on the correlations between brain volumes was not unexpected given prior multivariate twin studies. One study methodologically similar to the present one, performed by Barré et al., examined relationships between height, intracranial volume (ICV), total gray matter, total white matter, and lateral ventricular volumes in 54 MZ and 58 DZ adult twin pairs and 34 sibs of DZ pairs via variance component analyses (Baare et al., 2001a). They found remarkably similar estimates of

genetic (.68) and unique environmental (.04) correlations between gray and white matter, and no statistically significant evidence of genetic correlations between the lateral ventricles and other regions of interest. Nevertheless, the two studies do differ in several aspects, most notably in that the present study includes several neuroanatomic regions of interest while the study by Barré et al. focused on a few global cerebral measures and correlations between these measures and height and ICV. A similar approach was taken in an earlier study by Posthuma et al. which used a trivariate Cholesky decomposition of height, intracranial space, and cerebellar volume in an extended twin design (Posthuma et al., 2000b) of 111 twin pairs and 34 sibs. They estimate cerebellar heritability of .88 with significant sex effects on mean cerebellar volume, with a relatively high genetic correlation to the ICV (.57) and a low genetic correlation to height (.25). Though this study represents an important contribution to methodological design and advancement of the use of volumetric data as a novel endophenotype, its focus is not on relationships between brain regions but rather on relationships between brain volumes and non-neural phenotypes.

To date, only two other studies, to our knowledge, have employed genetically informative data to describe multivariate neuroanatomic relationships. A principle components analyses by Pennington et al. on a modest sample of 34 MZ and 32 DZ late teen or young adult twin pairs parcellated the brain into 7 cortical gray compartments and 6 noncortical structures (white matter, basal ganglia, brain stem, hippocampus, cerebellum, and the central gray nuclei including the thalamus) found that two factors could account for 64% of the total phenotypic variance. While cerebral structures loaded

primarily on the first factor, all other structures loaded on the second (except central gray, which loaded equally on both). Both factors were significantly more correlated in MZ than in DZ pairs, suggesting a strong genetic component to each. This approach differs substantially from the present study, not only in its use of principal components analyses rather than factor analyses, but also because it generated factors prior to decomposing variance. By contrast, we determined factor structure and variance components simultaneously using maximum likelihood. The study by Pennington et al. also has been criticized since greater than 70% of both MZ and DZ samples had dyslexia, though it is unclear how large of an effect this difference would have on a global multivariate analysis.

Despite the differences in study design, the findings between the two studies are largely complementary. Both find two strong genetic factors influencing inter-structural covariance. The factor loading pattern of the Pennington study does differ in that non-cortical structures are not particularly correlated with cortical structures. This discrepancy may be owed in part to the use of ICV as a covariate in the Pennington study. After regressing out the effects of total brain volume, we did observe a genetic factor that was primarily cerebral (total cerebral volume and corpus callosum), with a second genetic factor that loaded on non-genetic structures (with thalamus loading on both). However, the cerebellar measure in the present study had no genetic covariance with other structures after adjusting for brain volume, while in the Pennington study the cerebellum had a factor loading of .71 on the "non-cortical" factor. Though the exact cause for the discrepancy is unclear, it could be due to differences in statistical methodology, as

principle components analyses include structure-specific variance within its factors, while the factor analytic approach explicitly defines this variance as independent of common factors. Differences in cerebellar quantification also may play a role.

The final extant multivariate twin study by Wright et al. (Wright et al., 2002) parcellated the brain into regions with extremely high spatial resolution. Ninety-two (primarily cerebral) gray matter ROIs were automatically defined, roughly according to Brodmann's areas. Global effects were accounted for by adjusting for total gray volumes. Genetic correlations for each ROI pair were first calculated via a series of bivariate factor analyses, and then principle components analyses were applied to the resultant correlation matrix. This study identified two putative supra-regional principle components under genetic control. Specifically, a frontoparietal limbic/paralimbic factor and a factor related to audition (lateral temporal cortex, insula, occipitofrontal, and other frontal regions) were found; factor loadings, however, were quite low ($< |0.25|$). These findings would suggest that genes are involved in generating functional relationships between distant brain regions. Though extremely provocative, Wright et al.'s study is limited by low power, due to small sample size (10 MZ and 10 same sex DZ pairs) and issues of multiple testing.

The process of neurogenesis is extraordinarily complex. Though neurovolumetric changes are observed throughout childhood (Giedd et al., 1996; Gogtay et al., 2004; Sowell et al., 2004a; Sowell, Thompson, Holmes, Jernigan, & Toga, 1999; Sowell et al., 1999), the majority of brain formation occurs *in utero* and most of the genes involved in

neurodevelopment are also expressed at this time (Rakic & Lombroso, 1998; Rubenstein & Rakic, 1999b; Rubenstein et al., 1999a). In animal models, a multitude of genes responsible for brain patterning have now been identified, whose products include transcription factors, morphogens, and apoptotic factors (Rubenstein et al., 1999b). The initial discovery of the *Hox* family of transcription factors and their segmental patterns of expression in the hindbrain have argued strongly for the neuromeric models of brain organization (Lumsden & Krumlauf, 1996; Mcginnis & Krumlauf, 1992; Puelles, 2001a); more recent studies on the forebrain have suggested that although its development is more plastic and cell lineages appear less restricted, the prosencephalon also follows segmental (i.e. prosomeric) patterning based on expression of homeotic and related genes (Anderson, Mione, Yun, & Rubenstein, 1999; Puelles, 2001a; Rubenstein et al., 1999b; Puelles, 2001a; Rubenstein et al., 1999b) . Though mutations in neurodevelopmental genes have been shown to produce severe pathological states in humans (Clark, 2004), the genetic and environmental agents responsible for typical human variation are still unknown.

Theoretically, genetic associations between neuroanatomic structures could arise via numerous putative mechanisms; several general models can be considered while interpreting the present data. First, brain volumes may be related genetically via ubiquitous gene products involved in basic cellular metabolism, cell growth, differentiation, or other global processes expressed throughout neuroectodermal derivatives (Rakic, 1995). For example, functional variation in housekeeping genes or cell cycle regulators might be expected to produce genetic correlations between all brain

regions that express them (and perhaps other tissues), if they produce downstream effects on volumetric measures via changes in cell proliferation or survival (Figure 7.4). Second, correlations in brain volumes may represent vestigial relationships generated prenatally between structures with shared ontogenetic origins. Region-specific expression of transcription factors during neuroembryonic patterning would be one example of gene products producing regional correlations during embryogenesis. In this case, one would expect stronger genetic relationships among structures whose development diverged more recently (e.g. thalamic and hypothalamic volumes to be correlated via their shared diencephalic origin). Third, functional interrelationships between structures may generate volumetric correlations via morphological changes associated with increased connectivity. This hypothesis is essentially a generalization of the Protocortex model, which states that neocortical development is determined by extrinsic influences, such as effects of thalamic innervation (Schlaggar & O'Leary, 1991; O'Leary, 1989). Thus, one might expect structures in the visual processing network, such as V1 and the lateral geniculate nucleus, to be structurally correlated despite being potentially unrelated spatially or ontogenetically. Finally, genetic correlations may result from shared supra-regional gene expression triggered postnatally, in the present data from birth to the age of scan acquisition, approximately mid-childhood.

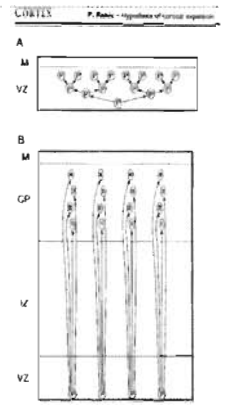

Figure 7.4: Rakic's hypothesis of cortical expansion. Proliferation (panel A) of progenitor cells (P) in the ventricular zone (VZ) precedes migration (panel B) to the cortical plate (CP). An increase in the number of cell cycles prior to migration would produce a dramatic increase in the number of cortical neurons at maturity. Adapted from Rakic et al, 1995.

The present data indicates that much of the variability in brain volumes is caused by genes shared between all tissue compartments. This finding is concordant with evolutionary genetic models of brain development which hypothesize global, genetically-mediated differences in cell division as the driving force behind interspecies differences in total brain volume (Finlay & Darlington, 1995) as well as with the radial unit hypothesis of neocortical expansion proposed by Rakic (Rakic, 1995). Comparative neuroanatomic analyses of multiple mammalian species (e.g. Figure 7.5) have shown that total brain volume is highly correlated with regional volumes, irrespective of region (including neocortex, striatum, thalamus, and cerebellum), and accounts for the vast majority (>96%) of the observed volumetric variance in all regions measured except for the olfactory bulb (Darlington, Dunlop, & Finlay, 1999; Finlay et al., 1995). Such strong correlations are thought to reflect a generalized adaption to specific selective pressures; although it is more expensive, in terms of energy, to expand the computational resources of the entire brain when only specific functions are needed, the molecular adjustments required are far fewer than those required to completely repattern gross neural architecture.

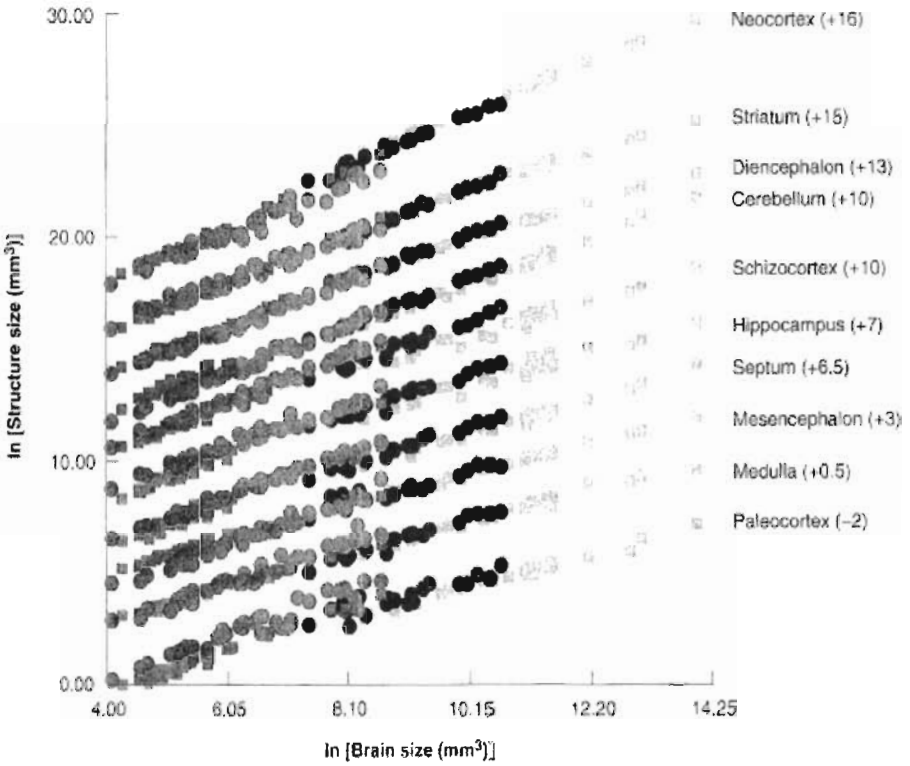

Figure 7.5: Scatterplots regressing the size of several neuroanatomic substructures (labeled at right) on total brain volume for 131 mammalian species. Parameters in parenthesis represent arbitrary constants added in order to prevent overlap.

In contrast, we found little evidence of genetic factors mediating region-specific neurodevelopment. The most notable ontological "oddball" in the present study was the cerebellum. Developmentally, the cerebellum diverges from the other regions soon after neural tube formation; while cerebrum, corpus callosum, and subcortical structures all are derived from the embryonic prosencephalon, cerebellar tissue is primarily derived from the rombencephalon (Kandel et al., 2000). However, differences in genetic correlations between the cerebellum and other structures were not particularly striking, either before or after removing the effects of TBV. Similarly, we did not detect weaker genetic associations between the thalamus when compared to the telencephalic cerebral volumes or the predominantly telencephalic basal ganglia (Fishell, 1997; Kandel et al., 2000;

Puelles, 2001a). Though genetically-mediated regional brain patterning certainly plays a major and undisputed role in mammalian neurodevelopment, our data would suggest that it plays a surprisingly minor role, at least at our level of volumetric measurement, in the generation of structure-specific *variation* within the typical human population. Functional relationships, for example, may be more important for defining volumetric correlations between the structures measured as basal ganglia, thalamus, and neocortex all are tightly linked functionally.

Though the unique environment had a relatively minor effect on the volumes of the structures measured, our relatively large sample allowed us to describe its role on the correlations between structures with high precision. We found that structures in spatial proximity were significantly and positively correlated via individual-specific environmental factors shared between multiple anatomic regions. In other words, the environment tends to influence nearby structures similarly. The principle exception was that correlations between subcortical nuclei and the lateral ventricles were significantly negatively correlated. Given that atrophy of either the basal ganglia or the thalamus can be associated with increased lateral ventricular volume in several diseases (Harris et al., 1999; Gaser, Nenadic, Buchsbaum, Hazlett, & Buchsbaum, 2004; Harris et al., 1999), an antagonistic effect between ventricles and subcortical nuclei was not unexpected. However, as our calculations represent environmental effects in typically developing children, these findings suggest that the correlation is not always pathological. Structural modeling identified two statistically significant environmental factors mediating the environmental correlations, one representing subcortical structures and one representing

the cerebrum and cerebellum. It is possible that common environmental effects reflect stochastic processes of major effect occurring early in development, or smaller, more continuous processes whose effects are additive. Though the exact nature of these factors cannot be deduced, this finding suggests the tantalizing possibility of an internal/external dichotomy for environmental effects.

Despite the wealth of information obtained from this study, certain limitations must be considered. Fundamental to its complex design involving intricate multistep techniques, this study inherits all of the limitations and assumptions of its component pieces, namely studies of twins, volumetric MRI, and structural equation modeling. The twin design is often criticized for its reliance on the equal environment assumption (EEA), which states that, on average, MZ and DZ twin pairs do not differ *relative to the phenotypes of interest.* It is now widely believed that much of the concerns regarding the EEA are overstated at best (Evans et al., 2002); regardless, it is unlikely that general violations of the EEA would substantially impact regional brain volumes (Hulshoff Pol et al., 2002). Secondly, the nature of our predominantly Caucasian, pediatric sample may limit generalizations to other populations. Aging, in particular, could reduce the strength of genetic factors on explaining neurovolumetric variance. Twin studies on geriatric populations, however, have shown that heritability for brain volumes remains high even into the seventh decade of life (Carmelli et al., 2002b; Carmelli et al., 2002a; Pfefferbaum et al., 2004; Pfefferbaum et al., 2000), and it is thus unlikely that patterns of neuroanatomic covariance change dramatically over the human lifespan. Thirdly, it is possible that a proportion of the large genetic covariance observed between structures is

owed to genes responsible for general body size, rather than brain-specific genetic factors. Though the present study could not examine the contribution of body size on brain volume, Barré et al. have shown that the genetic correlations between height and total gray or white matter are low (.19 and .16, respectively), suggesting that most of the observed genetic correlations between neuroanatomic structures can not be explained by body size alone (Baare et al., 2001a).

Finally, our volumetric measures may be disproportionately sensitive to the proliferative and apoptotic components of neurodevelopment. The use of morphometrics, such as deformation-based morphometry (Ashburner et al., 1998) rather than volumetric approaches might be more able to detect regionalized topological similarities that reflect common embryologic origins.

8

MULTIVARIATE ANALYSES OF CEREBRAL VOLUMETRIC RELATIONSHIPS

"If it were demonstrated...that the lesions that abolish speech consistently occupy one determinate convolution, one could hardly fail to admit that this convolution is the seat of the faculty of articulated language, and, that once the existence of a first localization was admitted, the principle of localization by convolutions would be established."

> --Paul Broca, "Remarks on the Seat of the Faculty of Articulated Language, Following an Observation of Amphemia." (1861). Translated by Christopher Green.

ABSTRACT

In this chapter, we examine the interrelationships between eight cerebral lobar volumetric measures via both exploratory and confirmatory factor analyses. These analyses suggest the presence of strong genetic correlations between cerebral structures, particularly between regions of like tissue type or in spatial proximity. Structural modeling estimated that most of the variance in all structures is associated with highly correlated lobar latent factors, with differences in genetic covariance and heritability driven by a common genetic factor that influenced gray and white matter differently. Reanalysis including total brain volume as a covariate dramatically reduced the total residual variance and disproportionately influenced the additive genetic variance in all regions of interest.

Introduction

The human telencephalon, or cerebrum, is approximately 950 grams at adulthood and represents over 80% of total brain weight (Jenkins & Truex, 1963). The cerebrum has long been considered the region of the brain most central to higher cognitive functions such as thought, memory, and complex sensory processing; functions that are associated with particular spatial locations within the cerebral hemispheres (Kandel et al., 2000). These facts are so obvious to us today that it may difficult to contemplate that, prior to the pioneering work of Paul Broca on aphasia in the mid-nineteenth century, little was known about the regional specificity within the cerebrum or indeed, whether cerebral function was localized at all. Broca's identification of a replicable functional center for productive language initiated the ongoing inquiries into the nature of functional neuroanatomy. Though debate continues regarding the specific locations associated with very specific functions, the overarching geography of the brain has been reasonably mapped. As the neuroanatomic "continents" have come into focus, it is now well-established that the gross sensory, motoric, and cognitive functions roughly correspond to the lobar subdivisions identified by early neuroanatomists (Nolte, 1999).

In this chapter, attempt to address question of whether individual differences in cerebral lobar volumes are generated by genetic factors exhibit regional specificity within the cerebrum, or rather are dominated by global or tissue-specific effects. This end, we

employ similar methods to those detailed in the previous chapter, as well as a novel, confirmatory approach.

Methods

The sample was identical to that described in the previous chapter. To briefly restate, we modeled MRI data from 127 MZ twin pairs (mean age = 11.6, SD = 3.3; age range = 5.6-18.7; 74 [58%] male, 53 female), 36 same-sex DZ twin pairs (mean age = 11.0, SD = 3.7; age range = 5.5-18.2; 18 [60%] male, 12 female), and 158 singletons (mean age = 11.3, SD = 3.5; age range = 5.2-18.7; 94 [59%] male, 64 female). Image processing of the native images was performed as described in Chapter Four. In these multivariate analyses, however, we included only data from cerebral lobar volumes (frontal, parietal, temporal, and occipital lobes), for gray and white tissue compartments separately.

Statistical Analyses

Preliminary inspection of normal quantile plots of the observed variables demonstrated that they met the normality assumptions of structural equation modeling with likelihood based optimization. Using R (Ihaka & Gentleman, 1996; R Development Core Team, 2005) we calculated correlations between all volumes for MZ and DZ groups separately.

Structural Modeling

The overall analytic strategy in this chapter largely parallels that of the previous one. After importing the data into Mx, we started by constructing a preliminary 8-variable triple Cholesky decomposition, the multivariate analog of the classical ACE model, in order to calculate relatively unbiased genetic and environmental correlations between the observed variables. We also calculated eigenvalues on the decomposed covariance matrices to obtain an approximate number of factors required to explain most of the observed variance. As in the previous chapter, we then performed an exploratory factor analysis using independent pathway models. Scree plots of eigenvalues from the Cholesky decomposition suggested that three common factors, at most, would be required to explain the covariance matrix for each variance component. Thus, our full model included three factors for each of the three variance components, as well as structure-specific factors for each variance component. This model is subsequently referred to as the 333-ACE IPM.

Unlike the more global analyses in the previous chapter, modeling of cerebral volumes also included confirmatory factor analyses (CFA), as the nature of the cerebral measures implied a straightforward factor structure. Each of the eight variables measured was hypothesized to be influenced by factors related to tissue type (e.g. gray versus white matter) or spatial location (e.g lobe). These relationships are visualized in Figure 8.1A, in which each observed variable is influenced by two latent factors based on its unique combination of region and tissue. Coincidentally, the factor structure of this model is identical to the multitrait-multimethod model (MTMM) originally proposed by Campbell

and Fiske for the assessment of construct validity (Campbell & Fiske, 1959). Our parameterization is similar to the correlated traits, correlated methods version of MTMM devised by Jöreskog for CFA using structural equation modeling (Jöreskog, 1971). Given our twin sample, the MTMM model was expanded in order to decompose observed intercerebral covariances into genetic and nongenetic sources (Figure 8.1B). Thus, intercerebral relationships due to genetic (A), shared environmental (C), and unique environmental (E) could be estimated separately.

Figure 8.1: Confirmatory factor models Panel A is a sample path diagram of the MTMM model factor pattern. Two classes of latent variables are defined, those pertaining to tissue or spatial location. Though not shown, each path corresponds to a unique, freely-estimated parameter. The first letter of the observed variable name corresponds to spatial location (F=frontal, P=parietal, O=occipital, T=temporal) and the second to tissue (G=gray, W=white). Given data from twins and family members, the variance can be decomposed into genetic and nongenetic sources (Panel B). For simplicity, model from only one twin is shown.

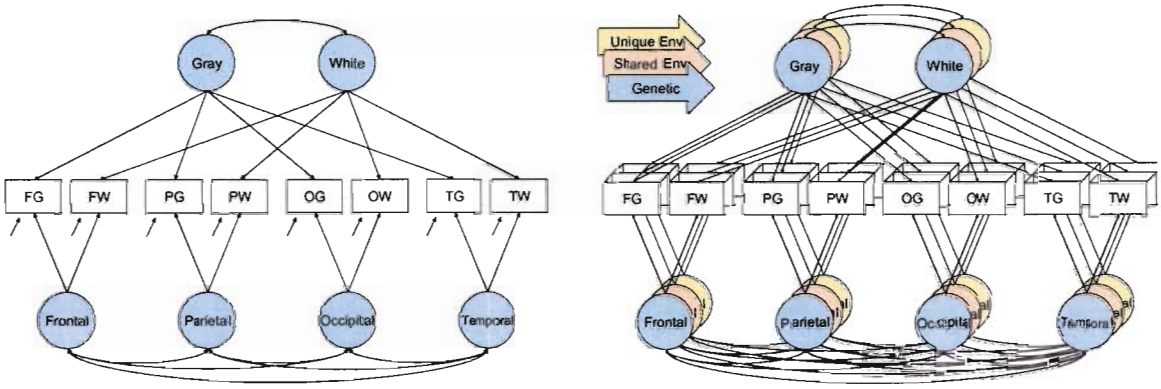

The MTMM has been extensively used in the social sciences, though the principles of the model can be easily generalized (Bechger T.M. & Maris, 2004). Unfortunately, the widespread use of MTMM (particularly Jöreskog's parameterization) over several decades has revealed many limitations of the approach, such as identification problems for small numbers of factors, easy misspecification, unidentified submodels due to

inadequate local information, and errors in estimation. Some of the problems are specific to the use of ordinal data or to assessing psychological constructs, however (Tomás, Hontangas, & Oliver, 2000). Additive MTMM models, for example, have been shown to fit well for other continuous, normally-distributed variables even though ordinal data often does not (Corten et al., 2002). Nevertheless, because of the inherent problems associated with the MTMM factor structure, we elected to pursue a cautious approach in our own data. Since prior research has demonstrated a trivial role of the shared environment on absolute cerebral volumes, we attempted to remove all factors related to the shared environment. Because of the risk of unidentification, however, we did not attempt more subtle simplifications of the model (e.g. removing tissue factors), but rather report maximum likelihood estimates from a less restricted model.

As with other structural modeling, we employed maximum likelihood (Edwards, 1972). In these analyses, best-fit models were chosen using AIC (Akaike, 1987), though we also performed likelihood ratio chi-squared tests to compare model fits without rewarding parsimony. Since preliminary simple linear regressions demonstrated a significant effect of age, race, and sex, we used residuals from multiple regressions including age sex and race as explanatory variables for all models.

Covarying for Global Effects

We then repeated our statistical analyses, but included total brain volume (TBV) as a regressor on mean ROI volumes.

Results

Cross-twin, cross-trait correlations are given in Table 8.1. Within individuals, correlations between cerebral structures were high. The highest correlations, approximately .80-.95, were between frontal gray matter and both temporal and parietal gray, as well as between frontal white and parietal and temporal white matter. The lowest correlations, approximately .30-.60, were between occipital structures and structures of different tissue type in different lobes. In general, variables that differed only by one qualitative trait were more correlated than if they differed by both tissue type and spatial location. For example, frontal gray matter was highly correlated with frontal white, temporal, gray, and parietal gray, but to a lesser extent to parietal and temporal white. The most prominent exception to this observation was a high correlation between temporal gray and parietal white matter.

Similar to our prior univariate studies on a slightly smaller sample, the within-region, cross twin correlations were substantially higher in MZ twins relative to DZ twins for cerebral volumes. The differences between groups were strongest for white matter structures, though these descriptive statistics suggest that both gray and white matter are highly heritable. Similarly, cross-twin, cross-structure correlations tended to be substantially higher in the MZ group, suggesting that most of the covariance between variables is genetically-mediated.

Table 8.1: Within and cross twin correlations between cerebral volumes for MZ (below diagonal) and DZ (above diagonal) groups. Cross twin correlations are shown in shaded boxes; cross-twin, within trait correlations are in boldface.

	FG1	FW1	OG1	OW1	PG1	PW1	TG1	TW1	FG2	FW2	OG2	OW2	PG2	PW2	TG2	TW2
FG1	1.00	0.75	0.54	0.60	0.80	0.67	0.87	0.68	**0.46**	0.32	0.20	0.22	0.37	0.23	0.36	0.24
FW1	0.67	1.00	0.48	0.77	0.59	0.94	0.79	0.92	0.29	**0.49**	0.10	0.43	0.19	0.48	0.34	0.53
OG1	0.64	0.58	1.00	0.69	0.59	0.52	0.61	0.52	0.23	0.13	**0.44**	0.31	0.25	0.14	0.28	0.25
OW1	0.39	0.73	0.70	1.00	0.54	0.84	0.71	0.82	0.20	0.32	0.33	**0.51**	0.19	0.45	0.26	0.44
PG1	0.84	0.61	0.73	0.51	1.00	0.62	0.70	0.53	0.23	0.19	0.14	0.21	**0.28**	0.19	0.14	0.11
PW1	0.44	0.86	0.60	0.83	0.55	1.00	0.71	0.90	0.13	0.40	0.03	0.40	0.07	**0.48**	0.19	0.47
TG1	0.85	0.67	0.71	0.51	0.74	0.53	1.00	0.83	0.38	0.39	0.37	0.46	0.36	0.38	**0.45**	0.48
TW1	0.48	0.83	0.52	0.77	0.46	0.84	0.64	1.00	0.30	0.50	0.27	0.57	0.26	0.56	0.42	**0.65**
FG2	**0.82**	0.62	0.62	0.50	0.74	0.49	0.70	0.53	1.00	0.58	0.51	0.22	0.89	0.42	0.88	0.43
FW2	0.62	**0.90**	0.58	0.69	0.55	0.80	0.68	0.81	0.63	1.00	0.29	0.59	0.49	0.84	0.68	0.77
OG2	0.53	0.57	**0.71**	0.65	0.59	0.57	0.58	0.60	0.63	0.55	1.00	0.60	0.66	0.39	0.63	0.39
OW2	0.39	0.66	0.59	**0.82**	0.43	0.72	0.51	0.74	0.42	0.70	0.73	1.00	0.32	0.71	0.41	0.72
PG2	0.66	0.57	0.60	0.58	**0.80**	0.54	0.56	0.52	0.87	0.57	0.70	0.49	1.00	0.46	0.82	0.39
PW2	0.43	0.81	0.56	0.76	0.50	**0.90**	0.55	0.83	0.50	0.87	0.61	0.80	0.57	1.00	0.60	0.79
TG2	0.71	0.66	0.63	0.60	0.66	0.57	**0.83**	0.70	0.86	0.68	0.69	0.53	0.76	0.61	1.00	0.68
TW2	0.47	0.74	0.52	0.68	0.42	0.74	0.67	**0.91**	0.50	0.82	0.60	0.76	0.47	0.85	0.70	1.00

Genetic and Environmental Correlations

Genetic and unique environmental correlations are given in Table 8.2; the covariances attributable to the shared environment were substantially smaller, and the corresponding correlation matrix therefore is not shown. Maximum likelihood estimates for the genetic correlations were quite high, ranging from .56 to .94. As with the within-individual phenotypic correlations, structures of like tissue type or location tended to be slightly more correlated via genetic factors than those without these similarities. In contrast, unique environmental correlations were, in general, lower and more variable, ranging from -.22 to .86. By far, the strongest correlations were between gray matter structures excepting the occipital lobe (>.80). Unique environmental correlations between regions of unlike tissue composition tended to be small or even negative.

Table 8.2 Genetic and unique environmental correlations between cerebral substructures, with 95% confidence intervals in parenthesis. Genetic correlations are given below the diagonal. Cross-tissue, within-lobe correlations are in boldface.

	FG	FW	OG	OW	PG	PW	TG	TW
FG	1	**.20 (0 .39)**	.26 (.07 .43)	-.28 (-.44 -.09)	.82 (.74 .88)	.11 (-.09 .31	.86 (.80 .91)	-.08 (-.28 .12)
FW	**.75 (.57 .94)**	1	-.05 (-.24 .16)	.32 (.14 .49)	.12 (-.09 .32)	.66 (.54 .76)	.04 (-.17 .24)	.52 (.36 .65)
OG	.83 (.57 .98)	.69 (.43 .93)	1	**.41 (.24 .56)**	.47 (.30 .62)	.27 (.08 .47)	.39 (.21 .55)	.03 (-.17 .23)
OW	.76 (.44 1)	.74 (.56 .96)	**.86 (.63 .98)**	1	-.11 (-.31 .09)	.54 (.38 .67)	-.22 (-.40 -.01)	.43 (.26 .58)
PG	.91 (.79 .98)	.58 (.39 .79)	.86 (.68 .97)	.66 (.41 .95)	1	**.29 (.08 .47)**	.81 (.73 .88)	-.10 (-.30 .12)
PW	.88 (.64 .99)	.91 (.84 .98)	.89 (.68 .99)	.83 (.69 .98)	**.74 (.57 .93)**	1	.11 (-.09 .32)	.63 (.48 .74)
TG	.94 (.85 .99)	.75 (.57 .93)	.63 (.40 .85)	.64 (.40 .98)	.79 (.67 .89)	.79 (.60 .94)	1	**-.13 (-.33 .08)**
TW	.82 (.49 1)	.92 (.80 1)	.61 (.25 .90)	.72 (.45 .97)	.56 (.29 .88)	.84 (.70 .96)	**.81 (.55 1)**	1

Exploratory Factor Analysis

The full 3-3-3-ACE IPM fit the data significantly worse than the Cholesky decomposition (χ^2_{21} = 37.35, p-value=.0153) but was preferred by fit statistics favoring parsimony (AIC = -4.65, Δ BIC = -40.80). Attempts to simplify this model resulted in the elimination of one shared environmental common factor and the shared environmental specific factors with little deterioration in model fit compared to the full IPM (compared to 3-3-3-ACE: χ^2_{14} = 3.10, p-value = .99, AIC = -24.90). Maximum likelihood parameter estimates from this best-fit model (a 3-2-3:AE IPM) are shown in Table 8.3.

Table 8.3 Standardized, varimax rotated factor loadings for the best fit exploratory model (3-2-3-AE).

ROI	A1	A2	A3	C1	C2	E1	E2	E3	As	Es
FG	0.57	0.37	0.28	0.43	-0.15	0.47	0.01	-0.04	0.00	0.13
FW	0.24	0.78	0.37	0.02	-0.06	0.06	0.30	-0.05	0.24	0.21
OG	0.28	0.18	0.57	0.39	0.32	0.18	0.00	0.47	0.00	0.22
OW	0.22	0.46	0.48	0.08	0.28	-0.15	0.26	0.31	0.38	0.31
PG	0.64	0.15	0.50	0.16	-0.01	0.41	0.03	0.10	0.26	0.19
PW	0.32	0.59	0.59	-0.22	0.04	0.04	0.32	0.10	0.08	0.15
TG	0.58	0.39	0.21	0.34	0.08	0.44	-0.03	0.04	0.34	0.18
TW	0.35	0.79	0.14	-0.05	0.29	-0.06	0.27	0.04	0.00	0.27

For all structures, the largest factor loadings were on genetic factors. The first common genetic factor loaded at least moderately on all structures, but gray structures in particular. The second genetic factor clearly loaded preferentially on white matter structures, while the third had high loadings primarily on the posterior cerebrum (occipital and parietal lobes), irrespective of tissue type. The shared environmental factor loadings were substantially smaller than the genetic loadings. The first factor primarily

loaded on frontal, occipital, and temporal gray, with the second on the occipital lobe and temporal white matter. The three unique environmental common factors were clearly identifiable as a gray matter, white matter, and an occipital lobe factor, respectively.

Confirmatory Factor Analysis

The full ACE MTMM model did not fit the data significantly worse than the more parameterized Cholesky decomposition (Cholesky decomposition: -2LL 20882.58, 180 parameters; MTMM Full model -2LL 20893.70, 165 parameters, $\chi^2_{15} = 11.20$, p-value=.74, AIC = -18.88). Similarly, the removal of shared environmental factors had little effect on the fit of the model (compared to Full Model: $\chi^2_{31} = 24.19$, p-value=.80, AIC= -37.81) and had a substantially better fit than the best-fit exploratory model. As the correlation between the gray and white matter factors was near unity for both genetic and environmental sources of variance, these could be fixed to one without a significant effect on model fit or parameter estimates (compared to Full model: -2LL 20919.36, χ^2_{33}=25.66, p-value=.8192, AIC=-40.34). Fixing these values does, however, simplify presentation of the complex model since the two tissue factors can be represented as a single, common factor. Though many correlations between the lobar factors were high, these could not be fixed to unity without substantial deterioration in model fit for both genetic ($\chi^2_{37} = 84.47$, p-value < .0001, AIC = 10.47) or environmental ($\chi^2_{37} = 71.37$, p-value < .0006, AIC = -2.634) variance components.

Table 8.3: Standardized maximum likelihood estimates for the best fit MTMM model. Columns represent factors contributing to either genetic (A) or unique environmental (E) variance. Negative estimates are shown in red. Columns with subscript *c* are common factors, those with subscript *s* are specific to a single structure, and those with the *lobe* subscript represent factors that are lobe-specific, but correlated with other lobar factors. These correlations are shown in Figure 8.2.

	A_c	E_c	A_{lobe}	E_{lobe}	A_s	E_s	a^2	e^2
Frontal Gray	.25	.36	.81	.36	.09	.01	.74 [.63 .81]	.26 [.19 .37]
Frontal White	-.41	-.16	.80	.26	.22	.21	.86 [.81 .90]	.14 [.10 .19]
Occipital Gray	.13	.16	.74	.55	.34	.01	.68 [.55 .76]	.32 [.24 .45]
Occipital White	-.18	-.31	.79	.29	.23	.32	.71 [.61 .79]	.29 [.21 .39]
Parietal Gray	.21	.33	.79	.34	.30	.15	.75 [.64 .83]	.25 [.17 .36]
Parietal White	-.43	-.18	.81	.32	.15	.04	.86 [.81 .90]	.14 [.10 .19]
Temporal Gray	.17	.37	.81	.29	.26	.20	.74 [.64 .82]	.26 [.18 .36]
Temporal White	-.37	-.25	.79	.16	.29	.27	.84 [.77 .89]	.16 [.11 .23]

The standardized maximum likelihood estimates from this model are presented both in Table 8.3 and Figure 8.3. By far, most of the variance in all cerebral structures was attributable to genetic factors common to lobes. As shown in Figure 8.3, these factors, in turn, were highly correlated. The subtle differences in phenotypic correlations between gray and white matter could be explained by the second genetic factor which had modest loadings, but with negative loadings on white matter structures. Though loadings were substantially lower, a very similar pattern emerged for environmental variance. The principal differences were that the relative contributions and tissue and lobar factors to structure variances were more similar for the unique environmental factors, high loadings on the occipital lobe latent factor, and less homogenous correlations between lobar factors.

Figure 8.2: Maximum likelihood parameter estimates for the best-fit MTMM model. For simplicity, genetic (panel A) and unique environmental (panel B) factor loadings are shown separately.

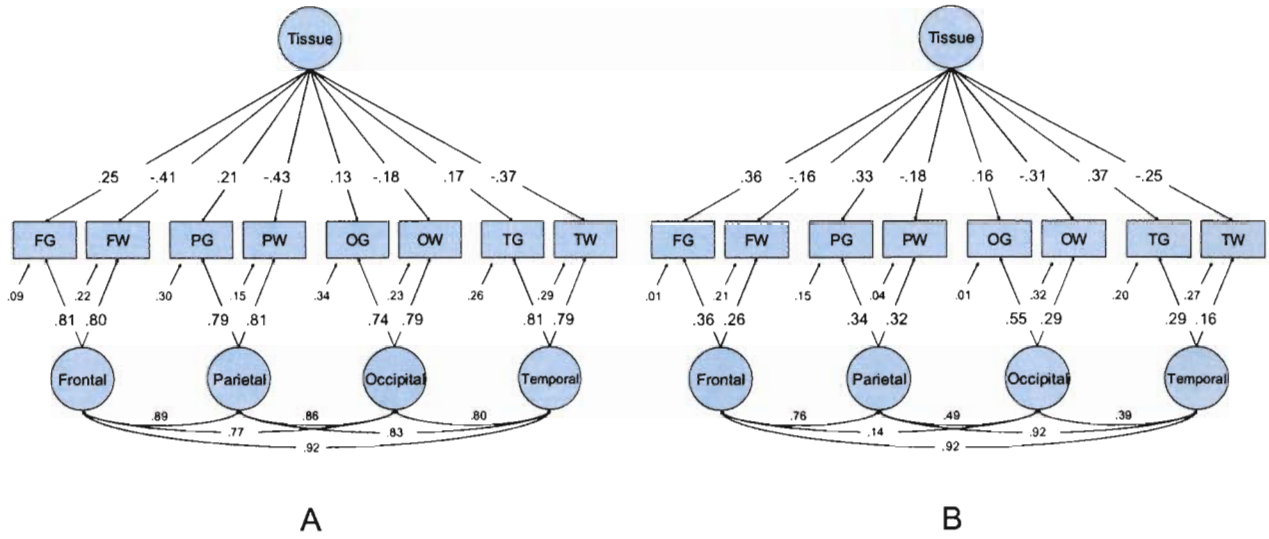

Models Including Global Covariates

The Cholesky decomposition allowing for linear effects of total brain volume on mean cerebral volumes fit the data substantially (-2LL=19102.57) better than the model without this regressor (-2LL = 20882.58). After adding the covariate, the total residual variance decreased precipitously for all regions (Figure 8.4). Without a global covariate, additive genetic variance always was the dominant variance component; the use of a global covariate had a disproportionately greater influence on the genetic variance compared to the environmental variance components. Thus, after controlling for global effects, additive genetic factors became relatively less important in explaining the residual variance.

Figure 8.3. Residual variance for variance components with and without a global covariate, organized by cerebral region of interest. Variance components (A,C, and E) are labeled and colored in red, green, and blue, respectively. Total variance (V) is shown as a solid black line.

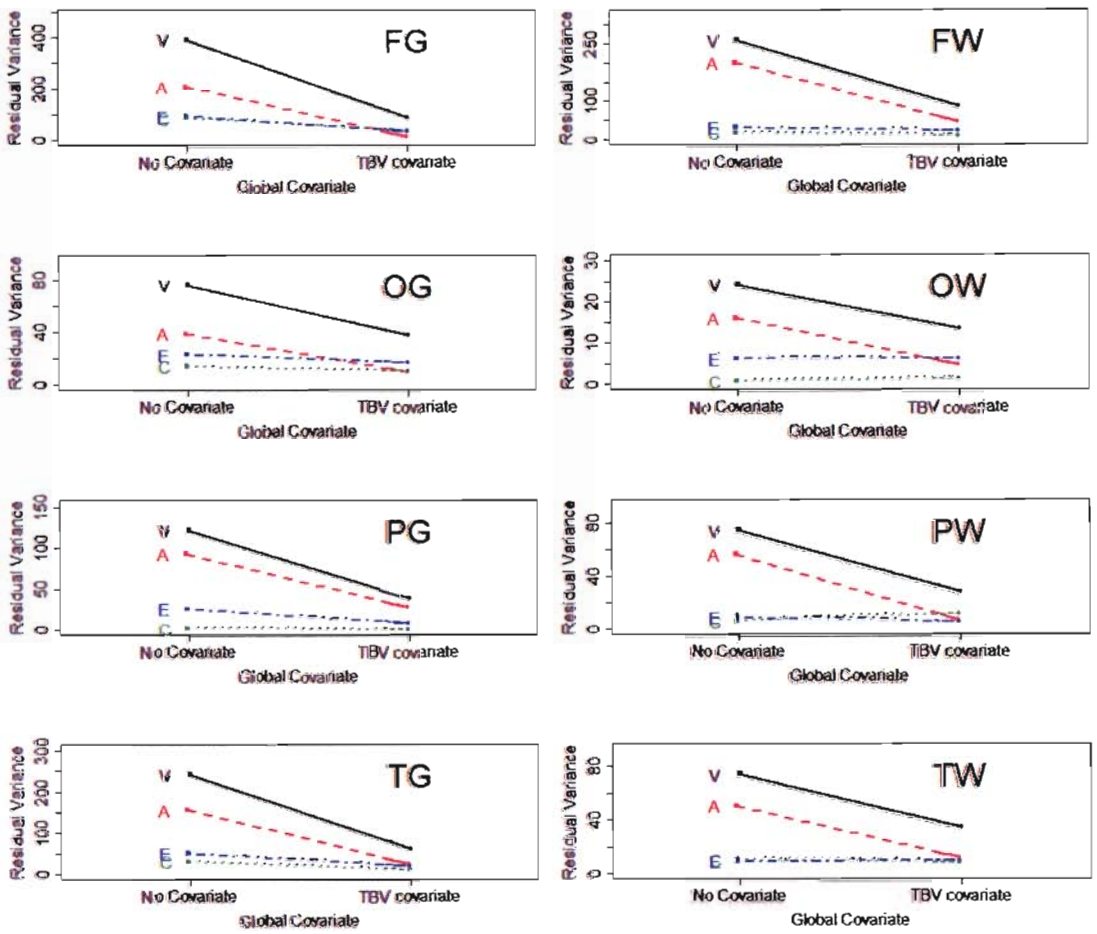

Table 8.4 provides correlations for individual variance components from this model. Unlike the strong positive genetic correlations observed for absolute volumes, genetic correlations between TBV-covaried structures varied widely and were often negative. For all variance components, negative correlations tended to be between gray and white matter structures. In effect, controlling for TBV removed a sizable, positive partial correlation between all structures.

Table 8.4: Genetic, shared environmental, and unique environmental correlations after use of a global covariate on mean volumes for all structures. Within-lobe correlations are shown in boldface.

	FG	FW	OG	OW	PG	PW	TG	TW
FG	1.00							
FW	**-0.94**	1.00					**GENETIC**	
OG	0.21	-0.33	1.00					
OW	-0.36	0.22	**0.34**	1.00				
PG	0.80	-0.63	0.46	-0.21	1.00			
PW	-0.67	0.63	0.26	0.34	**-0.22**	1.00		
TG	0.52	-0.41	-0.62	-0.56	0.19	-0.56	1.00	
TW	-0.66	0.67	-0.56	0.26	-0.65	0.21	**-0.25**	1.00

	FG	FW	OG	OW	PG	PW	TG	TW
FG	1.00							
FW	**-0.12**	1.00					**SHARED ENVIRONMENTAL**	
OG	-0.15	-0.96	1.00					
OW	-0.91	-0.19	**0.40**	1.00				
PG	-0.32	0.11	-0.07	0.41	1.00			
PW	-0.69	0.62	-0.47	0.60	**0.38**	1.00		
TG	0.34	-0.89	0.81	-0.12	-0.53	-0.76	1.00	
TW	-0.70	0.33	-0.13	0.51	-0.36	0.63	**-0.22**	1.00

	FG	FW	OG	OW	PG	PW	TG	TW
FG	1.00							
FW	**-0.45**	1.00					**UNIQUE ENVIRONMENTAL**	
OG	-0.30	-0.41	1.00					
OW	-0.76	0.30	**0.37**	1.00				
PG	0.51	-0.66	0.12	-0.51	1.00			
PW	-0.72	0.54	-0.02	0.56	**-0.43**	1.00		
TG	0.66	-0.67	-0.01	-0.59	0.52	-0.63	1.00	
TW	-0.58	0.49	-0.13	0.44	-0.64	0.62	**-0.58**	1.00

Attempts to model the relationships between TBV-covaried structures were only marginally successful. The 333-IPM fit worse than Cholesky decomposition based on χ^2 but not by AIC ($\chi^2_{21} = 41.53$, p-value = .0048, AIC = -0.47). As with the initial analyses on absolute volumes, the 323-AE IPM was found to be the most parsimonious model after a stepwise removal of latent factors (compared to Cholesky: χ^2_{35}=44.45, p-value = .13, AIC = -25.55; compared to 333-IPM: χ^2_{14}=2.91, p-value = .99, AIC = -25.09).

Table 8.5 reports the parameter estimates from this model, which were substantially more difficult to interpret then those on absolute volumes. Genetic effects were no longer predominant. Additionally, strong negative factor loadings were a prominent feature of the TBV-covaried factor models. The common factors still demonstrated evidence of the gray/white dichotomy, but these effects were somewhat obscured by loadings that did not fit the pattern. For example, the most prominent loadings for the third genetic factor were a positive loading on occipital gray matter, and a negative loading on temporal gray; these structures were uncorrelated via other common genetic factors.

Table 8.5: Varimax-rotated, standardized maximum likelihood parameter estimates of best-fit exploratory model after covarying for total cerebral volume.

ROI	A1	A2	A3	C1	C2	E1	E2	E3	As	Es
FG	-0.28	0.27	-0.08	0.64	0.00	0.52	0.20	-0.18	0.19	0.24
FW	0.62	-0.37	0.01	-0.07	0.40	-0.31	0.28	0.26	0.00	0.26
OG	0.00	0.29	0.43	-0.09	-0.52	-0.04	-0.57	-0.06	0.00	0.34
OW	0.04	-0.09	0.35	-0.39	-0.05	-0.45	-0.29	0.26	0.47	0.38
PG	-0.20	0.76	-0.04	-0.04	0.03	0.16	-0.04	-0.46	0.38	0.00
PW	0.34	-0.02	0.11	-0.53	0.38	-0.42	0.02	0.09	0.44	0.27
TG	-0.27	0.01	-0.58	0.18	-0.46	0.44	-0.04	0.17	0.00	0.35
TW	0.09	-0.51	0.03	-0.40	0.16	-0.33	0.07	0.28	0.44	0.39

Confirmatory analyses were somewhat more successful. The Full MTMM did not fit significantly worse than Cholesky decomposition (-2LL=19119.070, $\chi^2_{16} = 16.50$, p-value = .42, AIC = -16.50). Parameter estimates from the best-fit MTMM submodel (-2LL 19149.989; relative to Cholesky $\chi^2_{56} = 47.42$, p-value = .79, AIC = -64.581; relative to full MTMM $\chi^2_{40} = 30.92$, p-value = .85, AIC = -49.01) are shown in Figure 8.2. The most striking differences compared to the MTMM without a global covariate were 1) the substantial decrease in variance explained by genetic lobar factors, 2) a reversal in the correlations between these factors from strongly positive to negative, and 3) a relative increase in the importance of the path coefficients of the common genetic factor with a similar pattern of positive and negative values.

Figure 8.4: Maximum likelihood parameter estimates for the best-fit MTMM model after covarying for total brain volume. For simplicity, genetic (panel A) and unique environmental (panel B) factor loadings are shown separately.

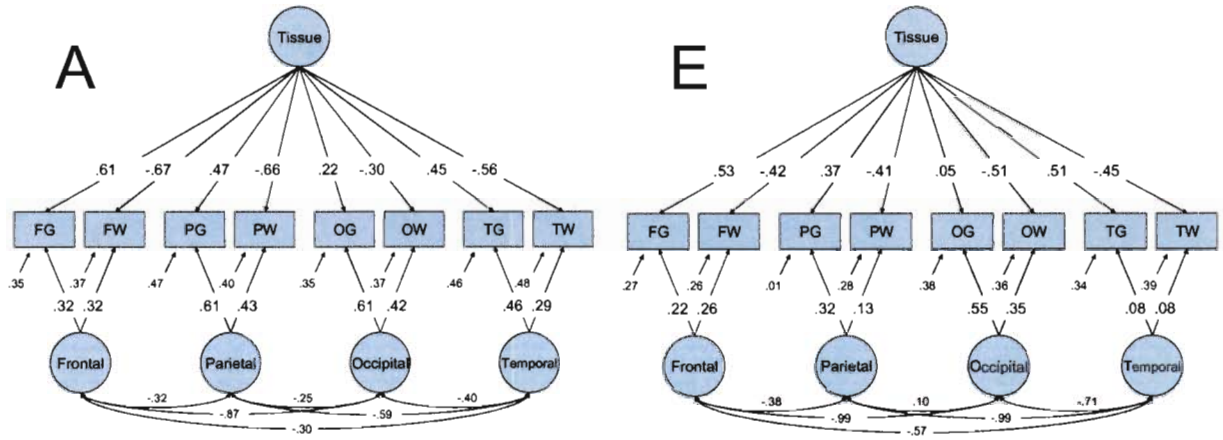

A B

Discussion

Similar to the results reported in the previous chapter on more ontogenetically diverse regions of interest, a more focused statistical genetic analysis on cerebral volumes suggests that genetic factors play the dominant role in the generation of covariance between observed structures. Because of the availability of segmentation data in the cerebrum, however, we were able to detect subtle differences in the relationships between gray and white matter. Genetic correlation matrices, EFA, and CFA all suggest that genetically-mediated covariance is greater between brain regions of similar tissue type. Since segmentation data from the rest of the brain are not available, it is unclear whether these relationships are unique to the cerebrum.

EFA and CFA models differ somewhat in how best to model cerebral relationships. In the best-fit EFA model, a gray-dominant and a white-dominant common genetic factor were present, with positive, moderate loadings on non-dominant structures (e.g. temporal white on the "gray" factor) for both factors. In the best fit CFA model, in contrast, genetic variance was almost entirely mediated via the lobar factor structure, with subtle gray-white differences modulated by a common factor. While in many ways the results from these two models are alternative perspectives of the same reality, it is noteworthy that the CFA model fit far better than the best fit EFA models. Thus, subtle inter-regional lobar differences appear to be an important determinant to both genetic and environmental covariance. The presence of the correlated lobar structure of the MTMM allows for all regions to be highly correlated via this factor structure, but not uniformly so as would be

the case with a single common factor; correlations between genetically-mediated latent lobar factors were all very high but not perfect.

As the cerebrum is the largest structure in the brain, it was not surprising that its eight major subcomponents were highly influenced by total brain volume. It is interesting, however, that the use of the TBV disproportionately decreased the additive genetic variance component with respect to the environmental components, reducing the heritability of all regions of interest substantially. This effect suggests strong genetic correlations between TBV and the cerebral ROIs in this study. In other words, as observed in the previous chapter, a strong single genetic factor or several highly correlated factors drives covariation between the observed variables. When the effects of this factor are largely removed by adding the TVB covariate, the positive partial correlations it generates also disappear, producing more complex interrelationships within the residual variance. The MTMM factor structure still fit well after the covariate was added, but the importance of the lobar factors relative to a common "tissue" factor was reversed and the interlobar correlations flipped to negative values.

Though a few studies have reported on cerebral lobar heritability (Carmelli et al., 2002b; Geschwind et al., 2002; Wallace & Giedd, 2004), the present analyses are unfortunately the only extant information on intralobar relationships. The prior observation by Barré et al of a .68 genetic correlation between total brain gray and white matter is, broadly speaking, consistent with the more detailed analyses reported here (Baare et al., 2001a).

9

IDENTIFICATION OF GENETICALLY-MEDIATED CORTICAL NETWORKS

"Our 20,000-25,000 genes can be compared to the residents of an average-sized town, each with names and addresses, all speaking a language for which the essential grammatical elements are understood. The brain, on the other hand, still evokes celestial metaphors, with its vast numbers of neurons compounded by the 10,000-fold complexity of the interconnections between them."

> --Jordan P. Amadio and Christopher A. Walsh. "Brain Evolution and the Human Genome." *Cell.* (126), 2006

ADAPTED FROM:

SCHMITT JE, LENROOT RK, WALLACE G, ORDAZ SE, LERCH JP, EVANS AC, KENDLER KS, NEALE MC, GIEDD JN. IDENTIFICATION OF GENETICALLY-MEDIATED CORTICAL NETWORKS. *CEREBRAL CORTEX*. UNDER REVISION.

ABSTRACT

Despite great interest in the role of genes in driving individual differences in cortical patterning, very little information on the topic is available for typically-developing individuals. We acquired high resolution anatomic MRI images on a large pediatric sample of twins, siblings of twins, and singleton families. We subsequently modeled familial relationships to obtain estimates of the additive genetic correlations between 54 gyral-level measures of cortical thickness. Both cluster and principal components analysis revealed several factors underlying the associations. The most dominant factor influenced the variability of non-orbital frontal lobe structures, dorsal parietal gyri, and somatosensory cortex. Other networks included two distinct factors driving associations between occipital lobe structures, and a factor influencing variability tempro-insular cortex. These findings are largely concordant with other multivariate studies of brain structure, the twin literature, and current understanding on the role of genes in cortical neurodevelopment.

Introduction

Though the role of genetics in brain patterning is of great scientific interest, many of the most basic questions in the field remain unanswered. That proper gene expression is critical for proper brain development has become self evident; both the large animal literature as well as structural and functional studies of neurogenetic syndromes provide overwhelming support of the obvious—genes help construct the brain, maintain and develop it through life, and perform its perceptual, computational, and motor activities (Kandel et al., 2000). The role of genetics on the tremendous intra-species variability in most neurobiological phenotypes, however, is substantially less well understood. For example, it still is unclear whether polymorphisms in the genes responsible for neuropathology also play a role in generating population-wide individual differences in neurobiological phenotypes, nor is it apparent how different genetic factors simultaneously influence multiple neurobiological measures during typical development.

Studies are only beginning to map out the relative strength of genetic effects on different aspects of human neuroanatomy. The advent of non-invasive techniques such as magnetic MRI in combination with twin and family-based methodologies has enabled the estimation of the fraction of population variability in the size of brain structures attributable to genetic effects (i.e. the heritability). In general, the heritability of brain volumes is high; approximately .80 for both total brain volume and cerebral cortex (Baare et al., 2001a; Geschwind et al., 2002; Wallace et al., 2004). Information on the heritability of smaller structures is more limited as fewer studies have been performed;

the most comprehensive parcellation to date by Wright et al. reported substantial heterogenetity in heritability of regions of interest (ROIs) based on Brodmann areas in a sample of 10 monozygotic (MZ) and 10 dizygotic (DZ) twin pairs. This study found the strongest genetic effects (heritabilities > .50) in pre- and postcentral gyrus, frontal and orbitofrontal regions, supramarginal gyrus, superior temporal gyrus, temporal pole, and cingulate gyrus, though only three out of ninety-two measured regions had statistically significant genetic effects (Wright et al., 2002). Additionally, two voxel-level studies have suggested that genetic effects are stronger in frontal areas and language centers, both for measures of gray matter density and cortical thickness (Lenroot et al., 2007; Thompson et al., 2001).

Multivariate studies examining how genetic effects influence multiple regions are more uncommon (Baare et al., 2001a; Pennington et al., 2000; Schmitt et al., 2006; Wright et al., 2002), and to date only two have parcellated the cerebrum with high resolution. The present study represents an extension to the important yet sparse previous work on the genetic contributions to variability in high-resolution neuroanatomic structure. Below, we describe analyses of gyral-level structures measured in a large sample of twins and family members using similar statistical to prior studies, but with substantially enhanced statistical power, and an alternative endophenotype, cortical thickness.

Methods

Subjects

The analyses reported in this chapter are based on MRI from a sample of 600 children in total (mean age 11.1, SD 3.4, range 5.4-18.7), including 214 MZ and 94 DZ twins, 64 singleton siblings of twins (1-2 per family), 116 members of entirely singleton families (2-5 members per family), and 112 unrelated singletons. The distribution of subjects and basic demographic information are given in Table 5.1. Findings on the heritability of voxel level cortical thickness measures have been reported previously with this sample (Lenroot et al., 2007).

Image Processing

A probabilistic atlas was used to assign cortical points to specific neuroanatomic regions (Collins et al., 1999). Mean CT was calculated for each of 54 cortical subregions (Table 9.1), which roughly corresponded to cerebral gyri and were based on the sulcal definitions of Ono (Ono, Kubik, & Abernathey, 1990).

Table 9.1: Cortical regions of interest in the present study and abbreviations used in subsequent Tables and Figures.

Structure Name	Left Abbreviation	Right Abbreviation
Superior Frontal Gyrus	SFG-L	SFG-R
Middle Frontal Gyrus	MFG-L	MFG-R
Inferior Frontal Gyrus	IFG-L	IFG-R
Precentral Gyrus	PreCG-L	PreCG-R
Lateral Orbitofrontal Gyrus	LFOrbG-L	LFOrbG-R
Medial Orbitofrontal Gyrus	MFOrbG-L	MFOrbG-R
Cingulate Cortex	Cingulate-L	Cingulate-R
Medial Frontal Gyrus	MedialFG-L	MedialFG-R
Superior Parietal Gyrus	SupParGy-L	SupParGy-R
Supramarginal Gyrus	SMG-L	SMG-R
Angular Gyrus	AngularGy-L	AngularGy-R
Precuneus	Precuneus-L	Precuneus-R
Postcentral Gyrus	PostCenGy-L	PostCenGy-R
Superior Temporal Gyrus	STG-L	STG-R
Middle Temporal Gyrus	MTG-L	MTG-R
Inferior Temporal Gyrus	ITG-L	ITG-R
Uncus	Uncus-L	Uncus-R
Medial Occipitotemporal Gyrus	MedialoccipitemporalGy-L	MedialoccipitemporalGy-R
Lateral Occipitotemporal Gyrus	LateraloccipitemporalGy-L	LateraloccipitemporalGy-R
Parahippocampal Gyrus	ParahippocampalGy-L	ParahippocampalGy-R
Occipital Pole	OccipitalPole-L	OccipitalPole-R
Superior Occipital Gyrus	SupOccGy-L	SupOccGy-R
Middle Occipital Gyrus	MidOccGy-L	MidOccGy-R
Inferior Occipital Gyrus	InfOccGy-L	InfOccGy-R
Cuneus	Cuneus-L	Cuneus-R
Lingual Gyrus	LingualGy-L	LingualGy-R
Insula	Insula-L	Insula-R

Statistical Analysis

The resultant data were iteratively passed from the statistical programming environment R (Ihaka et al., 1996; R Development Core Team, 2005) to Mx (Neale et al., 2002), a matrix-based structural equation modeling package (Neale et al., 1992). Univariate variance decomposition was accomplished using an extended twin design of the classical ACE model, which increases the statistical power to detect genetic effects on phenotypes (Posthuma et al., 2000b). Models included a simultaneous means regression to adjust for sex, nonlinear age effects, and interactions between age and sex. In these models, the

differences in the correlation between MZ twins, DZ twins, and related singletons enabled the parsing of the observed variance in the observed cortical thickness measured into variance of genetic (a^2), non genetic familial (c^2), and unique environmental (e^2) origin. Optimization was performed using maximum likelihood (ML) (Edwards, 1972). We also we tested for the significance of both genetic and shared environmental effects for each neuroanatomic region via likelihood ratio χ^2.

Figure 9.1: Example of a path diagram describing the bivariate Cholesky decomposition used to estimate genetic correlations between regions of interest (ROIs). The variance in observed variables (denoted as rectangles) are modeled to be mediated by latent additive genetic (A.), shared environmental (C.) or unique environmental (E.) sources of variance (circles) with latent variances standardized to unity. The model is identified since the correlation between genetic factors (α) is perfect in MZ twins, but ½ between DZ twins and singleton siblings. The expected covariances of this model produce nine simultaneous equations from which the values of the nine free parameters (a., c., e.) can be estimated. In this example, two related family members (S1 and S2) are shown. For families with more than two individuals, this model is easily expanded, with families of size k generating $(2k)^2$ informative variance/covariance relationships. Unrelated individuals provide useful information for the estimation of ROI variances as well as the within-person phenotypic covariance.

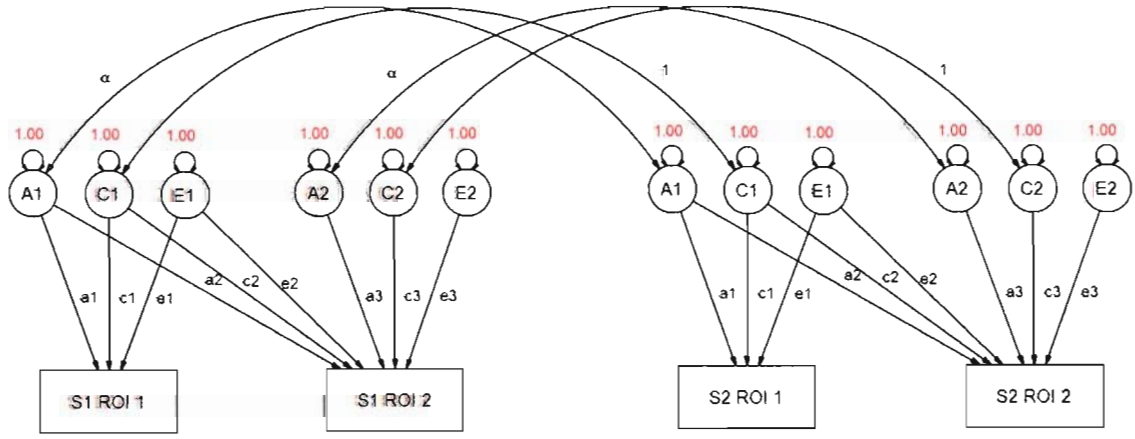

Multivariate Modeling

In order to analyze the pattern of genetic relationships between neuroanatomic structures, we employed a modified version of the multistep multivariate analyses reported by Wright et al. (Wright et al., 2002). First, we constructed extended twin versions of bivariate ACE Cholesky decompositions for each pair of neuroanatomic variables (Figure 9.1). In addition to adjusting for age and sex, mean global CT was included as a regressor. The genetic correlation between any two structures was then calculated by standardizing their genetic covariance matrix. The genetic correlation is defined as;

$$r_{x,y} = \frac{A_{xy}}{\sqrt{(A_x * A_y)}}$$

where A_{xy} is the genetic covariance between structures x and y, and A_x and A_y represent the heritability of x and y (Falconer et al., 1996). The sequential bivariate analyses of 2862 pairwise models populated a 54 x 54 genetic correlation matrix; despite the redundancy, calculations both above and below the diagonal were performed in order to ensure that the optimizer had converged to the proper solution. The correlation matrix was visualized using the heatmap.2 function in R (from the gplots package), which also performed a preliminary cluster analysis using Euclidian distances (Hastie, Tibshirani, & Friedman, 2001).

We then completed a principal components analyses (PCA) on the genetic correlation matrix and extracted the factors with the six highest eigenvalues. PCA is a linear

transformation that attempts to reduce the dimensionality of the data structure by identifying uncorrelated factors that account for a disproportionate amount of the *total* variance within the observed measures (Hastie et al., 2001; Norman & Streiner, 2000); in essence PCA rotates the axes of measurement to optimally align with the dominant axes of the observed data, with the constraint that all components lie orthogonal to one another. To facilitate interpretation of the factor structure, varimax rotation was subsequently applied (Kaiser, 1958). These adjusted factors represent the predominant patterns of relationships between the neuroanatomic regions that are caused by additive genetic factors. To determine the multivariate relationships between absolute measures of cortical thickness, we repeated these analyses without a global covariate.

Graph Theory

As an alternate method to characterize relationships between gyral regions, we constructed simple graph theoretical models using Bioconductor (Carey, Gentry, Whalen, & Gentleman, 2005), a collection of R packages for the analysis of genomic data. Graph theory is a branch of discrete mathematics for the analysis of complex networks, with applications in telecommunications, social networking, bioinformatics, and molecular biology, among others. Recently, there has been increasing interest in using graph theory in systems biological analyses of the most complex network known, i.e. the brain, with applications ranging from examining neuronal circuitry to understanding structural and functional connectivity between large neuroanatomic regions (Sporns, Chialvo, Kaiser, & Hilgetag, 2004).

The two fundamental components of these models are nodes, which represent units in a large system (e.g. computers, proteins, neurons, or gyri), and edges, which represent the connections between them. To identify important edges within our data, we ran AE Cholesky decompositions and compared the fit of this model to the submodel in which the path allowing for genetic covariance (a2 in Figure 1) was removed. Statistically significant positive correlations at an $\alpha = .05$ were identified as undirected edges. From this graph, we calculated statistics that evaluate properties of the network, namely the characteristic path length (L) and the clustering coefficient (C) (Watts & Strogatz, 1998). The average path length simply refers to the average shortest distance between a node and other nodes in the system; the clustering coefficient of a node is the average number of edges connecting a node's neighbors, relative to the total number possible. Values of L and C for the system as a whole were calculated by taking mean values for all nodes in the graph (Watts et al., 1998). We compared these calculations to those from 1000 simulated random networks, each with the same number of nodes and edges as the real data. In the simulations, for each of *i* edges, two nodes were identified by sampling from a pool of 54 nodes (with replacement) with uniform probability, with the constraints that an edge could not connect a node to itself, nor could edges be redundant. Visualization of graphs was performed using modifications of functions in the GeneTS package (Schafer & Strimmer, 2005).

Results

Variance component analyses

Variance decomposition demonstrated substantial heterogeneity in heritability between cortical regions. Table 9.2 presents both parameter estimates and tests of the statistical significance of genetic and shared environmental effects to the variation in each region. In general, genetic effects were strongest in frontal lobes, with temporal, parietal, and occipital variance progressively less influenced by genes. The specific regions with the highest genetically-mediated individual differences included the superior and inferior frontal gyri, the pre- and postcentral gyri, left medial frontal gyrus, left supramarginal gyrus, the left inferior temporal gyrus, and the left occipital pole. Global trends can be seen in Figure 9.2, which projects point estimates on the brain surface. In contrast to genetic factors, the familial environment appeared to have virtually no role in the observed variability in CT. While the genetic effects on most of structures were statistically significant at an α of .05, no shared environmental factors were significant at this level, and the c^2 maximum likelihood estimate for nearly every structure was zero.

Table 9.2: Maximum likelihood parameter estimates and p-values from hypothesis testing of univariate ACE models.95% confidence intervals for point estimates are in parentheses. P-values test the hypotheses of no genetic (A), shared environmental (C), or familial (A&C) effects on phenotypic variance. Statistically significant effects (at an α=.05) are shown in red.

	Variance Components									Hypothesis Testing		
ROI	a^2			c^2			e^2			A	C	A & C
SFG-R	0.45	(0.20	0.60)	0.00	(0.00	0.15)	0.55	(0.40	0.72)	0.004	1.000	0.00
SFG-L	0.51	(0.24	0.64)	0.00	(0.00	0.17)	0.49	(0.36	0.65)	0.002	1.000	0.00
MFG-R	0.43	(0.21	0.59)	0.00	(0.00	0.10)	0.57	(0.41	0.76)	0.002	1.000	0.00
MFG-L	0.38	(0.05	0.52)	0.00	(0.00	0.21)	0.62	(0.48	0.80)	0.027	1.000	0.00
IFG-R	0.52	(0.32	0.66)	0.00	(0.00	0.09)	0.48	(0.34	0.67)	0.000	1.000	0.00
IFG-L	0.44	(0.15	0.58)	0.00	(0.00	0.19)	0.56	(0.42	0.73)	0.007	1.000	0.00
PreCG-R	0.43	(0.20	0.58)	0.00	(0.00	0.13)	0.57	(0.42	0.75)	0.004	1.000	0.00
PreCG-L	0.52	(0.27	0.65)	0.00	(0.00	0.15)	0.48	(0.35	0.65)	0.001	1.000	0.00
LFOrbG-R	0.38	(0.12	0.54)	0.00	(0.00	0.15)	0.62	(0.46	0.81)	0.010	1.000	0.00
LFOrbG-L	0.34	(0.03	0.49)	0.00	(0.00	0.19)	0.66	(0.51	0.84)	0.037	1.000	0.00
MForbG-R	0.22	(0.00	0.38)	0.00	(0.00	0.17)	0.78	(0.62	0.96)	0.099	1.000	0.05
MForbG-L	0.27	(0.00	0.43)	0.00	(0.00	0.21)	0.73	(0.57	0.91)	0.087	1.000	0.01
Cingulate-R	0.36	(0.16	0.53)	0.00	(0.00	0.09)	0.64	(0.47	0.83)	0.003	1.000	0.00
Cingulate-L	0.40	(0.18	0.56)	0.00	(0.00	0.10)	0.60	(0.44	0.80)	0.003	1.000	0.00
MedialFG-R	0.38	(0.10	0.54)	0.00	(0.00	0.17)	0.62	(0.46	0.80)	0.016	1.000	0.00
MedialFG-L	0.50	(0.27	0.64)	0.00	(0.00	0.13)	0.50	(0.31	0.68)	0.001	1.000	0.00
SupParGy-R	0.44	(0.20	0.59)	0.00	(0.00	0.13)	0.56	(0.41	0.76)	0.004	1.000	0.00
SupParGy-L	0.30	(0.04	0.47)	0.00	(0.00	0.15)	0.70	(0.54	0.89)	0.032	1.000	0.01
SMG-R	0.39	(0.00	0.53)	0.00	(0.00	0.28)	0.61	(0.47	0.79)	0.056	1.000	0.00
SMG-L	0.51	(0.22	0.63)	0.00	(0.00	0.21)	0.49	(0.37	0.64)	0.003	1.000	0.00

ROI	a^2			c^2			e^2			A	C	A & C
AngularGy-R	0.20	(0.00	0.39)	0.00	(0.00	0.18)	0.80	(0.61	0.99)	0.171	1.000	0.12
AngularGy-L	0.24	(0.00	0.41)	0.00	(0.00	0.18)	0.76	(0.59	0.95)	0.113	1.000	0.04
Precuneus-R	0.19	(0.00	0.36)	0.00	(0.00	0.21)	0.81	(0.64	0.98)	0.227	1.000	0.09
Precuneus-L	0.12	(0.00	0.28)	0.00	(0.00	0.16)	0.88	(0.72	1.00)	0.367	1.000	0.32
PostCenGy-R	0.57	(0.36	0.68)	0.00	(0.00	0.13)	0.43	(0.32	0.58)	0.000	1.000	0.00
PostCenGy-L	0.48	(0.25	0.61)	0.00	(0.00	0.14)	0.52	(0.39	0.68)	0.001	1.000	0.00
STG-R	0.41	(0.13	0.56)	0.00	(0.00	0.17)	0.59	(0.44	0.77)	0.010	1.000	0.00
STG-L	0.40	(0.14	0.55)	0.00	(0.00	0.16)	0.60	(0.45	0.77)	0.007	1.000	0.00
MTG-R	0.33	(0.00	0.49)	0.00	(0.00	0.21)	0.67	(0.51	0.86)	0.047	1.000	0.00
MTG-L	0.39	(0.04	0.54)	0.00	(0.00	0.22)	0.61	(0.46	0.80)	0.031	1.000	0.00
ITG-R	0.38	(0.17	0.53)	0.00	(0.00	0.12)	0.62	(0.47	0.70)	0.003	1.000	0.00
ITG-L	0.47	(0.18	0.60)	0.00	(0.00	0.20)	0.53	(0.40	0.69)	0.004	1.000	0.00
Uncus-R	0.01	(0.00	0.16)	0.00	(0.00	0.09)	0.99	(0.84	1.00)	1.000	1.000	1.00
Uncus-L	0.05	(0.00	0.24)	0.00	(0.00	0.10)	0.95	(0.76	1.00)	0.584	1.000	0.86
MediooccipitemporalGy-R	0.31	(0.00	0.47)	0.01	(0.00	0.30)	0.68	(0.53	0.87)	0.196	0.938	0.00
MediooccipitemporalGy-L	0.26	(0.00	0.42)	0.00	(0.00	0.22)	0.74	(0.59	0.92)	0.128	1.000	0.01
LateralOccipitotrmporalGy-R	0.33	(0.00	0.48)	0.00	(0.00	0.22)	0.67	(0.52	0.85)	0.052	1.000	0.00
LateralOccipitotrmporalGy-L	0.28	(0.00	0.44)	0.00	(0.00	0.20)	0.72	(0.56	0.90)	0.074	1.000	0.01
ParahippocampalGy-R	0.06	(0.00	0.24)	0.01	(0.00	0.16)	0.93	(0.76	1.00)	0.808	0.929	0.61
ParahippocampalGy-L	0.10	(0.00	0.33)	0.06	(0.00	0.25)	0.84	(0.67	0.98)	0.651	0.705	0.07
OccipitalPole-R	0.30	(0.00	0.50)	0.05	(0.00	0.32)	0.65	(0.50	0.84)	0.183	0.764	0.00
OccipitalPole-L	0.47	(0.09	0.60)	0.00	(0.00	0.27)	0.53	(0.40	0.70)	0.018	1.000	0.00
SupOccGy-R	0.37	(0.01	0.52)	0.00	(0.00	0.24)	0.63	(0.48	0.81)	0.045	1.000	0.00

ROI	a^2			c^2			e^2			A	C	A & C
SupOccGy-L	0.31	(0.00	0.48)	0.00	(0.00	0.30)	0.69	(0.52	0.91)	0.216	1.000	0.01
MidOccGy-R	0.26	(0.00	0.43)	0.00	(0.00	0.22)	0.74	(0.57	0.94)	0.136	1.000	0.02
MidOccGy-L	0.33	(0.04	0.51)	0.00	(0.00	0.16)	0.67	(0.49	0.87)	0.032	1.000	0.01
InfOccGy-R	0.23	(0.00	0.40)	0.00	(0.00	0.21)	0.77	(0.60	0.96)	0.193	1.000	0.04
InfOccGy-L	0.12	(0.00	0.49)	0.21	(0.00	0.39)	0.67	(0.50	0.83)	0.580	0.200	0.00
Cuneus-R	0.35	(0.02	0.50)	0.00	(0.00	0.22)	0.65	(0.50	0.83)	0.039	1.000	0.00
Cuneus-L	0.15	(0.00	0.32)	0.00	(0.00	0.19)	0.85	(0.68	1.00)	0.307	1.000	0.25
LingualGyrus-R	0.01	(0.00	0.33)	0.13	(0.00	0.25)	0.86	(0.67	0.98)	1.000	0.349	0.06
LingualGyrus-L	0.22	(0.00	0.39)	0.00	(0.00	0.24)	0.78	(0.61	0.97)	0.325	1.000	0.06
Insula-R	0.30	(0.00	0.46)	0.00	(0.00	0.20)	0.70	(0.54	0.88)	0.059	1.000	0.01
Insula-L	0.26	(0.00	0.43)	0.00	(0.00	0.20)	0.74	(0.57	0.95)	0.120	1.000	0.03

Figure 9.2: Visualization of variance components analysis for fifty-four measures of cortical thickness. The maximum likelihood estimates for heritability (a^2) and the unique environmental variance (e^2) reported in Table 1 are rendered onto the brain surface. Since the estimates for familial variance approach zero for most structures, these are not shown.

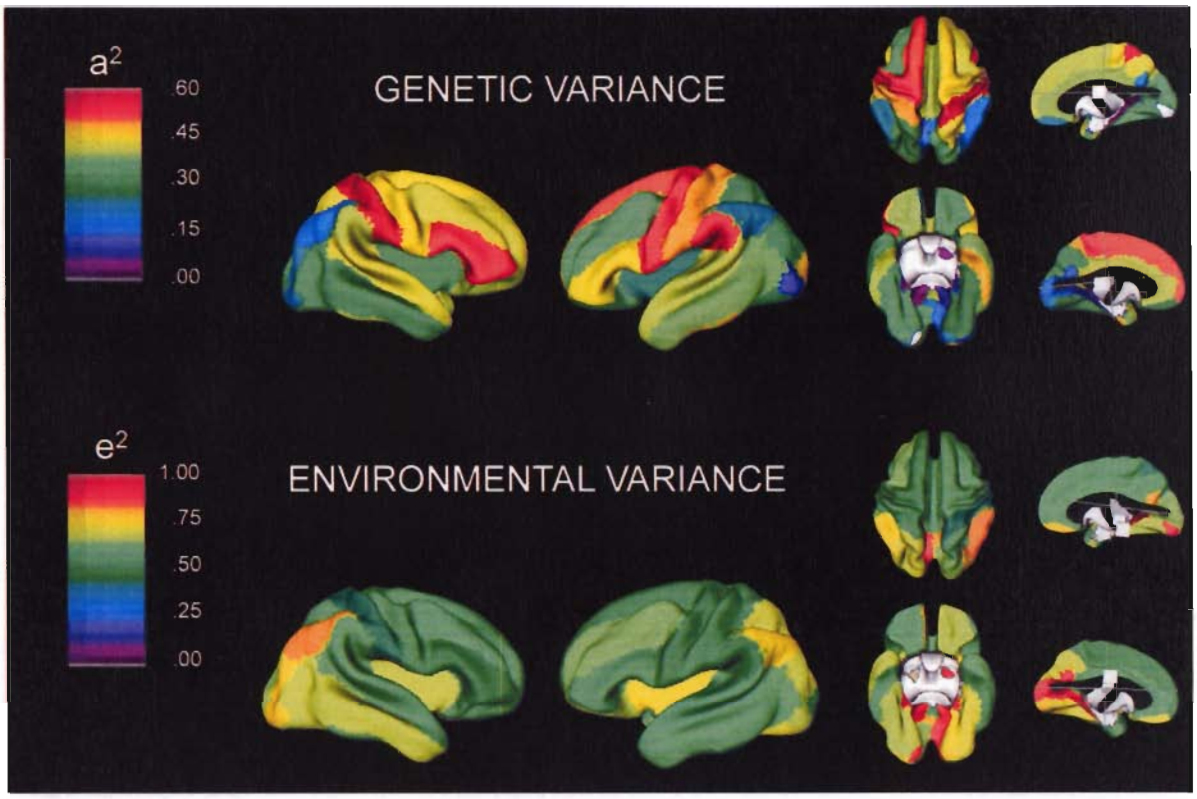

Multivariate Relationships

A color map of the genetic correlation matrix is shown in Figure 9.3. Genetic correlations between the measured cortical structures ranged from -.67 to .76. Gyri in contralateral regions were more likely to be positively correlated via genetic factors, as were regions in spatial proximity though this observation was far from absolute. The neuroanatomic relationships are apparent in the dendrogram that accompanies Figure 3 (reproduced on

Figure 9.3: Heatmap of the genetic correlations between measures of cortical thickness, reordered by the results from hierarchal cluster analysis (dendrogram reproduced on both margins).

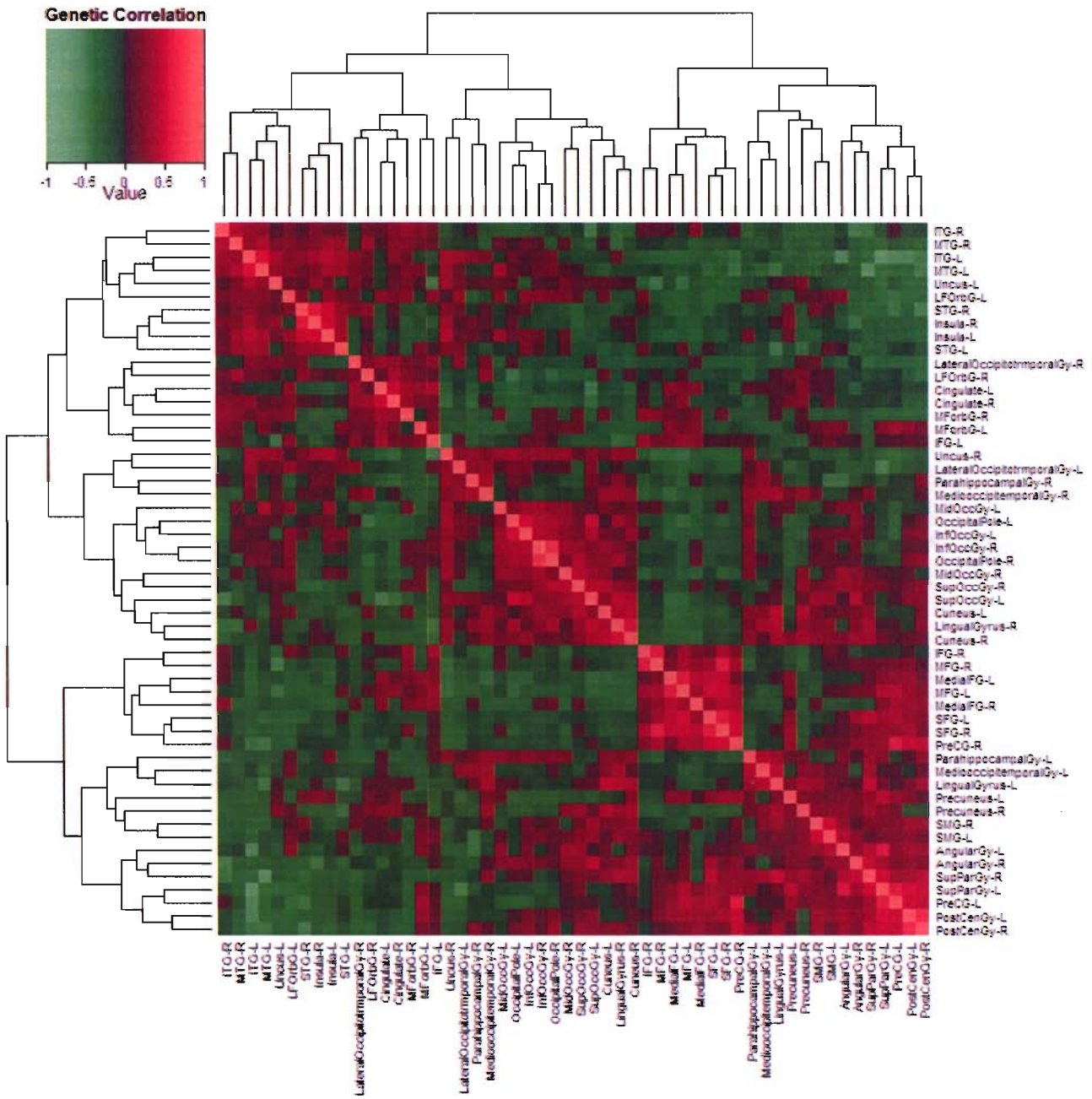

both axes). Approximately five blocks of related structures emerged; temporal/insular/left lateral orbitofrontal, cingulate/orbitofrontal, occipital/occipitotemporal, frontal (excluding

orbitofrontal gyri), and parietal including precuneus and primary somatosensory cortex bilaterally. Positive genetic correlations were largely clustered within these blocks, but there also were several strong correlations, such as between superior/middle frontal structures and primary somatosensory cortex. Structures on the inferior of the brain were dispersed between the parietal and occipital blocks and had correlational patterns similar to those of the occipitotemporal structures. Other prominent between-block correlations included between the frontal block and superior parietal lobe, frontal lobe and cingulate cortices, and between orbitofrontal, cingulate, and middle/inferior temporal structures.

The first six components of the PCA explained over half (58%) of the total genetic variance in all 54 measures, with each factor explaining about 10% of the observed variability. The component loadings are projected onto the brain in Figure 9.4, which visualizes the most important factors for explaining genetically-mediated individual differences in cortical thickness. The first and most prominent component strongly tapped frontal and superior parietal structures, including superior, middle, and medial frontal gyrus, pre- and postcentral gyrus, right superior frontal gyrus, and left precuneus. Several temporal structures and the inferior surface of the cortex, including the left lateral orbitofrontal gyrus, had negative factor loadings, suggesting a relationship between these structures via this factor. The second factor loaded predominantly on the occipital lobes, with high negative loadings in left fronto-orbital gyrus and cingulate gyrus bilateral

Figure 9.4: Results of PCA. Panel A is a barplot of factor loadings on the 54 measured regions, with columns representing the six most important components in explaining the total genetic variability in cortical thickness after adjusting for global effects. Since this PCA was performed on a (genetic) correlation matrix, factor loadings can be interpreted as the correlation between an ROI and a (genetic) component. Division lines are given for orientation purposes only. Panel B is an alternate representation of the same information projected on the brain surface.

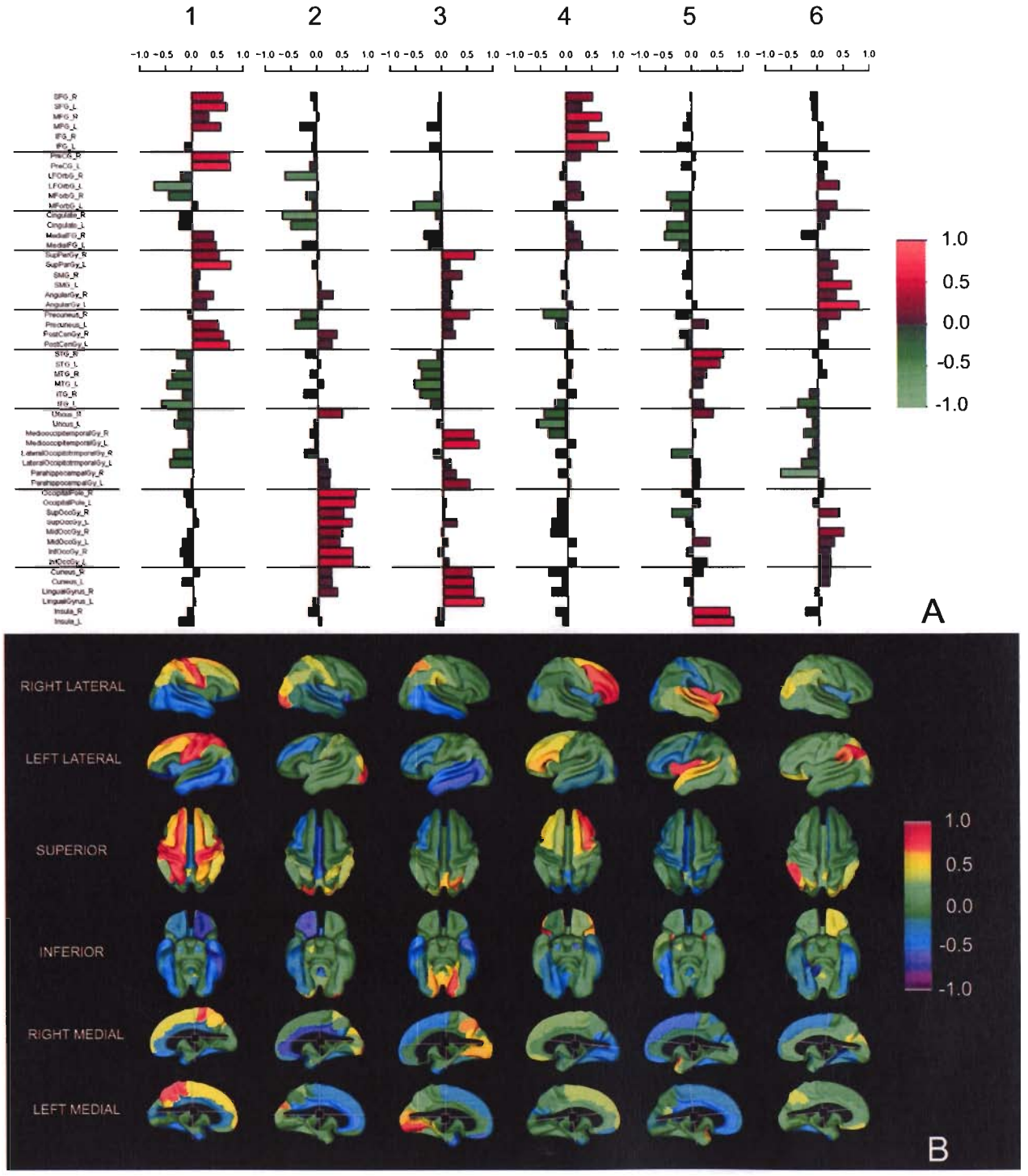

The remaining factors showed similar patterns, with high loadings on structures from lobar subregions, and prominent negative loadings on distal structures such as orbitofrontal gyri, cingulate, or inferior temporal lobe. The third factor could be identified as mediating genetic relationships between cuneus, lingual gyrus, mediooccipitotemporal gyrus, and right superior parietal gyrus, while the fourth strongly demonstrated associations within the frontal lobe; unlike the fronto-parietal factor described above, this factor included the inferior frontal gyri but neither the superior parietal lobes nor primary somatosensory cortex. The final two factors represented genetic associations between superior temporal gyrus and insula bilaterally (with modest negative loadings in orbitofrontal cortex and left cingulate), and inferior parietal lobe, with a stronger influence on the left hemisphere.

Absolute measures

When we repeated the analysis without a global covariate, all structures had strong positive correlations (Figure 9.5A). PCA identified a single genetic factor that could explain over 60% of genetic variability (Figure 9.5B), with the second factor explaining more than ten times less of the total variance. Most structures in the brain showed high loadings on this single factor.

Figure 9.5: Multivariate findings when measures are analyzed without global adjustment. Panel A is the heatmap of genetic correlations between absolute measures of cortical thickness, while Panel B plots the factor loadings from the largest principal component obtained via PCA.

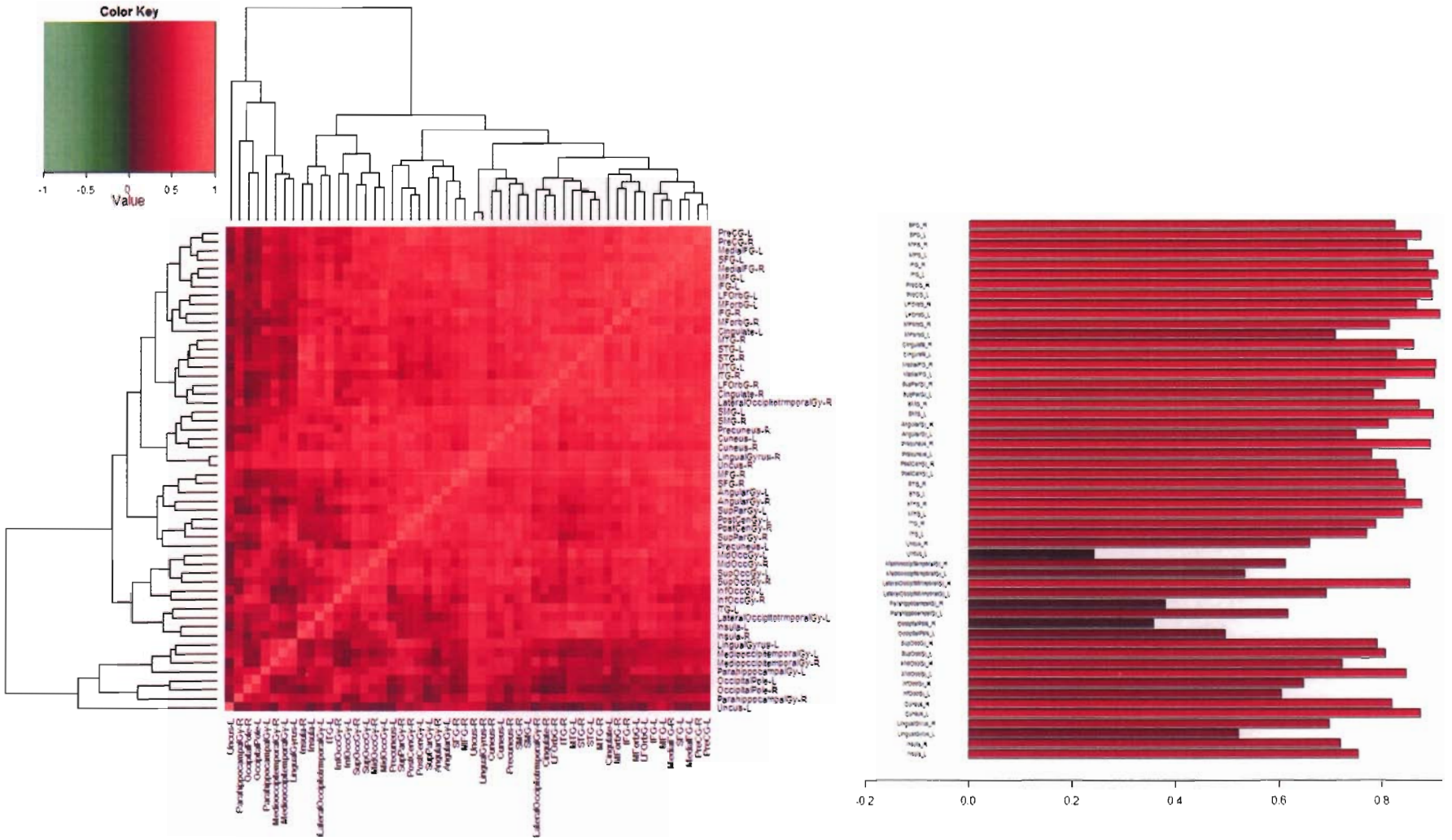

A B

Graph Theory

Using statistically significant genetic correlations as a threshold for edge placement, we identified 185 edges connecting the 54 neuroanatomic structures. Table 9.3 summarizes statistics by region. The distribution of edges was not uniform; regions with the highest number of edges (i.e. the degree of the node) were the superior and middle frontal gyri, pre- and postcentral gyri, superior parietal gyrus, and the occipital pole. The clustering coefficient and characteristic path length were similarly heterogeneous for different structures, with ranges from 0.17-1.0 and 2.3-3.7, respectively. The characteristic path length for the entire observed system was 2.8, which was marginally (1.2 times) larger than that in simulation of random networks (L=2.3, SD=.03). In contrast, the clustering coefficient for the entire system was .50, 4.2 times higher the average value for the simulated networks (C = .12, SD=.03). Figure 9.6A displays this graphically. The tight local clustering of the data relative to random networks is apparent in Figure 9.6B-C; in the observed data, most edges from a given node connect to other nodes nearby in the network, with occasional connections to distant nodes. Like prior analyses, the graph theoretical approach found strong relationships within fronto-parietal and occipital subnetworks (Figure 9.6D).

Table 9.3: Network statistics for gyral subregions

Structure	Degree	Clustering Coefficient	Average Path Length
SFG-R	12	0.62	2.74
SFG-L	11	0.69	2.78
MFG-R	7	0.52	2.85
MFG-L	10	0.38	2.65
IFG-R	6	0.47	3.19
IFG-L	9	0.22	2.63
PreCG-R	9	0.83	2.81
PreCG-L	12	0.58	2.63
LFOrbG-R	3	0.33	3.09
LFOrbG-L	5	0.50	2.56
MForbG-R	3	0.67	3.30
MForbG-L	6	0.40	2.70
Cingulate-R	5	0.20	2.63
Cingulate-L	8	0.36	2.65
MedialFG-R	11	0.51	2.57
MedialFG-L	7	0.57	2.98
SupParGy-R	12	0.59	2.44
SupParGy-L	11	0.64	2.52
SMG-R	7	0.52	2.74
SMG-L	5	0.50	2.83
AngularGy-R	6	0.60	2.63
AngularGy-L	6	0.67	2.83
Precuneus-R	3	0.33	3.04
Precuneus-L	1	.	3.65
PostCenGy-R	12	0.61	2.59
PostCenGy-L	12	0.50	2.50
STG-R	3	0.67	3.48
STG-L	6	0.47	2.93
MTG-R	3	1.00	3.33
MTG-L	10	0.24	2.48
ITG-R	3	0.33	2.70
ITG-L	7	0.33	2.81
Uncus-R	3	0.33	3.00
Uncus-L	4	0.17	2.85
MediooccipitemporalGy-R	5	0.30	3.02
MediooccipitemporalGy-L	5	0.30	2.87
LateralOccipitotrmporalGy-R	2	1.00	3.69
LateralOccipitotrmporalGy-L	5	0.30	3.04
ParahippocampalGy-R	3	0.33	3.02
ParahippocampalGy-L	4	0.67	3.07
OccipitalPole-R	11	0.51	2.31
OccipitalPole-L	10	0.44	2.41
SupOccGy-R	10	0.42	2.31
SupOccGy-L	7	0.81	2.63
MidOccGy-R	9	0.56	2.39
MidOccGy-L	9	0.42	2.37
InfOccGy-R	7	0.76	2.85
InfOccGy-L	10	0.58	2.35
Cuneus-R	8	0.43	2.69
Cuneus-L	5	0.60	2.63
LingualGyrus-R	5	0.40	2.78
LingualGyrus-L	6	0.20	2.69
Insula-R	5	0.40	3.19
Insula-L	6	0.47	3.17
Global Average	**6.85**	**0.50**	**2.81**

Figure 9.6: Genetically-mediated neuroanatomic networks modeled using graph theory. Panel A displays the distribution of the clustering coefficient (C) for 1000 random networks generated using permutation of observed data. The value of C from the observed data is given as an asterisk. Panels B and C represent graphs of a randomly generated network and the observed graph, respectively. In these graphs, nodes are represented as dots on the periphery of the circle and edges as lines; nodes are placed such that overlap of edges is minimized. Panel D represents an alternative layout of the observed data; darker edges represent stronger correlations.

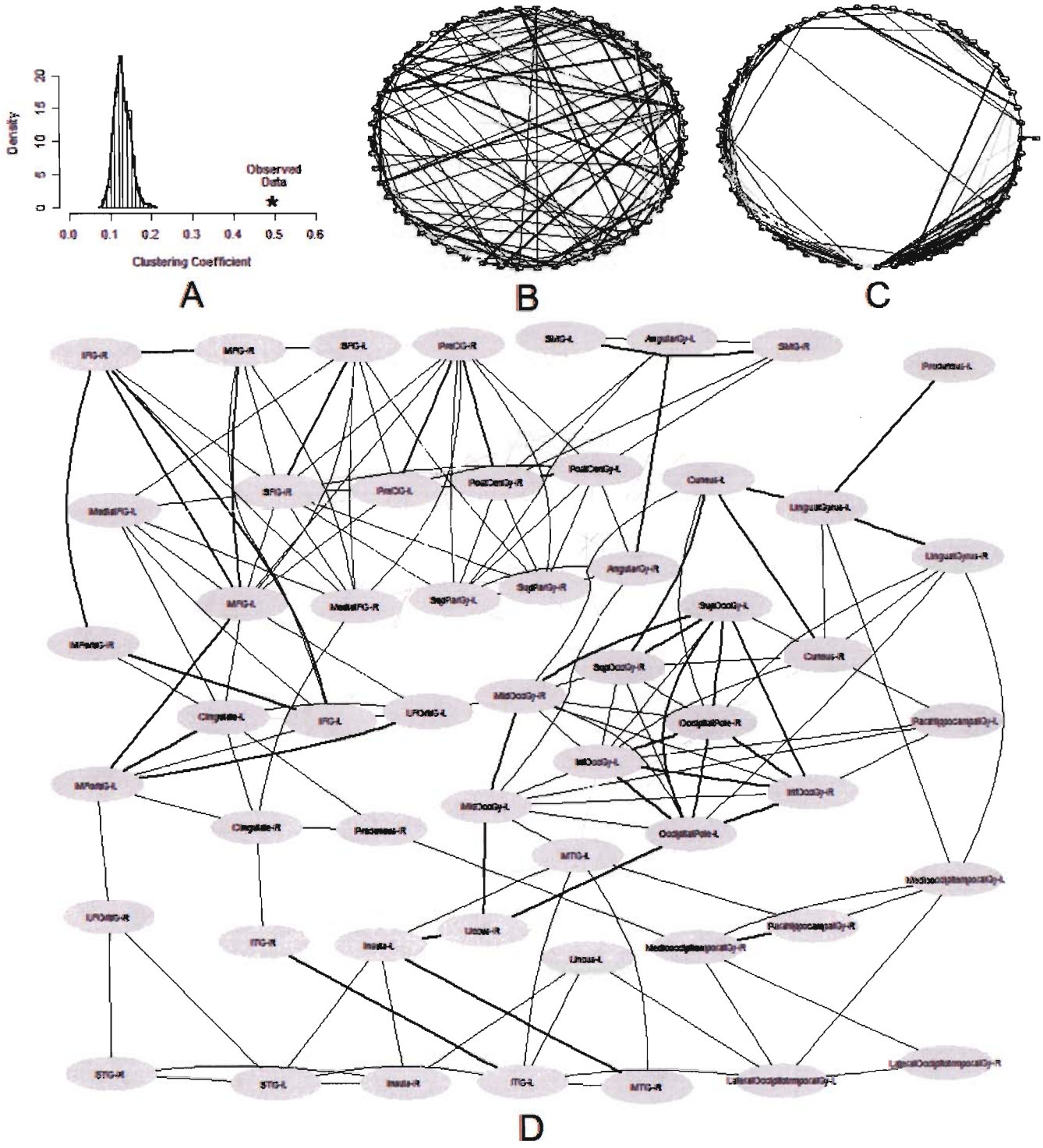

Discussion

The results from univariate analysis found substantial heterogeneity in the heritability of cortical thickness throughout the cerebrum, with the most heritable structures having about half of their variability explained by additive genetic effects. The most heritable structures were primarily frontal, somatosensory, supramarginal, or superior temporal. In general, gyri in the posterior and inferior cerebrum had lower heritability measures. These findings are largely consistent with the few prior studies at or above the level of resolution of the present study, with the exception that the heritability of cortical thickness appears to be smaller in magnitude when compared to measures of gray matter density (Thompson et al., 2001) or volumes (Wright et al., 2002). Studies of heritability on the lobar level have similarly found lower heritability for occipital lobe volumes relative to the remainder of the brain (Geschwind et al., 2002; Wallace et al., 2004), though between-lobe differences are less pronounced than differences between gyral-level measures.

Our multivariate analyses identified several distinct genetic factors that may be involved in gyral variability. Cluster analyses largely reproduced lobar segmentation patterns using the genetic correlations alone, suggesting that genetic control of the variation in cortical thickness may in part be controlled regionally. Molecular genetic studies have demonstrated that gene expression of cadherins and other molecules demarcate the gross lobar patterns of the cortex by birth (Rash & Grove, 2006), and therefore a similar pattern of genetic variability might be expected if polymorphisms exist in the genes responsible for prenatal neurodevelopment. Interpretation of these data, however, is somewhat limited because clustering imposes a structure to the data which may not be present in reality (Hastie et al., 2001). Nevertheless, we believe that in this case the exercise has proven fruitful, as it produces findings that largely mimic well-established neuroanatomic relationships; additionally heatmaps such as Figure 3 have the advantage that they allow for simultaneous inspection of the results and the data used to produce them.

Though there are no equivalent multivariate analyses in humans, the correlational blocks that we observed are strikingly similar to those produced in functional analyses of primate cortical connectivity using the large public database CoCoMac (Collections of Connectivity on the Macaque) (Passingham, Stephan, & Kotter, 2002; Stephan et al., 2000; Young, 1993; Young et al., 1995; Young, 1992). For example, Stephen et al. performed a multivariate meta-analysis of strychnine nonograpgy in macaque cortex. The application of strychnine, which locally inhibits $GABA_A$ and glycine, generates increases in activity in distal areas that can subsequently be measured. By using several different multivariate techniques, including cluster analysis, multidimensional scaling, and graph

theoretical models, Stephen examined the effects of 245 different local cortical applications of strychnine on 3897 tests of activity throughout the cortex. They identified three major clusters comprising 1) primary motor area, premotor areas, primary somatosensory cortex, and superior parietal regions (PEp and PEm) , 2) A "visual" cluster including primary visual cortex, extrastriate visual cortex, tempro-occipital regions, and medial temporal cortex, and 3) an "orbito-temporal-insular" cortical cluster including frontal operculum, anterior insula, and "polar, medial, and allocortical regions of the temporal lobe." There also were a few smaller clusters identified, whose structure varied depending on analyses methods; one included area 10 (orbitofrontal) and subcallossal region (FL), and one involved parietal operculum, area TB, and posterior insula. Given the remarkable concordance between these data and our own despite substantial methodological differences, it seems possible that variation in human cortical networks is related to genes that predate human speciation.

Multivariate analyses in primates also suggest that the organization of the primate brain follows small world architectural rules, by which inter-structural connectivity is dense within blocks and more sparse between them (Kotter & Sommer, 2000; Sporns et al., 2004; Sporns, Tononi, & Edelman, 2002; Sporns, Tononi, & Edelman, 2000). It has been suggested that this type of architecture is an appealing model of neural function since it allows both for modularization and efficient integration between functional subregions, resulting in enhanced computational power and transmission speeds (2000; Sporns et al., 2004; Stephan et al., 2000). Despite the fact that structural organization is an area of great interest to the field of systems neuroscience, at present there have been few

multivariate structural MRI studies in humans (2000; Crick & Jones, 1993; Mesulam, 2000; Sporns et al., 2004); this fact is somewhat surprising given the rapid increase in the use of multivariate techniques for the analysis of data from functional and diffusion tensor imaging (Ramnani et al., 2004). Though the present study is limited by several factors when compared to studies on nonhuman primates (not the least of which are level of resolution, implicit rather than explicit physical distances, and a lack of rigorous graph theoretical analysis), the dense clustering observable at the gyral level also implies a small world architecture. To our knowledge, this is the first evidence of this effect for anatomic MRI in humans, though several recent fMRI and DTI studies have reported small world properties in human neural function and white matter orientation (Achard, Salvador, Whitcher, Suckling, & Bullmore, 2006; Sporns, Tononi, & Kotter, 2005). Since our analyses were based on genetic, rather than phenotypic variances, it also appears that genetic factors are involved in the patterning of the human cortex in this manner.

Using PCA, we found that 6 principle components could explain the majority of the variance in all 54 gyral measurements. The components resembled the high-level groupings identified with hierarchical cluster analysis. Discrepancies between the two methods are at least partially owed to the discrete nature of clustering versus the more continuous approach in PCA; while a given structure may belong to only one cluster, it can have strong loadings on multiple components. The largest principle component in our study identified a superior frontoparietal network. Other important components included two factors primarily representing structures involved in visual processing (one

including the occipital pole, surrounding occipital gyri, and cingulate cortex, and the second influencing medial and ventral occipital lobe and occipitotemporal gyri), a purely frontal factor, a temporo-insular factor, and a parietal component most strongly influencing structures of the inferior parietal cortex.

Unfortunately, only a small number of imaging studies have investigated multivariate relationships in genetically-informative samples (Baare et al., 2001a; Pennington et al., 2000; Posthuma et al., 2000b; Schmitt et al., 2006). Of these, the most methodologically similar to the present study was that of Wright et al., on which many of our own methods were based (Wright et al., 2002). Their analyses found that two principal components could account for 24% of the total genetic variance in 92 regions, which they interpreted as representing a frontoparietal-limbic system and a supra-regional network involved in audition. The structures tapped by the second factor primarily were located in temporal lobe, dorsolateral prefrontal and orbitofrontal cortex, insula, and extracortical regions. The factor loadings were quite low for both factors ($|loadings| < .25$). Potential reasons for the discrepancies between the two studies are numerous, including 1) differing phenotypes both in measure (volume versus cortical thickness) and parcellation scheme, 2) the bivariate model used by Wright constrained genetic correlations to be positive while the present study allowed for negative values, 3) the former study used twins only while the latter included information from related family members, 4) an adult versus pediatric sample, and 5) a fifteen-fold difference in sample size.

Given these differences, it is reassuring that our dominant fronto-parietal component is similar to the largest component reported by Wright et al, as well as to findings from studies on primate cortical connectivity. With the strong structural and functional interrelationships between motor cortex, premotor cortex, and parietal lobe, it may come as no surprise to find evidence of regionalized genetic influences on structural variability. In addition, the fifth component reported in the present study somewhat resembles Wright's auditory factor, with large effects on STG and insular cortex and moderate loadings on orbitofrontal cortex. The remaining patterns in our data are a bit more enigmatic, though structures with high loadings on a particular factor tend to have anatomic or functional connectivity with each other. To reverse the problem, however, it is unclear why some regions dissociate so clearly, such as superior versus inferior parietal lobe, or lateral versus medioventral occipital lobes, despite being in close spatial proximity and thought to have related (albeit distinct) functionality.

Finally, it is important to keep in mind that these analyses do not account for all of the genetic variation in the cerebral cortex. In particular, the use of a global covariate obscures the presence of a genetic factor that strongly influences the thickness of nearly the entire cerebral cortex. A prior volumetric study by our group showed a similar phenomenon in a multivariate study of cerebrum and 5 other brain structures of diverse ontogenetic origins (cerebellum, basal ganglia, thalamus, corpus callosum, and the lateral ventricles) in a genetically informative sample (Schmitt et al., 2006). Thus, although the present study suggests that genes play a regional role in overall brain patterning, it appears secondary to global effects. As the genes influencing individual differences in

brain structure are discovered, it is likely that the genes with the largest effect size will influence the entire cortex in concert, with genes of lesser effect acting on specific subregions and local networks.

10

VARIANCE DECOMPOSITION OF MRI-BASED COVARIANCE MAPS USING GENETICALLY-INFORMATIVE SAMPLES AND STRUCTURAL EQUATION MODELING

"The brain is a world consisting of a number of unexplored continents and great stretches of unknown territory"

--Santiago Ramón y Cajal

ADAPTED FROM:

SCHMITT JE, LENROOT R, ORDAZ SE, WALLACE GL, LERCH JP, NEALE MC, KENDLER KS, GIEDD JN. VARIANCE DECOMPOSITION OF MRI-BASED COVARIANCE MAPS USING GENETICALLY-INFORMATIVE SAMPLES AND STRUCTURAL EQUATION MODELING. *NEUROIMAGE*. SUBMITTED.

ABSTRACT

Multivariate statistical genetic analysis of the cortex has, thus far, been limited to the gyral level. In this chapter, we combine classical behavioral genetic methodologies for variance decomposition with novel semi-multivariate algorithms for high-resolution measurement of phenotypic covariance. Using these tools, we produced correlational maps of genetic and environmental relationships between several regions of interest and the cortical surface. These analyses demonstrated high, fairly uniform genetic correlations between the entire cortex and global mean cortical thickness. Using several gyri as seed regions, we found a consistent pattern of bilateral genetic correlations between structural homologues, with environmental correlations more restricted to the same hemisphere as the seed region. These findings are consistent with the limited existing knowledge on the genetics underlying cortical variability, as well as our prior multivariate studies on cortical gyri.

Introduction

The development of non-invasive technologies for the acquisition of neuroanatomic information has revolutionized our ability both to obtain and to analyze human brain structure *in vivo*. Over the last several decades, magnetic resonance imaging (MRI) in particular has greatly expanded our understanding of the neural substrates of many psychiatric and neurological diseases, neurogenetic syndromes, typical human neurodevelopment, and aging. But with a few notable exceptions (Lerch et al., 2006; Worsley, Chen, Lerch, & Evans, 2005), the vast majority of the work on anatomic MRI to date has been univariate. The interrelationships between different regions are fundamentally important, however, given the compartmentalization of essential neural functions and the formation of complex neural networks. Many neuroanatomic circuits, such as the limbic system, perceptual and motor systems, and networks involved in higher cognition, language, and mood might be expected to result in morphological correlations between related regions. The mechanisms underlying these observed correlations in brain structure are of great neurodevelopmental interest; are they generated via shared genetic programming, or rather environmental effects that similarly influence different neuroanatomic structures?

Many research modalities such as axon tracing studies, diffusion tensor imaging, positron emission tomography, and even functional imaging have actively pursued methods on generating maps of neuroanatomic interrelatedness (Ramnani et al., 2004). Multivariate analyses in high-resolution structural data are particularly challenging, however, given

the extremely large number of voxels and subsequent immense computational requirements (the so-called "curse of dimensionality") for traditional multivariate approaches. Recently, semi-multivariate methods for high-resolution mapping of cortical correlations have been proposed that provide a work around to the problem of multidimensionality, by calculating correlations between all voxels and a target region of interest (ROI) (Lerch et al., 2006; Worsley et al., 2005). These semi-multivariate approaches, in particular, are easily integrated into quantitative genetic analyses.

In this article, we describe a simple statistical genetic extension to these maps of neuroanatomic relatedness. Using a similar global strategy, we use structural equation modeling (SEM) on genetically-informative data in order to decompose neuroanatomic relationships into those driven by either genetic or non-genetic factors. With these extensions we can begin to answer not only which regions are structurally related, but also whether observed phenotypic relationships are determined by shared genes or environmental forces.

Methods

Subjects

Subjects were recruited as part of an ongoing longitudinal study of pediatric brain development at the Child Psychiatry branch of the National Institutes of Mental Health (NIMH). Recruitment was performed via local and national advertisements and participants were screened via an initial telephone interview, parent and teacher rating

versions of the Child Behavior Checklist (Achenbach and Ruffle, 2000), and physical and neurological assessment. Exclusion criteria included psychiatric diagnosis in the subject or a first degree relative, and head injury or other conditions that might have affected gross brain development. Twin zygosity was determined by DNA analysis of buccal cheek swabs using 9-21 unlinked short tandem repeat loci for a minimum certainty of 99%, by BRT Laboratories, Inc. (Baltimore, MD). Twins were included in the analysis only if quantifiable MRI scans free from motion or other artifact were obtained on both twins at the same age. Written assent from the child and written consent from a parent were obtained for all participants. The study protocol was approved by the institutional review board of the National Institute of Mental Health.

The resultant sample consisted of 600 children in total (mean age 11.1, SD 3.4, range 5.4-18.7), including 214 MZ and 94 DZ twins, 64 singleton siblings of twins (1-2 per family), 116 members of entirely singleton families (2-5 members per family), and 112 unrelated singletons. The distribution of subjects and basic demographic information are given in Table 5.1. Findings on the heritability of high-resolution cortical thickness measures have been reported previously with this sample (Lenroot et al., 2007).

Image Acquisition

All subjects were scanned on the same GE 1.5 Tesla Signa scanner using the same three-dimensional spoiled gradient recalled echo in the steady state (3D SPGR) imaging protocol (axial slice thickness = 1.5 mm, time to echo = 5 msec, repetition time = 24 msec, flip angle = 45 degrees, acquisition matrix = 192 x 256, number of

excitations = 1, and field of view = 24 cm). A clinical neuroradiologist evaluated all scans and no gross abnormalities were reported.

Image Analysis

The native MRI scans first were registered into standardized stereotaxic space using a linear transformation (Collins et al., 1994) and subsequently corrected for non-uniformity artifacts (Sled et al., 1998). The registered and corrected volumes were segmented into white matter, gray matter, cerebro-spinal fluid and background using a neural net classifier (Zijdenbos et al., 2002). The white and gray matter surfaces are then fitted using deformable models resulting in two surfaces with 81920 polygons each (MacDonald et al., 2000). The white and grey matter surfaces are resampled into native space and CT was then computed in native space. Each subject's cortical thickness map was then blurred using a 30mm surface based blurring kernel which respects anatomical boundaries, resulting in 40962 unique cortical measures (Lerch et al., 2005a).

Statistical Analysis

Our overall analytic approach is similar to many of the MACAAC methods described in Lerch et al. which calculate Pearson cross-correlations between a target ROI and all cortical vertices (Lerch et al., 2006). The present methods differ in that 1) data records were based on families rather than individuals and 2) variance decomposition for each vertex were computed using SEM in Mx (Neale et al., 2002), a linear algebra interpreter and numeric optimizer commonly used in quantitative genetics (Neale et al., 1992). The parsing of variation into subcomponents is possible because of the known differences in

genetic relatedness between different types of family members. In the simpler univariate case, for example, differences between MZ and DZ cross-twin correlations can be used to compute the variance attributable to genetic factors across all vertices via the formula:

$$\forall i : Var_{A_i} = 2\left(\sum_{j=1}^{N_{MZ}} \frac{(v_{ij1} - \mu_{iMZ1})(v_{ij2} - \mu_{iMZ2})}{N_{MZ}} - \sum_{k=1}^{N_{DZ}} \frac{(v_{ik1} - \mu_{iDZ1})(v_{ik2} - \mu_{iDZ2})}{N_{DZ}} \right)$$

Where VAR_A is a N_v x 1 vector of genetic variances equal in length to the observed measurements (e.g., in our case, $N_v = 40962$), v_i is the measured cortical thickness for the i^{th} vertex, and subscripts 1 and 2 denote twin number. N_{MZ} and N_{DZ}, μ_{MZ} and μ_{DZ}, and j and k are the number of twin pairs, means, and twin pair index for MZ and DZ groups, respectively. This formulation is more simply and familiarly expressed as $Var_{Ai} = 2(\text{cov}_{iMZ} - \text{cov}_{iDZ})$ for the i^{th} vertex; the variance analog of Falconer estimation (Falconer et al., 1996). A similar procedure can be employed to calculate the genetic covariance between two phenotypes of interest by comparing the cross-twin, cross-trait covariances between MZ and DZ groups rather than the within-trait covariances. For the i^{th} vertex, in order to calculate the genetic covariation with a seed ROI the formula can be modified to:

$$Cov_A(V_i, ROI) = 2\left(\sum_{j=1}^{N_{MZ}} \frac{(v_{ij1} - \mu_{iMZ})(ROI_{j2} - \mu_{roiMZ1})}{N_{MZ}} - \sum_{k=1}^{N_{DZ}} \frac{(v_{ik1} - \mu_{iDZ})(ROI_{k2} - \mu_{roiDZ2})}{N_{DZ}} \right)$$

which simplifies to $Cov_A(V_i, ROI) = 2\left(Cov_{MZ}(V_{i1}, ROI_2) - Cov_{DZ}(V_{i1}, ROI_2)\right)$. These simple formulations have some important limitations. The calculation of genetic

covariance shown above, for example, effectively ignores half of the available information on cross twin covariance. Though including this information is possible, several other problems with this approach remain, including 1) these statistics do not easily generalize to more than two individuals per family group, 2) no information regarding the relative precision of the MZ and DZ correlations is incorporated, which are dependent both on sample size and correlation magnitude, 3) generating test statistics to determine whether covariation is statistically important is not straightforward, and 4) the addition of covariates, such as age and sex, is difficult.

SEM based approaches provide a straightforward solution to these problems. In the present study, family relationships were modeled using a statistical genetic extension of the Cholesky decomposition (e.g., Figure 10.1), which factors any symmetric positive definite matrix into a lower triangular matrix postmultiplied by its transpose (Neale et al., 1992). This approach allows for the covariance between two phenotypes to be decomposed into covariance resulting from genetic, shared environmental, or unique environmental sources but places few *a priori* constraints on the data. The variance in observed variables (denoted as rectangles in Figure 1) are modeled to be mediated by latent additive genetic (A.), shared environmental (C.) or unique environmental (E.) sources of variance (circles) with latent variances standardized to unity.

Figure 10.1: Figure 9.1, reproduced for convenience. Like the previous chapter, a simple bivariate model was used to assess neuroanatomic relationships. The analyses differ in that rather than investigating all pairwise relationships in 54 gyral regions, each analyses wave in the present study compares 40,962 cortical points to a single, target ROI.

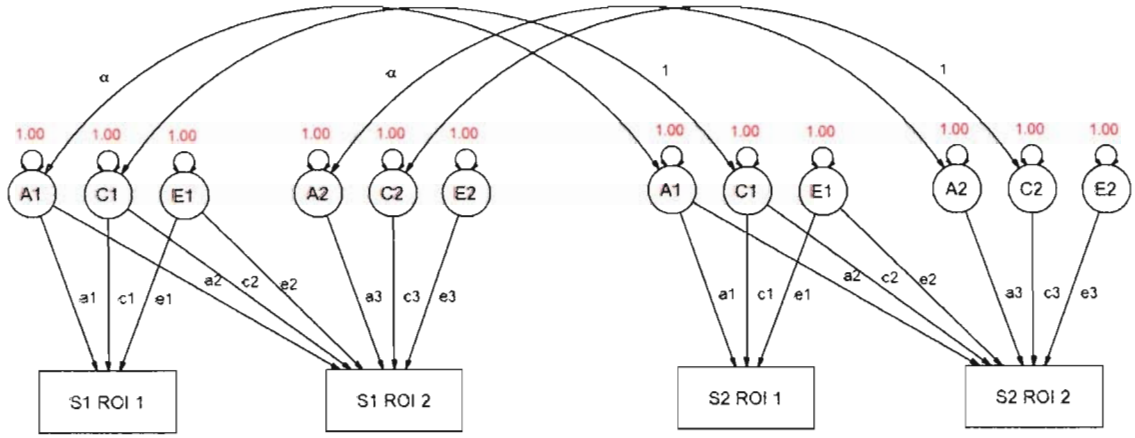

This model is identified since the correlation between genetic factors is perfect in MZ twins, but, on average, ½ between DZ twins and singleton siblings. In the path diagram shown in Figure 10.1, single-headed arrows are causal, double headed arrows represent correlations, with values on causal arrows (e.g. a1, a2, and a3) representing freely estimated parameters. The expected covariances of this model produce nine simultaneous equations from which the values of the nine free parameters (a., c., e.) can be estimated. In practice, the expected covariance matrices varied from 2 x 2 to 10 x 10 depending on the number of members in the family (e.g. 1-5). The addition of siblings of twins and a large sample of siblings from singleton families (i.e. families with no twins) provided substantially increased power to detect genetic signal due to a greater number of observed covariance statistics (Posthuma et al., 2000b; Posthuma et al., 2000a). This extended design assumes that the shared environment operates similarly in both twins and singleton births, with respect to the phenotype of interest. In our sample, families

contained a twin pair and up to three additional siblings, or singleton families with up to five members in total. Consistent with our univariate analyses (Lenroot et al., 2007), the role of the shared environment was minimal for all seed regions, and following the rules of parsimony it was removed from the findings reported below.

Optimization was performed using maximum likelihood (ML) (Edwards, 1972), which produces unbiased estimates of model parameters. From the parameter estimates calculations of the genetic and unique environmental covariance (cov_G and cov_E) between an ROI and all vertices could be determined. In addition, the genetic and environmental correlations were calculated by standardizing the decomposed variance-covariance matrices:

$$r_G(v_i, ROI) = \frac{Cov_A(v_i, ROI)}{\sqrt{(Var_A(v_i) * Var_A(ROI)}} \quad \text{and} \quad r_E(v_i, ROI) = \frac{Cov_E(v_i, ROI)}{\sqrt{(Var_E(v_i) * Var_E(ROI)}}$$

ML also allows for straightforward hypothesis testing, since the removal of parameters of interest from the original model produces nested submodels in which the difference in ML generally follows a χ^2 distribution, with degrees of freedom equal to the difference in the number of free parameters (Neale et al., 1992). Thus, probability maps indicating regions of significant covariances could be constructed.

Assessment of Global Covariation

We first wanted to determine how genetic factors contribute to global covariation patterns. MACAAC algorithms include a measure of correlational strength (MACAAC-strength), which is the average correlation between vertex *i* and all other vertices:

$$MACACCs_i = \frac{\sum_{j=1}^{N_v} r}{N_v}$$

Unfortunately, this approach is computationally demanding, as correlations for all pairwise combinations of vertices must be calculated. The computational cost is magnified with SEM, as numeric optimization must be performed for each pairwise combination of vertices. However, it has been demonstrated that use of global mean cortical thickness as a target ROI provides a reasonable approximation for the average correlation across all *j* (Lerch et al., 2006). This approach represents a special case of the general bivariate method of comparing a single ROI to a large vector of vertices.

Therefore, we employed our general bivariate SEM using mean global cortical thickness as the target ROI (μ_G). In addition to modeling the variances as described previously, we also simultaneously adjusted for mean effects of sex and age on the phenotypes of interest. Sex effects were estimated using a linear model and age was estimated using a cubic model, based on prior evidence of age interactions with cortical thickness (Lenroot, 2005). The resultant parameter estimates provide measures of the dominant forces driving interrelationships in cortical thickness. These findings provide similar information to that

which would be gleaned from examining the dominant eigenvalues of a principle component analyses on the N_v x N_v (40962 x 40962) covariance matrix, after decomposing the matrix into genetic and environmental subcomponents.

The maximal likelihood parameter estimates for the analyses were then projected onto the brain surface. In order to gain a thorough understanding of the strength of relationships, both covariances and correlation maps were constructed. Additionally, probability maps (H_0: $r_G = 0$ and H_0: $r_E = 0$) were constructed. The risk of type I error associated with multiple testing was controlled by setting a false discovery rate of .10 (Genovese et al., 2002), with η_0 calculated by bootstrap (Storey, 2002).

Analyses of target ROIs

We also examined covariances with respect to more localized ROIs, which were chosen based on prior univariate studies on the genetic contributions to brain structure (Lenroot et al., 2007). Because this study had shown particularly high heritability in Broca's area, we chose as our first seed region those vertices in the left inferior gyrus with the highest univariate heritability. To generate the remaining seed ROIs, a probabilistic atlas was used to assign cortical points to specific neuroanatomic regions (Collins et al., 1999), which roughly corresponded to cerebral gyri and were based on the sulcal definitions of Ono (Ono et al., 1990). The mean CT for this region was then calculated. In these studies, we controlled for global effects by including μ_G as a covariate in addition to age and sex. Our previous research demonstrated that the most heritable regions of the cortex lie in superior and inferior frontal gyri (SFG and IFG, respectively), left supramarginal gyrus (SMG), and superior temporal lobe (STG).

Results

Global Covariation

Genetic correlations with μ_G approached unity and were substantially higher than environmental correlations, though both had similar patterns. The genetic correlations were uniformly high except in the superior parietal lobule and the occipital pole (Figure 10.2). The regions with the strongest genetic correlations were the frontal cortex, SMG, STG, and in parieto-temporal cortex centered on the angular gyrus and continuing into lateral temporal lobe. Most primary somatosensory cortex, primary motor cortex, and primary visual cortex had lower genetic correlations with μ_G. The most notable differences in *pattern* between the two measures were that genetic correlations in the frontal poles, left SMG and STG, and inferior pre- and postcentral gyri bilaterally were among the highest in the brain, while environmental correlations were unremarkable in these regions. Probability maps (not shown) were uniformly significant, with 86% and 99% of all vertices significantly correlated with μ_G via genetic and environmental factors, respectively, at an α of .05. Correlational patterns for both genetic and environmental correlations were remarkably similar to measures of phenotypic cross correlations reported by Lerch et al., with the genetic correlational maps more similar in magnitude.

Figure 10.2: Maps of genetic and environmental relationships between global mean CT and individual vertices. Genetic and environmental correlations (r_G and r_E), covariances (cov_G and cov_E), and probability maps testing for significant genetic and environmental covariance. Map of MACAACs statistic (lower right) is adapted from Lerch et al.

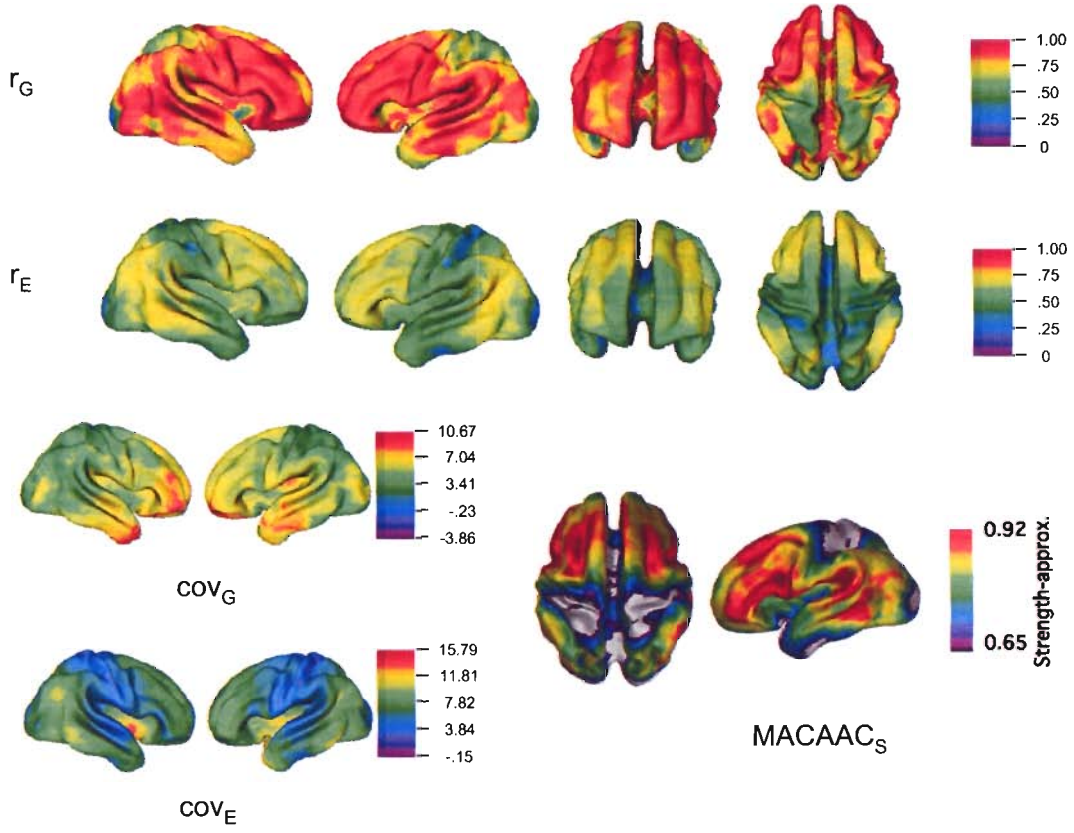

Correlations with target ROIs

When modeling relationships with target ROIs, striking differences were observed between the genetic and environmental correlations. Figures 10.3, 10.4, and 10.5 provide surface renderings of the results of analyses using several seed ROIs. In general, we observed that environmental correlations and covariances tend to be greatest in regions in close spatial proximity to the seed, gradually decreasing with greater distance along the cortical surface. Environmental correlations were almost entirely unilateral, with some notable exceptions. The most obvious of these were environmental correlations between

the superior frontal gyrus and its contralateral homologue, though correlations remained highly asymmetrical. Environmental correlations appeared almost entirely positive.

Genetic correlations, in contrast, were typically bilateral and were occasionally negative. Genetic correlations were high both spatially proximal to the seed itself, but also in and near the corresponding gyrus in the contralateral hemisphere. In many cases, the genetic correlations were, in fact, stronger in the contralateral hemisphere. Negative genetic correlations were most commonly observed between distal structures, such as between frontal ROIs and the occipitotemporal cortex. We also observed some differences in the pattern of genetic correlations when the ROI seed was in the left or right hemisphere, particularly for the IFG. Though the genetic correlations were strong bilaterally in both cases, they were very high between RIFG and the entire frontal lobe, while genetic correlations to LIFG were more restricted to inferior frontal and orbitofrontal cortex.

Figure 10.3: Covariance Maps between CT and four seed ROIs with high univariate heritability. Genetic and environmental correlations (r_G and r_E), covariances (cov_G and cov_E), and probability maps testing for significant genetic and environmental covariance.

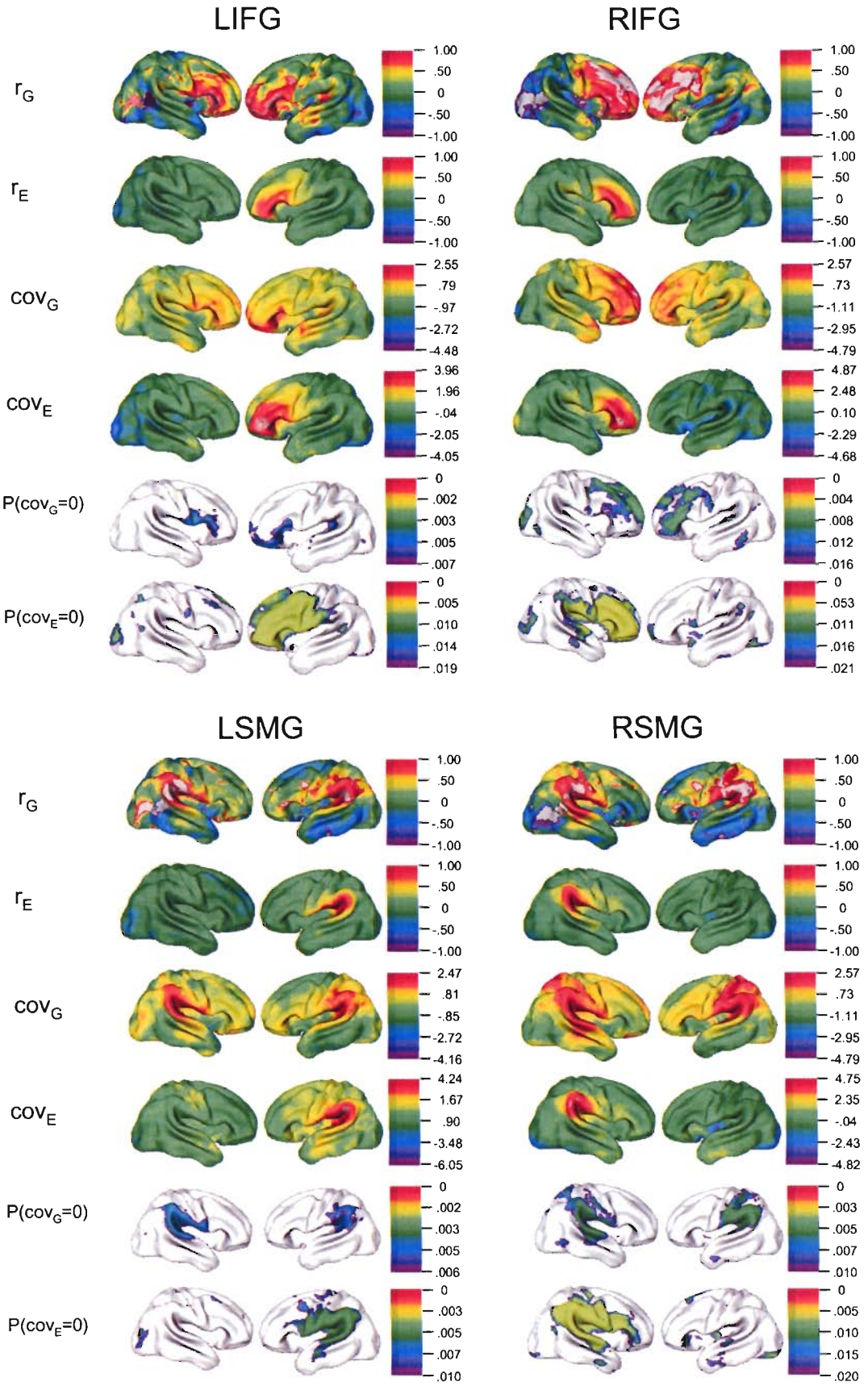

Figure 10.4: Maps of the genetic and environmental relationships with the superior frontal gyri.

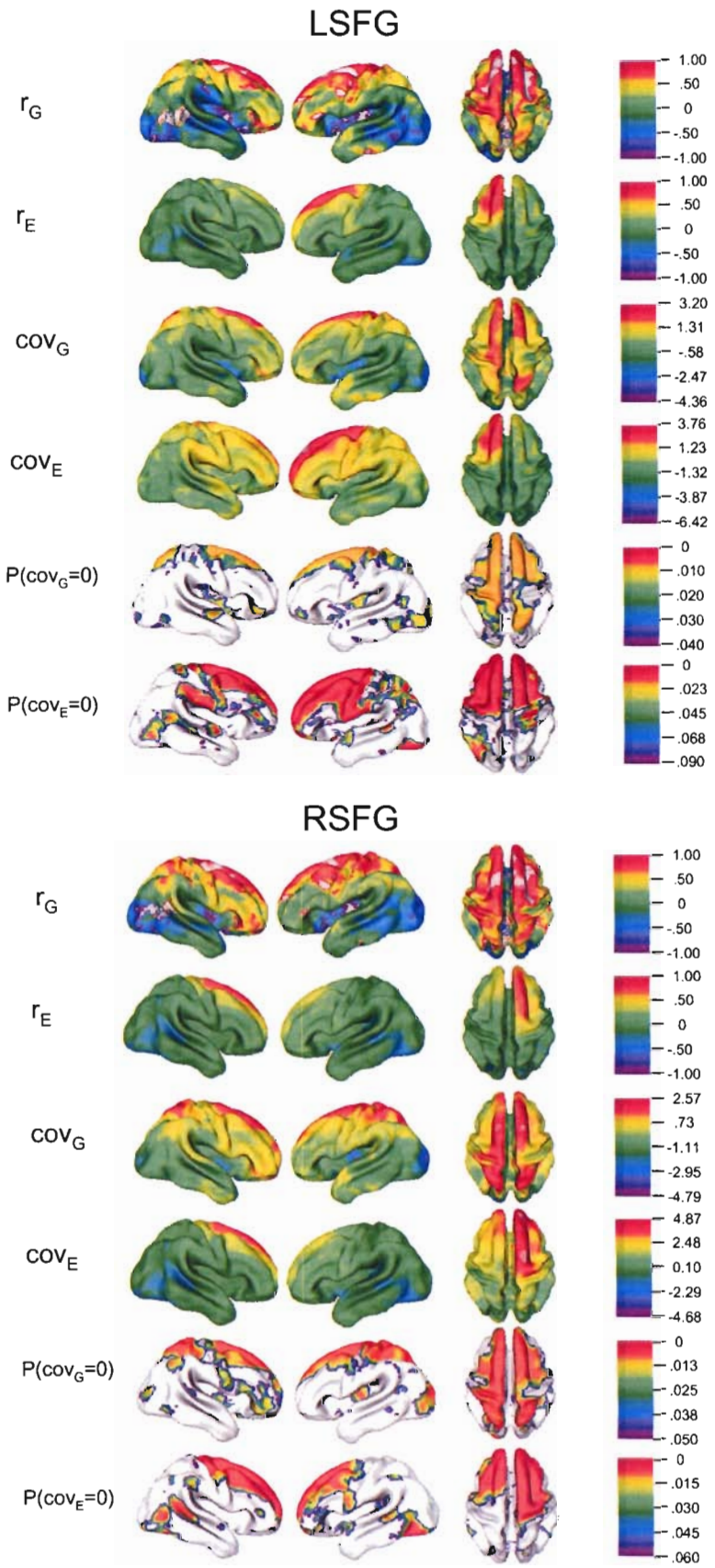

Among the most prominent exceptions to this rule were the results from analyses using a seed in Broca's area (Figure 10.5), which resulted in predominantly left-sided genetic correlations and included, in addition to adjacent regions of the inferior frontal lobe and orbitofrontal cortex, portions of the superior and middle temporal gyrus. Additionally, in contrast to the predominant unilateral correlations of larger seed regions, Broca's area had significant environmental covariance with right dorsolateral prefrontal cortex.

Figure 10.5: Correlation maps using Broca's area as a seed region.

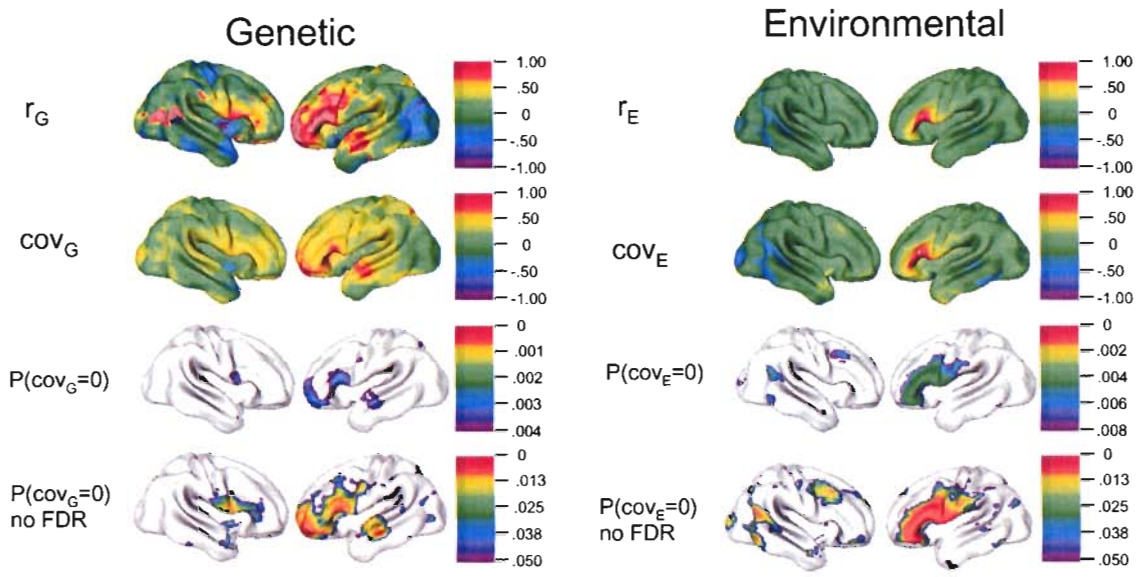

Discussion

These analyses demonstrate that traditional quantitative methodologies for the assessment of genetic variance can be integrated with novel multivariate tools for assessing cortical connectivity at high levels of resolution. This addition allowed us to decompose phenotypic correlational maps into maps of genetic and environmental correlations.

Using these methods, we found several differences between genetically-mediated and environmentally-mediated cortical relationships. While nearly all cortical vertices were highly correlated with μ_G via shared genetic origins, global environmental correlations were somewhat lower. Both genetic and environmental global correlations were highest in frontal and tempro-parietal association cortex, and were virtually identical to the $MACACC_s$ map of phenotypic correlations reported by Lerch et al. (see Figure 10.1). Since the $MACACC_s$ statistic identifies voxels with the highest average global associations, it is logical that association cortex would be most implicated. Interestingly, it appears as if this correlational pattern is determined by both common genetic and environmental effects. Given recent studies demonstrating that relatively minor environmental stimuli can produce changes in brain structure, it is reasonable to speculate that the establishment of these cortical networks is dependent on perceptual cues and responses to these cues (Draganski et al., 2004; Draganski et al., 2006) as well as contributions from one's genetic background.

The high genetic correlations between nearly the entire cortical surface and μ_G are consistent with the multivariate genetic studies on volumes, which show a single genetic factor accounting for the majority of both total genetic variance and the total phenotypic variance (Schmitt et al., 2006). Environmental factors appear to be somewhat more important to CT phenotypic variance than for volumes, but global genetically-mediated CT correlations appear largely dominated by a single genetic factor. In other words, genetic variation in the human population primarily influences the brain as a whole rather than regionally. Such a finding is consistent with radial models of neocortical evolution (Rakic, 1995) as well as the more recent modifications of this hypothesis (Kriegstein, Noctor, & Martinez-Cerdeno, 2006). It is important to note, however, that genetic *covariances* with μ_G were not uniform, but substantially higher in the frontal lobe, middle temporal lobe, and supramarginal gyrus, particularly on the left. The discrepancy between genetic correlations and covariances likely is due to a larger amount of genetic variance within the pediatric population in these regions (Lenroot et al., 2007).

Seed ROIs

For most seed ROIs, we observed strong localized environmental correlations and regionalized, bilateral genetic correlations, after adjusting for μ_G. In general, most of the covariance between the left and right hemispheres was a result of shared genetic mechanisms. A regionalized genetic role in bilateral cortical patterning, of course, is not a novel concept. Numerous neurogenetic syndromes are associated with bilateral abnormalities with very specific anatomical patterns, including several forms of

polymicrogyria, Smith Magenis syndrome, Turner syndrome, and language disorder associated with FOXP2 (2000; Boddaert et al., 2004; Guerrini & Marini, 2006; Mochida, 2005; Molko et al., 2004; Piao et al., 2005; Watkins et al., 2002). Recent anatomic MRI studies have shown that several common genetic polymorphisms influence brain structure bilaterally and in a regionally-specific manner, including variants of COMT, DISC1, BDNF, PCF1, and APOE (2000; Gurling et al., 2006; Hashimoto & Lewis, 2006; McIntosh et al., 2006; Nemoto et al., 2006; Wishart et al., 2006). For example, in a study of the apolipoprotein E gene (APOE), Wishart et al. found regionalized bilateral gray matter reductions in frontal and temporal regions in ε4/ε3 heterozygotes relative to individuals homozygous for the ε3 allele (Wishart et al., 2006). The aggregate effects of many polymorphisms such as these could explain the patterns we observed in population genetic variance in CT. Conversely, the information gleaned from studies on genetic covariance may facilitate the identification of the genes responsible for structural brain variation, by suggesting novel endophenotypic constructs or targets for multivariate analysis.

Dramatic advances in the molecular genetics of cortical patterning have been made in the last half decade, though it remains perhaps the least understood region of the brain. Considered as a whole, the brain appears to follow the same general developmental rules as the rest of the body, using gradients of intrinsic and extrinsic diffusible signaling molecules, regulatory factors, and structural proteins to identify the principal neuroanatomic axes (2000; Grove et al., 2003; Monuki et al., 2001). In the developing central nervous system, signaling centers have been shown to regulate anterior/posterior,

dorsal/ventral, and forebrain/hindbrain polarity (Grove et al., 2003). The expression of transcriptional regulator Pax6, for example, distinguishes progenitors of the cortex from subpallial structures, which instead express Gsh2 (Guillemot, Molnar, Tarabykin, & Stoykova, 2006; Molnar et al., 2006). There is some evidence that the principals of intracortical patterning are similar, with genes such as FGF 3, 7 8, 18, and Pax6 implicated in specification of the anteriorposterior cortical axis, and several members of the Wnt and Bone Morphogenetic Protein (BMP) families in establishment of the mediolateral axis in mice (Ciani & Salinas, 2005; Grove et al., 2003; Mallamaci & Stoykova, 2006). The molecular determinants of more regionalized cortical arealization are less certain, though several proteins (e.g. ephrins, cadherins, and members of the immunoglobulin superfamily) are expressed in specific patterns in the cortex (Monuki et al., 2001). Of these, the ephrins (diffusible molecules involved in axonal guidance), have been shown to have roles in the pattering of retinotectal, thalamocortical, and somatosensory circuitry (Flanagan, 2006; Price et al., 2006).

The principle exception to bilateral genetic correlations was our analyses of Broca's area, and to a lesser extent, the LIFG as a whole. In the case of Broca's area, remarkably, the highest genetic correlations were largely found in left orbitofrontal and middle frontal regions, as well as the superior and middle temporal gyri, and, in the case of LIFG, left supramarginal gyrus. The association between structures implicated in language is highly suggestive of a role of additive genetic factors in language development, particularly given the hemispheric specificity of the findings.

Although these findings represent a unique perspective on the genetics of brain structure, the limitations of the analyses must be considered in order to evaluate their utility. As this research represents a fusion of high-resolution anatomic methods as well as genetic techniques for twin and family covariance modeling, the general caveats for both apply to this research. Also, as our sample was entirely derived from a pediatric population, its generalizability to other ages is unclear. Indeed it is likely that future work on adults may find distinctly different patterns of genetic covariance, as childhood brain structure may be more strongly influenced by ontogenetic processes underlying brain formation itself, while adult brains will have had more time for these effects to attenuate, as well as the potential novel genetic and experiential effects on covariance to manifest. Finally, it is noteworthy that due to the inherent flexibility of SEM, the models reported here can easily be expanded to address more subtle questions about genetic and environmental etiology, such as the effects of age or other moderators on covariance patterns, or how intracortical relationships influence behavior measures.

11

A Brief Note on Brain and Behavior

"The mere fact that so much genetic variation [in intelligence] exists should provide a powerful incentive to research workers in psychology and many other related disciplines to search for the physical basis of intelligent behavior. The existence of this genetic variation guarantees that differences between people do, indeed, have a physical as well as experiential basis."

> --David W. Fulker and Hans J. Eysenk, "Nature and Nurture: Environment." In Eysenk's *The Structure and Measurement of Intelligence,* 1979.

King Arthur: Surely you've not given up your quest for the Holy Grail?
Minstrel: *He is sneaking away and buggering off--*
Sir Robin: [*to minstrel*] Shut up! [*to Arthur*] No, no no-- far from it.

> --Graham Chapman, Neil Innes, and Eric Idle, *Monty Python and the Holy Grail, 1975.*

The integration of biological data with behavioral phenotypes typically represents the climax of nearly any serious study of neurobiology, and the lack of behavioral data in the previous ten hefty chapters likely was noted by the reader long ago. Yet it is with no coincidence that we have disregarded the subject of behavior to the final pages of this long text, as identifying meaningful brain-behavioral correlates in our sample has proven quite challenging.

Difficulty in finding strong relationships between complex biological phenotypes and brain structure is nothing new, however. Neuroscientists have long endeavored, for example, to identify strong links between intelligence and brain volumes and with only modest success; both Broca and Galton struggled, largely in vain, to understand this relationship. Even with modern technology, until very recently there has been little consensus on the role of brain volume on IQ. Neuroimaging studies have produced quite inconsistent evidence, with correlations between IQ and total brain volume between .00 and .60, with most estimates reporting small but significant correlations of about .35 (Andreasen et al., 1993; Gur et al., 1999; Reiss et al., 1996; Vernon, Wickett, Bazana, & Stelmack, 2000). Subdividing the brain into substructures historically has provided only modest increases in the predictive power for the most correlated subregions.

What are we to make of these findings? The twin literature on common behavioral measures is extensive and informs us that IQ is among the most heritable of all behavioral phenotypes (Bouchard & Mcgue, 1981; Posthuma, 2002), an observation confirmed in our own sample (Figure 11.1). Thus, as its variance is largely determined

by biological sources, IQ is arguably among the best behavioral candidates for twin studies including data from biological endophenotypes. As reviewed in Chapter 3, there is some evidence of genetic correlations between large brain volumes and intelligence, though the overlap is disappointingly small (.29 versus total gray matter, .24 versus total white matter) (Posthuma et al., 2002).

Figure 11.1: Maximum likelihood parameter estimates from ACTE decomposition of several behavioral phenotypes from the Giedd sample. Behavioral measures include IQ, VIQ, and PIQ (left), the "trailmaking task" (TRAILS A and B), CANTAB tests of spatial working memory (SWM) and spatial recognition memory (SRM), and handedness measures (GP) from the PANESS.

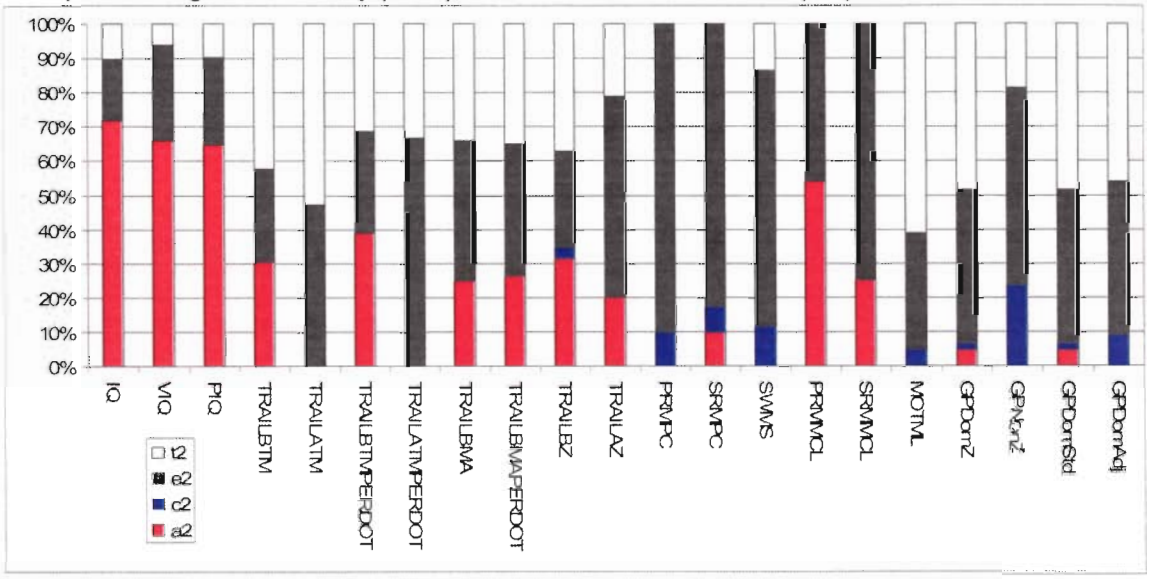

Prior to a retreat into Cartesian dualism, however, it is important to realize that volume is merely one (albeit highly heritable) metric of brain *structure*. Functional endophenotypes such as fMRI, EEG and PET notwithstanding, numerous other physical characteristics are of great interest to brain functionality (Gray & Thompson, 2004). Both gray and white matter density, for example, have been shown to be correlated with IQ, and there is some evidence of genetic contributions to the relationship (Hulshoff Pol et al., 2006; Thompson et al., 2001).

For both pragmatic and theoretical reasons, we opted to examine the relationships between IQ and cortical thickness rather than volumetric measures in our initial analyses. For the same sample and ROIs reported in Chapter 9 (54 gyral measures of mean cortical thickness on 600 children), we used bivariate SEM to decompose the variance between IQ and CT into generated by either genetic or nongenetic sources. The covariance and correlation maximum likelihood parameter estimates from these analyses are given in Figures 11.2 and 11.3.

Phenotypic correlations between IQ and the ROIs were universally low. Interestingly, however, the genetic and unique environmental covariances were substantially larger and of opposite sign. Thus, it appears as if the effects of genes and environment appear to mask one another in the phenotypic correlation, an effect that has long been considered possible on theoretical grounds but rarely is observed. This phenomenon may be, at least in part, responsible for the long tradition of weak correlations observed between structural endophenotypes and measures of intelligence.

Interestingly, the environmental correlation between IQ and CT is positive; in other words, environmental effects that increase CT also appear to increase IQ. Is such a result believable? In a landmark study, Draganski et al. demonstrated that environmental

Figure 11.2: Covariances between IQ, VIQ, and PIQ and mean cortical thickness for 54 gyral subregions. Phenotypic covariances are shown in black, genetic covariances in red, shared environmental covariances in blue, and unique environmental covariances in green.

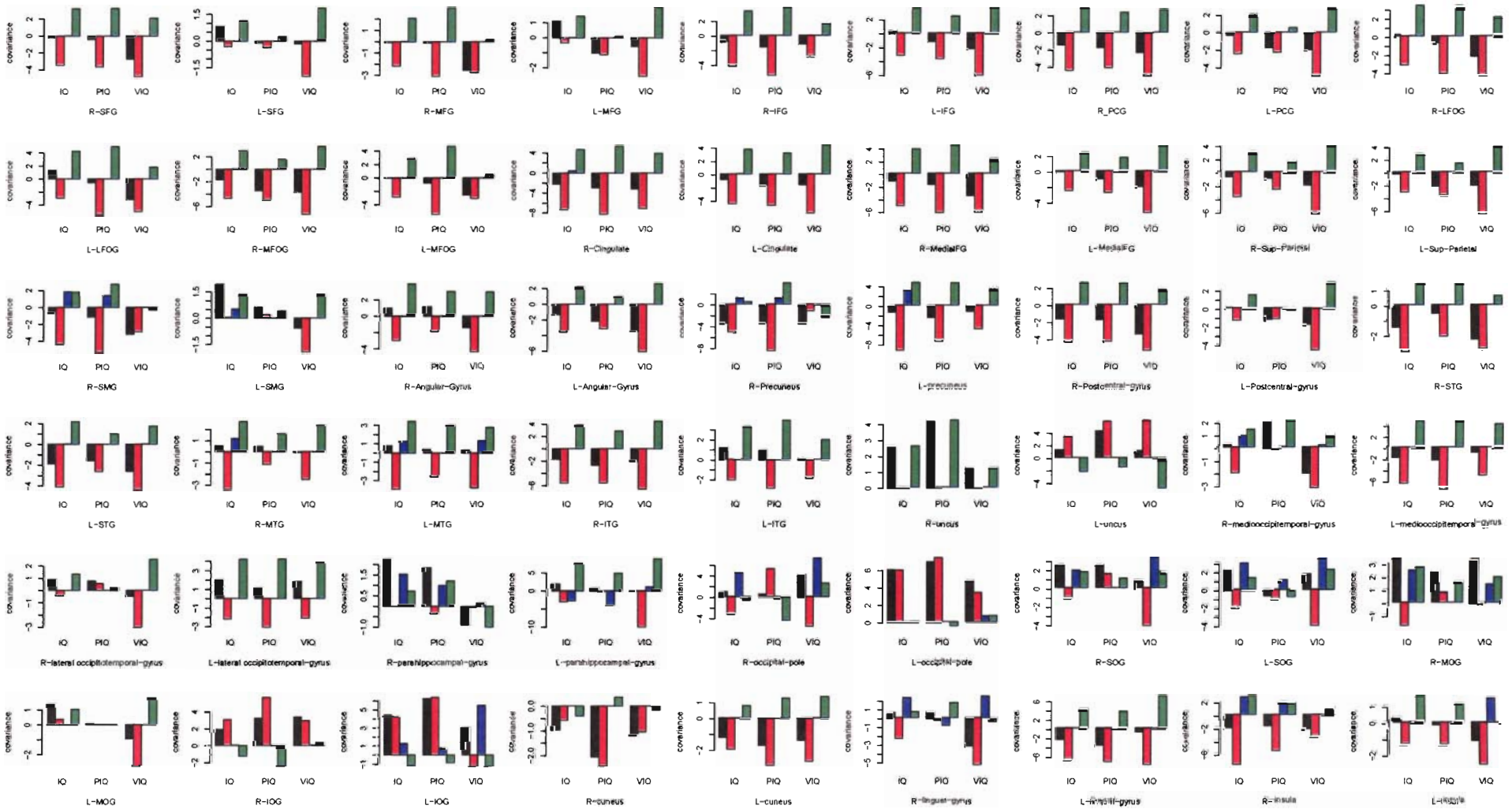

Figure 11.3: Correlations between IQ, VIQ, and PIQ and mean cortical thickness for 54 gyral subregions. Phenotypic correlations are shown in black, genetic correlations in red, and unique environmental correlations in green.

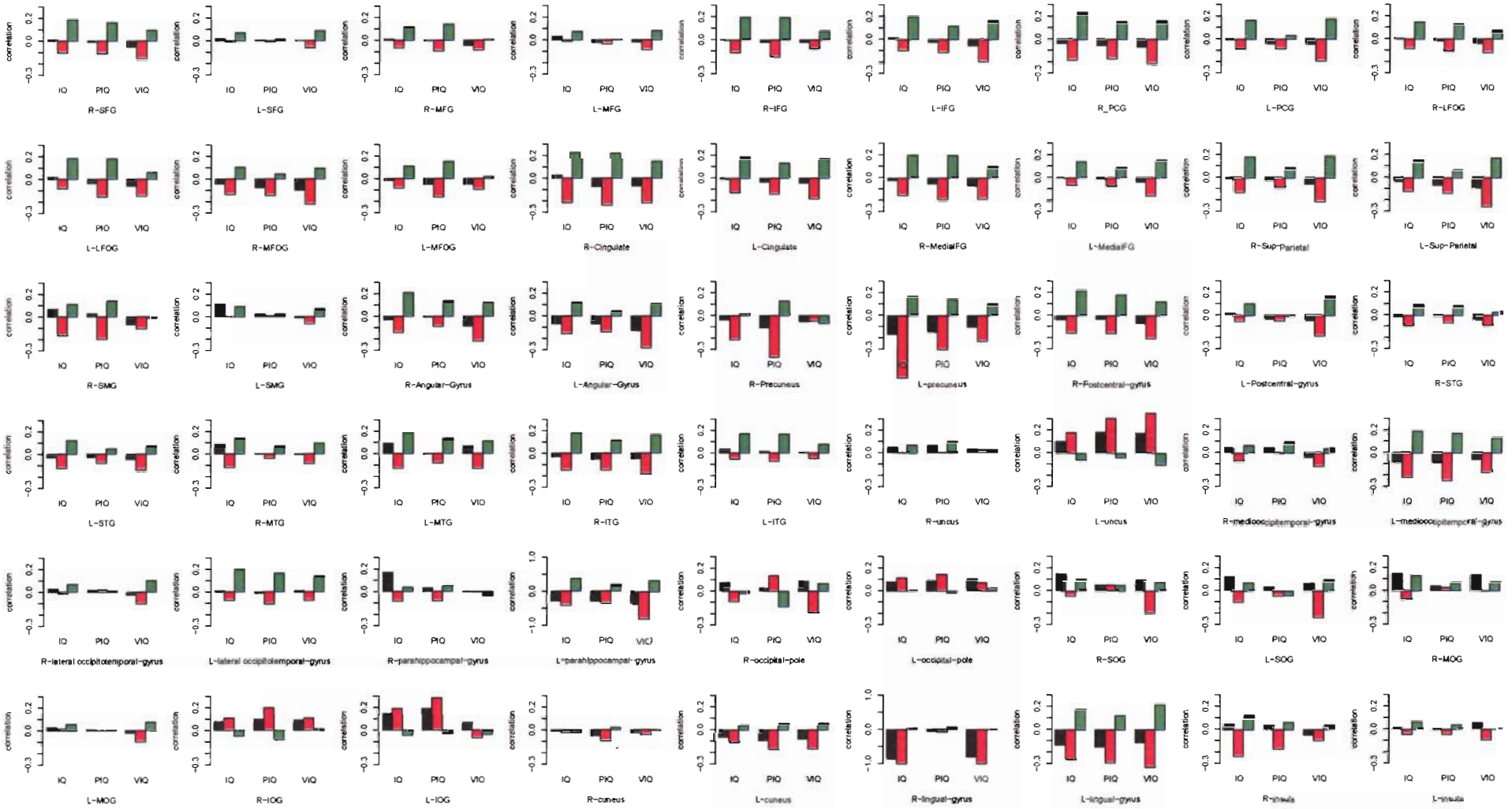

exposure to a complex motor activity (juggling) produced a 3% increase in mid temporal gray matter (Draganski et al., 2004) after only 3 months of exposure. Similarly, medical students subjected to their 2-year comprehensive examination ("Physikum", roughly the German equivalent of USMLE step 1) had increases in gray matter in the posterior and inferior parietal lobe and hippocampus, regions associated with learning within months (Draganski et al., 2006). Several studies have shown that taxi drivers' unremitting exposure to the streets of London, renown even to Dickens and Byron for their labyrinthine network, increase hippocampal volumes (Biegler, McGregor, Krebs, & Healy, 2001; Maguire, Woollett, & Spiers, 2006; Maguire, Nannery, & Spiers, 2006; Maguire et al., 2000). Thus, it is not impossible that intellectual ability and brain structure could be correlated by certain environmental exposures. An obvious possibility is the mutual effect of learning environment on both CT and IQ, though other possibilities and confounds can not be ruled out with these basic models.

In contrast to environmental correlations, genetic correlations between IQ and CT are generally negative, implying that some of the genetic factors that increase IQ also decrease CT. Such an observation is not inconsistent with the biology of neuronal pruning and synaptic plasticity. Recent longitudinal research on pediatric brain development has shown that the relationship between cortical thickness and intelligence is a dynamic process. A study by Shaw et al. demonstrated that cortical thickness is negatively correlated with IQ in young children but positively correlated in older children (Shaw et al., 2006a). Furthermore, longitudinal models revealed a significant differential trajectories in cortical development, depending on IQ, for several anatomic regions (Figure 11.4). Considered with our data, this finding suggests the intriguing possibility of

interactions between genes, age, and IQ on cortical development, with genetic factors playing the dominant role at early ages (when IQ/CT phenotypic correlations are negative), and environmental factors becoming relatively more important in late childhood and adolescence.

Figure 11.4: Figure by Shaw et al. on differences in the developmental trajectory of mean cortical depending on IQ status in a pediatric sample. The significant (colored) regions in the brain renderings at center were used to construct a ROI for genetic analyses (Shaw et al., 2006a).

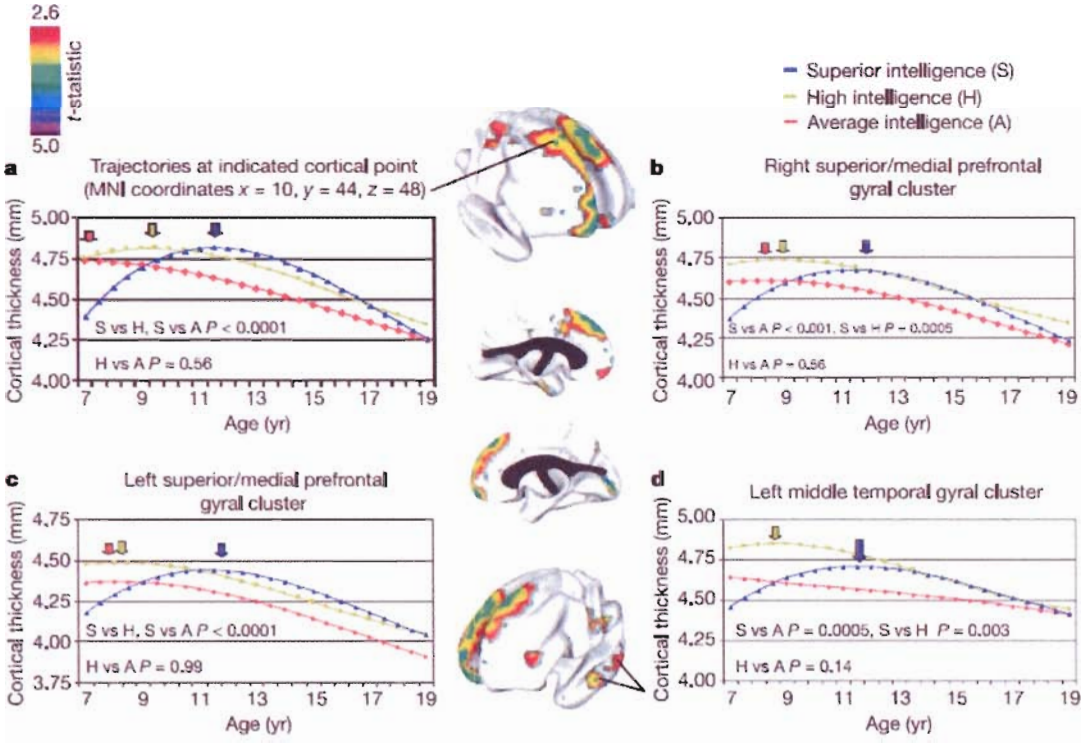

In order to test this hypothesis, we first constructed two ROIs, one encompassing the vertices from significant regions reported by Shaw et al. (colored vertices in Figure 11.4, ROI_S) and a second negative control region encompassing the rest of the brain (ROI_C). For each subject, we calculated mean CT values for both regions. Preliminary univariate modeling found that the heritability of ROI_S (a^2 = .66 [.34, .75], c^2 =.00 [.00, .26], e^2 = .34

[.25, .46]) was substantially higher than the ROI_C control region (a^2 = .39 [.07, .55], c^2 =.00 [.00, .18], e^2 = .61 [.45, .82]). Interaction models were then constructed in which moderators allowing for age, IQ (dichotomized into low or high IQ groups by the median IQ of 110), or their interaction to influence the contributions of genetic and nongenetic factors to influence mean cortical thickness.

The results of these models are summarized in Figure 11.4. Within the ROI, strong gene by age interactions were observed in the high IQ group, with no interactions observable in the low IQ group. Interactions with age via environmental factors were substantially smaller in both IQ groups, but in older children the role of environment on the total variance became relatively more important. The age by IQ interaction was statistically significant for both genetic (χ_1^2 = 9.8, AIC = 7.8, p-value = .0017) and environmental factors (χ_1^2 = 4.3, AIC = 2.3, p-value = .0371). Attempts to create a scalar model by equating the interaction terms also were not possible (χ_1^2=4.6, AIC = 2.6, p-value = .0321). A similar pattern was observed in the control ROI_C, but the magnitude of the interaction was substantially smaller than those in ROI_S.

Figure 11.4: Changes in variance in mean CT with age inside and outside of an ROI based on Shaw et al.. Line color represents variance component (red=additive genetic, green=unique environmental), while line type represents IQ group (solid=high IQ, dashed=low IQ). Panel A displays results from ROI_S while Panel B are findings from ROI_C.

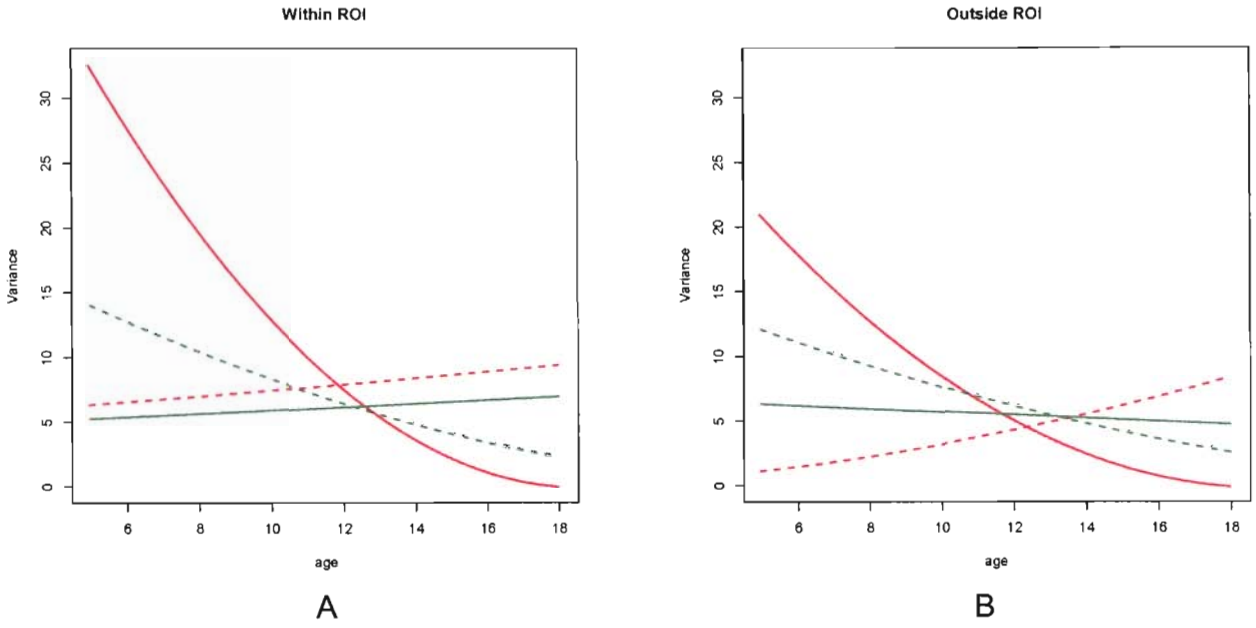

Although functional forms in Figure 11.4 do not parallel the mean CT age trajectories, it is noteworthy that there are striking similarities between changes in CT variance and the *rate* of change in mean CT (Figure 11.5) when splitting by IQ group. This similarity may reflect a genetic effect on the level of neuronal proliferation or neuropil formation in those genetically predisposed for higher IQ.

Figure 11.5: Comparison between derivatives of mean CT trajectories, from Shaw et. al. (Panel A) and changes in total CT variance in high (solid) and low (dashed) IQ groups (Panel B).

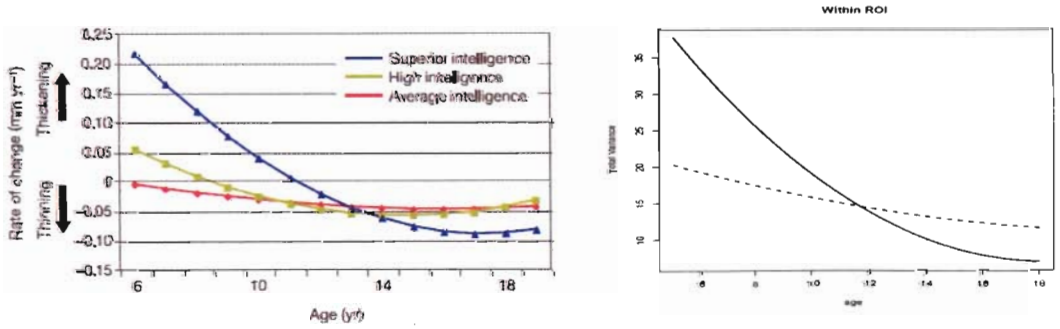

Conclusions

Our findings suggest that genetic and nongenetic factors influence the relationship between CT and IQ differently, and that observed relationships between phenotypes and endophenotypes may represent an amalgam of different biological processes that often work via opposing mechanisms. Additionally, more complex models suggest that like many aspects of child neurodevelopment, the associations between genes, brain and behavior must be considered to be dynamic processes in order to fully understand their relationships. Although these analyses represent a provocative first glimpse into the genetic role in brain-behavioral correlations, much more work needs to be done. Further longitudinal modeling will be required in order to quantify age interactions with a higher level of certainty.

12

GENERAL CONCLUSION

"Our field may be in particular need of integrative pluralism, where scientists, without abandoning conceptual rigor, cross borders between different etiological frameworks or levels of explanation. Such efforts may be unusually scientifically fruitful and work bit by bit toward broader integrative paradigms."

--Kenneth Kendler, "Toward a Philosophical Structure for Psychiatry" *American Journal of Psychiatry*. 162:433-440, 2005.

In the final chapter of a scientific dissertation, it is customary to dedicate many words to restating the principal findings of all preceding chapters. As these findings are summarized in the general abstract preceding this document and with increased detail in the individual chapter abstracts (reproduced collectively in Appendix E), I would instead like to discuss emerging themes from the work and the potential for future research in behavioral neurogenetics.

Sir Humphrey Davy once said that "nothing tends so much to the advancement of knowledge as the application of a new instrument. The native intellectual powers of men in different times are not so much the causes of the different success of their labours, as the peculiar nature of the means and artificial resources in their possession" (Davy, 1995). While this perspective may understate the general importance of creativity in scientific endeavor, it is largely the case in this work. Curiosity about the etiological underpinnings of the brain and its dynamics are not novel questions, but rather can be traced back thousands of years to Aristotle and before. With the availability of modern neurobiological, psychological, and statistical tools, our work has been a simple and natural extension of existing research. Thus, at minimum, our research is a lesson in the unrealized potential of interdisciplinary studies that combine knowledge of genetics, classical neuroscience, statistics, psychology, and psychiatry.

Yet methodological development, in this case, was merely a means to an end. Looking back at the amassed results of several years of research, it is natural to ask epistemological questions. Do calculations of heritability on brain volumes, for example,

increase scientific knowledge about the role of genetics in brain structure, or are the findings so obvious *a priori* as to make them meaningless? Is the investigation of neurobiological structure useful when it is performed largely independent of measures of function? Or for the more complex findings, are the modern computational methods used so dependent on so many constituent algorithms (and their inherent assumptions) as to make any inferences gleaned from them tenuous? In other words, have we gained knowledge from this endeavor, and if so, is this knowledge useful?

Although some of the findings of the work strongly conform to common sensibilities about the nature of the brain, there is still inherent value in demonstrating that they are true empirically. Confirming *a priori* knowledge about neuroanatomic variability represents a critical improvement in the bedrock understanding of behavioral neurogenetics. Most findings from our more complex multivariate examinations of brain structure integrate remarkably with the limited existing knowledge of neurodevelopment and the genetics of brain evolution. Yet at the same time, these examinations address these questions from quite a unique perspective. Novel information is often most useful when it simultaneously confirms and challenges the zeitgeist; many of the results from our work adhere to this principle.

Considered as a whole, these analyses show that genetic factors are extremely important in generating neuroanatomic variability throughout the brain. Notably, interpretation of the data differs depending on its level of resolution. Indeed, this dissertation can largely be considered as two sequential surveys of brain genetics (the first univariate, the second

multivariate) for different levels of anatomic magnification. Most of the variance in large structures is explained by strong, ubiquitous genetic factors, hypothesized to be involved in cell growth and proliferation. Nevertheless, exquisite genetically-mediated patterns of neuroanatomic variance and covariance emerge when examining smaller structures. For example, perhaps our most sensational observation was that of cortical thickness heritabilities being highest the regions of the cerebrum most unique to *homo sapiens*, suggesting a correlation between the genes that make us human and the genes that make us individuals. These patterns from HIA integrate nicely with more global and intermediate-level analyses, but each level conveys slightly different information about brain structure.

Yet as this dissertation comes to a close, it is most clear that there is far more work ahead than work accomplished. Examinations of neurodevelopment, in particular, have been limited by the cross-sectional nature of the data. As NIMH's longitudinal pediatric twin project progresses, it will soon become possible to address developmental questions more definitively. Similarly, identification of the specific genes involved in brain structure, perhaps partially informed by the present work, are likely to occur with increasing rapidity and will enable a better understanding the processes underlying our complex neural architecture. More comprehensive information about the genetics underlying brain-behavioral correlations also will be required. Our preliminary investigations suggest that the work in this area will be difficult and complicated by the dynamics of childhood, but not impossible with carefully-crafted developmental models.

APPENDIX A: SYNOPSIS OF MAMMALIAN BRAIN EVOLUTION

"Seen in the light of evolution, biology is, perhaps, intellectually the most satisfying and inspiring science. Without that light it becomes a pile of sundry facts some of them interesting or curious but making no meaningful picture as a whole."

> --Theodosius Dobzhansky. "Nothing in Biology makes sense, except in the light of evolution." *The American Biology Teacher* (35:125-129) 1973.

ABSTRACT

This appendix outlines the dominant theories on the evolution of the mammalian brain, with a focus on what volumetric research has revealed about the development of the cerebral cortex. Within the context of natural selection as an evolutionary force, the prevailing theories of the events leading to mammalian divergence from reptiles are discussed. Additionally, the current understanding about the origins of mammalian neurodiversity are outlined. It is argued that the development of cortical lamination, driven by an increased requirement for olfactory processing, was the most probable impetus for the development of the distinctly mammalian cerebral cortex. Further, the extant evidence suggests that the enormous variability in mammalian brain size was caused by a combination of traditional neo-Darwinian selective mechanisms and a series of developmental constraints that are unique to the central nervous system.

Perhaps the most unique trait of members of the human species is the desire to understand our origins and those of the world. Millennia of philosophical, scientific, and religious inquiry on the former topic can be condensed into two deceptively simple questions, namely 1) who are we? and 2) how did we get here? From a modern biological perspective, the first question is the fundamental goal of the neurosciences, and the latter is the unifying theory of genetics, i.e. evolution.

The present chapter is an attempt to summarize the current understanding of brain evolution, which is essentially a fusion of these two questions. In particular, the focus is on the development of the mammalian brain, though several other vertebrates are briefly mentioned as useful comparisons. The topic is quite complex and can be intimidating for the reader not fluent in the often esoteric language of evolutionary neurobiology. However, it is not the intention to overwhelm but rather to demonstrate that the core ideas are both intuitive and fascinating, hopefully without an excess of quickly-forgotten nomenclature.

Historical Background

Throughout the history of evolutionary theory, understanding the origin of behavior and cognition has been a central and controversial topic in the scientific debate on evolution. Long after the scientific community had accepted evolution as the dominant mediator of biological diversity, many resisted evolution as an explanation for psychological traits, particularly in humans. In this contentious discussion, the evolution of the brain became

the critical link between the biological forces of evolution and the more ethereal qualities of the mind (Larson, 2002).

Lamarck appears to be the first to attempt to unify evolutionary theory with the origins of brain and behavior. He postulated (incorrectly) that inter-species variation in brain size was caused by increased cognitive use (Lamarck, 1963). Thus, Lamarck's opinions about the evolution of brain and mind are consistent with his general theory of evolution, and completely analogous to his example of a giraffe evolving a long neck by stretching to access ever-higher vegetation. Darwin later proposed that selective advantage was the cause of increased brain size as part of his theory of natural selection, with selection indirectly influencing neuroanatomic physiology via the outward manifestation of its structure, namely cognitive and behavioral ability (Darwin, 1871). It was hypothesized that the brain, as a biological organ, followed the same general evolutionary rules as other biological structures. An important point, however, is that in brain evolution, selection is largely not operating on the structure itself. The brain has no outward phenotype on which most selective pressures could exert evolutionary changes. But selection for cunning, increased perceptual ability, and motor skill would indirectly influence the physical properties of neural tissue. According to the classical view, changes in the brain are merely the physical manifestations of these intangible yet highly adaptive traits.

The first true evolutionary models of the brain, linking actual brain structure with phylogenetic "progress" were proposed by Edinger in 1908. His model literally stratified the brain into subdivisions based on comparative neuroanatomic research of vertebrate

species (Swanson, 2000). According to Edinger's general model, species generated improved computational abilities and novel cognitive skills by layering new brain tissue on top of the previously existing neural systems of their ancestors with little change in older structures. For example, the most basic of functions, such as respiration and digestion, were the domain of the reptilian brain, the evolutionarily oldest region. Edinger viewed vertebrate evolution as a linear progression from simple (e.g. reptiles) to advanced (e.g. humans), with a corresponding increase in behavioral complexity with each new layer of neural tissue laid down. This theory persists in medicine in the form of MacLean's theory of the Triune brain (Figure A1.1) which divides the brain into reptilian, paleomammalian, and neomammalian components (MacLean, 1990). According to MacLean's model, advancements in primate evolution resulted from the application of the last layer (neomammalian brain) laid down most recently, in the form of cerebral cortex. This is essentially the classic "march of progress" for neuroanatomy, which considers advanced cognitive functions as restricted to higher primates. The theory of the Triune brain persists in the literature to this day. The research presented below, however, suggests that the theory is highly flawed (Swanson, 2000).

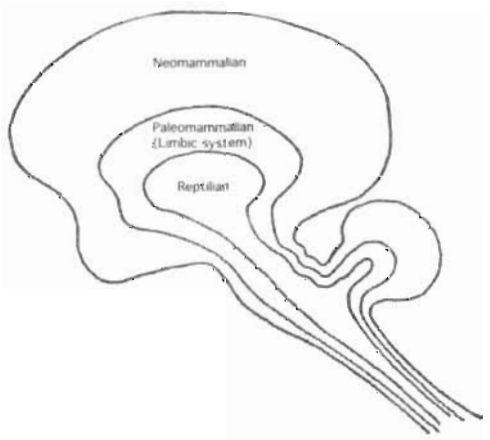

Figure A1.1: MacLean's Triune Brain

From Serapsid to Mammal

What are the origins of the mammalian brain? All vertebrates, including mammals, share a common ancestral origin. Within modern vertebrates, however, there is tremendous diversity in neural structure. For example, even after controlling for body size, total brain size varies 30-fold in vertebrates (Northcutt, 2002). Yet as Northcutt notes, there are some predictable characteristics that apply to the nearly all species in the *Vertebrata* subphyla. First, nearly all vertebrates have the same number of basic neuroanatomic subdivisions, though they can be quite morphologically different (Figure A1.2). The only known exceptions are the agnathans (e.g lampreys) that lack a definitive cerebellum. Second, substantial differences in brain size are seen when making comparisons between classes (e.g. *Mammalia*, *Reptilia*, and *Aves*), and increasing size, both within and between taxa, usually corresponds to increasing functional specificity and behavioral complexity. Unique mammalian neuroarchitecture began 200 million years ago as the primordial mammal diverged from ancestral reptiles (Northcutt & Kaas, 1995).

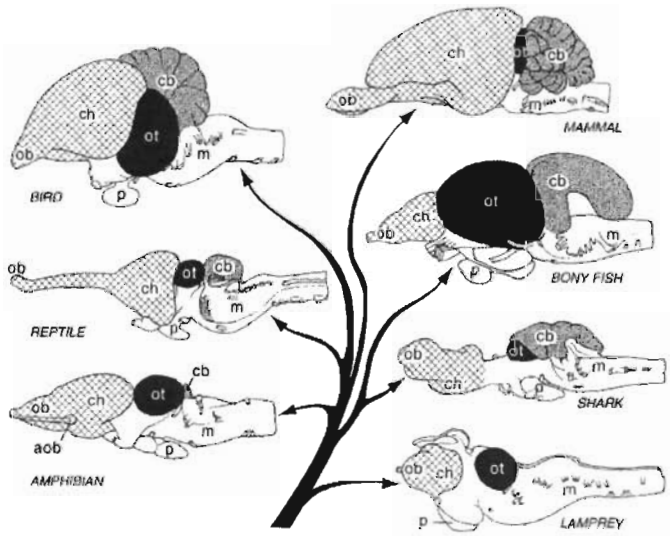

Figure A1.2: Neuroanatomic structure of vertebrates of different orders. Regions denoted in like patterns are structural homologues. Ch = cerebral cortex, Cb = cerebellum. (From Northcutt and Kaas 1995)

The most striking difference between mammals and other vertebrates is in the size and structure of the cortex. The cortex is essentially a vast sheet of neurons that forms at the most rostral end of the developing nervous system. There has been a dramatic expansion in cortical volume in mammals compared to the most phylogenetically similar modern amniotes, namely reptiles and amphibians (Rakic & Lombroso, 1998). The *iso*cortex itself is unique to mammals and all mammals have it; though reptiles, birds, and amphibians have cortical tissue as well, the mammalian isocortex represents a revolutionary change in design. This suggests that isocortex evolved only once and at a timepoint prior to the mammalian radiation (Aboitiz, Morales, & Montiel, 2003; Northcutt et al., 1995).

The fundamental structure of the cortex is distinctly altered in the mammalian isocortex. There is an expansion of cellular layering from three layers to six, which in turn influences computational ability and neural circuitry (Aboitiz et al., 2003). Also of note is that the development of the mammalian isocortex occurs in reverse order relative to most other structures in the mammalian brain and to the entirety of brain development in reptiles. The reptilian brain develops "outside in," a process in which neurons migrate to the brain surface first, then slightly preceding to the first set of neurons, and so on. In isocortex, younger neurons migrate past established neurons to rest at the brain surface. Finally, the mammalian isocortex has developed an entirely novel type of neuron, the multilayered pyramidal cell, which represents a substantial advance in computation and inter-neuronal communication (Marin-Padilla, 2003).

How did mammals develop such a radically different neural structure? Two predominant hypotheses have been developed to explain how this unique isocortex was generated, denoted the "recapitulation hypothesis" and the "outgroup hypothesis" (Northcutt et al., 1995). The details of both theories are complex and highly dependent on understanding neuroanatomic jargon. The premises, however, are quite simple (Figure A1.3). The out-group hypothesis states that the mammalian isocortex resulted from an expansion of the dorsal-most cortex of the common ancestor of reptiles and mammals (a synapsid). In contrast, the recapitulation hypothesis posits that the isocortex developed not from synapsid cortical tissue at all but instead evolved from an entirely different region known as the dorsal ventricular ridge (DVR) which is present in modern day reptiles but absent in mammals (Aboitiz et al., 2003). The out-group hypothesis posits that the DVR develops independently in reptiles after they have diverged from other taxa.

The recapitulation hypothesis, originally proposed by Karten, has been the dominant explanation for isocortex development for the last thirty years but the outgroup hypothesis has been rapidly gaining favor (Puelles, 2001b). Which theory is correct? Unfortunately, there is still an active, ongoing controversy. In a groundbreaking review, Aboitiz presents comprehensive evidence from comparative neuroanatomic, developmental, and paleoentological approaches (Aboitiz et al., 2003). Dispute arises because of strong yet conflicting evidence. The outgroup hypothesis is supported by detailed analyses of neuroanatomic connections, which show that the DVR in reptiles and the isocortex in mammals have similar relationships with other structures. For example,

many sensory connections from the thalamus project to the DVR in reptiles but to the cerebral cortex in mammals (Karten, 1997; Karten, 2005). However, the analogy is not perfect. In particular, the mammalian isocortex and archicortex (limbic system) are strongly associated, while the archicortex and the DVR are virtually unconnected in reptiles (Aboitiz et al., 2003).

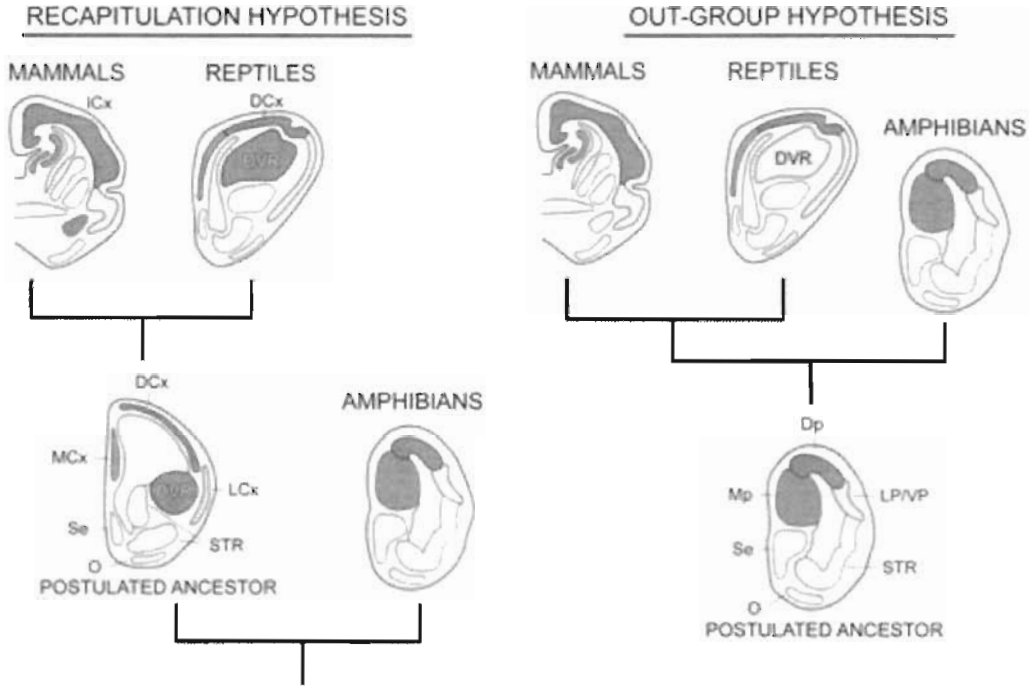

Figure A1.3: Two hypotheses of isocortical development. In the recapitulation hypothesis, the dorsal ventricular ridge (DVR) in a shared reptilian-mammalian ancestor develops into isocortex in mammals but remains DVR in reptiles. In the outgroup hypothesis, isocortex develops from ancestral dorsal cortex and the DVR evolves independently in reptiles. (adapted from Aboitiz et al., 2003)

The outgroup hypothesis is largely supported by developmental evidence. Streitder et al. has shown that the embryological origins of the DVR and the isocortex are markedly different (Aboitiz et al., 2003; Striedter, Marchant, & Beydler, 1998), with the DVR originating deep within the brain and the isocortex originating on its dorsal surface.

Molecular genetic evidence also supports the outgroup hypothesis. Immunohistochemistry of transcription factors critical for embryogenesis (e.g. homeotic-like genes such as Otx and Pax) with precise spatial expression demonstrate homologous patterns between isocortex in mammals and dorsal cortex (rather than DVR) in reptiles, as the outgroup hypothesis would suggest (Gellon & McGinnis, 1998; Puelles & Rubenstein, 1993). There are, however problems with developmental studies. detractor of the work, Northcutt, has correctly noted that similarities between structures do not necessarily mean common origins (homology). Other explanations, such as convergent evolution (homoplasmy), could also describe the observed data (Northcutt, 2003).

Despite the controversy, most experts agree that the outgroup hypothesis is more likely. Most of the twenty experts that provided peer commentary on Aboitiz' review agreed that the evolution of isocortex from dorsal cortex is the more probable hypothesis. The molecular genetic evidence would also seem to be highly suggestive of this hypothesis, as would the rules of parsimony. The DVR is developmentally distinct from cortical regions, which means that the switch to isocortex (as put forth in the recapitulation model) would represent a more drastic change. Thus, the outgroup hypothesis would mean a simpler (though still substantial) change from ancestral structure to the generation of isocortex. If it is true, however, then several problematic questions arise. Namely, it is unclear how genetic programming would have radically altered neural connections when isocortex was generated, and why reptiles (and particularly their more cognitively advanced avian relatives) did not also evolve isocortex, under similar pressures toward increased computational power.

If the outgroup hypothesis is true, then it has profound implications regarding what evolutionary pressures created mammals. In reptiles, the dorsal cortex is primarily responsible for olfaction, i.e. the sense of smell, and spatial mapping (Aboitiz et al., 2003; Bota, 2003). This suggests that selective pressures for increased olfactory processing ability may have been the driving evolutionary force that created divergence between the neuroanatomy of mammals and reptiles. The critical event that allowed this generation of isocortex may have been the ability to develop "inside out," as described previously (Super & Uylings, 2001). In "outside in" development, the expansion of cortex outward is constrained by outgoing neuronal fibers (axons) sending their projections to other regions. In other words, the axons are located closer to the brain surface than neuron bodies and these axons create a physical barrier to neuronal expansion. In "inside out" development, neurons migrate past the ultimate location of axons to rest closer to the brain surface. This situation allows for unrestricted enlargement outward. Further, the genetic alterations that would be required to produce isocortical expansion could have been relatively minor. For example, a few mutations in chemotaxic signaling pathways could have altered the paths of migrating neurons (Super et al., 2001).

This hypothesis of mammalian evolution also is not difficult to reconcile with the general conception of ancestral mammals as small rodent-like reptilian creatures in the age of dinosaurs. One can almost picture these tiny creatures filling a specific, perhaps nocturnal niche in a world of giant predators. This would be a place where a keen sense of smell

and an ability to remember important environmental locations could be the means for survival.

Brain Evolution Within Order Mammalia

Endocasts from primitive mammals have shown that although there is an anatomical divergence from reptiles more than 200 million years ago, brain size in mammals remained virtually constant until about 60 million years ago (~5 million years after the Cretaceous extinction). This places cortical expansion approximately at a time when placental and marsupial mammals diverged from each other rather than at the mammalian divergence from reptiles (Northcutt et al., 1995). Thus, at least two fundamental innovations led to the evolution of intelligent mammals: 1) a change in *design* of neurocircuitry (200 million years ago) and 2) a change in *amount* of neurocircuitry (beginning 60 million years ago) over 100 million years later. This section will focus on the latter process.

Figure A1.4: Examples of diversity in mammalian brain size and structure. Specimens include cetaceans, rodents, insectivores, humans, and primates (from the Comparative Mammalian Brain museum at http://brainmuseum.org.).

From the Cretaceous to the present, both endocasts and comparative biological approaches show that a tremendous amount of diversity in total mammalian brain exists

(Figure A1.4). For example, the surface area of the isocortical sheet ranges from 6-10 cm^2 in insectivores to about 2200 cm^2 in humans (Northcutt et al., 1995). The expansion of isocortex appears to have evolved independently within several mammalian radiations. Every major mammalian class has this high level of variability (Northcutt et al., 1995). Thus, increases in brain size in mammals appear to be an example of convergent evolution, in contrast to the singular evolutionary event that created isocortex.

Classical evolutionary notions postulate that the variability in brain volumes results from selective pressures on behavioral traits. For example, insectivores rely almost solely on olfaction with little need for other senses, complex motor skills, social cognition, or sensory integration (Brown, 2001). Conventional wisdom would dictate that relatively little computational power is required for an insectivore to function. Therefore the brain would have little reason to evolve larger than that of the ancestral mammal. Insectivores, in fact, have small, relatively undeveloped brains. In contrast, the combination of selective pressures towards bipedal locomotion, tool use, social structure, and hunting behaviors resulted in the need for vast increases in processing requirements and functional specificity in human ancestors, which placed selective pressures on evolving a larger brain (Darwin, 1871; Finlay, Darlington, & Nicastro, 2001a).

Absolute brain size, however, is not the sole determinant of computational power. Finlay and Darlington give the pointed example of volumetric differences between a ruby throated hummingbird and a baleen whale (Finlay et al., 2001a). The former has a brain size of less than one gram, while the latter has a brain volume of approximately 5000

grams. Although it is certainly true that these animals have quite different environmental niches and neuroprocessing needs, both animals have complex behaviors and it is difficult to quantify which one is computationally "superior." However, it is hard to believe that whales have 5000 times greater computational requirements. Perhaps a better example would be to compare the whale to another mammal, such as *Saimiri sciureus* (the squirrel monkey) which has a brain weight that is about 45 times smaller than that of the whale but a remarkable (perhaps more complex) behavioral repertoire as well (personal calculations and observations). Thus, simple selection based on increased cognitive needs alone cannot be the only determinant of brain size. It follows that computational power probably is not entirely dependent on absolute brain size.

Allometry, a mathematical subfield of comparative anatomy, was founded because of this problem. The goal of allometry is to attempt to quantify relationships between key evolutionary variables. Analyses have shown that total brain size increases with body size at an exponential rate (Finlay et al., 2001a). Mathematically, the relationship has been demonstrated to be:

$$\log(y) = a\log(x) + \log(b)$$

where y = brain size, x = body size, a = slope, and b = y-intercept, and the slope is generally estimated from .56 to .75 depending on the mammalian species used in the analyses (Kruska, 2005). Simply put, larger mammals have larger brains independent of their cognitive ability (Figure 5A). The exact reasons for this have not yet been

elucidated. One hypothesis is that larger animals require increased neural innervation to skeletal muscles and more computational power for motoric processing in order to control the larger muscles in their larger bodies. Similarly, increased sensory processing would be required to handle an increased number of messages from sensory neurons in a body with a larger volume. However, this could not be the whole story as the *entire* brain scales with body size and not just the regions responsible for sensory and motor functions (Finlay et al., 2001a).

Exactly how the brain scales is the source of greatest controversy in mammalian evolution. There is general agreement that species with larger brains than predicted based on body size (encephalization) are more likely to be cognitively advanced than those with brains equal to or smaller than predicted (Finlay et al., 2001a). For example, dolphins, non-human primates, and humans are the most encephalized mammals and also are believed to be among the most behaviorally advanced of all animals (Kruska, 2005). All things equal, a larger brain size is a good predictor of a more cognitively "advanced" species (Figure A1.5B).

Controversy arises over the role of selection on brain organization beyond total brain size. If we examine the brain's functional subregions, what should we see? The traditional viewpoint, coined the "mosaic hypothesis," is quite similar to what Darwin would postulate (Brown, 2001). It simply argues that subregions within the brain with different computational functions are going to be differentially influenced by selective pressures based on those functions (Finlay et al., 2001a). For example, an animal

particularly dependent on sight would be under selective pressure to improve visual acuity which would, in turn, disproportionately increase the computational power of centers controlling visual processing. By contrast, the "developmental constraint" hypothesis says that evolutionary pressures largely act on the brain as a whole. Applying this hypothesis to the previous example, we should observe an increase in total brain size as a result of selective pressures on visual ability alone.

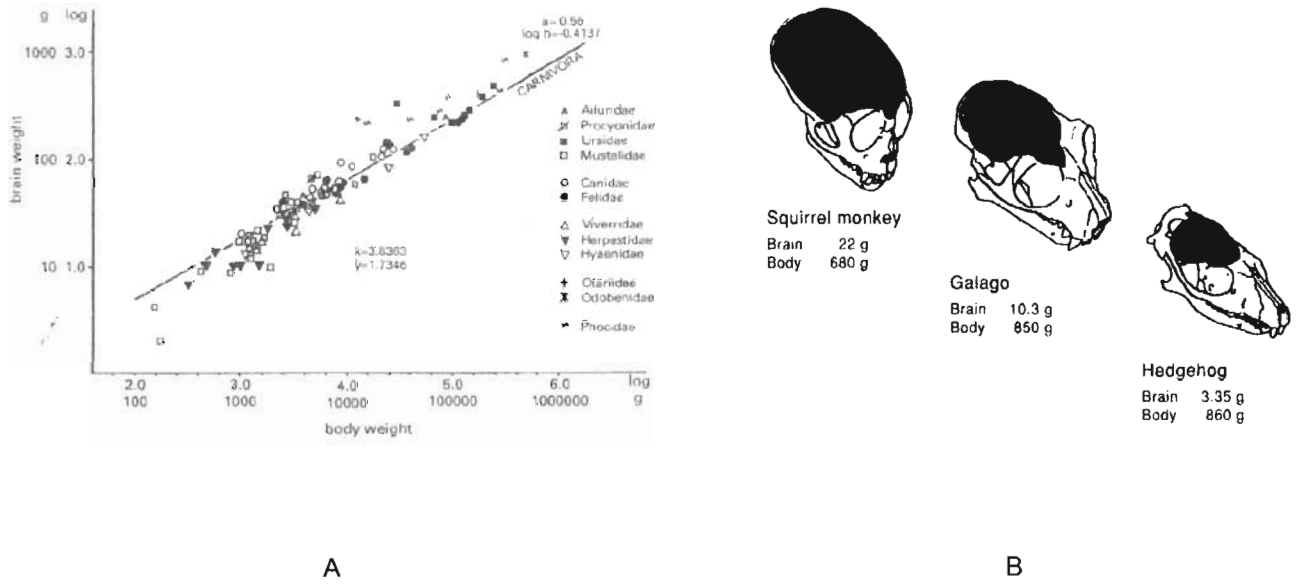

Figure A1.5: Mammalian brain weight to body weight comparisons. Panel A is a Log-log plot of body weight (g) and brain weight (g) for 93 species within the order Carnivora (includes cats, dogs, bears, etc). Note the *extremely* strong correlation between body size and brain size. (From Krushka 2004). Panel B: Exceptions to the rule. Even for mammals of comparable body mass, there can be substantial variability in brain volume. While body size increases from left to right, brain size and behavioral complexity increases from right to left (the galago is a prosimian). All things (more or less) equal, brain size is a good predictor of overall behavioral complexity. (From Northcutt 1995).

At first glance, the developmental constraint hypothesis may seem unlikely. There are numerous examples of one organ system component increasing in size relative to others; disproportionate growth is practically the rule rather than the exception. Under the

developmental constraint hypothesis, Lamarck's giraffe would grow proportionally in size until the vegetation could be reached, producing a giant horse-like creature rather than a long-necked one. Further, there are myriads of well-documented genetic regulators of brain patterning that selection could potentially act upon, each controlling specific regions (Gellon et al., 1998). This would provide a far more energetically favorable way to produce improved function, as these changes would not produce an excess of "useless" brain tissue, which is extremely expensive metabolically (Rubenstein & Rakic, 1999b).

However, there is extraordinarily compelling evidence that the developmental constraint hypothesis for brain evolution is at least partially true. Using comparative neuroanatomic analyses of multiple mammalian species, Finlay and Darlington have repeatedly shown that total brain volume is highly correlated with regional volumes (Figure 7.5), irrespective of region (including all neuroanatomic regions described in the present article). Further, total brain volumes account for the vast majority (>96%) of the observed volumetric variance in all regions measured except for the olfactory bulb (Darlington et al., 1999; Finlay & Darlington, 1995; Finlay et al., 2001a). These results suggest that the subcomponents of the brain are scaling together; if individual regions are selected for independently, then this should not happen.

Such strong correlations are thought to reflect a generalized adaptation to specific selective pressures; although it is more energetically expensive to expand the computational resources of the entire brain when only specific functions are needed, the molecular adjustments required to perform whole-brain scaling are far fewer than those

required to completely repattern the brain. Genes involved in regional patterning, such as Hox transcription factors, are tightly regulated (Gellon et al., 1998) and mutations in these genes may universally lethal, making mosaic evolution difficult. An alternative mechanism of modifying brain size would be to increase overall neuronal proliferation by relatively few alterations in cell cycle regulators, which would result in an increase in the total number of neurons and a larger brain. For example, prolonging progenitor cell division by a few cycles would be a way to exponentially increase the brain's computational power without tinkering with its overall design. Thus, although it may be less desirable to scale up the entire brain to obtain a specific function, it may be genetically easier to do so. Several well-designed neuroanatomic studies have supported this hypothesis by showing that increased cellular proliferation, at least in part, may be responsible for increased isocortical volumes in mammals (Rakic et al., 1998a).

Finlay and Darlington go so far as to speculate that the growth of the isocortex over mammalian evolution may be an indirect result of the need to increase some structure involved in lower functions, such as the brainstem, rather than *any* function of the isocortex at all (Finlay et al., 2001a). In this extension of their hypothesis, the cerebral cortex is essentially an evolutionary spandrel, whose initial development is only coincidentally related to the selective pressures that created it. However, the new cortical tissue does not go unused in their model, and is instead "pressed into service" to perform evolutionarily useful computational functions that the environment can select for. Exactly how this would work is never detailed, but it suggests that much of mammalian intelligence resulted from an evolutionary accident.

However, there are numerous studies that report evidence that the mosaic hypothesis, rather than the developmental constraint hypothesis, is the dominant force in brain evolution (Barton & Harvey, 2000; Brown, 2001; de Winter & Oxnard, 2001; Jones & MacLarnon, 2004). For example, Barton and Harvey use log-log plots of isocortical volumes versus total brain volume (Figure A1.7A) to show that primates have a higher y-intercept than insectivores, suggesting that primates have a 5-fold increase in cortex relative to predictions based on whole-brain scaling (Barton et al., 2000). Kaas and Collins provide an impressive anecdotal example by demonstrating that the size of the structure known as the superior colliculus (a structure

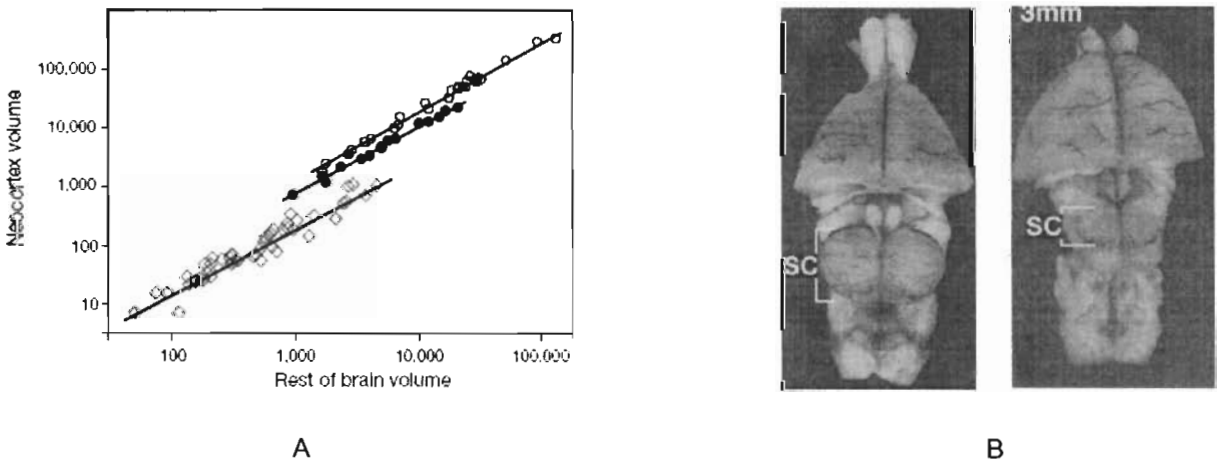

Figure A1.7. Differences in neocortical volume by species. Panel A is a log-log plot of neocortical volume versus whole brain volume in primate (open and closed circles) and insectivore (diamond) species. Upward displacement of primates relative to insectivores demonstrates that predicted neocortical size is higher in primates for a given total brain volume (from Barton and Harvey 2000). Panel B: comparison of the squirrel brain (left) to the rat brain (right). Though similar in volume, it is clear that the superior colliculis (SC) is not comparable in size between these species (modified from Kaas and Collins 2001).

important in basic visual processing) is dramatically different between rats and squirrels (Kaas & Collins, 2001) despite a comparable brain size (Figure A1.7B). Clearly, brain structures do not always scale together.

The debate over the relative merits of these two theories is intense. Proponents of mosaic brain evolution have provided convincing evidence that this mechanism does indeed occur. Often, however, studies employ the most extreme cases to support their theories (e.g. insectivores versus primates, or highly specialized mammals such as bats, marsupials, etc.). This sheds some doubt on their generalizability. Certainly mosaic evolution occurs, but is it the overriding force in the evolutionary process to the exclusion of all others? In plots of brain volume versus substructure volumes (e.g. Figure 6), the most prominent characteristic is not the magnitudes of deviations from the predicted values (i.e. residuals). Rather, what is striking is how little residual variation there after adjustment for brain volumes. Though Finlay and Darlington's spandrel hypothesis of cortical evolution is highly suspect, it does appear that the brain is under some developmental constraints. While some evolutionary biologists appear resistant to accept any form of neuoanatomic constraint (e.g. see Brown 2001), most realize that it likely had at least some role in general neural expansion (Finlay, Darlington, & Nicastro, 2001b).

Similarly, it seems highly unlikely that a developmental constraint hypothesis can be the only general mechanism for brain evolution. It is too dependent on brain volumes alone in order to defend its case. The mammalian brain represents a diversity of interconnecting

pathways, cell types, functional divisions, and numerous other properties that are often glossed over in traditional allometry (Northcutt, 2002). Certainly, brain volume is not everything. Not only do more intelligent mammalian species have larger brains, but their brains are also much more complex, with an increase in the number of total functional subunits, which reflect changes in design in addition to scale (Northcutt, 2002). These changes would not be predicted by developmental constraints alone. Perhaps a third fundamental theoretical mechanism will be required; the development of novel *functional* stratification of the brain following or concurrent with overall expansion, as well as interactions between volumes based on interrelated functions. Indeed, these theories are complementary; it is easy to see how developmental constraints could be driving the similarities in volumetric trends when making mammalian interclass comparisons, while mosaic evolution would explain deviations when examining how individual species adapt to their individual environmental niches.

Conclusions

The development of the mammalian brain is quite complex, but several general principles can be distilled from the compendious literature on the subject. It seems likely that the neuroanatomy of the oldest mammals diverged from reptiles as a consequence of increased olfactory requirements, which in turn resulted in the formation of a novel form of cortex. Later, the mammalian cortex expanded, allowing for several evolutionary innovations. Part of this increase in brain size is associated with increased body size

independent of cognitive ability. Within mammals, regulation of brain size probably resulted from a combination of selective pressures on individual brain regions with specific behavioral components, as well as developmental constraints imposed by the genetic elements that pattern the brain.

APPENDIX B: SAMPLE SCRIPTS FOR THE AUTOMATED ANALYSIS OF VOXEL-LEVEL DATA

"In inventing a model we may assume what we wish, but should avoid impossibilities"

--Aristotle

This appendix provides sample scripts for the automated analyses of neuroimaging data. The example is based on the first analyses attempted; that of basic ACE modeling and associated submodels (the printed version includes means regression that was added later, but otherwise is the original script constructed in Fall 2004). During the course of the Giedd project, the scripts were periodically optimized, modified for different purposes (e.g. bivariate models, multiple loops for generation of large correlation matrices), and simplified when possible, but the overall strategy is virtually identical in all analyses.

The present analysis consists of four scripts: 1) a large R script was used to control the analysis at a global level, performed data management, and calculated rudimentary statistics, 2) Mx performed iterative, customizable statistical genetic analyses, 3) a small shell script inserted starting values calculated in R into Mx, and 4) a second shell script to extract confidence intervals from the output file.

R Script

```
#SCRIPT TO RUN VOXELWISE ANALYSIS FOR ACE MODEL with CIs


#CD TO APPROPRIATE WD
#setwd("/home/schmitt/BRAIN/CT/FULL_ACTE")

#LOAD WORKSPACE FROM NIMH
load("~/BRAIN/CT/data/twin_ct_asc.txt");

#load vector of twin numbers (1 or 2) or sib number (1,2, or 3); later
versions calculate dynamically
rndor<-(read.table("~/BRAIN/CT/data/number.txt"))

#REMOVE OLD RESULTS FILES
system("rm -rf ACEbyvoxel.mxa",ignore.stderr=TRUE);
system("rm -rf fullbyvoxel.mxa",ignore.stderr=TRUE);

#REMOVE UNNECESSARY VARIABLES FROM DEMOGRAPHIC TABLE
gf$RACECOMT<-NULL;
gf$MRINUM <-NULL;
gf$DATESCAN <-NULL;
gf$BRACES <-NULL;
gf$SCANCOM <-NULL;
gf$Axial <-NULL;
gf$AxiNote <-NULL;
gf$Plane <-NULL;
gf$AxiSvrty <-NULL;
gf$ETHNICTY<-NULL;

#CONVERT FACTOR VARIABLES TO NUMERIC VALUES SO THEY ARE READABLE BY Mx
gf$SEX   <- factor(gf$SEX, c('F','M'),0:1);
gf$HAND   <- factor(gf$HAND, c('R','M','L'),0:2);
gf$GROUP <-
factor(gf$GROUP,c('MZTWN','DZTWN','SIBOFTWN','SINGLETON'),0:3);
gf$RACE <-factor(gf$RACE,c('W','B','A','M','U'),0:4);


#ENSURE NUMERIC CODING FOR ZYGOSITY (MZ 0, DZ 1, SIB 2, SIN 3)
gf[,1]<-as.numeric(substring(as.character(gf[,1]),33,37));
gf[,2]<-as.numeric(gf[,2]);
gf[,2]<-gf[,2]-1;

temp<-cbind(gf,rndor);

#BEGIN LOOP FOR ALL 40962 VERTICES
for (i in 1:length(dt[,1])){


#EXTRACT CT MEASURE FOR ALL SUBJECTS AT THE iTH SPATIAL LOCATION,
RESCALE
CT <- 10*dt[i,];


#ATTACH VOXEL CT VALUES TO DEMOGRAPHIC VARIABLES
```

```
comb<-cbind(temp,CT);

#EXTRACT AGE, SEX TO CALCUATE STARTING VALUES FOR MEANS BETA WEIGHTS
sex<-comb[,4]
age<-comb[,8]
age2<-age**2
age3<-age**3

#CALCULATE BETAS VIA REGRESSION
reg<-lm(CT~sex+age+age2+age3)
betas<-coef(reg)

#WRITE BETAS AND INTERCEPT TO FILE
write.table(t(betas[2:5]),file="betas.txt",row.names=FALSE,col.names=FA
LSE,quote=FALSE)
write.table(betas[1],file="mean.txt",row.names=FALSE,col.names=FALSE,qu
ote=FALSE)

#CALCULATE STARTING VALUES FOR VARIANCE COMPONENTS
sv<-(var(residuals(reg))/2)**.5
sv2<-(var(residuals(reg)))**.5
write.table(sv,file="sv.txt",row.names=FALSE,col.names=FALSE,quote=FALS
E)
write.table(sv2,file="sv2.txt",row.names=FALSE,col.names=FALSE,quote=FA
LSE)


#CREATE DATASETS BY PRIMARY GROUPS
twins<-subset(comb,GROUP<=1);
sibs<-subset(comb,GROUP==2);
singletons <-subset(comb,GROUP==3);

#SPLIT TWINS INTO TWIN1 and TWIN2
twin1<-subset(twins, twins[,9]==1);
twin2<-subset(twins, twins[,9]==2);


#COMBINE TWINS INTO A PAIRWISE DATASET
Twinpair<-merge(twin1,twin2,by="FAMID",all.x=TRUE,all.y=TRUE);


#SPLIT SIBS DATASETS
sib1<-subset(sibs,sibs[,9]==1);
sib2<-subset(sibs,sibs[,9]==2);
sib3<-subset(sibs,sibs[,9]==3);


#MERGE SIBS INTO A SINGLE DATASET
sibs1pair<-merge(sib1,sib2,by="FAMID",all.x=TRUE,all.y=TRUE);
sibsPair<-merge(sibs1pair,sib3,by="FAMID",all.x=TRUE,all.y=TRUE);


#MERGE TWINS AND SIBS
Fams<-merge(Twinpair,sibsPair,by="FAMID",all.x=TRUE,all.y=TRUE);

sin1<-subset(singletons,singletons[,9]==1);
sin2<-subset(singletons,singletons[,9]==2);
```

```
sin3<-subset(singletons,singletons[,9]==3);

sin4<-subset(singletons,singletons[,9]==4);
sin5<-subset(singletons,singletons[,9]==5);

sins1pair<-merge(sin1,sin2,by="FAMID",all.x=TRUE,all.y=TRUE);
sins2pair<-merge(sins1pair,sin3,by="FAMID",all.x=TRUE,all.y=TRUE);
sins3pair<-merge(sins2pair,sin4,by="FAMID",all.x=TRUE,all.y=TRUE);
sinsPair<-merge(sins3pair,sin5,by="FAMID",all.x=TRUE,all.y=TRUE);


#CONVERT MISSING AGE AND SEX TO DUMMY VARIABLE (-999) For Fams
Fams[is.na(Fams[,4]),4]<- 0
Fams[is.na(Fams[,8]),8]<- 0;
Fams[is.na(Fams[,13]),13]<- 0;
Fams[is.na(Fams[,17]),17]<- 0;
Fams[is.na(Fams[,22]),22]<- 0;
Fams[is.na(Fams[,26]),26]<- 0;
Fams[is.na(Fams[,31]),31]<- 0;
Fams[is.na(Fams[,35]),35]<- 0;
Fams[is.na(Fams[,40]),40]<- 0;
Fams[is.na(Fams[,44]),44]<- 0;

#SAME FOR SIBS
sinsPair[is.na(sinsPair[,4]),4]<- 0;
sinsPair[is.na(sinsPair[,8]),8]<- 0;
sinsPair[is.na(sinsPair[,13]),13]<- 0;
sinsPair[is.na(sinsPair[,17]),17]<- 0;
sinsPair[is.na(sinsPair[,22]),22]<- 0;
sinsPair[is.na(sinsPair[,26]),26]<- 0;
sinsPair[is.na(sinsPair[,31]),31]<- 0;
sinsPair[is.na(sinsPair[,35]),35]<- 0;
sinsPair[is.na(sinsPair[,40]),40]<- 0;
sinsPair[is.na(sinsPair[,44]),44]<- 0;

#WRITE DATA FILES
write.table(data.frame(Fams),file="CTtwinTemp.txt",na=".",quote=FALSE,r
ow.names=FALSE,col.names=FALSE);
write.table(data.frame(sinsPair),file="CTsinTemp.txt",na=".",quote=FALS
E,row.names=FALSE,col.names=FALSE);


#FIND/REPLACE KEYWORDS WITH STARTING VALUES
system("repmeanvar")

#RUN Mx!!!
system("/usr/local/bin/mxt161f < brain2.mx > brain.mxo")

#EXTRACT CONFIDENCE INTERVALS FROM TEMPORARY OUTPUT FILE
system("cicalc")

#SAVE OUTPUT IN APPENDING FILE
system("cat brain.mxo>>brainLOG.mxo")

}
```

Mx Script for Running ACE models in an Extended Twin Design

```
! SCRIPT FOR RUNNING ACE Models on voxel-level data in an Extended twin
Design

!Script based on twin modeling designs in Mx (see Neale and Cardon)
with

! Address all complaints to Eric Schmitt (schmittje@vcu.edu)

!DESCRIPTION: this script is intended to run all voxel-level analyses
serially,
!saving relevant parameter estimates and fit statistics along the way.

!ASSUMPTIONS: in the current model all means and variance components
!parameter estimates are assumed to be the same for all individuals.
!Relaxing this assumption for means values can be done without
specifying
!new variables; for other parameters more programming would be
required.

!remove existing output file since append option will be active
system rm -rf output.mxa
system rm -rf withchi.mxa


#define nummodels 6
#define numpars 10
#define numpars2 12

!BEGIN MODEL
G1: General Model parameters
Calc Ngroups=6 !number of program segments

!declare initial matrices
Begin Matrices;

!DIRECT PATHS from latent to observed variables
A full 1 1 free !additive genetic
C full 1 1 free !shared environment
E full 1 1 free !unique environment

!FIXED SCALAR MULTIPLIERS
H full 1 1 !fixed scalar = .5
K full 1 1 !fixed scalar = 2

L full 1 1 !fixed scalar = 3

! Parameter estimates sex age for multiple regression predicting mean

R Full 1 4 fixed  !sex age meanCT betas for means regression

End Matrices;
```

```
Ma H .5 !set H=.5 and ensure that it is fixed-used in halving DZ
genetic
!correlation
Ma K 2 !set K=2 and ensure that it is fixed-used in squaring variance
components
Ma L 3

!Optional: Set initial values for direct paths from ACE latent
variables
!based on descriptive statistics

Ma A
CTSTART
Ma C
CTSTART
Ma E
CTSTART

Ma R
INSERTBETAS


!creating A2/C2/E2  variables not necessary in this version-relevant
algebra
!performed in covariances command in individual groups

Begin algebra;
End Algebra;

option noout
End

G2: Monozygotic twin pairs for cortical thickness
Data Ninput_vars=46 Nobserved=159   !enter number of observations here
Rectangular file=CTtwinTemp.txt

Labels FAMID
ID1 ZYG1 SEX1 RACE1 HAND1 SES1 AGE1 V1 CT1
ID2 ZYG2 SEX2 RACE2 HAND2 SES2 AGE2 V2 CT2
ID3 ZYG3 SEX3 RACE3 HAND3 SES3 AGE3 V3 CT3
ID4 ZYG4 SEX4 RACE4 HAND4 SES4 AGE4 V4 CT4
ID5 ZYG5 SEX5 RACE5 HAND5 SES5 AGE5 V5 CT5

Select IF ZYG1=0; !ZYGOSITY=MZ ;    !MZ = 0; DZ = 1,

Select SEX1 AGE1 CT1 SEX2 AGE2 CT2 SEX3 AGE3 CT3 SEX4 AGE4 CT4;

Definition_variables  SEX1 AGE1 SEX2 AGE2 SEX3 AGE3 SEX4 AGE4; ! Female
= 0, Male = 1, age in years


Matrices=Group 1
G Full 1 1 Free   !  means for twins
F Full 1 1 Free   !  means for sibs

O Full 1 1 fixed  ! definition variable age.x
Q full 1 1 fixed  ! definition variable age.y
```

```
S Full 1 1 fixed  ! definition variable sex.x

B Full 1 1 fixed  ! definition variable age (sib1)
D Full 1 1 fixed  ! definition variable sex (sib1)

I Full 1 1 fixed  ! definition variable age (sib2)
J Full 1 1 fixed  ! definition variable sex (sib2)

End Matrices;


Ma G
INSERTMEANCT
Ma F
INSERTMEANCT

Specify O AGE1!age twin1
Specify Q AGE2!age twin2
Specify S SEX1!sex twins

Specify B AGE3 !age sib1
Specify D SEX3 !sex sib1

Specify I AGE4!age sib2
Specify J SEX4!sex sib2

!MODELING OF MEANS
! y = u + (B1 * SEX) + (B2 * AGE)


Means
G+(S|O|O^K|O^L)*R'|G+(S|Q|Q^K|Q^L)*R'|F+(D|B|B^K|B^L)*R'|F+(J|I|I^K|I^L
)*R' /  !modeling means


!Expected covariance matrix; covariance formula could be simplified
!since age and sex are same between pairs in this sample.


!covariance statement must be modified to allow for sib to have less
correlated shared environment
Covariances

A^K+C^K+E^K | A^K+C^K     | H@A^K+C^K     |H@A^K+C^K _
A^K+C^K     | A^K+C^K+E^K | H@A^K+C^K     |H@A^K+C^K _
H@A^K+C^K   | H@A^K+C^K   | A^K+C^K+E^K   |H@A^K+C^K _
H@A^K+C^K   | H@A^K+C^K   | H@A^K+C^K     |A^K+C^K+E^K /

!Option Rs


option noout
End
```

```
G3: Dizygotic twin pairs for cortical thickness
Data Ninput_vars=46 Nobserved=159   !enter number of observations here
Rectangular file=CTtwinTemp.txt

Labels FAMID
ID1 ZYG1 SEX1 RACE1 HAND1 SES1 AGE1 V1 CT1
ID2 ZYG2 SEX2 RACE2 HAND2 SES2 AGE2 V2 CT2
ID3 ZYG3 SEX3 RACE3 HAND3 SES3 AGE3 V3 CT3
ID4 ZYG4 SEX4 RACE4 HAND4 SES4 AGE4 V4 CT4
ID5 ZYG5 SEX5 RACE5 HAND5 SES5 AGE5 V5 CT5

Select IF ZYG1=1; !ZYGOSITY=MZ ; !MZ = 0; DZ = 1,

Select SEX1 AGE1 CT1 SEX2 AGE2 CT2 SEX3 AGE3 CT3 SEX4 AGE4 CT4;

Definition_variables  SEX1 AGE1 SEX2 AGE2 SEX3 AGE3 SEX4 AGE4; ! Female
= 0, Male = 1, age in years


Matrices=Group 1
G Full 1 1 Free   !  means for twins
F Full 1 1 Free   !  means for sibs

O Full 1 1 fixed  ! definition variable age.x
Q full 1 1 fixed  ! definition variable age.y
S Full 1 1 fixed  ! definition variable sex.x

B Full 1 1 fixed  ! definition variable age (sib1)
D Full 1 1 fixed  ! definition variable sex (sib1)

I Full 1 1 fixed  ! definition variable age (sib2)
J Full 1 1 fixed  ! definition variable sex (sib2)

!L Full 1 1 fixed  ! definition variable age (sib3)
!M Full 1 1 fixed  ! definition variable sex (sib3)

End Matrices;

Specify G 43 !specify parameter assignments for means
Specify F 44

Equate G 2 1 1 G 3 1 1
Equate F 2 1 1 F 3 1 1

Ma G
INSERTMEANCT

Ma F
INSERTMEANCT

Specify O AGE1!age twin1
Specify Q AGE2!age twin2
Specify S SEX1!sex twins

Specify B AGE3 !age sib1
Specify D SEX3 !sex sib1
```

```
Specify I AGE4!age sib2
Specify J SEX4!sex sib2

!MODELING OF MEANS
! y = u + (B1 * SEX) + (B2 * AGE)

Means
G+(S|O|O^K|O^L)*R'|G+(S|Q|Q^K|Q^L)*R'|F+(D|B|B^K|B^L)*R'|F+(J|I|I^K|I^L
)*R'/  !modeling means


!Expected covariance matrix; covariance formula could be simplified
!since age and sex are same between pairs in this sample.

!covariance statement must be modified to allow for sib to have less
correlated shared environment
Covariances

A^K+C^K+E^K | H@A^K+C^K     | H@A^K+C^K     |H@A^K+C^K _
H@A^K+C^K   | A^K+C^K+E^K   | H@A^K+C^K     |H@A^K+C^K _
H@A^K+C^K   | H@A^K+C^K     | A^K+C^K+E^K   |H@A^K+C^K _
H@A^K+C^K   | H@A^K+C^K     | H@A^K+C^K     |A^K+C^K+E^K /


!Option Rs


option noout
End

G4: Singleton families and true singletons for cortical thickness
Data Ninput_vars=46 Nobserved=159   !enter number of observations here
Rectangular file=CTsinTemp.txt

Labels FAMID
ID1 ZYG1 SEX1 RACE1 HAND1 SES1 AGE1 V1 CT1
ID2 ZYG2 SEX2 RACE2 HAND2 SES2 AGE2 V2 CT2
ID3 ZYG3 SEX3 RACE3 HAND3 SES3 AGE3 V3 CT3
ID4 ZYG4 SEX4 RACE4 HAND4 SES4 AGE4 V4 CT4
ID5 ZYG5 SEX5 RACE5 HAND5 SES5 AGE5 V5 CT5

Select SEX1 AGE1 CT1 SEX2 AGE2 CT2 SEX3 AGE3 CT3 SEX4 AGE4 CT4 SEX5
AGE5 CT5;

Definition_variables  SEX1 AGE1 SEX2 AGE2 SEX3 AGE3 SEX4 AGE4 SEX5
AGE5; ! Female = 0, Male = 1, age in years


Matrices=Group 1
F Full 1 1 Free   !  means for sibs

O Full 1 1 fixed  ! definition variable age sib1
Q full 1 1 fixed  ! definition variable age sib2
S Full 1 1 fixed  ! definition variable sex sib1
N Full 1 1 fixed  ! definition variable sex sib2

B Full 1 1 fixed  ! definition variable age (sib3)
```

```
D Full 1 1 fixed  ! definition variable sex (sib3)

I Full 1 1 fixed  ! definition variable age (sib4)
J Full 1 1 fixed  ! definition variable sex (sib4)

X Full 1 1 fixed  ! definition variable age (sib5)
M Full 1 1 fixed  ! definition variable sex (sib5)

End Matrices;


Ma F
INSERTMEANCT

Equate F 2 1 1 F 4 1 1

Specify O AGE1!age sib1
Specify S SEX1!sex sib1

Specify Q AGE2!age sib2
Specify N SEX2!sex sib2

Specify B AGE3 !age sib3
Specify D SEX3 !sex sib3

Specify I AGE4!age sib4
Specify J SEX4!sex sib4

Specify X AGE5!age sib5
Specify M SEX5!sex sib5


!MODELING OF MEANS
! y = u + (B1 * SEX) + (B2 * AGE)


Means
F+(S|O|O^K|O^L)*R'|F+(N|Q|Q^K|Q^L)*R'|F+(D|B|B^K|B^L)*R'|F+(J|I|I^K|I^L
)*R'|F+(M|X|X^K|X^L)*R'/  !modeling means


!Expected covariance matrix; covariance formula could be simplified
!since age and sex are same between pairs in this sample.

!covariance statement must be modified to allow for sib to have less
correlated shared environment
Covariances
A^K+C^K+E^K | H@A^K+C^K     | H@A^K+C^K     |H@A^K+C^K   |H@A^K+C^K_
H@A^K+C^K   | A^K+C^K+E^K   | H@A^K+C^K     |H@A^K+C^K   |H@A^K+C^K_
H@A^K+C^K   | H@A^K+C^K     | A^K+C^K+E^K   |H@A^K+C^K   |H@A^K+C^K_
H@A^K+C^K   | H@A^K+C^K     | H@A^K+C^K     |A^K+C^K+E^K |H@A^K+C^K_
H@A^K+C^K   | H@A^K+C^K     | H@A^K+C^K     |H@A^K+C^K   |A^K+C^K+E^K /


!Option Rs

option noout
```

```
End

G5: Concatenate parameters into a single vector
Data Calculation
!(Matrix Q concatenates output from this group)

Begin Matrices = Group 1
End Matrices;

Begin Algebra;
!Estimated Variance using mean values for age and sex
P = A|C|E|R; !approximate variance partitioning + parameters

End Algebra;

Option RS
End

G6: Calculate Fit statistics and concatenate local parameters (mean)
with global parameters
Data Calculation
Begin Matrices;
A Full 1 1 = %F2 !fit MZ
B Full 1 1 = %F3 !fit DZ
C Full 1 1 = %F4 !fit singletons
D Full 1 1 = G2  !mean twins
E Full 1 1 = F2  !mean sibs
P COMP 1 12 = P5  !
End matrices;

Begin Algebra;
M = D|E;
Z = A+B+C;
I = P|M|Z;      !parameter vector 'P' with means 'M' and fit 'Z'
concatenated
End Algebra;

Labels Columns I A C E R-sex R-age R-age2 R-age3 u-Twin u-Sib Fit
option noout
Option Format=(10D14.6)
Option mxi=output.mxa !output file for parameter vector (appended to
others)
Option append
Option rs multiple issat !multiple fit in effect
End

save full.mxs

!DROP A Genetic parameters
get full.mxs
DROP A 1 1 1
Ma 1 C
CTSTART
Ma 1 E
CTSTART

End
```

```
!DROP C Senv parameters
get full.mxs
DROP C 1 1 1
MA 1 A
CTSTART
MA 1 E
CTSTART

End

!DROP AC Uenv parameters
get full.mxs
DROP A 1 1 1 C 1 1 1
MA 1 E EONLYSTART

End

!DROP Sex regression
get full.mxs
DROP R 1 1 1
End

!DROP Age regression
get full.mxs
DROP R 1 1 1
Exit

!GRAB POTENTIAL STATISTICS OF INTEREST
G1: Calculate Chi-squared and AIC values relative to the full model
Calc Ngroups=1 !number of program segments

Begin Matrices;
P Full nummodels numpars
Q Full 1 4 !coordinates for Full model -2LL
A Full 1 4 !coordinates for VECTOR of -2LL values for submodels
K Full 1 1 !scalar 2
B Unit nummodels 1 !unit vactor
C Full nummodels 1 !df for AIC to FULL

End Matrices;

!HAVE TO MANUALLY INPUT DF HERE
 Ma C 0 1 1 2 1 1

Ma K 2 !parsimony bonus per df for AIC

Ma P File=output.mxa !input parameter file

Ma Q 1 numpars 1 numpars !definition of submatrix to extract Full Fit
Ma A 1 numpars nummodels numpars !definition of submatrix to extract
other fits

Begin Algebra;
R=\part(P,Q); !extract fit function of saturated model
S=B@R; !set up subtraction of submodel fits !turns a scalar to a column
FULL -2LL
```

```
T=\part(P,A); !extract fit functions

D=C@K; ! 2 * df to full

M=(T-S); !calculate X2 values to full

V=(M)-(D); !calculate AIC (X2 - 2 * df) (rel to Full)

Z=P|M|V;

End Algebra;


option format=(12D14.6)
option mxz=withchi.mxa
Exit


G2 GENERATE VOXELWISE OUTPUT FOR FULL MODEL (with X2 of submodels)
Calc Ngroups=1
Begin Matrices;
Z Full 6 12
A Full 1 4
B Full 1 4
C Full 1 4
D Full 1 4
E Full 1 4
F Full 1 4
End Matrices

Ma Z File=withchi.mxa !input parameter file

Ma A 1 1 1 10
Ma B 2 11 2 12
Ma C 3 11 3 12
Ma D 4 11 4 12
Ma E 5 11 5 12
Ma F 6 11 6 12

Begin Algebra;
Y = \part(Z,A)|\part(Z,B)|\part(Z,C)|\part(Z,D)|\part(Z,E)|\part(Z,F);

End Algebra;

!Labels columns Y a c e Reg-SEX Reg-AGE u-Twin u-Sib Fit X2-CE AIC-CE
X2-AE AIC-AE X2-E AIC-E X2-nosex AIC-nosex X2-noage AIC-noage

option append
option format=(25D15.6)
option mxy=fullbyvoxel.mxa
Exit
```

Shell Script to Insert Starting Values into Mx Script
(later versions use #include, which is less error prone)

```
#!/bin/sh

/bin/sed "s/INSERTMEANCT/$(cat mean.txt)/g" <brain.mx > braintemp2.txt
/bin/sed "s/INSERTBETAS/$(cat betas.txt)/g" <braintemp2.txt >
braintemp3.txt
/bin/sed "s/CTSTART/$(cat sv.txt)/g" < braintemp3.txt > braintemp4.txt
/bin/sed "s/EONLYSTART/$(cat sv2.txt)/g" < braintemp4.txt>
braintemp5.txt

/bin/cp braintemp5.txt brain2.mx

/bin/rm -rf braintemp1.txt braintemp2.txt braintemp3.txt braintemp4.txt
braintemp5.txt
```

Shell Script to Extract Confidence Intervals from Output Files and Save as Vectors
(later versions execute these commands via a system call from within the R script))

```
/bin/grep 'X   5   1   1' brain.mxo | awk '{print $6}' >> a2.txt
/bin/grep 'X   5   1   1' brain.mxo | awk '{print $7}' >> a2L.txt
/bin/grep 'X   5   1   1' brain.mxo | awk '{print $8}' >> a2U.txt


/bin/grep 'Y   5   1   1' brain.mxo | awk '{print $6}' >> c2.txt
/bin/grep 'Y   5   1   1' brain.mxo | awk '{print $7}' >> c2L.txt
/bin/grep 'Y   5   1   1' brain.mxo | awk '{print $8}' >> c2U.txt


/bin/grep 'Z   5   1   1' brain.mxo | awk '{print $6}' >> e2.txt
/bin/grep 'Z   5   1   1' brain.mxo | awk '{print $7}' >> e2L.txt
/bin/grep 'Z   5   1   1' brain.mxo | awk '{print $8}' >> e2U.txt
```

C

APPENDIX C: REPLICATION OF AUTOMATED METHODS IN OTHER SAMPLES: VETSA AND MATR

"Civilization advances by extending the number of important operations which we can perform without thinking about them. Operations of thought are like calvary in a battle—they are strictly limited in number, they require fresh horses, and must only be made at decisive moments."

--Alfred North Whitehead, *An Introduction to Mathematics,* 1948

The construction of automated methods for the analyses of voxel-level data were developed from the sheer impossibility of a manual analysis of tens of thousands of measurements. However, these methods are easily generalized to other applications. Perhaps the most obvious is the analysis of neuroanatomic volumes, which, like voxel data, are continuous variables that tend to be normally distributed. Much of the analyses on the NIMH dataset were performed in parallel with the development of the statistical pipeline, and much of the time required to generate results was a consequence of the necessity of algorithm creation. Thus, now that that the pipeline is more well-established, it would be useful to assess its utility in analyses in the situation in which there are no delays associated with pipeline development itself.

In collaboration with Bill Kremen at UCSD, we modified our algorithms to perform analyses on VETSA MRI data from the Vietnam Era Twin Study of Aging (VETSA), in a sample of 108 MZ and 114 DZ adult twin pairs 52-59 years of age. The resultant measures are volumes extracted using Freesurfer, a freeware application for the measurement of MRI data. Figure A3.1 shows raw correlations which, as with the NIMH pediatric sample, suggest high heritabilities for brain volumes.

Figure A3.1: Raw correlations for 37 volumetric ROIs on the VETSA sample. Black lines denote .5 of the MZ correlation, Purple lines .25 of the DZ correlation.

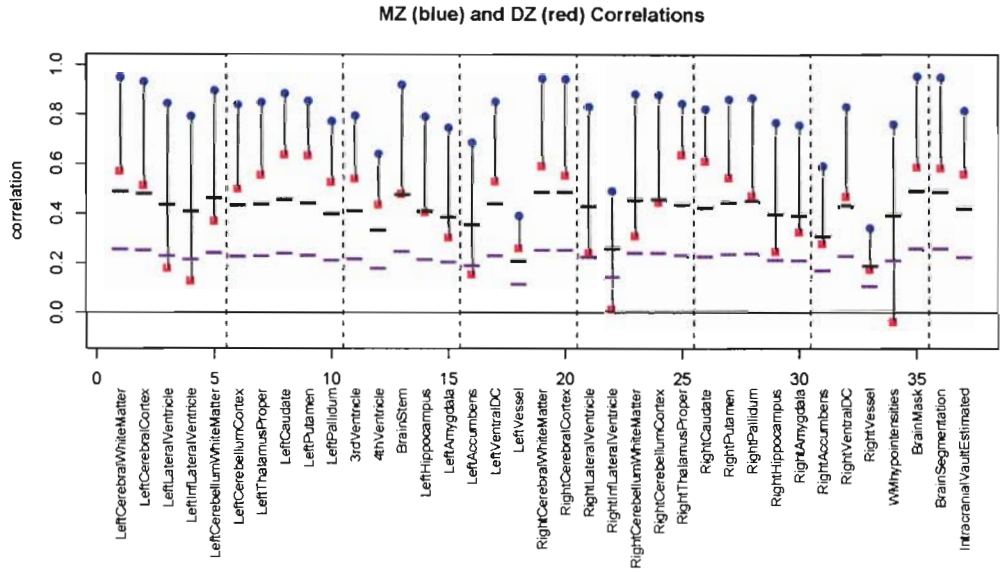

The data were subsequently passed to our ACE R/Mx hybrid scripts specifically designed for iterative analyses. Figures A3.2 provides MLEs from this model. As in children, heritabilities for most regions are quite high. Surprisingly, ventricular volume heritability was high as well. This difference compared to the NIMH sample is likely age related.

We also examined the effects of using ICV as a global covariate. The results from these models are in Figure A3.3. Surprisingly, despite decreases in residual variance (not shown), heritabilities remained high. Once again, age may be the causative factor here, although it has yet to be tested directly.

Figure A3.2: MLEs for the best fitting ACE models in the VETSA analysis. a^2 is shown in black, c^2 in red, and e^2 in blue. 95% confidence intervals also are given

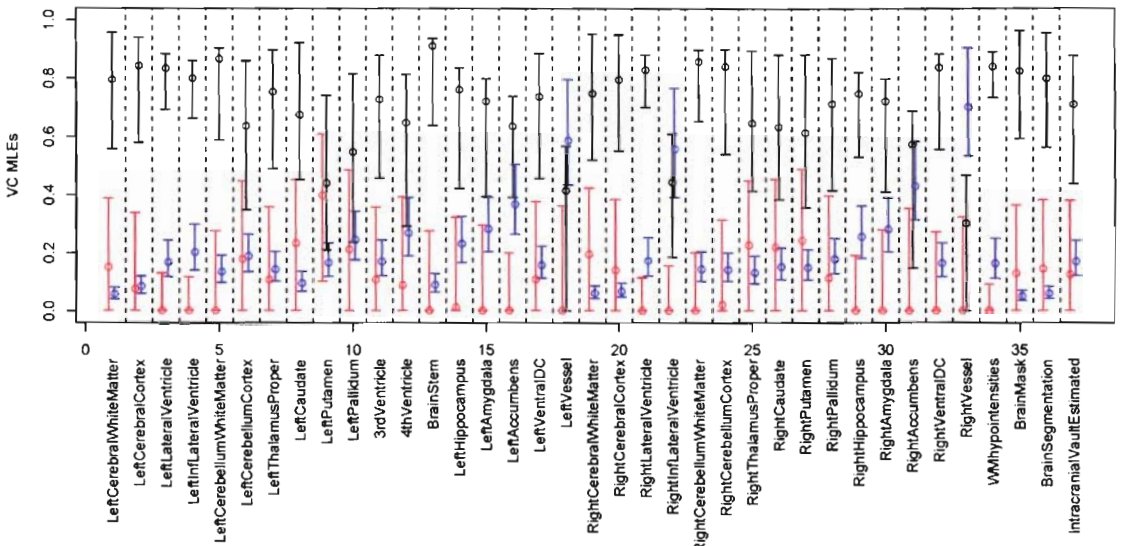

ADE models also were investigated, shown in Figure A3.3 without modification of R programs and only a subtle modification in Mx. The general trends were the same as with ACE models, with the exception that there is some evidence of dominance in ventricular volumes (as expected from the raw correlations). Consistent with confidence interval calculations, submodels removing either A or D did not produce significant reductions in fit; however, though in no instance could both be removed. Therefore it can be concluded that broad sense heritability is significant for all regions of the brain, but distinguishing between additive and dominant genetic effects is not possible.

Figure A3.3: MLEs for the best fitting ACE models in the VETSA analysis in models including a global covariate on mean volumes.

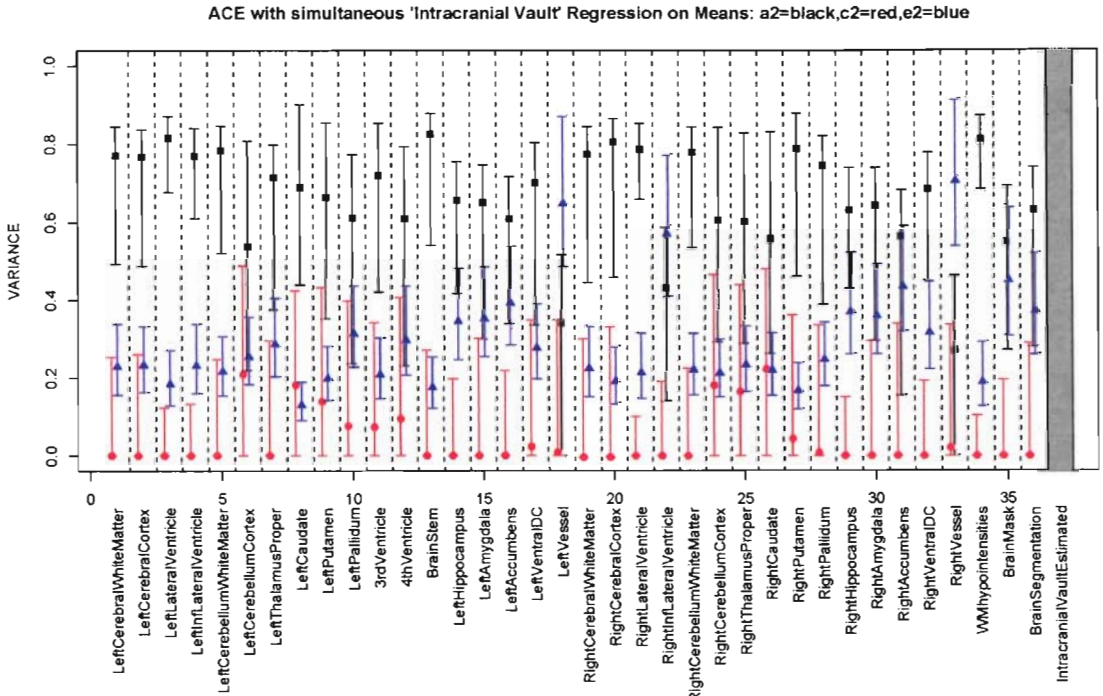

Figure A3.3: MLEs for the best fitting ADE models in the VETSA analysis.

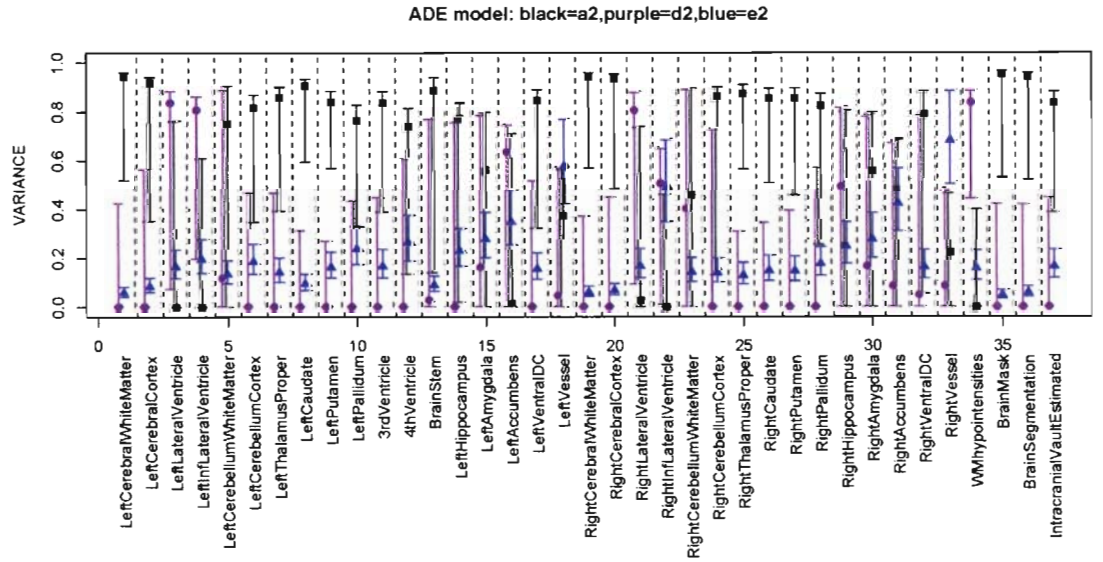

Interactions between individual variance components with age were performed, as shown in Figure A3.4. There were few significant interactions with tissue volumes, but there was some evidence of gene by age interactions in the ventral diencephalon, ventricular volumes, and white matter hypointensities.

Figure A3.4: Log p-values for tests of variance component interaction with age. Dotted lines represent various p-value thresholds

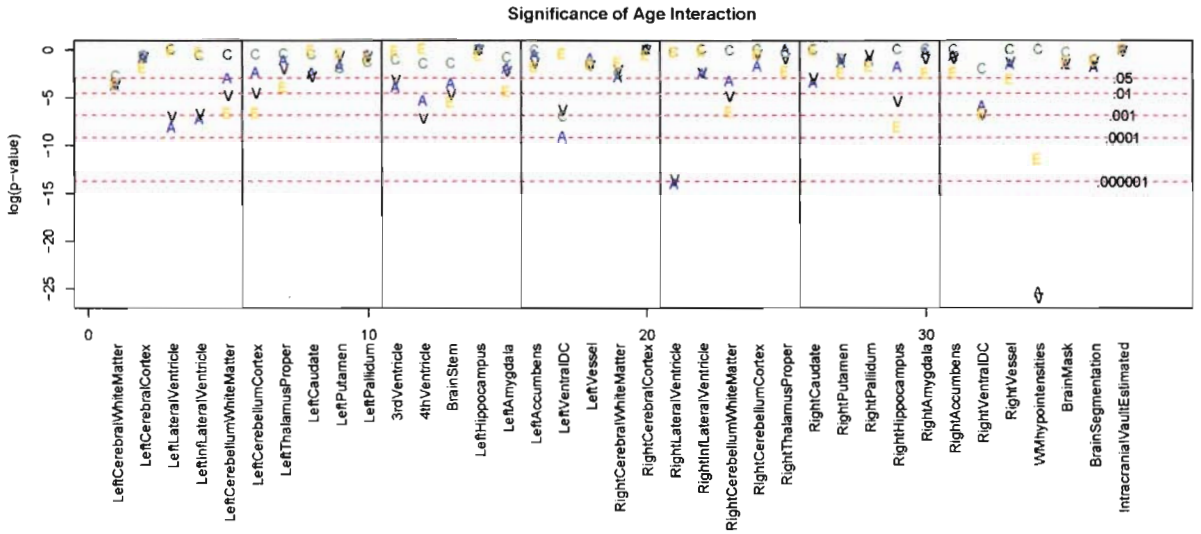

Due to the modular nature of the algorithms, the ACE Mx script could be replaced with a bivariate one with minimal labor. The addition of a second loop in the R script allowed for iteration over 2 dimensions, creating all pairwise combinations of ROIs. The genetic correlations from these analyses are shown in Figure A3.5, using the clustering capabilities of R to identify preliminary genetic associations between the measured structures. These results are shown in A3.5, which are in many aspects similar to the results reported in chapters 9 and 10. Left and right homologues were almost always highly associated. Three major clusters appeared, which represented 1) lateral ventricular measures, 2) 3rd ventricle, 4th ventricle, and nucleus accumbens, and 3) the remainder of the brain. Within brain tissue, the genetic correlations roughly clustered into 1) cerebral

are feasible. The findings on the VETSA sample were produced with less than two days of human labor, and include many analyses (such as inspecting for normality) not reported here. Thus, the use of automation allows for rapid generation of many statistics from basic SEMs, which makes them as readily obtainable now as descriptive statistics have been traditionally. Implementation of these methods may lead to increased time to devote to more complex and hypothesis-driven multivariate models (as well as the clues needed to create them), and carries the potential to rapidly screen phenotypes in much the same way that genome-wide association scans are performed presently.

For behavioral phenotypes, successful fusion of automation with ordinal data analyses will be required. Figure A3.6 demonstrates results from the first attempts to do so. Using calendar data on from the MM-III wave of the MATR, we analyzed an ordinal measure of smoking use via sequential univariate models. These analyses provide preliminary evidence on the trajectories of heritability throughout the lifespan. Interestingly, the shared environment appears the dominant source of covariance in adolescence, with genetic factors becoming most important for the remainder of the ages measured.

Future work should aim at 1) converting many of the capabilities of the R scripts into functions, which will increase generalizability, 2) the ability to call a library of Mx scripts based on arguments provided by the user, 3) development of functions to automatically convert individualwise to familywise datasets, 4) a library of functions for the visualization of raw data to facilitate rapid communication and minimize error owed to false assumptions, and 5) methods to address problems associated with multiple testing

cortex, amygdala, and hippocampus, 2) subcortical measures and cerebellar white matter, and 3) cerebellar cortex.

Figure A3.5: Genetic correlations from pairwise bivariate modeling for VETSA volumes.

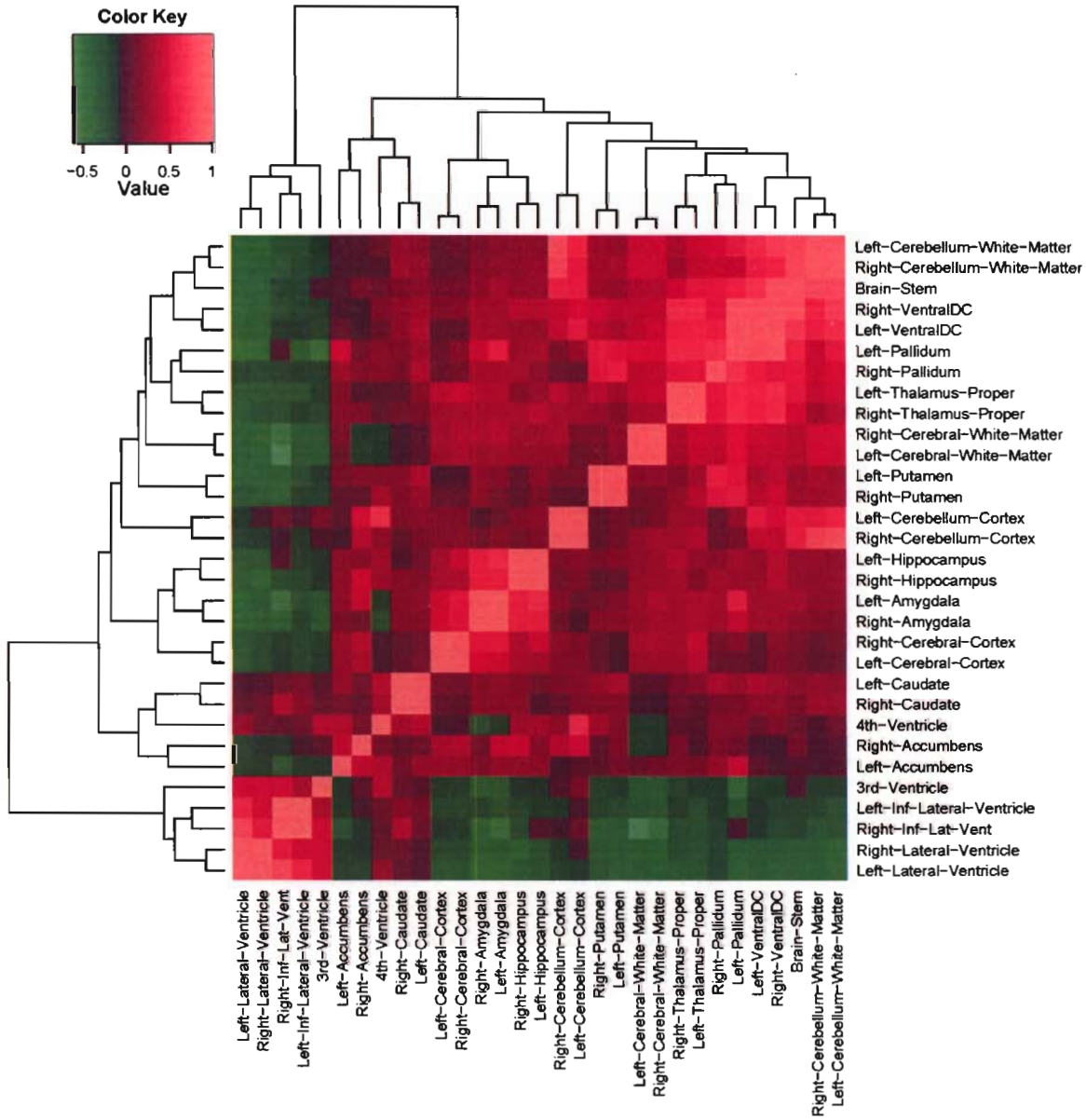

Though these findings provide exciting new evidence on the genetic role on adult brain structure, they also demonstrate the advantages of using iterative algorithms to perform classical behavioral genetic analyses even in situations where more manual techniques

Figure A3.6: ACE models on semi-longitudinal data on cigarette use. Panel A plots the proportion of response for 6 ordinal levels of smoking by age in the complete sample. Panel B represents results from ACE models (a^2=red, c^2=blue, e^2=green) from ages 10-50. Panel C shows a^2 and c^2, with significant results in red.

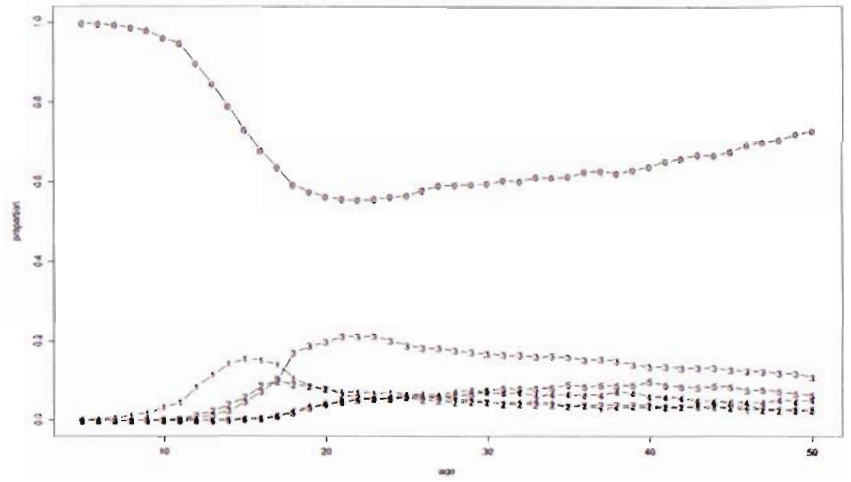

A

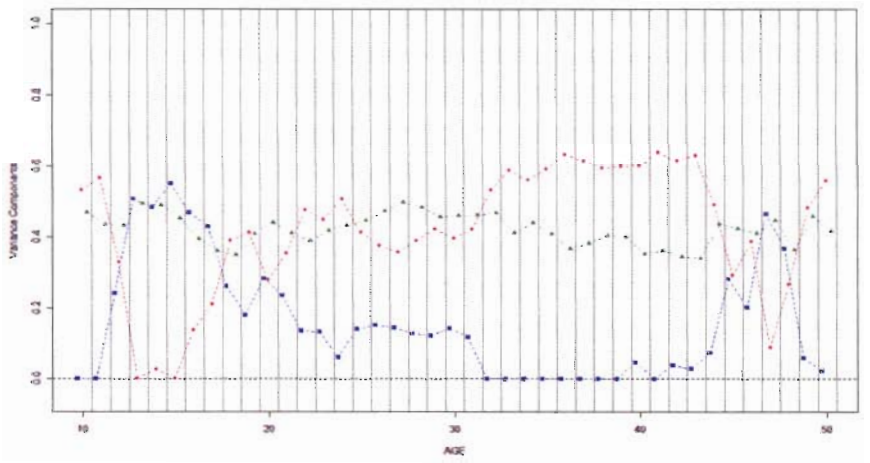

B

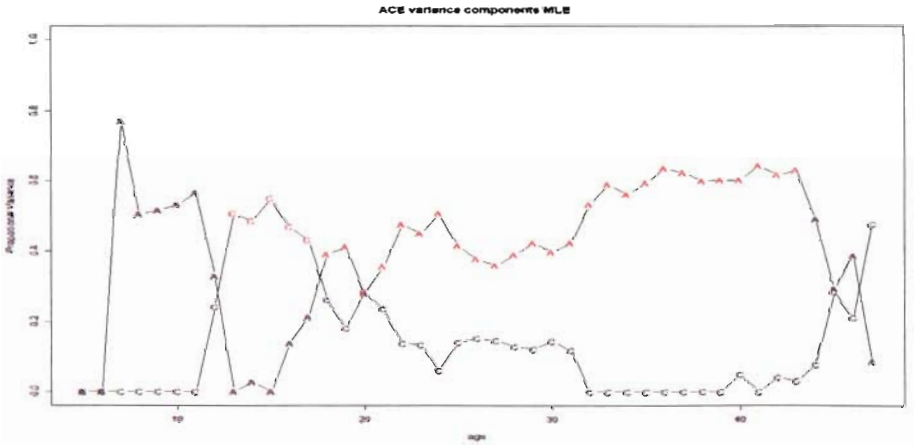

C

APPENDIX D: ODDS AND ENDS

Figure A4.1: Variance components MLEs for ADE model in twins only. Additive genetic variance is shown in the top panel, and dominance variance is shown at bottom. Uncorrected probability maps are shown in the inset.

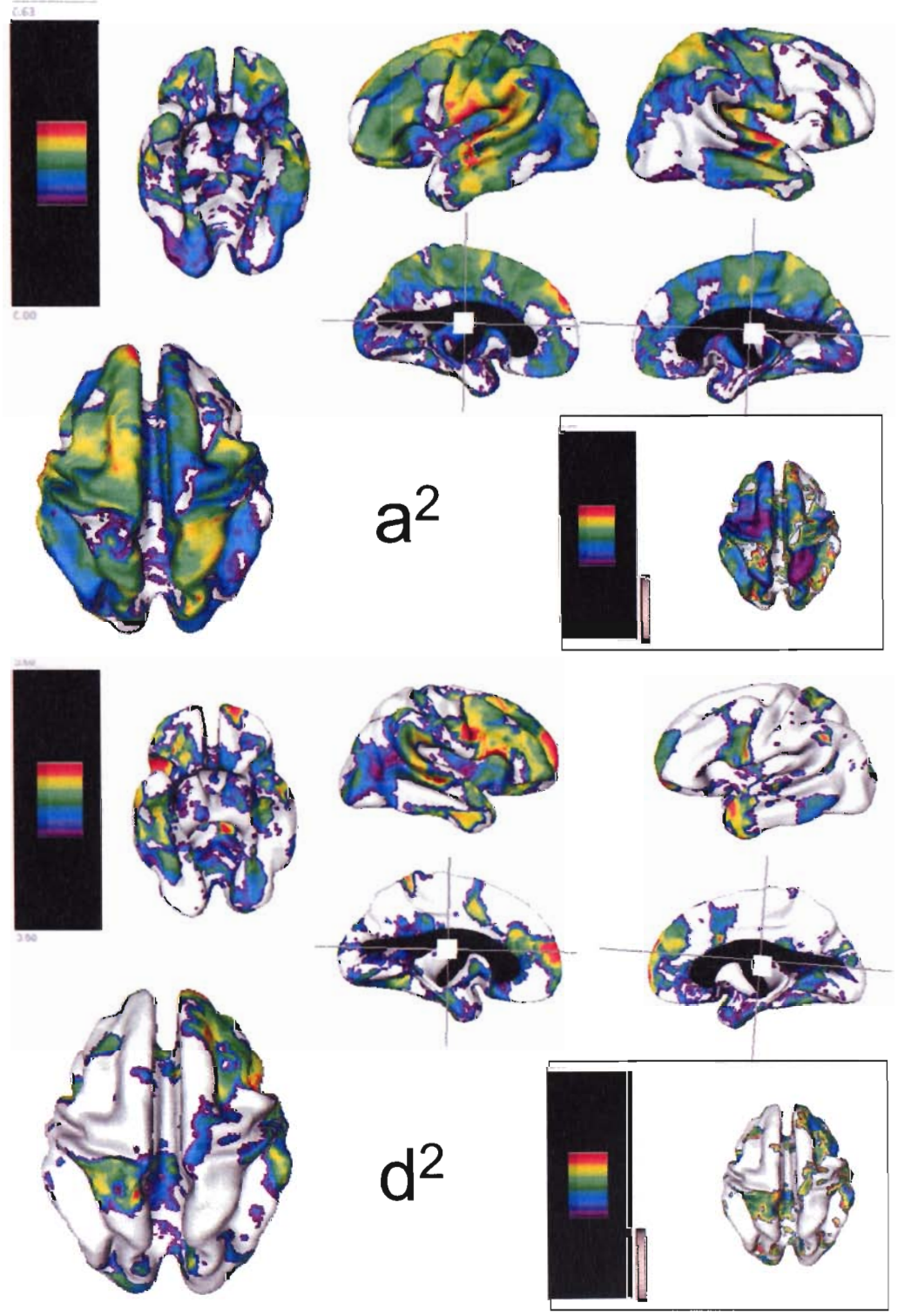

Figure A4.2: ACE models of cerebellar subregions

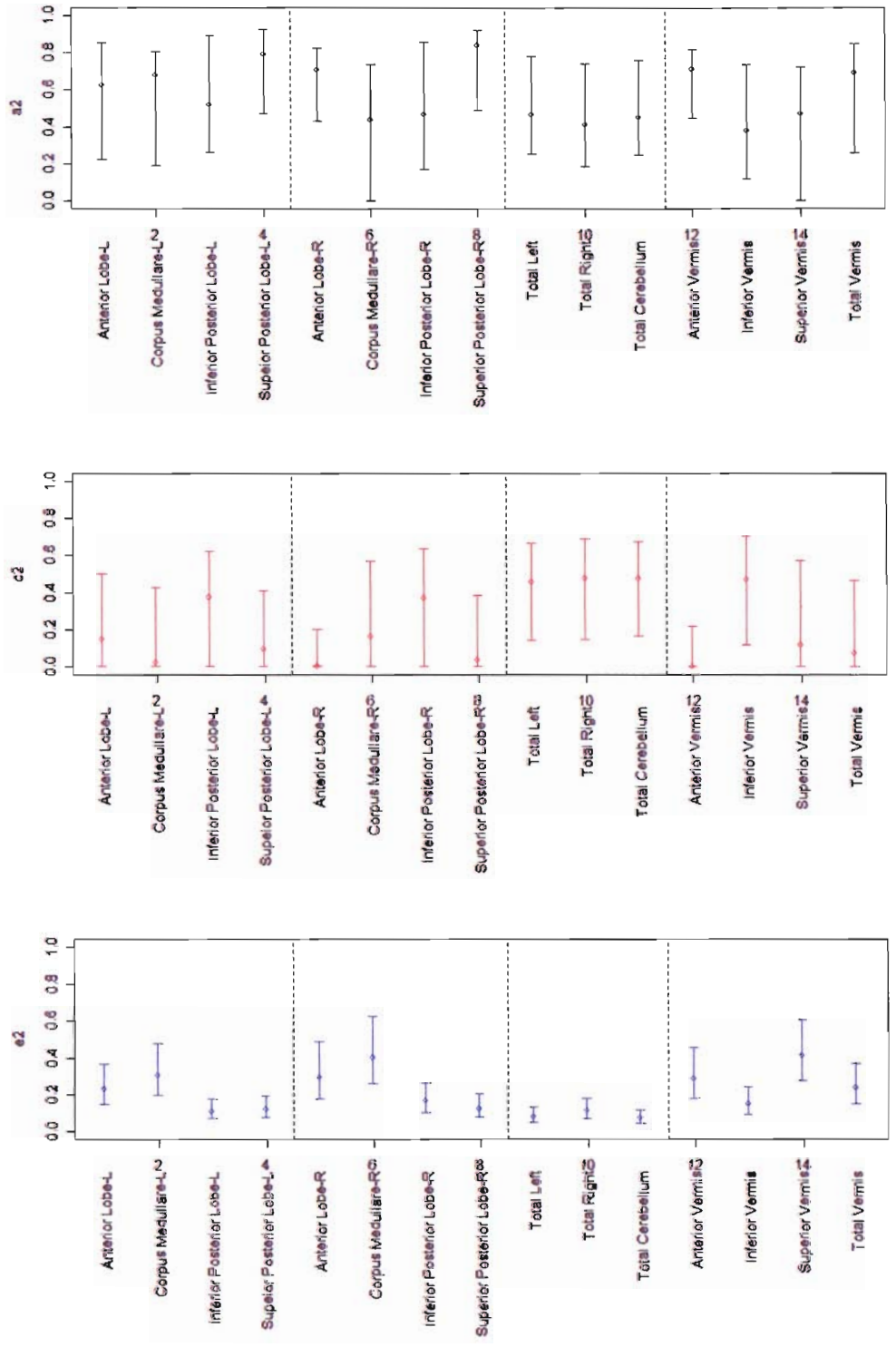

APPENDIX E: A COMPILATION OF DISSERTATION ABSTRACTS

GENERAL ABSTRACT

Understanding the causes of individual differences in brain structure may give clues about the etiology of cognition, personality, and psychopathology, and also may identify endophenotypes for molecular genetic studies on brain development. We performed a comprehensive statistical genetic study of anatomic neuroimaging data from a large pediatric sample (N=600+) of twins and family members from the Child Psychiatry Branch at the NIMH. These analyses included variance decomposition of structural volumetric endophenotypes at several levels of resolution, voxel-level analysis of cortical thickness, assessment of gene by age interaction, several multivariate genetic analyses, and a search for genetically-mediated brain-behavioral relationships.

These analyses found strong evidence for a genetic role in the generation of individual differences in brain volumes, with the exception of the cerebellum and the lateral ventricles. Subsequent multivariate analyses demonstrated that most of the genetic variance in large volumes shares a common source. More subtle analyses suggest that although this global genetic factor is the principal determinant of neuroanatomic variability, genetic factors also mediate regional variability in cortical thickness and are different for gray and white matter volumes. Models using graph theory show that brain structure follows small-world architectural rules, and that these relationships are genetically-determined. Structural homologues appeared to be strongly related genetically, which was further confirmed using novel methods for semi-multivariate quantitative genetic analysis at the voxel level.

Studies on interactions with age were mixed. We found evidence of gene by environment interaction on frontal and temporal lobar volumes, indicating that the role of genetic factors on these structures dynamic during childhood. Analyses on cortical thickness at a finer scale, however, showed that environmental factors are more important in childhood, and environmental changes were responsible for most of the changes in heritability over this age range. When assessing the relationship between brain and behavior, we found weak negative genetic correlations and positive environmental correlations between IQ and cortical thickness, which appear to partially cancel each other out. More complex

models allowing for age interactions suggest that high and low IQ groups have different patterns of gene by age interactions in concordance with prior literature on cortical phenotypes.

CHAPTER 2

The history of genetics and statistics largely overlap. Before the discovery of molecular genetic tools in the twentieth century, genetics was predominantly an inferential science. The development of appropriate statistical methods was a necessity for identifying heritable traits and to observe the effects of genes within populations. Today, despite technological advances in the basic sciences, the use of inferential statistics remains a powerful tool in elucidating thorny scientific questions, particularly when they involve extremely complex systems with multiple unknown or unmeasurable causal factors. Thus, statistical approaches retain great value when addressing general questions in genetics, psychology, neurobiology, and beyond. This chapter reviews the fundamental principles of behavioral genetics, with particular emphasis on methods central to this thesis.

CHAPTER 3

Investigations into the biology of typical neurodevelopment have greatly advanced the understanding of childhood psychiatric diseases. Yet despite extraordinary efforts to identify the molecular genetic factors influencing variability in human neuroanatomic volumes, this approach, thus far, has had limited success. Well-established behavioral genetic methodologies provide a means for investigating relationships between brain and behavior from a global perspective. Behavioral genetics, however, has only just begun to address neuroanatomical questions and to explore the associations between volumetric data and behavioral measures. Knowledge of heritability of brain endophenotypes in children is particularly limited. This chapter reviews the extant studies that report on the relative contributions of genetic and environmental influences on brain volumes via magnetic resonance imaging.

CHAPTER 4

The importance of genetic factors in generating variability in neuroanatomic endophenotypes is largely unquantified, particularly for developmental samples. We measured several neuroanatomic volumes via high-resolution MRI in a sample of 90 MZ twin pairs, 37 DZ twin pairs, and 158 unrelated singletons between the ages of 5 and 18. Statistical genetic analyses demonstrated high heritability for nearly all structures measured, with the exception of the lateral ventricles and the cerebellum. Moreover, allowing for changing genetic effects with age, we observed significant gene by age interactions in the frontal and temporal lobes, in both gray and white matter. These results suggest a strong and dynamic role of additive genetic differences on the population variability in pediatric brain structure.

CHAPTER 5

Using data from a large sample (N=600) of twins and family members, we combined voxel-level neuroimaging and statistical genetic analyses to produce the first high-resolution pediatric heritability maps of the human brain. The role of additive genetic factors on variance in cortical thickness varied substantially over the brain surface. Heritability was strongest in the frontal lobe (particularly on the right side and orbitofrontal regions bilaterally), superior parietal lobule, language centers (Broca's and Wernicke's area), inferior pre- and postcentral gyrus, and superior temporal gyrus bilaterally. In contrast, heritability was quite low in the occipital lobe and the inferior tempro-occipital cortex. The role of shared environmental factors on variance was insubstantial. These findings demonstrate regional effects of genes on cortical development, and could aid the hunt for genetic polymorphisms that affect variability in human brain structure.

CHAPTER 6

In this chapter, we have expanded our analyses of cortical thickness to allow for changes with age. Both genetic and environmental variance decreased in most regions, though genetic variance increased in the superior parietal lobule and environmental variance increased in superior primary motor and somatosensory cortex. As total phenotypic variance decreased, the relative importance of genetic factors increased in most regions, including superior temporal, frontal lobes, and the superior parietal lobule. The increase in heritability in these regions is temporally coincident with the development of many cognitive functions that have been associated with them. Though underpowered, these results are suggestive of a dynamic process underlying both genetic and nongenetic contributions to cortical variability.

CHAPTER 7

An important component of brain mapping is an understanding of the relationships between neuroanatomic structures, as well as the nature of shared causal factors. Prior twin studies have demonstrated that much of individual differences in human anatomy are caused by genetic differences, but information is limited on whether different structures share common genetic factors. We performed a multivariate statistical genetic analysis on volumetric MRI measures (cerebrum, cerebellum, lateral ventricles, corpus callosum, thalamus, and basal ganglia) from a pediatric sample of 326 twins and 158 singletons. Our results suggest that the great majority of variability in cerebrum, cerebellum, thalamus and basal ganglia is determined by a single genetic factor. Though most (75%) of the variability in corpus callosum was explained by additive genetic effects these were largely independent of other structures. We also observed relatively small but significant environmental effects common to multiple neuroanatomic regions, particularly between thalamus, basal ganglia, and lateral ventricles. These findings are concordant with prior volumetric twin studies and support radial models of brain evolution.

CHAPTER 8

In this chapter, we examine the interrelationships between eight cerebral lobar volumetric measures via both exploratory and confirmatory factor analyses. These analyses suggest the presence of strong genetic correlations between cerebral structures, particularly between regions of like tissue type or in spatial proximity. Structural modeling estimated that most of the variance in all structures is associated with highly correlated lobar latent factors, with differences in genetic covariance and heritability driven by a common genetic factor that influenced gray and white matter differently. Reanalysis including total brain volume as a covariate dramatically reduced the total residual variance and disproportionately influenced the additive genetic variance in all regions of interest.

CHAPTER 9

Despite great interest in the role of genes in driving individual differences in cortical patterning, very little information on the topic is available for typically-developing individuals. We acquired high resolution anatomic MRI images on a large pediatric sample of twins, siblings of twins, and singleton families. We subsequently modeled familial relationships to obtain estimates of the additive genetic correlations between 54 gyral-level measures of cortical thickness. Both cluster and principal components analysis revealed several factors underlying the associations. The most dominant factor influenced the variability of non-orbital frontal lobe structures, dorsal parietal gyri, and somatosensory cortex. Other networks included two distinct factors driving associations between occipital lobe structures, and a factor influencing variability tempro-insular cortex. These findings are largely concordant with other multivariate studies of brain structure, the twin literature, and current understanding on the role of genes in cortical neurodevelopment.

CHAPTER 10

Multivariate statistical genetic analysis of the cortex has, thus far, been limited to the gyral level. In this chapter, we combine classical behavioral genetic methodologies for variance decomposition with novel semi-multivariate algorithms for high-resolution measurement of phenotypic covariance. Using these tools, we produced correlational maps of genetic and environmental relationships between several regions of interest and the cortical surface. These analyses demonstrated high, fairly uniform genetic correlations between the entire cortex and global mean cortical thickness. Using several gyri as seed regions, we found a consistent pattern of bilateral genetic correlations between structural homologues, with environmental correlations more restricted to the same hemisphere as the seed region. These findings are consistent with the limited existing knowledge on the genetics underlying cortical variability, as well as our prior multivariate studies on cortical gyri.

Reference List

SAS/STAT User's Guide (2000). (Version version 8) [Computer software]. Cary, NC: SAS institute.

Aboitiz, F., Morales, D., & Montiel, J. (2003). The evolutionary origin of the mammalian isocortex: towards an integrated developmental and functional approach. *Behavioral and Brain Sciences, 26,* 535-586.

Achard, S., Salvador, R., Whitcher, B., Suckling, J., & Bullmore, E. T. (2006). A resilient, low-frequency, small-world brain functional network with highly connected association cortical hubs. *Joutnal of Neuroscience, 26,* 63-72.

Akaike, H. (1987). Factor analysis and AIC. *Psychometrika, 52,* 317-332.

Anderson, S., Mione, M., Yun, K., & Rubenstein, J. L. R. (1999). Differential origins of neocortical projection and local circuit neurons: Role of Dlx genes in neocortical interneuronogenesis. *Cerebral Cortex, 9,* 646-654.

Andreasen, N. C., Flaum, M., Swayze, V., Oleary, D. S., Alliger, R., Cohen, G. et al. (1993). Intelligence and Brain Structure in Normal Individuals. *American Journal of Psychiatry, 150,* 130-134.

Ashburner, J. & Friston, K. J. (2000). Voxel-based morphometry - The methods. *Neuroimage, 11,* 805-821.

Ashburner, J., Hutton, C., Frackowiak, R., Johnsrude, I., Price, C., & Friston, K. (1998). Identifying global anatomical differences: Deformation-based morphometry. *Human Brain Mapping, 6,* 348-357.

Baare, W. F., Hulshoff Pol, H. E., Boomsma, D. I., Posthuma, D., De Geus, E. J., Schnack, H. G. et al. (2001a). Quantitative genetic modeling of variation in human brain morphology. *Cerebral Cortex, 11,* 816-824.

Baare, W. F., van Oel, C. J., Hulshoff Pol, H. E., Schnack, H. G., Durston, S., Sitskoorn, M. M. et al. (2001b). Volumes of brain structures in twins discordant for schizophrenia. *Archives of General Psychiatry, 58,* 33-40.

Barnea-Goraly, N., Menon, V., Eckert, M., Tamm, L., Bammer, R., Karchemskiy, A. et al. (2005). White matter development during childhood and adolescence: A cross-sectional diffusion tensor imaging study. *Cerebral Cortex, 15,* 1848-1854.

Bartley, A. J., Jones, D. W., & Weinberger, D. R. (1997). Genetic variability of human brain size and cortical gyral patterns. *Brain, 120 (Pt 2),* 257-269.

Barton, R. A. & Harvey, P. H. (2000). Mosaic evolution of brain structure in mammals. *Nature, 405,* 1055-1058.

Bechger T.M. & Maris, G. (2004). Structural Equation Modeling of Multiple Facet Data: Extending Models for Multitrait-Multimethod Data. *Psicologica, 25,* 253-274.

Becker, L. E., Armstrong, D. L., Chan, F., & Wood, M. M. (1984). Dendritic Development in Human Occipital Cortical-Neurons. *Developmental Brain Research, 13,* 117-124.

Benes, F. M., Turtle, M., Khan, Y., & Farol, P. (1994). Myelination of A Key Relay Zone in the Hippocampal-Formation Occurs in the Human Brain During Childhood, Adolescence, and Adulthood. *Archives of General Psychiatry, 51,* 477-484.

Berger, K. S. & Thompson, R. A. (1995). *The Developing Person: Through Childhood and Adolescence.* (Fourth ed.) New York: Worth Publishers.

Biegler, R., McGregor, A., Krebs, J. R., & Healy, S. D. (2001). A larger hippocampus is associated with longer-lasting spatial memory. *Proceedings of the National Academy of Sciences of the United States of America, 98,* 6941-6944.

Biondi, A., Nogueira, H., Dormont, D., Duyme, M., Hasboun, D., Zouaoui, A. et al. (1998). Are the brains of monozygotic twins similar? A three-dimensional MR study. *AJNR American Journal of Neuroradiology, 19,* 1361-1367.

Boddaert, N., De Leersnyder, H., Bourgeois, M., Munnich, A., Brunelle, F., & Zilbovicius, M. (2004). Anatomical and functional brain imaging evidence of lenticulo-insular anomalies in Smith Magenis syndrome. *Neuroimage, 21,* 1021-1025.

Bonan, I., Argenti, A. M., Duyme, M., Hasboun, D., Dorion, A., Marsault, C. et al. (1998). Magnetic resonance imaging of cerebral central sulci: a study of monozygotic twins. *Acta Geneticae Mecicae et Gemellologiae (Roma.), 47,* 89-100.

Boomsma, D., Busjahn, A., & Peltonen, L. (2002). Classical twin studies and beyond. *Nat.Rev.Genet., 3,* 872-882.

Bota, M. (2003). From axis to triangle: The role of orbital cortex. *Behavioral and Brain Sciences, 26,* 552-553.

Bouchard, T. J. & Mcgue, M. (1981). Familial Studies of Intelligence - A Review. *Science, 212,* 1055-1059.

Brown, W. M. (2001). Natural selection of mammalian brain components. *Trends in Ecology & Evolution, 16,* 471-473.

Bushberg, J. T., Seibert, J. A., Leidholdt, E. M., & Boone, J. M. (1994). *The essential physics of medical imaging*. Baltimore: Williams and Wilkins.

Caceres, M., Lachuer, J., Zapala, M. A., Redmond, J. C., Kudo, L., Geschwind, D. H. et al. (2003). Elevated gene expression levels distinguish human from non-human primate brains. *Proc.Natl.Acad.Sci.U.S.A, 100,* 13030-13035.

Campbell, D. T. & Fiske, D. W. (1959). Convergent and discriminant validation by the multitrait-multimethod matrix. *Psychological Bulletin, 56,* 81-105.

Carey, V. J., Gentry, J., Whalen, E., & Gentleman, R. (2005). Network structures and algorithms in Bioconductor. *Bioinformatics, 21,* 135-136.

Carmelli, D., Reed, T., & DeCarli, C. (2002a). A bivariate genetic analysis of cerebral white matter hyperintensities and cognitive performance in elderly male twins. *Neurobiol.Aging, 23,* 413-420.

Carmelli, D., Swan, G. E., DeCarli, C., & Reed, T. (2002b). Quantitative genetic modeling of regional brain volumes and cognitive performance in older male twins. *Biol.Psychol., 61,* 139-155.

Carmelli, D., Swan, G. E., Reed, T., Wolf, P. A., Miller, B. L., & DeCarli, C. (1999). Midlife cardiovascular risk factors and brain morphology in identical older male twins. *Neurology, 52,* 1119-1124.

Carroll, S. B. (2003). Genetics and the making of Homo sapiens. *Nature, 422,* 849-857.

Casey, B. J., Giedd, J. N., & Thomas, K. M. (2000). Structural and functional brain development and its relation to cognitive development. *Biological Psychology, 54,* 241-257.

Ciani, L. & Salinas, P. C. (2005). WNTs in the vertebrate nervous system: From patterning to neuronal connectivity. *Nature Reviews Neuroscience, 6,* 351-U17.

Clark, G. D. (2004). The classification of cortical dysplasias through molecular genetics. *Brain & Development, 26,* 351-362.

Collins, D. L., Neelin, P., Peters, T. M., & Evans, A. C. (1994). Automatic 3D Intersubject Registration of Mr Volumetric Data in Standardized Talairach Space. *Journal of Computer Assisted Tomography, 18,* 192-205.

Collins, D. L., Zijdenbos, A. P., Barre, W. F. C., & Evans, A. C. (1999). ANIMAL+INSECT: Improved cortical structure segmentation. In A.Kuba, M. Samal, &

A. Todd-Pokropek (Eds.), *Information Processing in Medical Imaging: 16th International Conference, IPMI'99, Visegrad, Hungary, June/July 1999 Proceedings* (1613 ed., pp. 210-223). Berlin: Springer Verlag.

Corten, I. W., Saris, W. E., Coenders, G., van der Veld, W., Aalberts, C. E., & Kornelis, C. (2002). Fit of Different Models for Multitrait-Multimethod Experiments. *Structural Equation Modeling., 9,* 213-232.

Crawford, C. B. & DeFries, J. C. (1978). Factor analysis of genetic and environmental correlation matrices. *Multivar.Behav.Res., 13,* 297-318.

Crick, F. & Jones, E. (1993). Backwardness of human neuroanatomy. *Nature, 361,* 109-110.

Darlington, R. B., Dunlop, S. A., & Finlay, B. L. (1999). Neural development in metatherian and eutherian mammals: Variation and constraint. *Journal of Comparative Neurology, 411,* 359-368.

Darwin, C. R. (1871). *The Descent of Man and Selection in Relation to Sex.* Appleton.

Davy, S. H. (1995). *Force of Nature*. New York: Simon and Schuster.

de Winter, W. & Oxnard, C. E. (2001). Evolutionary radiations and convergences in the structural organization of mammalian brains. *Nature, 409,* 710-714.

Dekaban, A. S. & Sadowsky, D. (1978). Changes in Brain Weights During Span of Human Life - Relation of Brain Weights to Body Heights and Body Weights. *Annals of Neurology, 4,* 345-356.

Dorus, S., Vallender, E. J., Evans, P. D., Anderson, J. R., Gilbert, S. L., Mahowald, M. et al. (2004). Accelerated evolution of nervous system genes in the origin of Homo sapiens. *Cell, 119,* 1027-1040.

Draganski, B., Gaser, C., Busch, V., Schuierer, G., Bogdahn, U., & May, A. (2004). Neuroplasticity: Changes in grey matter induced by training - Newly honed juggling skills show up as a transient feature on a brain-imaging scan. *Nature, 427,* 311-312.

Draganski, B., Gaser, C., Kempermann, G., Kuhn, H. G., Winkler, J., Buchel, C. et al. (2006). Temporal and spatial dynamics of brain structure changes during extensive learning. *Journal of Neuroscience, 26,* 6314-6317.

Eckert, M. A., Leonard, C. M., Molloy, E. A., Blumenthal, J., Zijdenbos, A., & Giedd, J. N. (2002). The epigenesis of planum temporale asymmetry in twins. *Cereb.Cortex, 12,* 749-755.

Edwards, A. W. F. (1972). *Likelihood.* London: Cambridge.

Enard, W., Khaitovich, P., Klose, J., Zollner, S., Heissig, F., Giavalisco, P. et al. (2002). Intra- and interspecific variation in primate gene expression patterns. *Science, 296,* 340-343.

Evans, D. M., Gillespie, N. A., & Martin, N. G. (2002). Biometrical genetics. *Biological Psychology, 61,* 33-51.

Falconer, D. S. & Mackay, T. F. C. (1996). *Introduction to quantitative genetics.* Essex: Longman.

Falconer, D. S. (1965). The Inheritance of Liability to Certain Diseases, estimated from the incidence among relatives. *Ann Hum Genet,* 51-76.

Faraone, S. V., Seidman, L. J., Kremen, W. S., Kennedy, D., Makris, N., Caviness, V. S. et al. (2003). Structural brain abnormalities among relatives of patients with schizophrenia: implications for linkage studies. *Schizophrenia Research, 60,* 125-140.

Finlay, B. L. & Darlington, R. B. (1995). Linked Regularities in the Development and Evolution of Mammalian Brains. *Science, 268,* 1578-1584.

Finlay, B. L., Darlington, R. B., & Nicastro, N. (2001a). Developmental structure in brain evolution. *Behavioral and Brain Sciences, 24,* 263-+.

Finlay, B. L., Darlington, R. B., & Nicastro, N. (2001b). Developmental structure in brain evolution. *Behavioral and Brain Sciences, 24,* 298-308.

Fishell, G. (1997). Regionalization in the mammalian telencephalon. *Current Opinion in Neurobiology, 7,* 62-69.

Fisher, S. E. & Marcus, G. F. (2006). The eloquent ape: genes, brains and the evolution of language. *Nature Reviews Genetics, 7,* 9-20.

Flanagan, J. G. (2006). Neural map specification by gradients. *Current Opinion in Neurobiology, 16,* 59-66.

Flavell, J. H., Miller, P. H., & Miller, S. A. (1993). *Cognitive development.* Englewood Cliffs, N.J.: Prentice-Hall.

Gaser, C., Nenadic, I., Buchsbaum, B. R., Hazlett, E. A., & Buchsbaum, M. S. (2004). Ventricular enlargement in schizophrenia related to volume reduction of the thalamus, striatum, and superior temporal cortex. *American Journal of Psychiatry, 161,* 154-156.

Gellon, G. & McGinnis, W. (1998). Shaping animal body plans in development and evolution by modulation of Hox expression patterns. *Bioessays, 20,* 116-125.

Genovese, C. R., Lazar, N. A., & Nichols, T. (2002). Thresholding of statistical maps in functional neuroimaging using the false discovery rate. *Neuroimage, 15,* 870-878.

Geschwind, D. H., Miller, B. L., DeCarli, C., & Carmelli, D. (2002). Heritability of lobar brain volumes in twins supports genetic models of cerebral laterality and handedness. *Proc.Natl.Acad.Sci.U.S.A, 99,* 3176-3181.

Giedd, J. N., Blumenthal, J., Jeffries, N. O., Castellanos, F. X., Liu, H., Zijdenbos, A. et al. (1999). Brain development during childhood and adolescence: a longitudinal MRI study. *Nature Neuroscience, 2,* 861-863.

Giedd, J. N., Schmitt, J. E., & Neale, M. C. (2007). Structural brain magnetic resonance imaging of pediatric twins. *Human Brain Mapping*. In press.

Giedd, J. N., Snell, J. W., Lange, N., Rajapakse, J. C., Casey, B. J., Kozuch, P. L. et al. (1996). Quantitative magnetic resonance imaging of human brain development: Ages 4-18. *Cerebral Cortex, 6,* 551-560.

Gogtay, N., Giedd, J. N., Lusk, L., Hayashi, K. M., Greenstein, D., Vaituzis, A. C. et al. (2004). Dynamic mapping of human cortical development during childhood through early adulthood. *Proceedings of the National Academy of Sciences of the United States of America, 101,* 8174-8179.

Gottesman, I. I. & Gould, T. D. (2003). The endophenotype concept in psychiatry: etymology and strategic intentions. *Am.J.Psychiatry, 160,* 636-645.

Gray, J. R. & Thompson, P. M. (2004). Neurobiology of intelligence: Science and ethics. *Nature Reviews Neuroscience, 5,* 471-482.

Greenstein, D., Lerch, J., Shaw, P., Clasen, L., Giedd, J., Gochman, P. et al. (2006). Childhood onset schizophrenia: cortical brain abnormalities as young adults. *Journal of Child Psychology and Psychiatry, 47,* 1003-1012.

Grove, E. A. & Fukuchi-Shimogori, T. (2003). Generating the cerebral cortical area map. *Annual Review of Neuroscience, 26,* 355-380.

Gu, J. & Gu, X. (2003). Induced gene expression in human brain after the split from chimpanzee. *Trends Genet., 19,* 63-65.

Guerrini, R. & Marini, C. (2006). Genetic malformations of cortical development. *Experimental Brain Research, 173,* 322-333.

Guillemot, F., Molnar, Z., Tarabykin, V., & Stoykova, A. (2006). Molecular mechanisms of cortical differentiation. *European Journal of Neuroscience, 23,* 857-868.

Gur, R. C., Turetsky, B. I., Matsui, M., Yan, M., Bilker, W., Hughett, P. et al. (1999). Sex differences in brain gray and white matter in healthy young adults: Correlations with cognitive performance. *Journal of Neuroscience, 19,* 4065-4072.

Gurling, H. M. D., Critchley, H., Datta, S. R., McQuillin, A., Blaveri, E., Thirumalai, S. et al. (2006). Genetic association and brain morphology studies and the chromosome 8p22 pericentriolar material 1 (PCM1) gene in susceptibility to schizophrenia. *Archives of General Psychiatry, 63,* 844-854.

Haidekker, M. A., Evertsz, C. J., Fitzek, C., Boor, S., Andresen, R., Falkai, P. et al. (1998). Projecting the sulcal pattern of human brains onto a 2D plane--a new approach using potential theory and MRI. *Psychiatry Res., 83,* 75-84.

Hardan, A. Y., Muddasani, S., Vemulapalli, M., Keshavan, M. S., & Minshew, N. J. (2006). An MRI study of increased cortical thickness in autism. *American Journal of Psychiatry, 163,* 1290-1292.

Harris, G. J., Codori, A. M., Lewis, R. F., Schmidt, E., Bedi, A., & Brandt, J. (1999). Reduced basal ganglia blood flow and volume in pre-symptomatic, gene-tested persons at-risk for Huntington's disease. *Brain, 122,* 1667-1678.

Hashimoto, T. & Lewis, D. A. (2006). BDNF Val66Met polymorphism and GAD(67) mRNA expression in the prefrontal cortex of subjects with schizophrenia. *American Journal of Psychiatry, 163,* 534-5U2.

Hastie, T., Tibshirani, R., & Friedman, S. (2001). *The Elements of Statistical Learning; Data Mining, Inference, and Prediction.* New York: Springer-Verlag.

Herbert, M. R., Ziegler, D. A., Deutsch, C. K., O'Brien, L. M., Lange, N., Bakardjiev, A. et al. (2003). Dissociations of cerebral cortex, subcortical and cerebral white matter volumes in autistic boys. *Brain, 126,* 1182-1192.

Hsieh, W. P., Chu, T. M., Wolfinger, R. D., & Gibson, G. (2003). Mixed-model reanalysis of primate data suggests tissue and species biases in oligonucleotide-based gene expression profiles. *Genetics, 165,* 747-757.

Hulshoff Pol, H. E., Posthuma, D., Baare, W. F., De Geus, E. J., Schnack, H. G., Van Haren, N. E. et al. (2002). Twin-singleton differences in brain structure using structural equation modelling. *Brain, 125,* 384-390.

Hulshoff Pol, H. E., Schnack, H. G., Posthuma, D., Mandl, R. C. W., Baare, W. F., van Oel, C. et al. (2006). Genetic contributions to human brain morphology and intelligence. *Journal of Neuroscience, 26,* 10235-10242.

Huttenlocher, P. R. (1979). Synaptic Density in Human Frontal-Cortex - Developmental-Changes and Effects of Aging. *Brain Research, 163,* 195-205.

Huttenlocher, P. R. & Dabholkar, A. S. (1997). Regional differences in synaptogenesis in human cerebral cortex. *Journal of Comparative Neurology, 387,* 167-178.

Huxley, T. H. (1880). *The Crayfish.* London: C. Keegan Paul and Co.

Ihaka, R. & Gentleman, R. (1996). R: a language for data analysis and graphics. *J.Comput.Graph.Statist.,* 299-314.

Jenkins, T. W. & Truex, R. C. (1963). Dissection of the human brain as a method for its fractionation by weight. *Anatomical Record, 147,* 359-366.

Jinks, J. L. & Fulker, D. W. (1970). Comparison of Biometrical Genetical, Mava, and Classical Approaches to Analysis of Human Behavior. *Psychological Bulletin, 73,* 311-349.

Jones, K. E. & MacLarnon, A. M. (2004). Affording Larger Brains: Testing Hypothesis of Mammalian Brain Evolution on Bats. *The American Naturalist, 164,* E20-E31.

Jöreskog (1971). Statistical analysis of sets of congeneric tests. *Psychometrika, 52,* 101.

Kaas, J. H. & Collins, C. E. (2001). Variability in the sizes of brain parts. *Behavioral and Brain Sciences, 24,* 288-+.

Kaiser, H. F. (1958). The varimax criterion for analytic rotation in factor analysis. *Psychometrika, 23,* 187-200.

Kandel, E. & Jessl (2000). *Principles of Neural Science*. McGraw Hill.

Karten, H. J. (1997). Evolutionary developmental biology meets the brain: The origins of mammalian cortex. *Proceedings of the National Academy of Sciences of the United States of America, 94,* 2800-2804.

Karten, H. J. (2005). The ascending auditory pathway in the pigeon (*Columbia livia*). II. Telencephalic projections of the nucleus ovalis thalami. *Brain Research, 11,* 134-153.

Kendler, K. S., Heath, A., Martin, N. G., & Eaves, L. J. (1986). Symptoms of Anxiety and Depression in A Volunteer Twin Population - the Etiologic Role of Genetic and Environmental-Factors. *Archives of General Psychiatry, 43,* 213-221.

Kendler, K. S., Heath, A. C., Martin, N. G., & Eaves, L. J. (1987). Symptoms of Anxiety and Symptoms of Depression - Same Genes, Different Environments. *Archives of General Psychiatry, 44,* 451-457.

Kendler, K. S. & Kidd, K. K. (1986). Recurrence Risks in An Oligogenic Threshold-Model - the Effect of Alterations in Allele Frequency. *Annals of Human Genetics, 50,* 83-91.

Khaitovich, P., Hellmann, I., Enard, W., Nowick, K., Leinweber, M., Franz, H. et al. (2005). Parallel patterns of evolution in the genomes and transcriptomes of humans and chimpanzees. *Science, 309,* 1850-1854.

Kotter, R. & Sommer, F. T. (2000). Global relationship between anatomical connectivity and activity propagation in the cerebral cortex. *Philos.Trans.R.Soc.Lond B Biol.Sci., 355,* 127-134.

Kriegstein, A., Noctor, S., & Martinez-Cerdeno, V. (2006). Patterns of neural stem and progenitor cell division may underlie evolutionary cortical expansion. *Nature Reviews Neuroscience, 7,* 883-890.

Kruska, D. C. T. (2005). On the evolutionary significance of encephalization in some eutherian mammals: Effects of adaptive radiation, domestication, and feralization. *Brain Behavior and Evolution, 65,* 73-108.

Lamarck, J. B. (1963). *Zoological philosophy; an exposition with regard to the natural history of animals*. New York: Hafner Pub. Co.

Larson, E. J. (2002). Theory of Evolution: A History of Controversy. The Teaching Company.

Le Goualher, G., Argenti, A. M., Duyme, M., Baare, W. F., Hulshoff Pol, H. E., Boomsma, D. I. et al. (2000). Statistical sulcal shape comparisons: application to the detection of genetic encoding of the central sulcus shape. *Neuroimage., 11,* 564-574.

Lenroot, R., Schmitt, J. E., Ordaz, S., Wallace, G. W., Neale, M. C., Lerch, J. P. et al. (2007). Quantitative genetic analysis of cortical thickness in a pediatric twin population. *In preparation.*

Lenroot, R. K. (2005). Paper presented at the Human Brain Mapping conference, Toronto, Canada.

Lenroot, R. K. & Giedd, J. N. (2006). Brain development in children and adolescents: Insights from anatomical magnetic resonance imaging. *Neuroscience and Biobehavioral Reviews, 30,* 718-729.

Lerch, J., Pruessner, J., Zijdenbos, A., Collins, D. L., Teipel, S., Hampel, H. et al. (2004). Using cortical thickness to predict Alzheimer's disease. *Neurobiology of Aging, 25,* S295.

Lerch, J. P. & Evans, A. C. (2005a). Cortical thickness analysis examined through power analysis and a population simulation. *Neuroimage, 24,* 163-173.

Lerch, J. P., Pruessner, J. C., Zijdenbos, A., Hampel, H., Teipel, S. J., & Evans, A. C. (2005b). Focal decline of cortical thickness in Alzheimer's disease identified by computational neuroanatomy. *Cerebral Cortex, 15,* 995-1001.

Lerch, J. P., Worsley, K., Shaw, W. P., Greenstein, D. K., Lenroot, R. K., Gledd, J. et al. (2006). Mapping anatomical correlations across cerebral cortex (MACACC) using cortical thickness from MRI. *Neuroimage, 31,* 993-1003.

Loehlin, J. C. (1996). The Cholesky approach: A cautionary note. *Behavior Genetics, 26,* 65-69.

Loehlin, J. C. (1998). *Latent Variable Models: An introduction to factor, path, and structural analyses.*

Lohmann, G., von Cramon, D. Y., & Steinmetz, H. (1999). Sulcal variability of twins. *Cereb.Cortex, 9,* 754-763.

Lumsden, A. & Krumlauf, R. (1996). Patterning the vertebrate neuraxis. *Science, 274,* 1109-1115.

MacDonald, D., Kabani, N., Avis, D., & Evans, A. C. (2000). Automated 3-D extraction of inner and outer surfaces of cerebral cortex from MRI. *Neuroimage, 12,* 340-356.

MacLean, P. D. (1990). *The Triune Bain: Role in Paleocerebral Functions.* Plenum Press.

Maguire, E. A., Gadian, D. G., Johnsrude, I. S., Good, C. D., Ashburner, J., Frackowiak, R. S. J. et al. (2000). Navigation-related structural change in the hippocampi of taxi drivers. *Proceedings of the National Academy of Sciences of the United States of America, 97,* 4398-4403.

Maguire, E. A., Nannery, R., & Spiers, H. J. (2006). Navigation around London by a taxi driver with bilateral hippocampal lesions. *Brain, 129,* 2894-2907.

Maguire, E. A., Woollett, K., & Spiers, H. J. (2006). London taxi drivers and bus drivers: A structural MRI and neuropsychological analysis. *Hippocampus, 16,* 1091-1101.

Mallamaci, A. & Stoykova, A. (2006). Gene networks controlling early cerebral cortex arealization. *European Journal of Neuroscience, 23,* 847-856.

Marin-Padilla, M. (2003). Reptilian cortex and mammalian neocortex early developmental homologies. *Behavioral and Brain Sciences, 26,* 560-+.

Mcardle, J. J. & Goldsmith, H. H. (1990). Alternative Common Factor Models for Multivariate Biometric Analyses. *Behavior Genetics, 20,* 569-608.

Mcginnis, W. & Krumlauf, R. (1992). Homeobox Genes and Axial Patterning. *Cell, 68,* 283-302.

McIntosh, A. M., Baig, B., Hall, J., Job, D., Whalley, H. C., Owens, D. et al. (2006). Relationship of COMT variants to brain structure, function and risk of psychosis. *Schizophrenia Research, 81,* 192-193.

Mesulam, M. (2000). Brain, mind, and the evolution of connectivity. *Brain Cogn, 42,* 4-6.

Mochida, G. H. (2005). Cortical malformation and pediatric epilepsy: A molecular genetic approach. *Journal of Child Neurology, 20,* 300-303.

Mohr, A., Knauth, M., Weisbrod, M., Stippich, C., & Sartor, K. (2001). [Similarity of the brains of twins]. *Rofo, 173,* 515-521.

Mohr, A., Weisbrod, M., Schellinger, P., & Knauth, M. (2004). The similarity of brain morphology in healthy monozygotic twins. *Brain Res.Cogn Brain Res., 20,* 106-110.

Molko, N., Cachia, A., Riviere, D., Mangin, J. F., Bruandet, M., LeBihan, D. et al. (2004). Brain anatomy in Turner syndrome: Evidence for impaired social and spatial-numerical networks. *Cerebral Cortex, 14,* 840-850.

Molnar, Z., Metin, C., Stoykova, A., Tarabykin, V., Price, D. J., Francis, F. et al. (2006). Comparative aspects of cerebral cortical development. *European Journal of Neuroscience, 23,* 921-934.

Monuki, E. S. & Walsh, C. A. (2001). Mechanisms of cerebral cortical patterning in mice and humans. *Nature Neuroscience, 4,* 1199-1206.

Mrzljak, L., Uylings, H. B. M., Kostovic, I., & Vaneden, C. G. (1992). Prenatal Development of Neurons in the Human Prefrontal Cortex .2. A Quantitative Golgi-Study. *Journal of Comparative Neurology, 316,* 485-496.

Narr, K. L., Bilder, R. M., Toga, A. W., Woods, R. P., Rex, D. E., Szeszko, P. R. et al. (2005a). Mapping cortical thickness and gray matter concentration in first episode schizophrenia. *Cerebral Cortex, 15,* 708-719.

Narr, K. L., Toga, A. W., Szeszko, P., Thompson, P. M., Woods, R. P., Robinson, D. et al. (2005b). Cortical thinning in cingulate and occipital cortices in first episode schizophrenia. *Biological Psychiatry, 58,* 32-40.

Narr, K. L., van Erp, T. G., Cannon, T. D., Woods, R. P., Thompson, P. M., Jang, S. et al. (2002). A twin study of genetic contributions to hippocampal morphology in schizophrenia. *Neurobiol.Dis., 11,* 83-95.

Neale, M. C. Twins studies: software and algorithms. In *In: Encyclopedia of the human genome* (2000) Nature Publishing Group.

Neale, M. C., Boker, S. M., Xie, G., & Maes, H. H. (2002). Mx: Statistical Modeling (Version 5th edition) [Computer software]. Richmond, VA: Department of Psychiatry, Medical College of Virginia, Virginia Commonwealth University.

Neale, M. C. & Cardon, L. R. (1992). *Methodology for Genetic Studies of Twins and Families*. Dordrecht, the Netherlands: Kluwer Academic.

Neale, M. C. & Miller, M. B. (1997). The use of likelihood-based confidence intervals in genetic models. *Behavior Genetics, 27,* 113-120.

Nemoto, K., Ohnishi, T., Mori, T., Moriguchi, Y., Hashimoto, R., Asada, T. et al. (2006). The Val66Met polymorphism of the brain-derived neurotrophic factor gene affects age-related brain morphology. *Neuroscience Letters, 397,* 25-29.

Nolte, J. (1999). *The Human Brain: An Introduction to Its Functional Neuroanatomy*. St. Louis, MO: Mosby, Inc.

Norman, G. R. & Streiner, D. L. (2000). *Biostatistics: The bare essentials.* Hamilton, Ontario: B.C. Decker, Inc.

Northcutt, R. G. (2002). Understanding Vertebrate Brain Evolution. *Integ.and Comp.Biol., 42,* 743-756.

Northcutt, R. G. (2003). The use and abuse of developmental data. *Behavioral and Brain Sciences, 26,* 565-566.

Northcutt, R. G. & Kaas, J. H. (1995). The Emergence and Evolution of Mammalian Neocortex. *Trends in Neurosciences, 18,* 373-379.

O'Leary, D. D. M. (1989). Do Cortical Areas Emerge from A Protocortex. *Trends in Neurosciences, 12,* 400-406.

Ono, M., Kubik, S., & Abernathey, C. D. (1990). *Atlas of the Cerebral Sulci.* Stuttgart/New York: Thieme.

Oppenheim, J. S., Skerry, J. E., Tramo, M. J., & Gazzaniga, M. S. (1989). Magnetic resonance imaging morphology of the corpus callosum in monozygotic twins. *Ann.Neurol., 26,* 100-104.

Orr, H. A. (1887). Contribution to the embryology of the lizard. *J.Morphol, 1,* 311-372.

Passingham, R. E., Stephan, K. E., & Kotter, R. (2002). The anatomical basis of functional localization in the cortex. *Nat.Rev.Neurosci., 3,* 606-616.

Paus, T., Zijdenbos, A., Worsley, K., Collins, D. L., Blumenthal, J., Giedd, J. N. et al. (1999). Structural maturation of neural pathways in children and adolescents: In vivo study. *Science, 283,* 1908-1911.

Pennington, B. F., Filipek, P. A., Lefly, D., Chhabildas, N., Kennedy, D. N., Simon, J. H. et al. (2000). A twin MRI study of size variations in human brain. *J.Cogn Neurosci., 12,* 223-232.

Pfefferbaum, A., Sullivan, E. V., & Carmelli, D. (2004). Morphological changes in aging brain structures are differentially affected by time-linked environmental influences despite strong genetic stability. *Neurobiol.Aging, 25,* 175-183.

Pfefferbaum, A., Sullivan, E. V., Swan, G. E., & Carmelli, D. (2000). Brain structure in men remains highly heritable in the seventh and eighth decades of life. *Neurobiol.Aging, 21,* 63-74.

Piao, X. H., Chang, B. S., Bodell, A., Woods, K., BenZeev, B., Topcu, M. et al. (2005). Genotype-phenotype analysis of human frontoparietal polymicrogyria syndromes. *Annals of Neurology, 58,* 680-687.

Plomin, R., DeFries, J. C., & Fulker, D. W. (1988). *Nature and Nurture During Early Infancy and Childhood.* New York: Cambridge University Press.

Posthuma, D. (2002). *Genetic Variation and Cognitive Ability: Thesis.* Amsterdam, The Netherlands: Vrije Universiteit.

Posthuma, D., Baare, W. F., Hulshoff Pol, H. E., Kahn, R. S., Boomsma, D. I., & De Geus, E. J. (2003). Genetic correlations between brain volumes and the WAIS-III dimensions of verbal comprehension, working memory, perceptual organization, and processing speed. *Twin.Res., 6,* 131-139.

Posthuma, D. & Boomsma, D. I. (2000a). A note on the statistical power in extended twin designs. *Behavior Genetics, 30,* 147-158.

Posthuma, D., De Geus, E. J., Baare, W. F., Hulshoff Pol, H. E., Kahn, R. S., & Boomsma, D. I. (2002). The association between brain volume and intelligence is of genetic origin. *Nat.Neurosci., 5,* 83-84.

Posthuma, D., De Geus, E. J., Neale, M. C., Hulshoff Pol, H. E., Baare, W. E. C., Kahn, R. S. et al. (2000b). Multivariate genetic analysis of brain structure in an extended twin design. *Behav.Genet., 30,* 311-319.

Price, D. J., Kennedy, H., Dehay, C., Zhou, L. B., Mercier, M., Jossin, Y. et al. (2006). The development of cortical connections. *European Journal of Neuroscience, 23,* 910-920.

Puelles, L. (2001b). Brain segmentation and forebrain development in amniotes. *Brain Research Bulletin, 55,* 695-710.

Puelles, L. (2001a). Brain segmentation and forebrain development in amniotes. *Brain Research Bulletin, 55,* 695-710.

Puelles, L. & Rubenstein, J. L. R. (1993). Expression Patterns of Homeobox and Other Putative Regulatory Genes in the Embryonic Mouse Forebrain Suggest A Neuromeric Organization. *Trends in Neurosciences, 16,* 472-479.

Purcell, S. (2002). Variance components models for gene-environment interaction in twin analysis. *Twin Research, 5,* 554-571.

R Development Core Team (2005). R: A language and environment for statistical computing [Computer software]. Vienna, Austria.

Rakic, P. (1995). A Small Step for the Cell, A Giant Leap for Mankind - A Hypothesis of Neocortical Expansion During Evolution. *Trends in Neurosciences, 18,* 383-388.

Rakic, P., Bourgeois, J. P., Eckenhoff, M. F., Zecevic, N., & Goldmanrakic, P. S. (1986). Concurrent Overproduction of Synapses in Diverse Regions of the Primate Cerebral-Cortex. *Science, 232,* 232-235.

Rakic, P. & Lombroso, P. J. (1998). Development of the cerebral cortex: I. Forming the cortical structure. *Journal of the American Academy of Child and Adolescent Psychiatry, 37,* 116-117.

Ramnani, N., Behrens, T. E. J., Penny, W., & Matthews, P. M. (2004). New approaches for exploring anatomical and functional connectivity in the human brain. *Biological Psychiatry, 56,* 613-619.

Rash, B. G. & Grove, E. A. (2006). Area and layer patterning in the developing cerebral cortex. *Curr.Opin.Neurobiol., 16,* 25-34.

Reed, T., Pfefferbaum, A., Sullivan, E. V., & Carmelli, D. (2002). Influences of chorion type on measurements of the corpus callosum in adult monozygotic male twins? *Am.J.Hum.Biol., 14,* 338-346.

Reiss, A. L., Abrams, M. T., Singer, H. S., Ross, J. L., & Denckla, M. B. (1996). Brain development, gender and IQ in children - A volumetric imaging study. *Brain, 119,* 1763-1774.

Reveley, A. M., Reveley, M. A., Chitkara, B., & Clifford, C. (1984). The Genetic-Basis of Cerebral Ventricular Volume. *Psychiatry Research, 13,* 261-266.

Reveley, A. M., Reveley, M. A., Clifford, C., & Murray, R. M. (1982). Cerebral ventricular size in twins discordant for schizophrenia. Lancet 1, 540-541.

Ref Type: Generic

Rijsdijk, F. V., Van Haren, N. E., Picchioni, M. M., McDonald, C., Toulopoulou, T., Hulshoff Pol, H. E. et al. (2005). Brain MRI abnormalities in schizophrenia: same genes or same environment? *Psychological Medicine, 35,* 1-11.

Rubenstein, J. L. R., Anderson, S., Shi, L. M., Miyashita-Lin, E., Bulfone, A., & Hevner, R. (1999a). Genetic control of cortical regionalization and connectivity. *Cerebral Cortex, 9,* 524-532.

Rubenstein, J. L. R. & Rakic, P. (1999b). Genetic control of cortical development. *Cerebral Cortex, 9,* 521-523.

Scamvougeras, A., Kigar, D. L., Jones, D., Weinberger, D. R., & Witelson, S. F. (2003). Size of the human corpus callosum is genetically determined: an MRI study in mono and dizygotic twins. *Neurosci.Lett., 338,* 91-94.

Schafer, J. & Strimmer, K. (2005). An empirical Bayes approach to inferring large-scale gene association networks. *Bioinformatics, 21,* 754-764.

Schlaggar, B. L. & O'Leary, D. D. M. (1991). Potential of Visual-Cortex to Develop An Array of Functional Units Unique to Somatosensory Cortex. *Science, 252,* 1556-1560.

Schmitt, J. E., Wallace, G. W., Rosenthal, M. A., Molloy, E. A., Ordaz, S., Lenroot, R. et al. (2006). A multivariate analysis of neuroanatomic relationships in a genetically informative pediatric sample. *Neuroimage*.

Schmitz, S., Cherny, S. S., & Fulker, D. W. (1998). Increase in power through multivariate analyses. *Behavior Genetics, 28,* 357-363.

Shaw, P., Greenstein, D., Lerch, J., Clasen, L., Lenroot, R., Gogtay, N. et al. (2006a). Intellectual ability and cortical development in children and adolescents. *Nature, 440,* 676-679.

Shaw, P., Lerch, J., Greenstein, D., Sharp, W., Clasen, L., Evans, A. et al. (2006b). Longitudinal mapping of cortical thickness and clinical outcome in children and adolescents with attention-deficit/hyperactivity disorder. *Archives of General Psychiatry, 63,* 540-549.

Singh, V., Chertkow, H., Lerch, J. P., Evans, A. C., Dorr, A. E., & Kabani, N. J. (2006). Spatial patterns of cortical thinning in mild cognitive impairment and Alzheimer's disease. *Brain, 129,* 2885-2893.

Sled, J. G., Zijdenbos, A. P., & Evans, A. C. (1998). A nonparametric method for automatic correction of intensity nonuniformity in MRI data. *Ieee Transactions on Medical Imaging, 17,* 87-97.

Sowell, E. R., Thompson, P. M., Holmes, C. J., Jernigan, T. L., & Toga, A. W. (1999). In vivo evidence for post-adolescent brain maturation in frontal and striatal regions. *Nature Neuroscience, 2,* 859-861.

Sowell, E. R., Thompson, P. M., Leonard, C. M., Welcome, S. E., Kan, E., & Toga, A. W. (2004a). Longitudinal mapping of cortical thickness and brain growth in normal children. *Journal of Neuroscience, 24,* 8223-8231.

Sowell, E. R., Thompson, P. M., & Toga, A. W. (2004b). Mapping changes in the human cortex throughout the span of life. *Neuroscientist, 10,* 372-392.

Spiegelhalter, D. J., Best, N. G., Carlin, B. R., & van der Linde, A. (2002). Bayesian measures of model complexity and fit. *Journal of the Royal Statistical Society Series B-Statistical Methodology, 64,* 583-616.

Sporns, O., Chialvo, D. R., Kaiser, M., & Hilgetag, C. C. (2004). Organization, development and function of complex brain networks. *Trends Cogn Sci., 8,* 418-425.

Sporns, O., Tononi, G., & Edelman, G. M. (2000). Theoretical neuroanatomy: relating anatomical and functional connectivity in graphs and cortical connection matrices. *Cereb.Cortex, 10,* 127-141.

Sporns, O., Tononi, G., & Edelman, G. M. (2002). Theoretical neuroanatomy and the connectivity of the cerebral cortex. *Behav.Brain Res., 135,* 69-74.

Sporns, O., Tononi, G., & Kotter, R. (2005). The Human Connectome:A Structural Description of the Human brain. *PLoS Computational Biology, 1,* 32-42.

Steinmetz, H., Herzog, A., Huang, Y., & Hacklander, T. (1994). Discordant brain-surface anatomy in monozygotic twins. *N.Engl.J.Med., 331,* 951-952.

Steinmetz, H., Herzog, A., Schlaug, G., Huang, Y., & Jancke, L. (1995). Brain (A) symmetry in monozygotic twins. *Cereb.Cortex, 5,* 296-300.

Stephan, K. E., Hilgetag, C. C., Burns, G. A., O'Neill, M. A., Young, M. P., & Kotter, R. (2000). Computational analysis of functional connectivity between areas of primate cerebral cortex. *Philos.Trans.R.Soc.Lond B Biol.Sci., 355,* 111-126.

Storey, J. D. (2002). A direct approach to false discovery rates. *Journal of the Royal Statistical Society B., 64,* 479-498.

Strachan, T. & Reed, A. P. (2004). *Human Molecular Genetics*. (3rd ed.) London: Garland Press.

Striedter, G. F., Marchant, T. A., & Beydler, S. (1998). The "neostriatum" develops as part of the lateral pallium in birds. *Journal of Neuroscience, 18,* 5839-5849.

Sullivan, E. V., Pfefferbaum, A., Swan, G. E., & Carmelli, D. (2001). Heritability of hippocampal size in elderly twin men: equivalent influence from genes and environment. *Hippocampus, 11,* 754-762.

Sullivan, P. F. & Kendler, K. S. (1999). The genetic epidemiology of smoking. *Nicotine.Tob.Res., 1 Suppl 2,* S51-S57.

Super, H. & Uylings, H. B. M. (2001). The early differentiation of the neocortex: a hypothesis on neocortical evolution. *Cerebral Cortex, 11,* 1101-1109.

Swanson, L. W. (2000). What is the brain? *Trends in Neurosciences, 23,* 519-527.

Takane, Y. & de Leeuw, J. (1987). On the relationship between item response theory and factor analysis of discretized variables. *Psychometrika, 52,* 393-408.

The Chimpanzee Sequencing and Analysis Consortium (2005). Initial sequence of the chimpanzee genome and comparison with the human genome. *Nature, 437,* 69-87.

Thompson, P., Cannon, T. D., & Toga, A. W. (2002). Mapping genetic influences on human brain structure. *Ann.Med., 34,* 523-536.

Thompson, P. M., Cannon, T. D., Narr, K. L., van Erp, T., Poutanen, V. P., Huttunen, M. et al. (2001). Genetic influences on brain structure. *Nat.Neurosci., 4,* 1253-1258.

Thompson, P. M., Sowell, E. R., Gogtay, N., Giedd, J. N., Vidal, C. N., Hayashi, K. M. et al. (2005). Structural MRI and brain development. *Neuroimaging, Pt B, 67,* 285-+.

Tien, A. Y., Eaton, W. W., Schlaepfer, T. E., McGilchrist, I. K., Menon, R., Powers, R. et al. (1996). Exploratory factor analysis of MRI brain structure measures in schizophrenia. *Schizophrenia Research, 19,* 93-101.

Tomás, J. M., Hontangas, P. M., & Oliver, A. (2000). Linear Confirmatory Factor Models to Evaluate Multitrait-Multimethod Matrices: The Effects of Number of Indicators and Correlation Among Methods. *Multivar.Behav.Res., 35,* 469-499.

Tramo, M. J., Loftus, W. C., Stukel, T. A., Green, R. L., Weaver, J. B., & Gazzaniga, M. S. (1998). Brain size, head size, and intelligence quotient in monozygotic twins. *Neurology, 50,* 1246-1252.

Triarhou, L. C. (2006). The signalling contributions of Constantin von Economo to basic, clinical and evolutionary neuroscience. *Brain Research Bulletin, 69,* 223-243.

Uddin, M., Wildman, D. E., Liu, G., Xu, W., Johnson, R. M., Hof, P. R. et al. (2004). Sister grouping of chimpanzees and humans as revealed by genome-wide phylogenetic analysis of brain gene expression profiles. *Proc.Natl.Acad.Sci.U.S.A, 101,* 2957-2962.

van Erp, T. G., Saleh, P. A., Huttunen, M., Lonnqvist, J., Kaprio, J., Salonen, O. et al. (2004). Hippocampal volumes in schizophrenic twins. *Arch.Gen.Psychiatry, 61,* 346-353.

Van Haren, N. E., Picchioni, M. M., McDonald, C., Marshall, N., Davis, N., Ribchester, T. et al. (2004). A controlled study of brain structure in monozygotic twins concordant and discordant for schizophrenia. *Biol.Psychiatry, 56,* 454-461.

Vernon, P. A., Wickett, J. C., Bazana, P. G., & Stelmack, R. M. (2000). The Neuropsychology and Psychopathology of Human Intelligence. In *Handbook of Intelligence* (pp. 245-265). Cambridge, UK: Cambridge University Press.

von Baer, K. E. (1828). *Uber die Enwicklungsgeschichte der Thiere, Beobachtung und Reflexion.* Konigsberg: Borntrager.

von Economo, C. & Koskinas, G. N. (1925). *Die Cytoarchitekonic der Hirnrine des erwachsenen Menschen.* Vienna/Berlin: Springer.

Wallace, G. W. & Giedd, J. N. (2004). Genetic and Environmental Influences on Brain Morphometry: A Pediatric Twin Study.

Ref Type: Generic

Watkins, K. E., Vargha-Khadem, F., Ashburner, J., Passingham, R. E., Connelly, A., Friston, K. J. et al. (2002). MRI analysis of an inherited speech and language disorder: structural brain abnormalities. *Brain, 125,* 465-478.

Watts, D. J. & Strogatz, S. H. (1998). Collective dynamics of 'small-world' networks. *Nature, 393.*

White, T., Andreasen, N. C., & Nopoulos, P. (2002). Brain volumes and surface morphology in monozygotic twins. *Cereb.Cortex, 12,* 486-493.

Wishart, H. A., Saykin, A. J., McAllister, T. W., Rabin, L. A., McDonald, B. C., Flashman, L. A. et al. (2006). Regional brain atrophy in cognitively intact adults with a single APOE epsilon 4 allele. *Neurology, 67,* 1221-1224.

Worsley, K. J., Chen, J. I., Lerch, J., & Evans, A. C. (2005). Comparing functional connectivity via thresholding correlations and singular value decomposition. *Philosophical Transactions of the Royal Society B-Biological Sciences, 360,* 913-920.

Wright, I. C., Sham, P., Murray, R. M., Weinberger, D. R., & Bullmore, E. T. (2002). Genetic contributions to regional variability in human brain structure: methods and preliminary results. *Neuroimage., 17,* 256-271.

Wright, I. C., Sharma, T., Ellison, Z. R., McGuire, P. K., Friston, K. J., Brammer, M. J. et al. (1999). Supra-regional brain systems and the neuropathology of schizophrenia. *Cerebral Cortex, 9,* 366-378.

Young, M. P. (1992). Objective analysis of the topological organization of the primate cortical visual system. *Nature, 358,* 152-155.

Young, M. P. (1993). The organization of neural systems in the primate cerebral cortex. *Proc.Biol.Sci., 252,* 13-18.

Young, M. P., Scannell, J. W., O'Neill, M. A., Hilgetag, C. C., Burns, G., & Blakemore, C. (1995). Non-metric multidimensional scaling in the analysis of neuroanatomical connection data and the organization of the primate cortical visual system. *Philos.Trans.R.Soc.Lond B Biol.Sci., 348,* 281-308.

Zijdenbos, A. P., Forghani, R., & Evans, A. C. (2002). Automatic "pipeline" analysis of 3-D MRI data for clinical trials: Application to multiple sclerosis. *Ieee Transactions on Medical Imaging, 21,* 1280-1291.